

Some pages of this thesis may have been removed for copyright restrictions.

If you have discovered material in Aston Research Explorer which is unlawful e.g. breaches copyright, (either yours or that of a third party) or any other law, including but not limited to those relating to patent, trademark, confidentiality, data protection, obscenity, defamation, libel, then please read our [Takedown policy](#) and contact the service immediately (openaccess@aston.ac.uk)

Assessing the physiological and pathological functions of tissue Transglutaminase using FRET analysis

Shruti Sharma

Doctor of Philosophy

ASTON UNIVERSITY

December 2014

© Shruti Sharma, 2014

Shruti Sharma asserts her moral right to be identified as the author of this thesis

This copy of the thesis has been supplied on condition that anyone who consults it is understood to recognise that its copyright rest with its author and that no quotation from the thesis and no information derived from it may be published without appropriate permission or acknowledgement.

Thesis summary

Tissue Transglutaminase (TG2) is a cross-linking enzyme that links proteins by the formation of covalent bonds and confers resistance to proteolytic degradation. TG2 acts as a cell adhesion protein by binding to matrix fibronectin, cell surface heparan sulphates and integrins. TG2 has been implicated in a variety of diseases such as neurodegenerative disease, fibrosis and cancer. However, little is known about the mechanisms involved in its secretion, intracellular or extracellular activation or how these are regulated. The activity of TG2 is tightly controlled by GTP binding and calcium is required for its activation. TG2 assumes two strikingly different conformations, a catalytically inactive compact one in the presence of GTP and an active extended one in the presence of Ca^{2+} . This conformation change affects the functions of TG2 including its transamidating activity, its affinities and juxtaposition of binding sites for fibronectin, heparan sulphates and integrins. To study this, a FRET (Förster Resonance energy Transfer) sensor was constructed using the fluorescent proteins CFP and YFP fused to the N and C terminus of TG2, respectively. The FRET sensor has demonstrated different fluorescent characteristics depending on the conformation of TG2 and was used to monitor the conformational change that is induced by calcium or GTP binding.

Dedication

To my wonderful mother, Mrs Madhu Sharma, you have been my pillar of strength. You made me who I am today, I love you mom with all my heart.

To my dad, Mr Nagendra Sharma, my hero. Thank you for supporting me through joys and tears. So much of me is made of what I learned from you.

To my partner, Mr. Arzan Polishwalla. Your extraordinary love, friendship and humour, I will always cherish. I am truly blessed to have you by my side.

To Mrs Satyavati Singh, you will always be in my heart.

Acknowledgment

I would like to thank my supervisor Dr Russell Collighan for his support, guidance and time throughout this course. His expertise in the field and guidance has helped me tremendously. Thankyou for sharing your knowledge.

I gratefully acknowledge Prof. Martin Griffin for giving me this opportunity to work with him and his efficient team. His insight and productive comments have always been deeply appreciated.

I would also like to thank Dr. Wang Zhuo for her energetic support and understanding during my research.

I am thankful to Dr Andrew Dewitt for his encouragement.

A special thank you to Dr. Darius Kavaliauskas, you have truly been an inspiration. Thank you for all your support.

I am also grateful to Gill Pilfold and Matthew Richards for their assistance.

A very big thank you to Mrs Meenakshi Rehani, for being such a wonderful mentor and an amazing friend.

I would like to thank my friends Dr. Vidya Rajasekaran, Dr Vinod Nadella, Andrea Costanzi for sharing this experience with me.

Lastly I would like to thank my sisters, Priyanka Parmar and my lucky mascot Ekta Singh for always being there for me.

Table of contents

Thesis summary.....	2
Dedication.....	3
Acknowledgment.....	4
List of Abbreviations.....	12
List of figures.....	13
List of Tables.....	20
Chapter 1	21
Introduction	21
1.1 Introduction	22
1.2 Mechanism of cross linking	22
1.3 Types of Transglutaminase.....	23
1.3.1 TG1 or Keratinocyte Transglutaminase.....	23
1.3.2 TG2 or tissue transglutaminase	24
1.3.3 TG3 or epidermal transglutaminase	24
1.3.4 TG4 or prostate transglutaminase.....	25
1.3.5 TG5.....	25
1.3.6 Factor XIIIa	26
1.3.7 Protein 4.2.....	27
1.3.8 TG6 or TGM Y	27
1.3.9 Transglutaminase 7/ TGZ	28
1.4 Structure of transglutaminase	31
1.5 Tissue Transglutaminase (TG2).....	32
1.6 Structure of TG2	33
1.6.1 Catalytic site.....	33
1.6.2 Calcium binding site	34
1.6.3 Nucleotide pocket	35
1.6.4 Fibronectin binding site	36
1.6.5 Heparin binding site	36
1.7 Localisation and cellular distribution	37
1.8 Secretion of TG2.....	38
1.9 Regulation of TG2 activity	40
1.10 Roles of TG2.....	42

1.10.1 GTPase.....	42
1.10.2 Kinase activity	42
1.10.3 TG2: protein disulphide isomerase	42
1.10.4 Cell adhesion	43
1.11 TG2 involvement in pathological and disease state	44
1.11.1 Wound Healing	44
1.11.2 Neurodegenerative Disease.....	44
1.11.2.1 Huntington's disease.....	45
1.11.2.2 Parkinson's disease	45
1.11.2.3 Alzheimer's disease	45
1.11.3 Fibrosis	46
1.11.4 Coeliac disease.....	47
1.11.5 Cancer	47
1.12 TG2 inhibitors.....	48
1.12.1 Competitive amine inhibitors.....	48
1.12.2 Reversible inhibitors.....	49
1.12.3 Irreversible inhibitors.....	49
1.13 FRET (Förster Resonance Energy Transfer)	49
1.13.1 Green fluorescent protein.....	51
1.13.2 Crystal Structure of GFP	53
1.13.3 GFP mutants.....	55
1.14 Classification of GFPs.....	56
1.15 Intra-molecular FRET	58
1.16 Inter-molecular FRET	59
1.17 Mechanism of FRET	59
1.18 FRET quantification techniques	60
1.18.1 Donor de-quenching.....	60
1.18.2 Acceptor enhanced emission	61
1.18.3 Donor acceptor emission peak ratio.....	61
1.19 FRET measurement.....	62
1.20 Potential problems in FRET experiments.....	62
1.20.1 Measurement difficulties	62
1.20.2 Problems with construction and validation of fusion proteins	64

AIMS	66
Chapter 2	67
Material and Methods.....	67
2. METHODS	68
2.1 Media Recipe	68
2.1.1 LB Broth	68
2.1.2 LB Agar	68
2.2 Buffer Recipes	68
2.2.2 6x DNA loading buffer	68
2.2.3 Laemmli Buffer.....	69
2.2.4 Cracking buffer.....	69
2.2.5 Coomassie Blue stain	69
2.2.6 SDS electrode running buffer.....	69
2.2.7 SDS transfer buffer	69
2.3 10x dNTPs	69
2.4 SDS polyacrylamide Gel	70
2.5 General chemicals	70
2.6 Primers.....	70
2.7 General Techniques.....	72
2.7.1 Preparation of competent cells using calcium chloride	72
2.7.2 Transformation.....	73
2.7.3 Blue White screening procedure	74
2.7.4 Cracking procedure.....	74
2.7.5 Plasmid preparation	74
2.7.6 Phenol Chloroform Extraction of DNA.....	75
2.7.7 Isopropanol precipitation	75
2.7.8 Ethanol precipitation.....	76
2.7.9 Agarose gel electrophoresis.....	76
2.7.9.1 Agarose gel.....	76
2.7.9.2 Agarose gel purification (Low melting point gel).....	77
2.7.10 DNA quantification	77
2.8 Cloning Vectors.....	77
2.9 Dephosphorylation of DNA.....	78

2.10 Ligation reaction.....	78
2.11 Restriction Digestion	78
2.12 PCR reactions.....	79
2.13 Touchdown PCR.....	79
2.14 Colony PCR	80
2.15 Sequencing reactions.....	81
2.16 Klenow 3'end infilling.....	81
2.17 Expression and purification of Recombinant TG2	82
2.18 Chromatographic purification of His-tagged proteins using His GraviTrap column (GE Healthcare).	82
2.19 Gradient purification using GE AKTA prime FPLC.....	83
2.20 Desalting by gel filtration.....	83
2.21 SDS-PAGE	83
2.22 Western blotting of SDS PAGE separated proteins	84
2.23 Protein Assay.....	85
2.24 Transglutaminase Activity assay.....	85
2.25 Detection of TG2 antigen using ELISA.....	86
2.26 Binding of TG2 to Heparin-Sepharose	86
2.27 Trypsin Digestion Assay.....	87
2.28 Conformation dependent protease digestion	87
2.29 FRET reactions	88
Chapter 3	89
Construction of CFP-TG2-YFP recombinant protein in bacterial system.....	89
3.1 Introduction	90
3.2 RESULTS	93
3.3 PCR amplification	93
3.3.1 CFP amplification.....	94
3.3.4 YFP amplification	95
3.3.4 TG2 amplification	96
3.4 Cloning amplified products into pSTBlue-1	97
3.4.1 Identification of recombinant pSTBlue-1 plasmids.	97
3.4.2 CFP cracking	98
3.4.3 YFP cracking.....	99
3.4.5 TG2 cracking.....	100

3.5 Cloning of CFP, YFP and TG2 into expression vector pTrcHisB	101
3.6 Cloning CFP into pTrcHis B	102
3.7 Screening of recombinant CFP-pTrcHisB plasmids	104
3.8 Analysis of selected colonies of recombinant CFP-pTrcHis B clones.	106
3.9 Orientation of CFP into pTrcHisB	107
3.10 Colony PCR	109
3.11 Nucleotide sequencing	110
3.12 Cloning of TG2 into CFP-pTrcHis B	110
3.13 Restriction digestion of CFP-pTrcHisB 12 and TG2-pSTblue1 plasmid	112
3.14 Screening of CFP-TG2-pTrcHisB ligated colonies.	114
3.15 Nucleotide sequencing of CFP-TG2-pTrcHisB clones	115
3.16 Test <i>Bgl</i> III digest of CFP-TG2 clones	118
3.17 YFP cloning into CFP-TG2 pTrcHisB	118
3.18 <i>Hind</i> III digestion of YFP-psTBlue1 plasmid	119
3.19 <i>Eco</i> RI digestion of YFP-psTBlue1 plasmid	120
3.20 <i>Eco</i> RI digestion of CFP-TG2-pTrcHisB plasmid	123
3.21 Screening of recombinant CFP-TG2-YFP-pTrcHisB clones	124
3.22 Restriction digestion test on selected CFP-TG2-YFP-pTrcHisB clones.	125
3.23 Discussion	127
Chapter 4	130
Expression and characterisation of construct	130
4.1 Introduction	131
4.2 Expression of CFP-pTrcHisB	132
4.3 Expression and Purification of CFP-TG2-YFP recombinant protein	133
4.4 Chromatographic purification of His-tagged proteins using His GraviTrap column	133
4.5 Fractions of protein purified on His GraviTrap column	134
4.6 Gradient purification using GE AKTA prime FPLC	135
4.6.1 Western blot analysis of 20mM-200mM imidazole gradient eluted fractions	136
4.6.2 25mM-500mM imidazole gradient eluted fractions	139
4.6.3 30mM-500mM imidazole gradient eluted fractions	140
4.6.4 Steep 25mM-200mM imidazole gradient eluted fractions	144
4.7 Control CFP-TG2 recombinant protein purification	145

4.7.1 Western blot analysis of control CFP-TG2 purification eluted fractions	146
4.8 Control wild type TG2-pET30ek/LIC purification (wild type TG2)	146
4.9 Binding of TG2 to Heparin-Sepharose	147
4.9.1 Western blot analysis of CFPTG2YFP purification through heparin-Sepharose column	149
4.9.2 Western blot analysis of wild type TG2 purification eluted using heparin-Sepharose column	150
4.9.3 Western blot analysis of CFPTG2 purification eluted fractions	151
4.9.4 Downstream cleaning of Ni-affinity purified protein using Heparin column.	153
4.10 Affinity purification of control pET30Ek/LIC TG2 using GE AKTA prime FPLC	154
4.10.1 Purified wild type TG2 through heparin column	155
4.11 Affinity purification of CFP-TG2-YFP using GE AKTA prime FPLC	157
4.11.2 Purified CFP-TG2-YFP fractions through heparin column	158
4.12 Conformational changes due to effect of monodansyl cadaverin, biotin cadaverin, inhibitors R281 / R283	160
4.12.1 Effect of Biotin cadaverin (BTC)	160
4.12.2 Effect of monodansyl cadaverin	163
4.12.3 Effect of Inhibitors R281 and R283	166
4.12.4 R281 and wild type	166
4.12.5 R283 and wild type	167
4.12.6 R281 and CFP-TG2-YFP recombinant protein	169
4.13 Presence of TG2 antigen by ELISA	172
4.14 Biotin-cadaverine incorporation into N,N'-dimethylcasein	173
4.15 Biotin-cadaverine incorporation into Fibronectin	173
4.16 Calcium activation assay	174
4.17 GTP inhibition curve	176
4.18 Discussion	178
Chapter 5	180
FRET analysis	180
5.1 Introduction	181
5.2 FRET data analysis	182
5.2.1 Effect of GTP on conformation using FRET analysis	182
5.3 Control CFP-TG2 recombinant protein FRET analysis	186

5.4 Effect of Calcium on conformation using FRET analysis.....	191
5.5 Control CFP-TG2 recombinant protein FRET analysis	195
5.6 Comparison of Calcium activity curve and FRET efficiency	200
5.7 Discussion.....	201
Chapter 6	202
Construction of CFP-TG2-YFP recombinant protein in mammalian system.....	202
6.1 Introduction	203
6.2 PCR amplification	204
6.3 CFP-TG2-YFP amplification.....	204
6.4 Cloning amplified products into pSTBlue-1	206
6.5 His-CFP-TG2-YFP cracking.....	206
6.6 NotICFP-TG2-YFP cracking.....	207
6.7 Cloning of CFP-TG2-YFP construct into expression vector pcDNA3.1-.....	209
6.8 Cloning NotCFP-TG2-YFP and HisCFP-TG2-YFP into pcDNA3.1-	210
6.9 Screening of recombinant CFP-TG2-YFP-pcDNA3.1- plasmids	213
6.10 Discussion.....	217
Chapter 7	218
Discussion.....	218
References.....	229

List of Abbreviations

ATP Adenosine 5'- triphosphate
APP Amyloid precursor protein
BTC Biotin Cadaverin
CaCl₂ Calcium Chloride
CD Celiac disease
DMSO Dimethyl sulphoxide
DNA Deoxyribonucleic acid
dNTP Deoxyribonucleotide
DTT Dithiothreitol
ECL Enhanced chemiluminescence
ECM Extracellular matrix
EDTA Ethylene diamine tetra acetic acid
EGTA Ethylene glycol tetra acetic acid
FCS Fluorescence correlation spectroscopy
FN Fibronectin
FXIII Factor XIII
FXIII A Factor XIII subunit A
FXIII B Factor XIII subunit B
GDP Guanosine 5'diphosphate
RhTG2 Recombinant human transglutaminase
GFP Green fluorescent protein
GTP Guanosine 5'- triphosphate
GTPase Guanosine 5'- triphosphatase
HRP Horseradish peroxidase
HS Heparan sulphate
IgG Immunoglobulin
IGF1 insulin like growth factor 1
IL-6 Interleukin - 6
I κ B Inhibitor of - κ B
IPTG isopropyl-beta-D-thiogalactopyranoside
kDa Kilo Dalton
MDC Monodansyl Cadaverin
MMP matrix metalloproteinases
NF κ B Nuclear factor kappa - light chain enhancer of activated B cells
OPD o-phenylenediamine
ORF Open reading frame
PAGE Polyacrylamide gel electrophoresis
PBS Phosphate buffer saline
PCR Polymerase chain reaction
PDI Protein disulphide isomerase
PKC α protein kinases c alpha
PMA α phorbol 12, 13 didecanole
PMSF Phenylmethylsulfonyl fluoride
PNRC Perinuclear recycling compartment
SCR Small consensus repeat
SDS Sodium dodecyl sulphate
SDS- PAGE Sodium dodecyl sulphate- polyacrylamide gel electrophoresis
TEMED N, N, N', N'-tetramethylene diamine
TG Transglutaminase
TG2 Tissue transglutaminase
TGF β 1 Transforming growth factor beta 1
X-gal 5-bromo-4-chloro-3-indolyl-beta-D-galacto-pyranoside

List of figures

Figure 1.1 Crystal structure of GDP bound (closed conformation) and inhibitor bound TG (open conformation).

Figure 1.2 Calcium binding sites.

Figure 1.3 Secretion of cytoplasmic TG2.

Figure 1.4 Trafficking of TG2 into the extracellular matrix via syndecan shedding.

Figure 1.5 Timeline of major developments of GFP

Figure 1.6 Structure of monomeric WT GFP

Figure 1.7 Chromophore structures of CFP and YFP

Figure 1.8 Intramolecular FRET.

Figure 1.9 Intermolecular FRET.

Figure 1.10 Cross-talk.

Figure 1.11 Bleed-through

Figure 3 Overview of the cloning strategy

Figure 3.1 Agarose gel electrophoresis of amplified products using primers CFP For3/Rev3.

Figure 3.2 Agarose gel electrophoresis of amplified products using primers YFP For2/Rev2.

Figure 3.3 Agarose gel electrophoresis of amplified products using primers TG2 For/Rev.

Figure 3.4 Agarose gel electrophoresis of the cracking procedure performed on the selected CFP colonies after Blue White screening.

Figure 3.5 Agarose gel electrophoresis of the cracking procedure performed on the selected YFP colonies after Blue White screening

Figure 3.6 Agarose gel electrophoresis of the cracking procedure performed on the selected TG2 colonies after Blue White screening

Figure 3.7 Agarose gel electrophoresis of the purified plasmid of pTrcHis B.

Figure 3.8 Agarose gel electrophoresis of the digestion of purified CFP using *Bam HI* and *Bgl II*.

Figure 3.9 Agarose gel electrophoresis of the digestion of the purified pTrcHis B plasmid using *Bam HI*.

Figure 3.10A and 3.10B Agarose gel electrophoresis of the cracking procedure performed on the selected CFP-pTrcHis B clones.

Figure 3.11 Agarose gel electrophoresis of the purified plasmid of CFP-pTrcHis B clones.

Figure 3.12 Agarose gel electrophoresis of the *BamHI/EcoRI* digestion of the purified CFP-pTrcHis B clones.

Figure 3.13 Agarose gel electrophoresis of the colony PCR.

Figure 3.14 Agarose gel electrophoresis of the purified plasmid of CFP-pTrcHis B clones 12 and TG2-pSTblue 1 purified plasmid.

Figure 3.15 Agarose gel electrophoresis of *EcoRI/BglIII* digested CFP-pTrcHis B 12 and TG2-pSTBlue1 purified plasmid.

Figure 3.16 Agarose gel electrophoresis of gel purified plasmid of CFP-pTrcHis B clones 12 and TG2-pSTblue 1 purified plasmid.

Figure 3.17 Agarose gel electrophoresis of the cracking procedure performed on the selected CFP-TG2-pTrcHisB clones.

Figure 3.18 Agarose gel electrophoresis CFP-TG2-pTrcHisB clones which were treated with Klenow fragment and re-ligated

Figure 3.19 Agarose gel electrophoresis showing a test *BglIII* digested of re-ligated clones.

Figure 3.20 Agarose gel electrophoresis of the digestion of the purified YFP-pSTBlue1 plasmid using *HindIII*.

Figure 3.21 Agarose gel electrophoresis of the double digestion of the purified YFP-pSTBlue1 plasmid using *EcoRI*/*HindIII*.

Figure 3.22 Agarose gel electrophoresis of the double digestion of CFP-TG2-pTrcHisB plasmid using *HindIII*/*EcoRI*.

Figure 3.23A and 23B Agarose gel electrophoresis of the cracking procedure performed on the selected CFP-TG2-YFP-pTrcHisB clones.

Figure 3.24 Agarose gel electrophoresis of the double digestion of the purified CFP-TG2-YFP-pTrcHisB clones.

Figure 4.1 SDS PAGE analysis of expression of CFP by CFP-pTrcHisB clones. Lane 1 is the BLUeye prestained protein ladder.

Figure 4.2 SDS PAGE analysis CFP-TG2-YFP recombinant protein expressed in Novablu cells and purified using His GraviTrap column (GE Healthcare).

Figure 4.3 Western blot analysis of CFP-TG2-YFP recombinant protein purification using His GraviTrap column (GE Healthcare).

Figure 4.4 SDS PAGE analysis CFP-TG2-YFP recombinant protein expressed in Rosetta cells and purified using Ni-NTA column (GE AKTA prime FPLC).

Figure 4.5 Western blot analysis of CFP-TG2-YFP recombinant protein purification using Ni-NTA column.

Figure 4.6 SDS PAGE analysis CFP-TG2-YFP recombinant protein expressed in Rosetta cells and purified using Ni-NTA column (GE AKTA prime FPLC).

Figure 4.7 Western blot analysis of CFP-TG2-YFP recombinant protein purification using Ni-NTA column using 25-500mM imidazole gradient elution.

Figure 4.8 SDS PAGE analysis CFP-TG2-YFP recombinant protein expressed in Rosetta cells and purified using Ni-NTA column (GE AKTA prime FPLC).

Figure 4.9 Western blot analysis of CFP-TG2-YFP recombinant protein purification using Ni-NTA column using 30-500mM imidazole gradient elution.

Figure 4.10 SDS PAGE analysis CFP-TG2-YFP recombinant protein using a shallow gradient of 20ml.

Figure 4.11 SDS PAGE analysis CFP-TG2-YFP recombinant protein expressed in Rosetta cells and purified using Ni-NTA column (GE AKTA prime FPLC).

Figure 4.12 Western blot analysis of CFP-TG2-YFP recombinant protein purification using Ni-NTA column.

Figure 4.13 SDS PAGE analysis CFP-TG2 control recombinant protein expressed in Rosetta cells and purified using Ni-NTA column (GE AKTA prime FPLC).

Figure 4.14 Western blot analysis of CFP-TG2 recombinant protein purification using Ni-NTA column over a 20-200mM imidazole gradient elution

Figure 4.15 SDS PAGE analysis Control wild type TG2-pET30ek/LIC recombinant protein expressed in Rosetta cells and purified using Ni-NTA column (GE AKTA prime FPLC).

Figure 4.16 Western blot analysis of CFP-TG2-YFP recombinant protein purification over heparin sepharose column.

Figure 4.17 Western blot analysis of wild type recombinant protein purification over heparin sepharose column.

Figure 4.18 Western blot analysis of control CFP-TG2 recombinant protein purification over heparin sepharose column.

Figure 4.19 SDS PAGE analysis of wild type TG2 protein purification using Ni column.

Figure 4.20 SDS PAGE analysis of purified fractions of wild type TG2 protein purification using heparin column.

Figure 4.21 SDS PAGE analysis of CFP-TG2-YFP recombinant protein purification using Ni column.

Figure 4.22 SDS PAGE analysis of purified fractions of CFP-TG2-YFP recombinant protein purification using heparin column

Figure 4.23 SDS PAGE analysis of BTC treated wild type TG2.

Figure 4.24 SDS PAGE analysis of BTC treated CFP-TG2-YFP recombinant protein

Figure 4.25 SDS PAGE analysis of MDC treated wild type TG2.

Figure 4.26 SDS PAGE analysis of BTC treated CFP-TG2-YFP recombinant protein.

Figure 4.27 SDS PAGE analysis of R281 treated wild type recombinant TG2 protein.

Figure 4.28 A and B SDS PAGE analysis of R283 treated wild type recombinant TG2 protein.

Figure 4.29 A and B SDS PAGE analysis of R281 treated wild type recombinant TG2 protein.

Figure 4.30 Detection of TG2 antigen using ELISA

Figure 4.31 Comparison of specific activity of RhTG2 and purified CFP-TG2-YFP recombinant with respect to biotin cadaverin incorporation into N, N'-dimethylcasein.

Figure 4.32 Comparison of specific activity of RhTG2 and purified CFP-TG2-YFP recombinant with respect to biotin cadaverin incorporation into fibronectin.

Figure 4.33 Dose-response curve of transglutaminase activity for calcium with values plotted on a logarithmic scale.

Figure 4.34 Figure Dose-response curve of transglutaminase activity for GTP with values plotted on a logarithmic scale.

Figure 5.1 Effect of increasing concentration of GTP on CFP emission analysing CFP-TG2-YFP recombinant protein

Figure 5.2 Effect of increasing concentration of GTP on YFP emission analysing CFP-TG2-YFP recombinant protein.

Figure 5.3 Effect of increasing concentration of GTP on CFP excitation YFP emission analysing CFP-TG2-YFP recombinant protein.

Figure 5.4 Effect of increasing concentration of GTP on CFP emission analysing control CFP-TG2 recombinant protein.

Figure 5.5 Effect of increasing concentration of GTP on CFP excitation YFP emission analysing control CFP-TG2 recombinant protein.

Figure 5.6 Effect of increasing concentration of GTP on FRET.

Figure 5.7 Effect of increasing concentration of GTP on FRET efficiency.

Figure 5.8 Effect of increasing concentration of calcium on CFP emission analysing CFP-TG2-YFP recombinant protein

Figure 5.9 Effect of increasing concentration of calcium on YFP emission analysing CFP-TG2-YFP recombinant protein

Figure 5.10 Effect of increasing concentration of calcium on CFP excitation YFP emission analysing CFP-TG2-YFP recombinant protein.

Figure 5.11 Effect of increasing concentration of calcium on CFP emission analysing control CFP-TG2 recombinant protein

Figure 5.12 Effect of increasing concentration of calcium on CFP excitation YFP emission analysing CFP-TG2 recombinant protein.

Figure 5.13 Effect of increasing concentration of calcium on FRET.

Figure 5.14 Effect of increasing concentration of calcium on FRET efficiency

Figure 5.15 Comparison of calcium activity and FRET efficiency.

Figure 6.1 Agarose gel electrophoresis of amplified CFP-TG2-YFP plasmid using forward primers NotICFP and HisPtrc and YFP Rev2 primer

Figure 6.2 Agarose gel electrophoresis of the cracking procedure performed on the selected His CFP-TG2-YFP colonies after Blue White screening

Figure 6.3 Agarose gel electrophoresis of the cracking procedure performed on the selected NotI CFP-TG2-YFP colonies after Blue White screening

Figure 6.4 Agarose gel electrophoresis of the purified plasmid of pcDNA3.1-.

Figure 6.5 Agarose gel electrophoresis of the digestion of the His-CFP-TG2-YFP5 plasmid using *NotI* and *HindIII*.

Figure 6.6 Agarose gel electrophoresis of the digestion of the purified pcDNA3.1- plasmid using *NotI* and *HindIII*.

Figure 6.7 Agarose gel electrophoresis of the cracking procedure performed on the selected NotICFP-TG2-YFP-pcDNA3.1- colonies after transformation.

Figure 6.8 NotICFP-TG2-YFP-pcDNA3.1- colonies after transformation.

Figure 6.9 Agarose gel electrophoresis of the cracking procedure performed on the selected His-CFP-TG2-YFP-pcDNA3.1- colonies after transformation.

List of Tables

Table 1 Members of the transglutaminase family.

Table 2 Wide range of fluorescent proteins available

Chapter 1

Introduction

Transglutaminase

1.1 Introduction

Transglutaminases are multifunctional enzymes that cross-link proteins to form high molecular weight aggregates. This post-translational modification of proteins occurs through an acyl-transfer reaction between the γ -carboxamide group of a protein or peptide bound glutamine and the free ϵ -amino group of a lysine. The resulting cross-linked protein aggregates impart strength to tissues and enhance resistance to chemical and proteolytic degradation. Transglutaminase are involved in protein crosslinking and polyamidation which regulate cellular functions like apoptosis, extracellular matrix assembly, and stabilisation of skin epidermis.(Griffin et al., 2002)

1.2 Mechanism of cross linking

The calcium dependent cross linking reaction was well investigated in the 1960s by Jack Folk and the enzymatic reaction was depicted to follow a ping-pong mechanism. This reaction is a two step reaction where by the enzyme primarily recognises a glutamine bound peptide and interacts via the sulphur of the cysteine (C277) residue resulting in the formation of a thioester acyl intermediate with the release of ammonia. The second half of the reaction involves the intermediate undergoing a nucleophilic attack by a primary amine or water molecule. The unfavourable hydrolytic reaction results in the formation of glutamic acid and is called deamination. The alternate favourable transamidation reaction occurs when a primary amine acts as an acyl acceptor. This reaction can result in either incorporation of primary amines into proteins or crossing linking of proteins depending on the second substrate. The formation of iso-peptide bonds between donor and acceptor is particularly significant due to their property for being resistant to proteolytic and

chemical damage. Apart from this direct cross linking small polyamine are also involved in indirect crosslinking involving polymerisation of polyamine such as putrescine (Tsai et al., 1998),(Griffin et al., 2002).

1.3 Types of Transglutaminase

Transglutaminase (EC 2.3.2.13) is classified as follows

E.C. 2 Transferase

E.C. 2.3 Acyltransferase

E.C. 2.3.2 Aminoacyltransferase

E.C. 2.3.2.13 ProteinGlutamineGammaGlutamyltransferase

Transglutaminases are found in both eukaryotes and prokaryotes, including microorganisms(Kanaji et al., 1993), invertebrates(Singh and Mehta, 1994), plants(Del Duca et al., 1995), amphibians(Zhang and Masui, 1997), fish(Yasueda et al., 1994), and birds(Puszkina and Raghuraman, 1985). Mammalian transglutaminases are calcium dependent whereas bacterial transglutaminase are not regulated by cofactors.

All types of transglutaminase illustrate substrate specificity. Different TGs can recognise same protein substrate but differ in affinity and specificity. At the genetic level, nine members of the mammalian transglutaminase family have been identified, of which seven have been characterised at the protein level.

1.3.1 TG1 or Keratinocyte Transglutaminase

TG1 in proliferating cells exists as a membrane-bound 106kDa form but in terminally differentiating cells undergoes proteolysis to fragments of 67kDa, 33kDa and 10kDa . (Kim et al., 1995) TG1, expressed at basal levels in proliferating keratinocytes, is exponentially induced and activated by tarazotene induced protein 3 (TIG3) during

the differentiating phase of keratinocytes. It contributes to the cornified envelope formation by anchoring to the inner surface of plasma membrane via amino terminal lipid linkage. (Sturniolo et al., 2005) Apart from keratinocytes it is found to be expressed in epithelial tissue of the lung, kidney and liver at adherens junctions and also reported in myocardial microvascular endothelial cells and are involved in maintaining structural integrity.(Hiiragi et al., 1999) TG1 is involved in the cross linking of cell envelope proteins where during terminal differentiation of keratinocytes the plasma membrane bound TG1 is activated. Besides cross linking of keratins TG1 has been found to support the attachment of cell envelope proteins to the lipid envelope by cross linking terminal ω hydroxyceramides.(Iismaa et al., 2009)

1.3.2 TG2 or tissue transglutaminase

TG2 is 80kDa protein and is the most widely studied member of the family.TG2 cross-links cell surface fibronectin to promote cell-matrix interactions and are also associated with noncovalent bonding of integrins to fibronectin. This function is important in cell adhesion and in fibronectin assembly. (Wang et al., 2010)

1.3.3 TG3 or epidermal transglutaminase

TG3 is a 77 kDa inactive zymogen which on activation by cathepsin L is converted into its active form (50/27kDa)(Kim et al., 1990). It is involved in the cross linking of hair structural protein; e.g. trichohyalin to form keratin intermediate filament matrix protein and also participates in cell envelope formation.(Tarcza et al., 1997) It is observed that TG3 knockout mice do not show adverse effects, except for a delay in skin barrier formation before birth which is normalised until birth and irregular hair follicle function(Thiebach et al., 2007, Iismaa et al., 2009). TG3 cross links loricrin and SPRs (small proline rich proteins) during cell envelope formation in corneocytes

and may be involved in cross linking structural proteins of hair. Association of TG3 genetic variants with disease conditions have not been reported in humans (Stacey et al., 2014). It is known to play a pathological role in dermatitis herpetiformis (celiac disease)(Rose et al., 2009)

1.3.4 TG4 or prostate transglutaminase

TG4 is predominantly distributed and expressed in the prostate gland and has been indicated to be involved in prostate cancer. Dubbink *et al* has reported the androgen supported upregulation of TG4. (Dubbink et al., 1996) TG4 exhibits both transamidase and GTPase activity similar to that of TG2. (Spina et al., 1999)It is known to mask antigenicity of sperm cells by regulating immune responses in the female genital tract of rabbits.(Mukherjee et al., 1983) It is reported to be associated with prostate cancer cell growth and increases migration and invasiveness of these cells. It is also involved in membrane micromotion, cell-matrix adhesion, tumor – endothelial interaction and epithelial mesenchymal transition. It is referred to as a potential biomarker to differentiate between aggressive and nonaggressive cancer. (Jiang and Albin, 2011) (Cao et al., 2013)

1.3.5 TG5

TG5 is an 81kDa transglutaminase and is activated upon proteolytic processing and its expression found in upper layers of the epidermis and human hair follicle.(Candi et al., 2002) It is observed in the epithelial mesenchymal transition state of keratinocytes with substrates like loricrin, involucrin, SPR3 and is co-localised with vimentin.(Candi et al., 2001) A mutation in TG5 resulting in the loss of function has been implicated to cause APSS or acral peeling skin syndrome. There is a higher expression of TG5 in the skin of APPS patients where the enzyme is found between

the granular layer and the stratum corneum and localised to the position of the split. (Cassidy et al., 2005) Sequence analyses of APPS families have revealed two missense mutations p. T109M and p. G113C in affected individuals. (Bowden, 2011)

1.3.6 Factor XIIIa

FXIII is a heterotetramer found in the plasma comprising of two subunit A (83kDa), which belongs to the transglutaminase family, and two regulatory subunit B (80kDa) of the small consensus repeat (SCR) protein family. (Lehthinen et al., 2004) Subunit A is the catalytic domain and subunit B is the carrier protein. FXIII finds important functions both inside and outside the cell, predominantly present in the plasma, noncovalently bound to fibrinogen. Subunit B is known to play a role in stabilising subunit A and a mutation in subunit B leads to deficiency of subunit A. (Saito et al., 1990) The carrier subunit B also contributes by regulating the conversion of Plasma FXIII (pFXIII) to pXIIIa/(activated form) and binding the pFXIII heterotetramer zymogen to fibrinogen. During the activation of pFXIII the detaching of subunits A and B is initiated by thrombin and enhanced by polymers of fibrin. The dissociation of subunits is governed by calcium binding followed by a conformational change that results in access to the active site cysteine for crosslinking reaction to follow. It also incorporates plasminogen activator inhibitor-2 which prevents fibrinolysis and increases resistance during blood coagulation. (Ritchie et al., 2000) (Verderio et al., 2005) Apart from being found in blood platelets (Puszkun and Raghuraman, 1985) it has been reported that FXIIIa is associated with macrophages, (Törőcsik et al., 2005) and plays a role in wound healing, bone development and tumor progression.

1.3.7 Protein 4.2

Protein 4.2 is the catalytically inactive member of the transglutaminase family due to substitution of active cysteine with alanine. It is found in the cells of erythroid lineage and the protein has a myristoyl and palmitoyl group attached to it. It is associated with the association of erythrocyte membrane to the cytoskeleton via ankyrin and Band3. (Iismaa et al., 2009) Band 4.2 is suggested to be involved in providing stability and flexibility of RBCs and patients with deficiency suffer from spherocytosis and to an extent haemolytic anemia. (Zhu et al., 1998) Another intriguing fact that differentiates protein 4.2 is that it binds to ATP and not GTP. (Azim et al., 1996) In 4.2 knockout mice the RBCs were observed to be smaller than normal as an effect of membrane loss and altered cation concentrations. They are also observed to be spherical due to lack of lipid anchoring and are more fragile. (Iismaa et al., 2009)

1.3.8 TG6 or TGM Y

TG6 has been shown to have restricted expression pattern and is expressed in the neural tissue and is associated with pathogenesis of gluten sensitivity-related neurological problems. (Hadjivassiliou et al., 2008) TG6 has been found to have high specific activity in the absence of proteolytic processing and is sensitive to oxidative inactivation. Similar to TG2, TG6 require calcium binding for activation and data suggests potential to function as a guanine nucleotide exchange factor in signalling. Expression of TG6 was enhanced on induction of cell death by metal ion chelation in Neuro 2a cells relating the increase in TG6 expression during cerebral cortex development to programmed cell death. It is also suggested that TG6 may play an important role in neurons involved in motor control. (Thomas et al., 2013) TG6 is associated with gluten ataxia (Cascella et al., 2013)

1.3.9 Transglutaminase 7/ TGZ

TG7 is known to be expressed in osteosarcoma cells, dermal fibroblasts, erythroleukemia cells, primary keratinocytes, testis, skin, brain kidney, etc. TG7 is also known to be similar to TG2 in terms of structural requirements and calcium binding. The catalytic core comprise of Cys-279, His-338 and Asp-361. TG7 was observed that similar to TG5, Tyr at 538 is replaced by His. It is also present on the same chromosome 15q15.2 along with TG5 and band 4.2.(Grenard et al., 2001b)

Member of TG family	Gene location	Function	Molecular mass	Tissue expression	Distribution
Epidermal transglutaminase	Chromosome 20 q11-12	Involved in cornified cell envelop formation during terminal differentiation of keratinocytes. Keratinization of developing hair.	77kDa	Squamous epithelium	Cytosol
Factor XIII	Chromosome 6 p24-p25	Associated with blood clotting and wound healing Bone metabolism (ECM deposition and osteoblast differentiation)	83kDa	Monocytes, macrophages, dermal dendrocytes, astrocytes, chondrocytes, oosteoblasts, osteocytes	Cytosol and extracellular matrix
Tissue transglutaminase	Chromosome 20 q11-12	Involved in cell survival, cell differentiation, matrix stabilization, cell adhesion, apoptosis, transmembrane signalling	80kDa	Ubiquitous	Cytosol, nucleus, membrane, cell surface, extracellular, mitochondria
Keratinocyte transglutaminase	Chromosome 14 q11.2	Assembly of cornified cell envelope during terminal differentiation of keratinocytes (epidermal barrier formation)	106kDa	keratinocytes	Plasma membrane, cytosol

Prostate transglutaminase	Chromosome 3 p22-p21.33	Involved in formation of rodent copulatory plug and semen coagulation	77kDa	Prostate	Extracellular, seminal plasma
TG 5	Chromosome 15 q15.2	Associated with keratinocyte differentiation, cornified envelope formation	81kDa	Female reproductive tissue, skeletal muscle, epithelial barrier lining	Cytosol
Erythrocyte-bound 4.2	Chromosome 15	Inactive as an enzyme. Function is unknown but is suggested to be essential to stabilize erythrocyte membrane integrity, involved in scaffolding.	72kDa	Erythrocyte membrane, foetal liver, spleen	Erythrocyte plasma membrane (RBCs)
TG6	Chromosome 15 q15.2	Central nervous system Development and motor function	78kDa	Skin epidermis and hair follicle	Not defined
TG7	Chromosome 15 q15.2	Not characterized	71kDa	Ubiquitous (lung/testis)	

Table 1: Members of the transglutaminase family.

1.4 Structure of transglutaminase

Cysteine, histidine and aspartate/asparagine are the three amino acids that comprise the catalytic triad, which is conserved among all active members of the transglutaminase family (with the exception of erythrocyte Band 4.2, which contains alanine in place of the active site cysteine and hence is catalytically inactive). Other conserved amino acids in the TG family are Trp²⁴¹, Trp³³² and Thr³⁶⁰ (numbered for TG2). The TG isoenzymes differ in terms of substrate specificity and how the enzyme activity is regulated. GTP acts an inhibitor for tissue (TG 2), epidermal (TG 3) and prostate (TG 4) transglutaminase. Proteolytic cleavage of the connecting loop (between the catalytic core and C-terminal barrel 1) is essential for the activity of TG 3 whereas cleavage at this site leads to inactivation of TG 2 and Factor XIIIa. (Pinkas et al., 2007)Factor XIIIa is activated by thrombin cleavage of an N-terminal inhibitory peptide.

Using TG2 as an example, the structure is organised into four distinct domains, NH₂-terminal β sandwich (aa 1-139), Core domain (aa140-454) and COOH- terminal β barrels 1 (aa 479-584) and 2 (aa 586-687). These domains are highly conserved among other members of the TG family, with keratinocyte TG and Factor XIIIa having an additional pro-peptide sequence.

Domain 1 is folded into a β structure comprising of an initial flexible loop, five tightly packed anti-parallel strands (B₂-B₆) and two additional strands B₁ and B₇.

Domain 2 or core domain contains the catalytic site and other regulatory sites. It comprises the GTP binding site involving Ser¹⁷¹ and Lys¹⁷³ on the surface, guarded by two β strands (B8 and B9) which move up and down exposing this site. The core domain also comprises four additional β strands (B₁₀-B₁₃). Apart from this, three α -

helices pointing towards the catalytic triad and one α -helix protects the Ca^{2+} binding region (Ser⁴⁴⁹, Pro⁴⁴⁶, Glu⁴⁵¹ and Glu⁴⁵²)

Domain 3 is made up of six β strands and one β turn and domain 4 made up of seven anti-parallel β strands. Domain 3 and 4 protect the core domain thus regulating exposure of the active site. When Ca^{2+} binds, the structure unfolds disturbing the connecting loop. The resulting dislocation of domains 3 and 4 exposes the active site followed by transamination reaction (Griffin et al., 2002).



Figure 1.1 Crystal structure of GDP bound (closed conformation) and inhibitor bound TG (open conformation). A) Represents the different domains of TG2 B) Closed conformation of GDO bound TG2 C) Open conformation of TG2 showing the Ca^{2+} binding sites. (Bergamini et al., 2011)

1.5 Tissue Transglutaminase (TG2)

TG2 is the most ubiquitously expressed and most extensively studied member of the TG family. Like other mammalian transglutaminases, TG2 is a calcium dependent

enzyme. TG2 is found intracellularly in the cytosol, at the cell membrane and in the nucleus and is also associated with the extracellular matrix. The primary function of TG2 is transamidation.

1.6 Structure of TG2

1.6.1 Catalytic site

The crystal structures of TG2 bound with GDP, ATP and inhibitors have supported the understanding of the multi-functionality of TG2 depending on its structure. The catalytic triad is the site of transamidating activity comprised of Cys-277, His-335 and Asp-358. The guanine nucleotide binding site is found between the catalytic core and the first β barrel domain. Tyr-516 and its loop from β -barrel domain regulate the accessibility of Cys-277 to substrates. (Liu et al., 2002) Mutation of Cys-277 to serine inactivates the transamidation function of TG2. (Mian et al., 1995) This mutation also affects the GTP/GDP binding ability and increases the tendency of the protein to remain in its open conformation. (Begg et al., 2006) During the transamidation reaction residues W241 and W332 are critically important to stabilize the intermediate form. Mutation at W241A is known to abolish the transamidating activity but does not affect the GDP/GTP binding but mutation W332F decreases its ability to bind GDP/GTP. (Murthy et al., 2002) Mutation of T360A promotes the deamination reaction of TG2 as it affects the regulation of the acyl acceptors. (Pinkas et al., 2007) Cys-277 forms hydrogen bonds with Y516 which is known to promote stability of TG2 in its closed conformation. A substitution of Y516 with phenylalanine (Y516F) promotes TG2 to its open conformation (Begg et al., 2006). (Gundemir et al., 2012)

1.6.2 Calcium binding site

Although the crystal structure of TG2 bound to calcium has not been solved, X ray crystallography has revealed FXIIIa and TG3 calcium bound structures.(Fox et al., 1999, Ahvazi et al., 2003) X ray crystallography of calcium bound FXIIIa revealed that the calcium binding pocket is 10Å from barrel1 and regulates the exposure of the active site by inducing dynamical changes along Tyr-560. It is proposed that during crystallisation, factorXIII is in its inactive form. (Fox et al., 1999) Transglutaminase 3 binds to three calcium ions responsible for stability of the enzyme and opening the channel to the active site and thereby controlling access of substrates to the active site.(Ahvazi et al., 2003) Based on structural homology and site directed mutagenesis, studies have been undertaken to predict the calcium binding sites of TG2. It is evaluated that there are 6 calcium binding sites within the catalytic domain. Apart from importance S2 and S3 calcium binding sites (similar to TG3) S4 (149 YLDSEEERQEY) and S5 (432 GRDEREDIT) are equally important. Mutations at these sites lead to a total inactivation. A “sequential mechanism” is involved in binding of calcium to TG2 that is the binding of one calcium ion promotes or triggers the binding of additional calcium ions. Mutations at site 228 VNCNDDQGV 236 prevents this additional binding of other calcium ions without altering the GTPase activity.(Király et al., 2009)

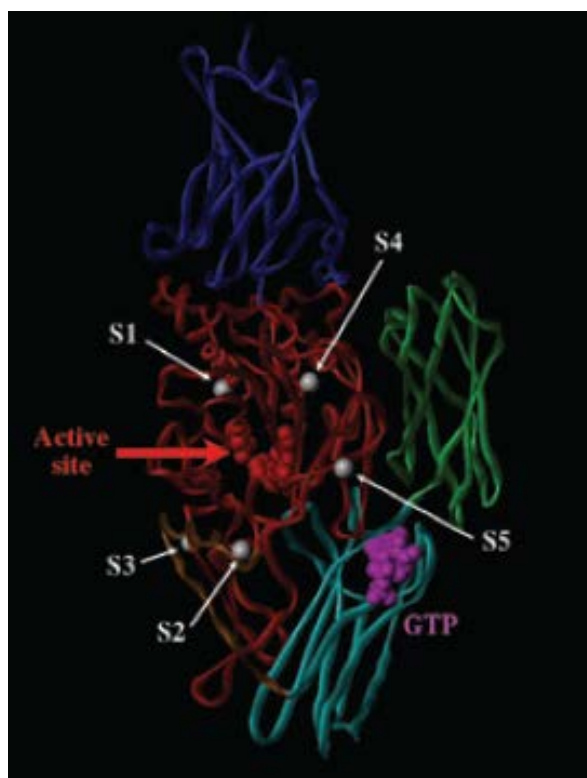


Figure 1.2 Calcium binding sites. In this figure represents the 4 domains of TG2, N-terminal (blue), core domain (red), β -barrel1 (cyan) and β -barrel2 (red). The calcium binding sites (grey), active site is represented using red spheres and bound GTP indicated by purple spheres.

1.6.3 Nucleotide pocket

The nucleotide binding pocket involving residues of the catalytic and β barrel domain is common to both GTP and ATP binding. This pocket is comprised of ten residues with Ser482 and Arg580 specifically binding guanine indicating stronger binding to TG2 and efficient inhibition of TG2 activity by GTP than ATP.(Jang et al., 2014, Han et al., 2010) A mutation R580A completely abolishes its GTP/GDP binding activity by decreasing affinity for both but has an opposite effect on GTP hydrolysis rate.(Gundemir and Johnson, 2009) Other residues like Ser171 and Lys173 play a critical role in the direct association with GTP binding.(Iismaa et al., 2000)

It has been suggested that under normal physiological conditions TG2 remains catalytically inactive intracellular (low calcium and high GTP) and extracellularly (due

to association with integrins). It remains inactive until induced upon by stress. (Siegel et al., 2008) The exact control mechanisms to support this, despite favourable conditions for TG2 activity outside the cell, still need further investigation. TG2 also has 5 intramolecular disulphide bridges which play a role in the redox state and regulation of TG2 activity. Disulphide bonds between C370 and C371 and between C370 and C230 were found to inactive the transamidating activity of TG2.(Gundemir et al., 2012)

1.6.4 Fibronectin binding site

The interaction of TG2 and fibronectin is important in cell adhesion, cell migration, matrix stabilisation and signalling. The fibronectin binding site is located in the N terminal domain and has been mapped to 88 WTATVVDQQDCTLSLQLTT 106. This is a hairpin like structure of antiparallel β strands 5 and 6 of the β sandwich domain. Amino acids site Asp94 and Asp97 are key residues of TG2 for fibronectin interaction. Mutagenesis of Asp94 or Asp97 to Ala result in reduction of fibronectin binding affinity and substitution of both with Ala leads to a further decrease in affinity. Mutation of other residues of antiparallel β strands 5 and 6 such as Cys98Ala does not affect fibronectin binding. Asp94 and Asp97 are conserved among other mammalian transglutaminases whereas Trp88 and Ala90 residues are conserved among the other seven transglutaminases. This indicates the uniqueness of TG2 with respect to its interaction with fibronectin, which is not seen with other transglutaminases.(Hang et al., 2005)

1.6.5 Heparin binding site

TG2 has a high affinity for cell surface heparin sulphate proteoglycans (HSPG) and syndecan-1 and syndecan-4 play a critical role in cell surface shedding of heparin

sulphates for translocation of TG2 into the extra cellular matrix(ECM). Mutations K205A and R209A showed a loss of binding affinity for heparin indicating that Lys-205 and Arg-209 play a direct role in high affinity binding to heparin. It is also suggested the heparin sulphate binding site of TG2 202 KFLKNAGRDCSRRSSPVYVGR 222 is essential for the translocation of TG2 to the extracellular compartment via cell surface shedding of HS. Heparin affinity chromatography showed that TG2 when in its compact GTP bound form binds with higher affinity as compared to its open conformation (inhibitor R281 treated) (Wang et al., 2012).

1.7 Localisation and cellular distribution

TG2 is predominantly present in the cytoplasm. It is also found in the mitochondria and the nucleus(Lesort et al., 1998) whereas no TG2 is detected in the endoplasmic reticulum or Golgi apparatus. TG2 is transported into the nucleus by interaction with importin $\alpha 3$ (Peng et al., 1999) and is found associated with chromatin. TG2 is involved in mitochondrial functions such as apoptosis. It also exhibits protein disulphide isomerase (PDI) activity and is involved in the assembly of respiratory chain complexes in the mitochondria.(Park et al., 2010) TG2 is also externalised both on the plasma membrane and into the ECM. Upon externalisation TG2 exhibits both enzymatic and non-enzymatic functions. It is known to cross link ECM proteins and regulates the interactions of cells with each other and the extracellular matrix. It is also associated with regulating non covalent interactions involving integrins, syndecan 4 and growth factor receptors. It also plays a role in cell survival and apoptotic responses both inside and outside the cell.

1.8 Secretion of TG2

TG2 is externalised from fibroblasts, osteoblasts, endothelial, smooth muscle cells, monocytes and macrophages and is found in the extracellular matrix. TG2 also lacks secretory signals or hydrophobic domains that direct externalisation. TG2 does not follow the conventional ER/Golgi-dependent pathway as TG2 lacks a signal peptide. A fraction of TG2 is associated with membranes. TG2 is also associated with fibronectin and heparin sulphates and these are likely to affect the retention of TG2 on the cell surface rather than its export. It was proposed earlier that TG2 is secreted as a soluble protein and then gets associated with the cell surface and ECM but now it is clear that this is not the case and it first appears on the outside of the plasma membrane and is then translocated to the ECM. A study by Zemskov et al. (2011) proposed an alternative mechanism. By using inhibitors including brefeldin and tunicamycin to block secretion via the ER/golgi pathway, they showed that TG2 was still externalised. Also the use of sodium chlorate and glyburide which inhibit unconventional secretion of FGF2 and IL-1 β respectively do not interfere with the secretion of TG2. Even the application of heat shock and copper chelator tetrathiomolybdate did not stop TG2 from being externalised. The rate of externalisation was reduced by the use of N ethylmaleimide. It is also certain that TG2 maintains its association with membranes during the secretion. The study proposed the secretion of TG2 by a vesicle-mediated route where the protein maintains its association with the intracellular membrane with the aid of Ca²⁺. Prior to externalisation, cytoplasmic TG2 first binds to phosphoinositides to be recruited to the endosomal membrane. The delivery of endosomal bound TG2 inside vesicles requires the recruitment of ATP. It then attaches to the recycling endosomal marker Rab11 in the perinuclear recycling compartment (PNRC). TG2 was also found to be

associated with $\beta 1$ integrins in the PNRC and is then delivered to the cell surface as a complex with recycled $\beta 1$ integrins. Proteins VAMP3 and SNAP23 SNARE are involved in the TG2-endosome fusion with plasma membrane. (Zemskov et al., 2011)



Figure 1.3 Secretion of cytoplasmic TG2 involving phospholipid-dependent delivery into recycling endosomes.(Belkin, 2011)

Interestingly in 2012 Wang et al, demonstrated that syndecan-4 bound TG2 in its closed conformation is deposited into the extracellular matrix by syndecan shedding. It was shown that matrix metalloproteinases, MMP-2 and MMP-9 are recruited for this deposition. TG2 deposition into the matrix was regulated by heparan sulfate shedding. It was restricted by treatment with PKC α inhibitor Go6976, upregulated by treatment with α -phorbol-12,13-didecanoate (PMA) and abolished by removal of

heparan sulfate chains. It was indicated that TG2 is retained at the cell surface associated with heparan sulphate in its compact conformation until syndecan shedding and deposition into the ECM. In the ECM, the TG2 structure opens up due to calcium. (Wang et al., 2012)



(Wang et al., 2012)

Figure 1.4 Trafficking of TG2 into the extracellular matrix via syndecan shedding. Cell surface TG2 associated with syndecan-4 is deposited into ECM by syndecan shedding. PKC α acts as an intracellular signalling molecule for activating syndecan-4 shedding. TG2 adapts to its open conformation once shed from cell surface.

1.9 Regulation of TG2 activity

It is known that under normal physiological conditions, extracellular TG2 adopts a closed conformation due to GTP inhibition and integrin binding in spite of the high calcium concentrations. In case of stress (physical or chemical injury) TG2 adopts its open active conformation. (Pinkas et al., 2007) Inside the cell TG2 functions as a G protein in phospholipase C signal transduction. (Nakaoka et al., 1994) Outside the cell TG2 plays an important role in the ECM by binding to cell surface integrins and fibronectin. (Akimov et al., 2000) TG2 is sensitive to redox changes which result in

oxidation and inactivation of TG2. The redox sensitive cysteine triad comprises of Cys-230, Cys-370 and Cys-371. Cys-370 can form disulphide bonds with either Cys-230 or Cys-371 which leads to inactivation. This disulphide bond formation is influenced by the presence of calcium which protects against formation of Cys230-Cys370 and Cys370-Cys371 disulphide bonds. (Stamnaes et al., 2009) Evidence suggests that TG2 activity is also regulated by nitric oxide. In the absence of calcium, 8 cysteine residues were nitrosylated with no disruption in TG2 activity whereas in the presence of calcium, 15 cysteine residues were nitrosylated with inhibition of TG2 activity. (Lai et al., 2001) This inhibitory regulation of TG2 by nitric oxide is reversible and affects matrix cross-linking and activation of TGF β -1, which is important in fibrogenesis and tissue scarring. (Telci et al., 2009) TG2 regulation is also affected by binding of calreticulin that down regulates both GTPase and TGase activity. (Feng et al., 1999) It was also found that at low calcium concentrations sphingosylphosphocholine (lyso-SM) was able to activate TG2 in the presence of phospholipid vesicles. Lyso-SM induces a conformational change in the protein that affects the calcium binding without affecting substrate binding ability. (Lai et al., 1997) In the cytoplasm of a healthy cell, the ATP concentration is 8-11mM, part of which may be in bound form. The GTP concentration in the cytosol of living cells is around 50-300 μ M with an estimated free GTP concentration of 100 μ M. The free Ca²⁺ concentration inside the cell is only about 100-200nM. In this state, the TG2 activity within the cytosol is inhibited (Smethurst and Griffin, 1996). The intracellular average GTP/Calcium ratio (~150 μ M/~100nM) is sufficient to keep TG2 in a relatively latent state as a transamidase (Gundemir et al., 2012). Structurally, domains 3 and 4 of TG2 are involved in this interaction where they mediate GTP and

phosphatidylinositide binding. It was also found that the Ca^{2+} binding protein calreticulin is associated with TG2 and leads to down regulation of the GTP binding.

1.10 Roles of TG2

1.10.1 GTPase

TG2 can bind and hydrolyse GTP, a function involved in signal transduction. Initial studies suggested that TG2 was implicated in signalling from $\alpha_{1B/D}$ adrenergic receptors to downstream effectors like $\delta 1$ isoform of phospholipase C (PLC $\delta 1$)(Murthy et al., 1999) GTP is known to inhibit the transamidase activity of TG2 (Achyuthan and Charles, 1987).

1.10.2 Kinase activity

TG2 also has intrinsic kinase activity. TG2 is associated with the cell membrane where it phosphorylates insulin like-growth factor- binding protein-3 (IGFBP-3), thereby enhancing the binding affinity towards IGF-1 (insulin like growth factor). Increasing the concentration of calcium leads to inhibition of kinase activity, and also promotes the cross-linking activity of TG2. The exact mechanism of this is not fully understood. Apart from IGFBP-3, TG2 has been reported to be involved in the phosphorylation of histones, retinoblastoma protein and oncoprotein p53. (Mishra and Murphy, 2004)

1.10.3 TG2: protein disulphide isomerase

TG2 has protein disulphide isomerase (PDI) activity. PDI activity is usually found in the endoplasmic reticulum where it forms disulphide bridges within polypeptides. This function is important in the folding of protein by the re-arrangement of disulphide

bonds, in order to achieve proper conformational state. It has been demonstrated that TG2 was able to catalyse the refolding of disulphide bond-scrambled RNase (inactive) by the rearrangement of disulphide bonds. The PDI and transamidation activities of TG2 are independent of each other. Also, PDI activity does not require Ca^{2+} and is not inhibited by the presence of nucleotides. It has been suggested that TG2 may function as a PDI in a moderately reducing environment as found in the cytosol. (Hasegawa et al., 2003)

1.10.4 Cell adhesion

TG2 acts as a cell adhesion protein by binding to matrix fibronectin and cell surface heparan sulphates. TG2 is localised into the extracellular matrix after cell damage and stress, where it plays an important role in matrix remodelling and stabilisation of the ECM proteins. It is also found to play an important role in integrin-mediated cell adhesion, spreading, migration, survival, differentiation, ECM (extracellular matrix) contraction, and fibronectin matrix deposition (Belkin, 2011). Various ECM proteins such as fibronectin, fibrinogen, collagen, vitronectin, osteopontin and laminin-nidogen complexes are cross-linked by cell surface TG2. TG2 interacts with the gelatin-binding domain of fibronectin, consisting of modules I₆II_{1,2}I₇₋₉, which are distinct from the integrin-binding sites on fibronectin. During cell adhesion, the $\beta 1$, $\beta 3$ and $\beta 5$ subunits of integrins interact with TG2-bound fibronectin, forming stable ternary structures. Syndecan-4 (one of the major group of cell surface heparan sulphate proteoglycans) binds to fibronectin and participates with integrin $\alpha_5\beta_1$ in focal adhesion formation and actin cytoskeleton organisation. The binding of TG2 to fibronectin and subsequent binding to heparan sulphate chains of syndecan-4 promotes RGD-independent cell adhesion. (Telci et al., 2008).

1.11 TG2 involvement in pathological and disease state

Extracellular TG2 is involved in inflammatory situations such as in wound healing, tissue fibrosis, autoimmune condition; neurodegenerative disease and cancer.

1.11.1 Wound Healing

TG2 activity is found to increase both intracellularly and extracellularly during wound healing and stabilisation. In conditions of tissue damage and cellular stress, TG2 is externalised, where it binds to fibronectin fibrils or plasma fibronectin. The ability of TG2 to form non-reducible multimers of ECM-fibronectin leads to the stabilisation of the ECM. The TG2-fibronectin complex can restore loss of cell adhesion following the inhibition of the classical fibronectin ArgGlyAsp (RGD)-dependent adhesion pathway mediated by $\alpha_5 \beta_1$ integrin receptors. TG2 also cross links collagen, leading to rapid synthesis of fibrils and formation of a stable substratum for cell adhesion (Collagen types 1 and 3). TG2 also activates TGF β_1 , thereby upregulating proliferation and synthesis of ECM. During the inflammatory phase of wound healing, an increase in TG2 activity has been reported particularly associated with macrophage adhesion and migration.(Verderio et al., 2005)

1.11.2 Neurodegenerative Disease

TG2 is found to be expressed in a number of neural cells and is suggested to be involved in the development of the nervous system. (Monsonogo et al., 1997) TG2 is involved in forebrain maturation and increased activity is observed at the start of neuronal differentiation or brain growth spurt (BGS)(Bailey and Johnson, 2004) Neurodegenerative disorders are known to be linked to disturbed calcium signalling. β -amyloid peptide is implicated in In Alzheimer's which is neurotoxic and is produced as a result of processing of amyloid precursor protein(APP). TG2 is suggested to be

involved in these disorders by facilitating the stabilisation of such toxic aggregates. It is also observed that in pathogenesis of neurodegenerative disorders like Parkinson's, Huntington's, Alzheimer's and schizophrenia demonstrate abnormalities in calcium homeostasis. (Palotas et al., 2004)

1.11.2.1 Huntington's disease is an inherited disease due to CAG repeat expansion mutation where as compared to normal population (6-35 repeats) over 40 repeats is observed in Huntington's patients. (Gusella et al., 1993) TG2 is indicated to contribute to Huntington's by inhibition of aggregate formation and promoting formation soluble protein complexes of mutant htt protein.(Michalik and Van Broeckhoven, 2003) In TG2 knockout studies it was observed that the Huntington's disease transgenic mice showed an increase in life span and improved motor dysfunction. (Ruan and Jonhson, 2007)

1.11.2.2 Parkinson's disease is the loss of neurons in the substantia nigra of the brain. These neurons regulated dopamine and a loss of these neurons develops disease state with symptoms of tremor, stiffness in muscles and slow movement. (Rascol et al., 2003) Significant amount of TG2 is detected in the membrane and cytosol extracts from substantia nigra. (Citron et al., 2002) TG2 cross links α -synuclein and facilitates formation of high molecular weight aggregates into insoluble cytoplasmic inclusions also known as Lewy bodies. This is followed by degeneration of dopamine neurons in the substantia nigra.(Andringa et al., 2004) (Ruan and Jonhson, 2007)

1.11.2.3 Alzheimer's disease is an age-related disorder involving memory loss, behaviour changes, and speech related difficulties. Alzheimer's disease is associated with the cross-linking of beta amyloid peptide to form insoluble

aggregates to form senile plaques found in the brain. TG2 is found to cross link beta-amyloid peptide to form multimers and leads to amyloid deposition and amyloidosis. (Dudek and Johnson, 1994) In the neocortex and hippocampus shows the presence of neurofibrillary tangles. Tau protein aggregates into soluble paired helical filaments and further covalently cross-linked by transglutaminase to form insoluble PHFs. (Johnson et al., 1997a)

1.11.3 Fibrosis

Tissue destruction seen with the heart, lung, liver, kidney and skin due to fibrosis is a result of excessive production of collagenous extracellular matrix and accumulation of fibroblasts. The expression of fibroblast and α -smooth muscle actin is seen by “fibroblastic loci” composed of myofibroblasts and contractile cells. It has been previously found that cytokine transforming growth factor ($\text{TGF}\beta$) is known to regulate the differentiation process of fibroblasts into myofibroblasts. (Broekelmann et al., 1991) Unlike normal physiology, these myofibroblasts fail to undergo apoptosis and the excessive deposition of collagen and fibronectin is seen in tissue. Myofibroblast survival is regulated by $\text{TGF}\beta$ and endothelin-1 via protein kinase B activation. (Kulasakaran et al., 2009) TG2 is known to contribute to fibrosis by cross-linking collagen and fibronectin in the ECM. (Verderio et al., 2004) TG2 mediated nuclear histone crosslinking is observed in liver fibrosis. Osteonectin is also a substrate of TG2 and is upregulated during fibrosis. TG2 (Grenard et al., 2001a) TG2 has also been implicated in kidney fibrosis. (Johnson et al., 1997b) An increase in TG2 expression is seen patients of idiopathic pulmonary fibrosis. Production of $\text{TGF}\beta$ in alveolar macrophages is involved in the onset of pulmonary fibrosis which in turn promotes TG2 crosslinking activity. (Olsen et al., 2011)

1.11.4 Coeliac disease

Coeliac disease is an inflammatory disorder of the small intestine due to gluten sensitivity found in wheat, barley and rye. Coeliac disease is associated with damage to the epithelial cells (IECs), destruction of small intestine villi, crypt hyperplasia and lymphocytic infiltration caused as a result of the immune response against specific gluten antigens. Coeliac disease is also marked by the development of autoantibodies (IgA and IgG) specific for tissue transglutaminase /TG2. Within the lumen of the gut, proline residues in gluten proteins cause them to be resistant to breakdown by intestinal proteases. TG2 is known to deamidate gluten fragments and convert glutamine residues to glutamate and triggering increased binding affinity to HLA-DQ2 and HLA-DQ8 (Arentz-Hansen et al., 2000). CD4⁺T cells also show preferred affinity towards deamidated peptides(Wal et al., 1998). (Jabri and Sollid, 2009) It is also suggested autoantibodies targeted against TG2 disturb angiogenesis and promote disorganisation of the actin cytoskeleton in endothelial and vascular mesenchymal cells.(Myrsky et al., 2008)

1.11.5 Cancer

The involvement of TG2 in cancer progression has further developed interest in this enzyme. The GTP binding and transamidating properties of TG2 are associated with proliferation of the malignant cells into the surrounding tissues. (Collighan and Griffin, 2009) Inflammatory responses play an important role in tumour initiation, promotion, invasion and metastasis. During tissue injury, cytokines and growth factors like TGF- β 1, TNF- α and IL-6 are secreted which induce TG2 expression. TG2 is down regulated in primary tumours which aid matrix destabilisation and thereby supporting angiogenesis and tumour invasion. TG2 is found to be up

regulated in secondary metastatic tumours. (Mehta et al., 2010) (Kotsakis and Griffin, 2007) The importance of TG2 is seen in various stages of tumour progression. Intracellular TG2 is observed to act as a pro-apoptotic factor through the cross-linking of intracellular proteins such as pRB, and also anti-apoptotic signals by activating the NF kappa B pathway (Mann et al., 2006). Extracellular TG2 interacts with fibronectin via integrins involved in cell survival by inducing anti-apoptotic protein Bcl-2. TG2 also binds to fibronectin through an RGD independent pathway via syndecan 4 thereby rescuing the cells from cell death. (Collighan and Griffin, 2009, Kotsakis and Griffin, 2007) Depending on the ECM composition the cell surface TG2 favours or opposes cell migration. The over-expression of MT-MMPs (membrane type matrix metalloproteinases) results in degradation of TG2, thereby suppressing cell adhesion and locomotion on fibronectin, whereas fibronectin protected cell surface TG2 from MT1-MMP digestion, promoting cell adhesion and locomotion (Belkin et al., 2001) (Collighan and Griffin, 2009).

1.12 TG2 inhibitors

The implication of TG2 in various diseases has led to development of peptidomimetic TG2 inhibitors. Depending on their mode of inhibition TG2 inhibitors are classified as competitive amine inhibitors, reversible inhibitors and irreversible inhibitors.

1.12.1 Competitive amine inhibitors

These inhibitors compete with natural amine substrates. In the presence of competitive inhibitors TG2 proceeds with its transamidation reactions but the isopeptide bond formed is between the glutamine substrate and the introduced amine inhibitors rather than its natural lysine residue. Some examples of such inhibitors include putrescine, monodansylcadaverine, 5-(biotinamido)pentylamine and 2-

mercaptoethylamine. These inhibitors are commercially accessible, found to be non toxic to cells and chemically stable.(Siegel and Khosla, 2007)

1.12.2 Reversible inhibitors

TG2 cofactors, GTP, GDP and Zn^{2+} are known to act as reversible inhibitors by hindering the access to the enzyme active site without any covalent modifications. (Lai et al., 1998) Similarly allosteric inhibitors having a thieno [2,3-d]pyrimidin-4-one acylhydrazide backbone are slow-binding competitive inhibitors that target the GTP binding site. (Duval et al., 2005, Case and Stein, 2007)

1.12.3 Irreversible inhibitors

This class of inhibitors tend to target the active site and result in covalent modification of TG2 thereby preventing the binding of substrates. This includes inhibitors like iodoacetamide, 3-halo-4,5-dihydroisoxazoles and 6-diazo-5-oxo-norleucine (DON) (Siegel and Khosla, 2007).

Griffin et al demonstrated the synthesis of cell permeable TG2 inhibitors R283 and cell impermeable inhibitors R294 and R281 that interfere with TG2 transamidation reaction by targeting the cysteine of the active site (Griffin et al., 2008).

1.13 FRET (Förster Resonance Energy Transfer)

In order to investigate the involvement of proteins in a disease state and develop drug targets it is critical to address fundamental questions like the structure of the protein, its expression and regulation, its dynamic interaction with other biomolecules, its localisation and its potential role within a cell. To answer these

questions some approaches include structural studies (e.g. X ray crystallography, NMR spectroscopy) expression proteomics (e.g. immunoassays, mass spectroscopy) and functional analysis (enzyme kinetics studies, development of fusion protein). The dynamic interaction of proteins and protein regulation that are implicated in human diseases can be analysed using different approaches. Förster Resonance Energy Transfer (FRET) also referred to as Fluorescence Resonance Energy Transfer permits the study of interactions between molecules in proximity, beyond the scope of light microscopic resolution. FRET can be used as a tool to visualize reactions in live cells that have the potential to give a better understanding to address these questions. This allows us to derive information of a protein and its interactions that best represents the actual reactions happening within the cell as compared to in-vitro methods. There are few alternate methods to study protein interactions that involve direct detection of interactions. For example, co-precipitation requires the removal of the proteins from their normal cellular environment. Proteins may behave differently once extracted from their natural environment and in turn affect analysis. Other limitations include fixing of cells (which restrains dynamic measurements of live cells), spatial resolution limits (diffraction limit of conventional optical microscopy) and lack of precise labelling strategies. These limitations can be overcome using FRET. It is also worth considering FRET before getting into animal testing and clinical trials as it provides cheaper and faster method to address some questions if not all regarding the pathogenesis of a disease at protein level. (Piston and Kremers, 2007) FRET provides another approach to analyse the regulation of TG2 via its large conformation change induced by calcium and GTP binding. FRET would also allow the titration of the calcium and GTP to observe this conformational change of TG2 that is critical for its regulation. This in turn could help bridge the

understanding as to how TG2 is implicated in various diseases and help in the development of better drug targets. FRET is the non-radiative transfer of electronic excitation energy between a pair of fluorophores, i.e. a fluorescent donor and acceptor molecule separated by a distance of 10 to 100Å (inter-chromophoric distance). FRET imaging microscopy not only enables us to visually localise the fluorescent protein within a living cell but also allows measurement of changes in FRET corresponding to cellular events at a millisecond time resolution. When two fluorophores are sufficiently close, such that the emission spectrum of the donor overlaps the excitation spectrum of the acceptor, energy flows via dipole-dipole coupling (resonance) from one molecule to another leading to a FRET signal (Wang and Wang, 2009). In other words this transfer of energy is reflective of the reduction of fluorescence intensity of the donor, a decrement in its excited state lifetime and in the presence of a fluorescent acceptor, a 're-emission' at its respective wavelength.(Heim and Tsein, 1996) FRET-based imaging microscopy can be used as a sensitive probe of protein-protein interactions and protein conformational changes *in vivo*. Real time *in vivo* imaging of dynamic molecular events provides a crucial insight into biological mechanisms as well as physiological functions of the cell. (Truong and Ikura, 2001) To construct a FRET based biosensor the gene of a bioluminescent protein is fused with that of a target molecule such that the resultant recombinant protein emits fluorescence reflecting the target protein and its interactions.(Wang and Wang, 2009)

1.13.1 Green fluorescent protein

Green fluorescent protein (GFP) is a protein that was first purified with another bioluminescent protein, aequorin, obtained from *Aequorea Victoria* jellyfish

(Shimomura et al., 1962). The major advances of GFP and its applications have been indicated in Figure 1.5 with columns indicating the number the scientific articles. GFP can be expressed in a variety of cells emitting fluorescence without being associated with a cofactor. A biosensor constructed incorporating GFP is known to retain the fluorescent properties of the GFP and the biochemical function of the original host. On addition of an appropriate signal peptide this GFP fused recombinant protein can be targeted to specific organelles. Lately many GFP mutants have been produced having different spectral properties, which can be used as donors and acceptors in the construction of a FRET based biosensor. (Truong and Ikura, 2001). In 1994 Martin Chalfie *et al* expressed GFP in *E.coli* using a T7 promoter system and discovered it fluoresced. Bacterial cells were grown in the presence of inducer isopropyl- β -D-thiogalactoside (IPTG) and were detected under a ultraviolet (UV) source. Previous methods to study gene expression and protein distribution were dependent on the introduction of exogenous substrates or cofactors whereas use of GFP is autonomous. It can also be used as a marker of transformation as it not found to hamper cell growth or function. (Chalfie et al., 1994) The use of GFP to tag proteins was made possible in living cells with the discovery of GFP and the principle that it preserved its fluorescent properties when produced in living organisms. Advances have been made to use fluorescent proteins as indicators of biological events. The use of organic dye labels to investigate FRET for cyclic AMP (cAMP) mediated pathways was implemented by Roger Tsien in 1991 (Adams et al., 1991). However organic dyes were substituted by genetically encoded fluorescent proteins due to difficulties with covalent labelling and cellular injection of organic dyes. The introduction of GFP as a tool for FRET studies launched the need to engineer new fluorescent proteins with enhanced characteristics. Advances have

been made to develop new fluorescent proteins emitting light from blue to red range of visible spectrum. GFP has been known to impact other biophysical fluorescence methods including fluorescence correlation spectroscopy (FCS), fluorescence cross-relation spectroscopy (FCCS), fluorescence recovery after photo-bleaching (FRAP) which can be applied to investigate intracellular events. GFP also contributes to techniques like fluorescence life-time imaging (FLIM), high-resolution photo-activation localisation microscopy (PALM). Cloning target protein that is labelled with fluorescent proteins has provided an innovative tool for studies related in cell biology, physiology and medicine. (Day and Davidson, 2012)



Figure 1.5 Timeline of major developments of GFP (Chudakov et al., 2010)

1.13.2 Crystal Structure of GFP

Wild type GFP has a size of 238-aa (25kDa). The chromophore of GFP, *p*-hydroxybenzylideneimidazolinone, is well protected by 11 β -barrel strands (Figure 1.6 - represented in green), making the molecule stable at physiological environment

of living organisms resistant to detergents, organic solvents and proteases (Ward and Bokman, 1982). The internal irregular helix of chromophore is well guarded by the β strands and threaded by an α helix (represented in red) that form a cylinder like structure extending about 42Å long and 24Å in diameter. The placement of the chromophore contributes to the high quantum yield of fluorescence; small Stoke's shift and inability of O₂ to quench the excited state. The key amino acids Ser⁶⁵ – Tyr⁶⁶-Gly⁶⁷ undergo conformational changes to form a mature chromophore by 'internal cyclization' and 1,2-dehydrogenation of the Tyr. (Wang and Wang, 2009) GFP absorbs blue light at 395nm and a small peak at 475nm (ionised chromophore) and emits green light at 508nm (Brejc et al., 1997).



(Brejc et al., 1997)

Figure 1.6 Structure of monomeric WT GFP. The compact 11 β strands forming a cylinder like structure as shown in green, the α -helices shown in red and the ball-and stick model indicating the chromophore (Brejc et al., 1997).

1.13.3 GFP mutants

There is a diverse range of available fluorescent proteins extending nearly the entire visible spectrum (Table 2) providing exclusive markers to simultaneously examine multiple cellular events and they can be used as donor: acceptor FRET pairs (Heim and Tsein, 1996). GFP based proteins are designed to be structurally stable and relatively inert.



Table 2 Wide range of fluorescent proteins available.
Selected dimeric and tetrameric FPs indication T, tetrameric; D, dimeric; B-, low brightness; Ps-, low photostability; pH-, low pH stability; Ag-, aggregation; Ps+, high photostability; pH+, high pH stability; mat+, fast maturation; B+, high brightness.(Chudakov et al., 2010)

Given the wide options of fluorescent proteins; some basic requirements for successful application for imaging experiments includes the efficient expression of the protein in the appropriate system, its signal should be bright enough for detection and should not oligomerize when co-expressed with protein of interest. The mutant of GFP used should be photostable and when used in association with each other

should have minimal crosstalk in their excitation and emission spectra. Generally fluorescent proteins are optimised for expression in mammalian cells but some proteins may differ in their efficiency of folding and maturation. Expression of fluorescent proteins in bacterial cells does give a good indication of the efficiency of a system. Bacterial cell expression of fluorescent proteins helps in early determination of potential folding inefficiencies and provides useful information on notable variations between different expression systems (Shaner et al., 2005).

1.14 Classification of GFPs

On the basis of chromophores GFP variants can be classified into seven different classes:

Class 1 wild type mixture of neutral phenol and anionic phenolate having two chemically distinct species one having major excitation peak at 395nm, emission peak at 508nm and second minor peak at 475nm, emission at 503nm. Even though this class can be visualised by exposure to UV using a blocking filter, scattering, autofluorescence and tissue damage provides an inconvenience. Excitation at 470nm would certainly be preferable in this case but anionic chromophore comprises only 15% of the total chromophores.

Class 2 GFP proteins have phenolate anions in the chromophore such as Ser65Thr mutant having enhanced brightness and having excitation peak at 489nm and emission peak at 511nm. This class of mutants fold efficiently when expressed at room temperature and below.

Class 3 or neutral phenol having excitation peak at 399nm and emission at 511nm having a large Stokes' shift.

Class 4 or phenolate anion with stacked π electron system have the longest wavelengths as His, Trp, Phe and Tyr residues at position 203 increase excitation to 516nm and emission 529nm. They are also called as yellow fluorescent proteins.

Class 5 or indole chromophores derived by Tyr66Trp having indole instead of phenol having excitation and emission wavelengths at 436nm and 476nm. They are also referred to as cyan fluorescent proteins due to their blue emission.

Imidazole chromophores or Class 6 are derived by substitution of Tyr66His and introducing an imidazole ring, having 383nm excitation and 447nm emission. This class is also called blue fluorescent proteins and has disadvantages like low quantum yield, high bleaching susceptibility.

Class 7 or phenyl chromophore or Tyr66Phe have very little applications due to such short wavelength which excitation at 360nm and emission at 442nm. (Tsein, 1998)

One of the most promising FRET pairs derived from mutagenesis of GFP is CFP (cyan fluorescent protein) and YFP (yellow fluorescent protein) because of the high quantum yield and enhanced photostability. CFP and YFP refer to the generic class of cyan and yellow mutants. CFP is a Tyr66Trp (figure 1.7) mutant of GFP which creates an excitation peak of 436nm and an emission peak 476nm. YFP was designed by introducing a Thr203Tyr (figure1.7) mutation in GFP which results in a π - π stacking interaction between Tyr²⁰³ and Tyr⁶⁶ creating excitation and emission peaks of 516nm and 529nm respectively. This CFP-YFP pair allows FRET to be detected at larger distances as compared to other FRET FP (fluorescent protein) pairs.



Figure 1.7 Chromophore structures of CFP and YFP (Shaner et al., 2007)

1.15 Intra-molecular FRET

When both the donor chromophore and acceptor chromophore are fused on the same host molecule which undergoes transition between open and closed conformations, intramolecular FRET is known to occur. The efficiency of FRET is dependent on the relative orientation and distance between the donor and acceptor chromophores. (Li et al., 2006) A larger FRET signal is generated when both the chromophore are oriented parallel to each other and shorter the distance between them.



(Kevin and Mitsuhiro, 2001)

Figure 1.8 Intramolecular FRET. Both donor and acceptor chromophores are present on same host molecule.

1.16 Inter-molecular FRET

FRET biosensors created by the fusion of donor and acceptor fluorescent proteins on two separate interacting proteins, inter-molecular FRET is known to occur. When these two fusion proteins interact the fluorescent proteins are brought closer together and create an inter-molecular signal. Such biosensors have been used to study protein associations for example the interaction of G protein coupled receptors (GPCR) with G proteins. (Li et al., 2006)



(Kevin and Mitsuhiro, 2001)

Figure 1.9 Intermolecular FRET. Both donor and acceptor chromophores are fused on different macromolecules. When protein A and protein B interact, FRET occurs, when they dissociate FRET diminishes.

1.17 Mechanism of FRET

There are three basic requirements for FRET to work efficiently. These include separation distance, angular dependence and spectral overlap. Since FRET involves dipole dipole interactions the efficiency of energy transfer varies as the inverse of the sixth power of the distance that separates the fluorescent molecules. In other words the FRET efficiency decreases rapidly with an increase in the separation distance.

The second requirement is the angular dependence where the efficiency is dependent on the favourable alignment of the electromagnetic dipoles of the donor emission and acceptor absorption. This angular dependence of the dipole interactions is denoted by orientation factor k^2 . Depending on the orientation value of k^2 from 0 to 4. Although it is difficult to measure k^2 in most experiments the orientations of the fluorescent protein tags randomize over the time-scale measurements. k^2 is often assumed to be two thirds. Lastly the spectral overlap is a basic requirement such that the fluorophores must share a strong overlap between the donor emission spectrum and the absorption spectrum of the acceptor. CFP and YFP are often used due to the large spectral overlap. However this also generates background fluorescence that is detected in the acceptor emission channel. This is due to the direct excitation of the acceptor by donor excitation wavelengths and donor emission signal that bleeds into the FRET detection channel. (Day and Davidson, 2012)

1.18 FRET quantification techniques

FRET can be measured either by the increase of the acceptor fluorescent emission or the decrease of the donor fluorescent emission. Apart from intensity based techniques there are other methods of measuring FRET too. Some of the commonly used techniques include

1.18.1 Donor de-quenching

This technique involves the use of photobleaching to destroy the acceptor and then measuring the increase in fluorescence intensity of the donor. Due to the absence of the acceptor the energy transfer between the donor and acceptor can no longer occur and thereby FRET can be measured as an increase in the donor emission.

The photobleaching process is irreversible hence measurements can be taken just once from a sample. The difference in fluorescence intensity of the donor pre and post photobleaching can be used to measure FRET directly as

$$\text{FRET}_{\text{eff}} = (D_{\text{post}} - D_{\text{pre}})/D_{\text{post}}$$

Where D_{post} is the fluorescence intensity of the donor after photobleaching and D_{pre} is the fluorescence intensity of the donor before photobleaching. (Lieca, 2007)

1.18.2 Acceptor enhanced emission

Instead of measuring the decrease in fluorescence of the donor, an increase in fluorescence of the acceptor is measured during FRET as the donor fluorophore transfers energy to the acceptor fluorophore. In this method contamination due to cross talk and bleed through are calculated separately from acceptor only and donor only samples. These contaminating values are then subtracted from the total fluorescent signal measured from the donor plus acceptor samples.

1.18.3 Donor acceptor emission peak ratio

This method involves the comparison of donor acceptor peak fluorescence ratios with and without FRET.(Miyawaki and Tsein, 2000) As FRET occurs the fluorescence intensity of the donor will decrease and that of the acceptor will increase. The ratio between the acceptor intensity over the donor intensity before FRET will be smaller than the ratio during FRET. This is a good method for measuring changes at a distance as measurement of this ratio can be quickly determined at the emission peak of each fluorophore.

1.19 FRET measurement

To experimentally measure efficiency (E). FRET, the differential decrease or increase of the donor and acceptor intensity respectively is determined.

$$E^{app} = (DA / D+DA) \times E$$

Where E^{app} is the apparent FRET efficiency of the system,

DA is the concentration of donor-acceptor pair

D is the concentration of free donor and

A is the concentration of free acceptor

Likewise FRET can be measured also by the increase in acceptor emission

$$E^{app} = (DA / A+DA) \times E$$

1.20 Potential problems in FRET experiments

1.20.1 Measurement difficulties

It is worth noting that FRET measurements are usually based on certain assumptions. For example, re-absorption of donor fluorescence by the acceptor is considered to be negligible using mutants with low fluorophore densities. Contamination due to “background light” must also be considered and subtracted from calculation by setting a control blank region for measurement. Some common contaminating factors include cross talk.

While analysing FRET it is observed that the donor emission spectrum overlaps the acceptor excitation spectrum. But the excitation spectrum overlap or emission spectrum overall is to an extent unavoidable and unfavourable as the smaller Stoke's shift and FRET pair getting excited by the same excitation light to different levels. This is referred to as cross talk and commonly observed as the direct excitation of the acceptor by donor excitation light.

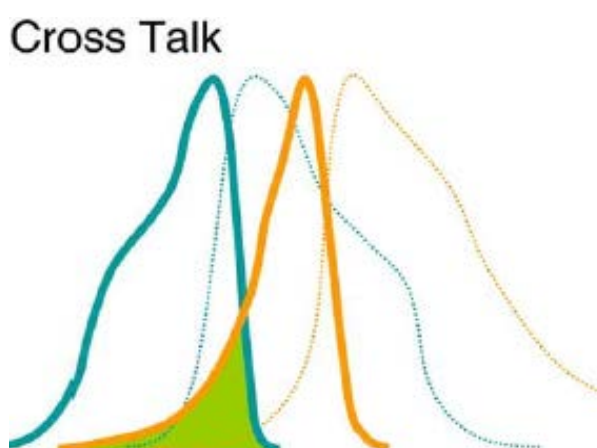


Figure 1.10 Cross-talk. Spectra of donor (blue) and acceptor (yellow) fluorophores are superimposed. Solid lines represent excitation spectra and dotted lines represent emission spectra. The overlap between donor and acceptor excitation spectra indicated by shaded area representing cross-talk.

Cross talk can be determined by comparing the fluorescence intensities of an acceptor only sample excited using donor excitation light.

Another essential consideration is “bleed-through” which is the overlapping of emission spectrums of donor and acceptor. This is where fluorescence emission of the donor fluorophore overlaps the emission range of the acceptor.

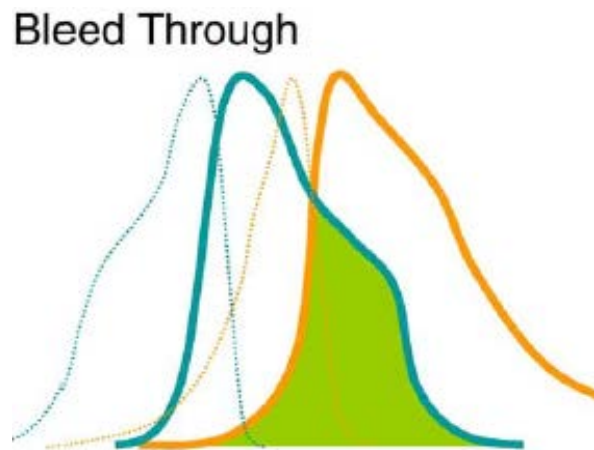


Figure 1.11 Bleed-through Spectra of donor (blue) and acceptor (yellow) fluorophores are superimposed. Excitation spectra shown as dotted curve and emission spectra shown as solid curve. The shaded area representing donor bleed-through emissions in the acceptor range.

Bleed through is estimated by analysing the emission range of the donor. (Takanishi et al., 2006)

1.20.2 Problems with construction and validation of fusion proteins

An interesting study conducted to study the effect of calcium binding to calmodulin, which causes subsequent binding of calmodulin to other proteins. In this study calmodulin-M13 peptide was fused with fluorescent proteins BFP and mutant S65T. The construct was expressed in bacteria and FRET analysed. A variety of mutations such as deletion, insertions and amino acids substitutions were analysed for fluorescence. It was discovered that many variants of the wild-type construct showed improper folding resulting in abolishment of fluorescence, possibly being proteolysed in bacteria or during the purification process. It was noted that trial and error was adopted to obtain fusions that express well and to avoid precipitation or proteolysis. (Miyawaki and Tsein, 2000) Further analysis of intact mutants response to calcium revealed dramatic differences in FRET efficiency due to single amino

acid substitutions. Uncertainty whether fusing two fluorescent proteins rigidly without the extra spacers at boundaries or introduction of Gly-Gly spacers, showed the construct without spacers to have improved FRET efficiency. Measuring FRET directly from bacterial colonies, in this case, by soaking with calcium followed by EGTA in presence of calcium ionophore was performed. The drawback of this method was the dependency of signal on size of colony, uncertainty of exposure of proteins to reagents and misfolding and/or proteolysis inside bacteria. Fluorescence activated cell sorting could not be applicable in this case for comparing changes in fluorescence in response to calcium. (Miyawaki and Tsein, 2000)

AIMS

The main objective of this project is to construct a FRET TG2 biosensor from which a better understanding about the conformation of TG2 in both solution and cell systems can be examined. To analyse this conformational change with respect to binding of TG2 to calcium and GTP suitable fluorescent proteins would be fused on the N and C termini of TG2. This construct will be further analysed for activity and it was proposed to characterise fluorescence changes depending on the conformation.

In order to do this, the following tasks were planned:

- Construction of a TG2 FRET sensor by PCR and cloning methods.
Suitable primers would be designed to PCR amplify the fluorescent protein genes allowing assembly of the fusion in a bacterial expression vector.
- The TG2 FRET sensor would be affinity purified using the bacterial expression system and characterised in terms of TG2 activity and regulation by Ca^{2+} and GTP.
- The ability to bind to fibronectin, heparan sulphate proteoglycans and ability to act as a mammalian cell adhesion protein would also be assessed using simple binding assays.
- Characterisation of the fluorescent properties of the purified TG2 fusion with respect to alterations in FRET due to conformational changes.
- TG2 fusions would also be attempted be subcloned into a mammalian expression plasmid

Chapter 2

Material and Methods

2. METHODS

2.1 Media Recipe

2.1.1 LB Broth

1 % (w/v) Tryptone (Melford, UK), 0.5 % (w/v) Yeast Extract (Oxoid, UK), 1 % (w/v) Sodium Chloride (Sigma Aldrich, UK)

2.1.2 LB Agar

1% (w/v) Tryptone (Melford, UK), 0.5% (w/v) Yeast Extract (Oxoid, UK), 1% (w/v) Sodium Chloride (Sigma Aldrich, UK), 2% (w/v) Granulated Agar (Melford, UK)

LB broth and LB Agar were autoclaved at 121°C for 20 minutes. Media was then cooled to below 50°C and antibiotic such as Ampicillin (final concentration 100 µg/ml) or Kanamycin (final concentration 30 µg/ml) were added.

2.2 Buffer Recipes

2.2.1 Tris Acetate EDTA (TAE) buffer

1x TAE buffer was prepared using Melford, UK 10 x stock solution (0.4M Tris, 0.1M Acetate, 0.01M EDTA pH8.2) by dilution with deionised water.

2.2.2 6x DNA loading buffer

DNA loading buffer was prepared using 30% (v/v) glycerol, 0.25% (w/v) bromophenol blue and 0.25% (w/v) Xylene cyanol. Aliquots were made and stored at -20°C.

2.2.3 Laemmli Buffer

125mM Tris-HCl, pH6.8, 20% (v/v) glycerol, 4% (w/v) SDS, 10% (v/v) 2- β -mercaptoethanol and 0.004% (w/v) bromophenol blue)

2.2.4 Cracking buffer

Cracking buffer (2X) was freshly prepared using 5M NaOH, 10% (w/v) SDS and 10g sucrose, deionised water for final volume of 50ml.

2.2.5 Coomassie Blue stain

0.05% (w/v) Coomassie Brilliant Blue R-250 (Thermo Scientific, UK) was dissolved in 50% (v/v) methanol (Fisher Scientific), 10% (v/v) acetic acid (Fisher Scientific, UK).

2.2.6 SDS electrode running buffer

Tris glycine running buffer was prepared using 25mM Tris, 192mM glycine, 0.1%(w/v) SDS

2.2.7 SDS transfer buffer

SDS transfer buffer pH9.7 was prepared using 48.8mM Tris, 39mM glycine and 20% (v/v) methanol

2.3 10x dNTPs

100mM of dTTP, 100mM of dGTP, 100mM of dATP and 100mM of dCTP were introduced into sterile nuclease free water. Appropriate aliquots were made and stored at -20°C.

2.4 SDS polyacrylamide Gel

Separating gel (10%w/v) pH 8.8 was prepared using 0.75M Tris, 0.2% (w/v) SDS stock solution. Stacking gel (3%w/v) pH 6.8 was prepared using 0.2M Tris, 0.2% (w/v) SDS stock solution. Polymerisation was initiated by addition of 10% (w/v) ammonium persulphate (freshly prepared) and 10 µL N,N,N',N'-Tetramethylethylenediamine (TEMED)

2.5 General chemicals

Recombinant human tissue transglutaminase (insect cells) was obtained from Zedira. Cub7402 antimouse monoclonal was purchased from Thermo Fisher. ID10 and TG2 inhibitors were a kind gift from Dr. Collighan, Aston University.

2.6 Primers

Primers were designed using Primerselect software (Lasergene, DNASTar) and obtained from Sigma, UK.

Primer sequences

- Forward primer for Cyan Fluorescent Protein/CFP (CFP For3)

5' **A G A T C T** A A T G G C C C T G T C C A A C A A G 3'
BglII

- Reverse primer for Cyan Fluorescent Protein/CFP (CFP Rev3)

5' **G G A T C C** C C G A A G G G C A C C A C G G A G G 3'
BamHI

- Forward primer for Yellow Fluorescent Protein/YFP (YFP For2)

5' **G A A T T C** T A T G G C C A C A A G C A A G C A C G G C 3'

EcoRI

- Reverse primer for Yellow Fluorescent Protein/YFP (YFP Rev2)

5' **A A G A T T C** A G G A C A G G G C G C T G G G G A A G 3'

HindIII

- Forward primer for TG2 (TG2 For)

5' **A G A T C T C** A A T G G C C G A G G A G C T G G T C T T A G 3'

BglII

- Reverse primer for TG2 (TG2 Rev)

5' **G A A T T C** C C G G C G G G G C C A A T G A T G A C A T T C 3'

EcoRI

- Forward primer for CFP-TG2-YFP (NotICFP)

5' **G C G G C C G C** A C C A T G G C C C T G T C C A A C A A 3'

NotI

- Forward primer for His-tag pTrcHisB-CFP-TG2-YFP (HispTrc)



Sequencing primers

- sp6 sequencing primer



- T7 Pro sequencing primer



2.7 General Techniques

2.7.1 Preparation of competent cells using calcium chloride

5ml of LB broth with Rosetta 2(DE3) or DH5α cells were grown overnight at 37°C using a benchtop orbital shaker. For inoculation, 1ml of this overnight grown culture was added to 100ml of LB broth and incubated at 37°C for about 4 hour (approximately 0.4 OD at 600nm). Cells were pelleted by centrifugation at 5000 rpm at 4°C for 10 min. Cell media was discarded and cell pellet was gently resuspended in ¼ volume of ice-cold 100mM MgCl₂ taking at least 3 to 5 min for this step. Cell suspension was centrifuged at 4000 rpm at 4°C for 10min. The cell pellet was resuspended in 1/20 volume of ice cold 100mM CaCl₂. Then 9/20 volume of ice cold 100mM CaCl₂ was added to the cell suspension and placed on ice for 20 min. The

cell suspension was then centrifuged at 4000 rpm at 4°C for 10 min. the cell pellet was resuspended in 1/50 volume of sterile ice cold 85mM CaCl₂, 15% glycerol w/v. For long term storage, aliquots of 100µL of this cell suspension were made into sterile 1.5mL microcentrifuge tubes and stored at -80°C.

2.7.2 Transformation

Transformation was carried out using heat-shock method. Agar plates with appropriate antibiotic (Ampicillin final concentration 100 µg/ml or Kanamycin final concentration 30µg/ml) were freshly prepared to carry out transformation. 100µL aliquots of Rosetta 2/DH5α cells (made competent using CaCl₂ method) were removed from -80°C and immediately placed on ice to thaw ice for approximately 5-10 min. 5µL of plasmid DNA was added to competent cells and gently mixed by flicking the bottom of centrifuge tube a few times. The same was done for positive control using control plasmid to ensure transformation efficiency. The mixture was incubated on ice for 20 min. Heat shock was performed at 42°C for 45sec using a water bath. The cells were immediately placed back on ice for 5 min. After incubation on ice, 900µL of LB medium or SOC medium was introduced into the transformation reaction and placed for 60min in a shaking incubator (225 rpm) at 37°C. Approximately 15min before plating, agar plates were kept inverted at 37°C in an incubator. Using a sterile spreader, 20µL of transformation reaction was evenly distributed onto an agar plate containing appropriate antibiotic for selection. Remaining reaction was similarly spread onto a plate. The plates were then placed inverted in an incubator overnight at 37°C.

Using Novablue competent cells, transformation was carried out according to manufacturer's instructions.

2.7.3 Blue White screening procedure

For blue white screening of recombinants the above transformation was followed. After heat shock and cooling on ice, SOC/LB medium was introduced to the competent cells. The ampicillin agar plates also included IPTG and X gal. 50mg/ml X-gal in dimethyl formamide and 100mM IPTG in water were spread and allowed to soak on ampicillin plates 30 min prior to plating cells.

2.7.4 Cracking procedure

Cracking procedure was carried out for screening bacterial colonies and for rapid analysis of plasmid. After transformation, individual colonies were streaked onto a freshly prepared agar plate with appropriate antibiotic and grown overnight at 37°C in an incubator. 50µL of 10mM EDTA, pH 8.0 was dispensed into a sterile 1.5ml eppendorf tubes. Using sterile pipet tips individual colonies were picked and smeared into the microcentrifuge tubes. Freshly prepared 2X cracking buffer (50µL) was used to resuspend the cells by vortexing. The samples were then heated at 70°C using a waterbath for approximately 5min. After cooling to room temperature, samples were mixed with 1.5µL of 4M KCl and 0.5µL of 0.4% bromophenol blue. The samples were incubated on ice for 5min. Samples were then centrifuged at 16,000 x g using a benchtop refrigerated centrifuge for 3min at 4°C. Carefully avoiding the precipitate, 20µL of the supernatant was run on a 1% agarose gel to rapidly estimate plasmid size. Appropriate colonies were further grown for plasmid preparation and restriction digestion analysis.

2.7.5 Plasmid preparation

A single colony of bacteria was grown overnight in LB medium containing antibiotic at 37°C using a benchtop orbital shaker. Plasmid was purified using Promega

Wizard Plus minipreps DNA purification kit. The centrifugation protocol was followed according to manufacturer's instructions. The eluted DNA was stored at -20°C for subsequent use.

2.7.6 Phenol Chloroform Extraction of DNA

An equal volume of Phenol:Chloroform:Isoamyl alcohol pH 8.05 (25:24:1) was added to DNA solution very carefully. The mixture was vortexed and a milky white suspension was observed due to denaturing of proteins into the hydrophobic phase. This was followed by centrifugation at 12,000 x g for 5 min at room temperature. Three distinct phases were observed after centrifugation, top aqueous layer containing DNA of interest, a disc-like interface of denatured proteins and bottom organic layer of lipids. Using a pipette the top aqueous layer was removed into a fresh centrifuge tube. Care was taken to avoid pipetting the interface layer along with aqueous layer. This step was repeated to remove any residual protein until no visible interface phase was observed. To the recovered aqueous phase equal part of Chloroform:Isoamyl alcohol (24:1) was mixed to remove residual phenol. Centrifugation was repeated at 12,000 x g for 5 min at room temperature. The top aqueous layer was removed into a fresh centrifuge tube for further processing.

2.7.7 Isopropanol precipitation

To the DNA sample, $1/10^{\text{th}}$ volume of 3M sodium acetate (pH 5.2) was added. To this 1 x volume of ice cold isopropanol (100%) was added. The mixture was placed at -20°C for 15 min to allow precipitation. To pellet the DNA, the mixture was centrifuged at 4°C at 12,000 x g for 5 min. The supernatant was decanted gently without disturbing the pellet. The pellet was then washed with 1ml 70% ice cold ethanol very gently by slowly inverting the tube. This was followed by centrifuging at

4°C at 12,000 x g for 2 min. The supernatant was decanted and the wash with 70% ethanol was repeated. After decanting the supernatant the pellet was air dried. The DNA pellet was resuspended in nuclease free water by vortexing and stored at -20°C for further use.

2.7.8 Ethanol precipitation

DNA was precipitated by adding 1/10th volume of 3M sodium acetate (pH 5.2) and 2 x volume of ice cold absolute ethanol. The mixture was vortexed and placed on ice for 30 min. To pellet the DNA the mixture was centrifuged at 4°C at 12, 000 x g for 15min. The supernatant was gently discarded without dislodging the pellet. The pellet was further processed by washing with 70% ice-cold ethanol. After centrifuging at 4°C at 12,000 x g for 2 min, the supernatant was discarded. This wash with ethanol was repeated. The pellet was air dried and resuspended in nuclease free water.

2.7.9 Agarose gel electrophoresis

2.7.9.1 Agarose gel

Agarose gels (1% w/v) were prepared using Molecular Biology Grade-High gel strength agarose by Melford and run using 1x TAE buffer. Agarose was melted in its appropriate gel mixture by heating for 1min and cooled by running under cold water. Ethidium bromide (final concentration 0.2µg/ml) was introduced to the cooled gel before pouring into the gel tray. The gel was incubated for about 20min for solidification at room temperature. DNA samples were loaded using 6x DNA loading buffer. Novagen perfect DNA marker 0.05-10Kb (or NEB 2-log DNA ladder 0.1-10.0 kb) was loaded to determine the size of DNA fragment. The agarose gel was run at

100V for about 40min. DNA was visualised using Syngene G:Box Chemi Fluorescent and Chemiluminescent imaging system.

2.7.9.2 Agarose gel purification (Low melting point gel)

Agarose gels (1.5% w/v) were prepared using Melford low melting point agarose and run using 1 x TAE buffer. Ethidium bromide (final concentration 0.2 µg/ml) was added to the cooled gel before pouring into the gel tray. The gel was solidified at room temperature for 20 min and kept at 4°C for 30min. DNA samples were loaded using 6x loading buffer and Novagen perfect DNA marker 0.05-10Kb was the preferred DNA marker. The low melting point gel was run at 75v over 60min. Using Syngene G:Box Chemi Fluorescent and Chemiluminescent imaging system the DNA fragments were visualised. DNA fragment of interest was excised using sterile scalpel blades and weighed into a microcentrifuge tube. Using Promega SV gel and PCR Clean Up kit DNA was purified using the centrifugation protocol according to manufacturer's instructions. Purified DNA was run on a test 1% w/v agarose gel.

2.7.10 DNA quantification

DNA was quantified using IMPLEN NanoPhotometer.

2.8 Cloning Vectors

pTrcHis B (Invitrogen)

pAM cyan1-c1 (Invitrogen) (CFP)

pZs Yellow1-N1 was a kind gift from Dr.Eric Hill ,Aston University, UK (YFP)

pcDNA3.1 CT GFP:hTG2 was a kind gift from Dr. Russell Collighan, Aston University,UK

pSTBlue-1 (Novagen)

pcDNA 3.1- (Invitrogen) was a kind gift from Dr. Eric Hill, Aston University

2.9 Dephosphorylation of DNA

Reaction was performed in 1x Antarctic Phosphatase reaction buffer containing 0.1mM ZnCl₂ according to manufacturer's instructions. The enzyme was employed to remove 5' phosphate and prevent vector self-ligation. 50ng of Purified DNA was treated with 1unit Antarctic phosphatase and incubated at 37°C for 30 min and heat inactivated at 70°C for 5min. Using the Promega SV gel and PCR Clean Up kit DNA was re-purified before proceeding to ligation.

2.10 Ligation reaction

Ligation reaction was setup using 50ng of appropriate vector DNA and a 3-fold molar excess of insert in a final reaction volume of 20µL. NEB T4 DNA ligase (1 Weiss unit) was the preferred ligase supplied with 10x DNA ligase reaction buffer containing ATP. The reaction was incubated overnight at 16°C; alternatively set up at room temperature for 2 hours. Appropriate ligation controls were set up. "Self-ligation control" reaction was set up omitting addition of insert into reaction to distinguish clones during cracking procedure. A "no ligase" control was also setup.

2.11 Restriction Digestion

Appropriate restriction enzymes (including *BamHI*, *BglII*, *EcoRI*, *HindIII*, *PvuI*, *NotI*) were obtained from Promega or NEB, supplemented with 10X reaction buffer. Restriction digest reaction was set up using 50ng of appropriate DNA and reaction was set up at 37°C for 4 hours. While setting up double digest, sequential digestion was the preferred protocol using the Promega SV gel and PCR Clean Up kit DNA

before proceeding to the second restriction digestion. A test 1% agarose gel was run to analyse restriction digestion products at the end of reaction.

2.12 PCR reactions

PCR reactions were set up using Finnzymes Phusion High-Fidelity DNA polymerase (unless stated otherwise). Phusion High Fidelity polymerase was provided with 5x Phusion HF buffer containing 1.5mM MgCl₂. Reaction was set up using 100μM dNTPs, 0.5μM of appropriate forward and reverse primer, 0.5ng of template DNA. Total reaction volume was set up to 50μL using nuclease free water. PCR reaction was optimised at initial denaturation at 98°C for 2 min, followed by 35 cycles of

98°C for 45s

65°C for 1min

72°C for 1 min,

Followed by a final extension step 72°C for 10min. This was the standard reaction set-up unless otherwise stated and was set up in MWG biotech Aviso Thermal cycler.

2.13 Touchdown PCR

Touchdown PCR was set up using Novagen KOD HOT start polymerase provided with a 10x reaction buffer to minimize nonspecific amplification. The PCR reaction was set up using 1x buffer, 25mM MgSO₄, 100mM dNTPs, forward and reverse primer (final concentration of 0.3μM), template DNA and 0.02U/μl of KOD Hot start DNA polymerase. The final reaction volume was 50μL. The PCR reaction was initiated with 95°C for 2 min. Followed by 8 cycles of,

95°C for 1 min

70°C for 1 min; with a 1°C decrement of annealing temperature with every round until it reached optimum annealing temperature of about 62°C

The next stage of PCR involved 35 cycles of

95°C for 1 min

62°C for 1 min

72°C for 4 min,

Followed by a final extension step at 72°C for 10min.

2.14 Colony PCR

Colony PCR was employed to determine the orientation of the insert into the vector while screening transformants. PCR amplification was set up using forward primer of vector and reverse primer of insert to produce amplicon of desired size only if the insert was in correct orientation. The PCR reaction was setup using Phusion Hot Start II DNA polymerase using 5x Phusion reaction buffer, 100µM dNTPs, 0.5µM of appropriate forward and reverse primer, 1.0U of Phusion Hot Start II DNA polymerase. To this mixture add a small amount of appropriate colony. The PCR reaction was set up by heating at 95°C for 2 min to lyse bacterial cells. This was followed by 35 cycles of

95°C for 45sec

52°C for 1min

72°C for 3 min

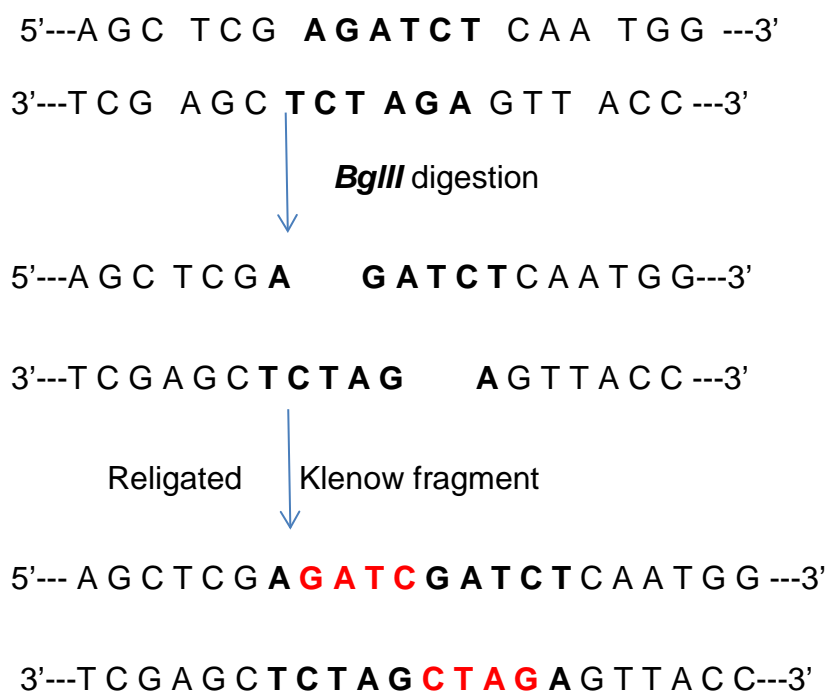
And a final extension step for 10min at 72°C. A test 1% agarose gel was used to analyse the results of the colony PCR.

2.15 Sequencing reactions

Samples for sequencing were sent to the Functional Genomic laboratory at University of Birmingham for analysis. The samples were subjected to Big dye 3 chain terminal reaction (functional genomic laboratory at University of Birmingham) according to manufacturer's instructions.

2.16 Klenow 3'end infilling

Klenow fragment was employed to infill 3' end of DNA fragment in order to shift the reading frame. Thermo scientific Klenow fragment (1unit) was mixed with 10x reaction buffer containing 50mM $MgCl_2$ and 10mM DTT. To the reaction 0.05mM dNTP mix was added along with 2µg of DNA and reaction volume was made up to 20µL using nuclease free water.



2.17 Expression and purification of Recombinant TG2

20ml of LB medium was inoculated with *E. coli* BL21 (DE3) recombinant CFP-TG2-YFP at 37°C for 4 hours. Cultures were diluted 1:20 into LB medium and then induced with 0.1 mM IPTG overnight at 16°C in an orbital shaking incubator. Cells were harvested by centrifugation at 10000g for 15min at 4°C, dissolved in Laemmli buffer and subjected to SDS-PAGE analysis.

2.18 Chromatographic purification of His-tagged proteins using His GraviTrap column (GE Healthcare).

500 ml of induced *E. coli* culture was prepared as above. Cells were resuspended in 10 ml of ice-cold 50mM Tris, 1mM EDTA, 1mM DTT and 5mM imidazole, pH7.5 and chilled on ice. Cells were lysed by sonication for six periods of 30 seconds at 18µm amplitude (with 1 minute of chilling on ice in between) using MSE Soniprep 150 sonicator. Cell debris was removed by centrifugation at 20000g for 30 minutes at

4°C. The clarified lysate was applied to a 1 ml GE Healthcare His GraviTrap column equilibrated in 50mM Tris HCl, 1 mM EDTA, 1mM DTT, 5 mM imidazole pH7.5 (buffer A). After loading the lysate the column was washed with Buffer A followed by a wash using 50mM Tris HCl, 1mM EDTA, 1mM DTT, 20mM imidazole pH7.5. Fractions (0.5 ml) were collected into microcentrifuge tubes at room temperature by elution with buffer B (50mM Tris HCl, 1 mM EDTA, 200 mM imidazole) and stored immediately on ice.

2.19 Gradient purification using GE AKTA prime FPLC

The Ni-NTA column (GE Healthcare) was washed and equilibrated with buffer A (50mM Tris, 1mM EDTA, 1mM DTT, 5mM imidazole and 500mM NaCl). The clarified lysate was diluted 1:1 using buffer A and loaded onto the column at 1ml/min flowrate. The column was then washed with approximately 15ml buffer A (unless absorbance is near to zero) and fractions were collected as wash fractions. This was followed by elution step. 2ml fractions were eluted and collected over an imidazole gradient from 20mM to 500mM imidazole over 40mls (unless stated otherwise)

2.20 Desalting by gel filtration

GE Healthcare PD-10 desalting columns which are packed with Sephadex G25 Medium were used for this technique. The gravity protocol was used for separation of molecules according to manufacturer's instructions.

2.21 SDS-PAGE

SDS-PAGE analysis was performed using a 3% (w/v) polyacrylamide stacking gel and a 10% (w/v) polyacrylamide separating gel at 125volts. 30% solution Acrylamide/Bis acrylamide (29:1) was used as a stock solution. Separating gel was

made using 2.5ml of 30%(w/v) acrylamide/bis-acrylamide solution, 2.5ml Tris SDS pH8.8 solution, 5ml distilled water, 10% of ammonium persulphate and 10 μ L TEMED. 200 μ l of isopropanol was poured on top of the resolving gel to level the upper surface. The gel was allowed to polymerise at room temperature for 40 minutes. To remove the isopropanol after polymerisation the upper surface was washed with distilled water and blotted dry using whatmann filter paper. Stacking gel was prepared using 0.5ml of 30% (w/v) acrylamide/bis-acrylamide solution, 1.25ml of Tris/SDS pH6.8 and 3.25ml of distilled water. Using 10% ammonium persulphate and 10 μ L TEMED the polymerisation was initiated. Gel was polymerised at room temperature for 45 minutes. Protein samples were quantified and 20 μ g of protein was mixed to 2x or 6x Laemmli loading buffer. GE Healthcare Amersham Full - Range Rainbow Molecular Weight marker- RPN800E was the marker of choice. Coomassie Brilliant Blue R250 was used to stain the gels for about 4 hours on a rotatory shaker. Destaining was performed by boiling the gel in distilled water until clear bands were observed.

2.22 Western blotting of SDS PAGE separated proteins

Transfer of separated proteins onto a nitrocellulose membrane was done electrophoretically using BioRad Mini-PROTEAN 3 wet blot system. Assembly of the apparatus was done according to manufacturers' instructions. Air bubbles trapped during the assembly were removed using a western blot roller. The electrophoretic transfer was performed at 150mA for 2 hours in a pre-chilled transfer buffer. After transfer, membrane was blocked using 5% (w.v) Marvel dried milk powder in 1x TBS-Tween at room temperature for 1 hour. Blots were then incubated overnight at 4°C with primary antibody (CUB 7402 or 1D10) in blocking buffer. This was followed

by washing the membrane three times (10minutes each) using TBS-Tween and one wash with PBS. The membrane was then incubated with secondary HRP-conjugated antibody (anti-mouse) in blocking buffer for 2 hours at room temperature. The membrane was then washed three times (10minutes each) with TBS-Tween followed by one wash with PBS. The HRP conjugate of the secondary antibody was treated with ECL chemiluminescence substrate according to manufacturer's instructions and blots were developed using Syngene G:Box Chemi Fluorescent and Chemiluminescent imaging system.

2.23 Protein Assay

Protein concentrations were determined using the Bio-Rad D_c Protein Assay Reagent A (25 µl) and Reagent B (200 µl). Change in the absorbance was measured using the absorbance plate reader at 750nm. Appropriate fractions were pooled.

2.24 Transglutaminase Activity assay

Biotin-cadaverine incorporation into N,N'-dimethylcasein or fibronectin

96 well plates were coated with 100µl of 100mg/ml N, N' dimethylcasein (or 5µg/ml fibronectin) in 100mM TrisHCl, pH8 overnight at 4°C. The plates were then washed with TBS-tween three times. Reaction was prepared using 100µL of 50mM TrisHCl pH7.4 containing TG2 samples with 0.1mM biotin-cadaverine, 10mM CaCl₂ and 1mM DTT. Reactions were performed in triplicates. For positive control 400ng of recombinant TG2 was used and recombinant TG2 containing 0.1mM biotin-cadaverine, 10mM EDTA was set up as the negative control. After 2 hours of incubation at 37°C, the plate was washed with TBS-tween three times. Blocking was performed using 3% heat inactivated BSA in Tris pH7.4 for 30min at 37°C. For the

detection of biotin-cadaverine incorporation, the plate was incubated with 1:1000 extravidin peroxidase conjugate in 3% BSA in TrisHCl pH7.4. Colour was developed using SIGMAFAST OPD (o-Phenylenediamine dihydrochloride) tablets and terminated with addition of 50µl 3N HCl and absorbance was read at 490nm on a spectrafluor plate reader.

2.25 Detection of TG2 antigen using ELISA

96 well plates were coated with 50µL of 5µg/ml fibronectin overnight at 4°C. Wells were washed with 100µL of 50mM Tris-HCl, pH7.4. Using of 3% BSA in PBS, pH 7.4 was used to block wells at 37°C for 30min. wells were then washed three times with 1xPBS and 50µg of protein in 1xPBS and 2mM EDTA was applied to each well and incubated at 37°C for 1 hour. This was followed by a washing with 1xPBS performed three times. Wells were blocked for 30min at 37°C using 3% BSA in PBS and then incubated for 2 hours with Cub7402 or 1D10 (1:1000 dilution in blocking buffer) at 37°C. The wells were washed 3 times with 1xPBS and anti-mouse IgG(1:1000dilution in blocking buffer) was incubated for 2 hours at 37°C. Wells were washed three times with PBS, pH7.4. Colour was developed using SIGMAFAST OPD (o-Phenylenediamine dihydrochloride) tablets and terminated with addition of 50µl 3N HCl and absorbance was read at 490nm on a spectrafluor plate reader.

2.26 Binding of TG2 to Heparin-Sepharose

20ml of LB medium containing antibiotic was inoculated from glycerol stock stored at -80°C. Cells were allowed to grow overnight at 37°C using a benchtop orbital shaker. 400ml of LB broth was inoculated with the 20ml overnight culture of *E.coli* Rosetta2 CFPTG2YFP, cCFPTG2, pET30Ek/LIC TG2 and grown for 4 hours at 37°C. This is followed by inducing cells with 1mM IPTG at 16°C overnight. Cells

were centrifuged at 10000g for 15 min at 4°C. Cells were resuspended in cold 50mM Tris, 1mM EDTA, 1mM DTT pH 7.5 (bufferA) and thereafter sonicated on ice for 6 sonication cycles of 30sec each with 1min cooling over ice. The cell lysate was centrifuged at 20000g for 30 min at 4°C. 5ml GE Healthcare Heparin column was equilibrated using buffer A and the clarified lysate was loaded onto the column. Purification was performed using protocol by Wang *et al*, 2012. The column was washed with 25ml of buffer A and 1ml fractions were eluted with a linear gradient of increasing NaCl concentration from 0 to 0.5M. Every alternate fraction of the gradient was run on a SDS page and analysed by western blotting.

2.27 Trypsin Digestion Assay

Purified recombinant TG2 protein was digested with trypsin using protocol adapted from Fesus *et al* (2013). Purified protein was eluted in 20mM Tris, 300mM NaCl and 10% glycerol using PD-10column. 3µg of purified protein was mixed with trypsin at concentrations including 80ng, 0.4µg, 0.8µg, 1.6µg, 3.2µg and 8µg. The reaction was incubated for 2h on ice and terminated by addition of laemmli buffer. The samples were boiled and resolved by SDS-PAGE. Control reactions including no trypsin digestion and pre- treated inhibitor treated samples were set up similarly.

2.28 Conformation dependent protease digestion

Purified recombinant TG2 was pre-treated with increasing amounts of Monodansyl cadaverin (MDC). After treatment samples were subjected to trypsin digestion and incubated for 2h. The reaction was stopped by boiling with laemmli buffer for 5 min over a waterbath. The samples were resolved by SDS PAGE and analysed by staining with coomassie blue.

2.29 FRET reactions

FRET reactions performed using increasing concentration of calcium and GTP were performed using black 96 well immune plates (Thermo Scientific) and read using SpectraMAX GeminiXS microplate spectrofluorometer.

Chapter 3

Construction of CFP-TG2-YFP recombinant protein in bacterial system


3.1 Introduction

For the construction of TG2 FRET based sensor, fluorescent proteins CFP and YFP were designed to fuse at the N and C terminal of TG2. This chapter goes through the step by step strategy for cloning. CFP, TG2 and YFP plasmid were PCR amplified and first cloned individually into the cloning vector pSTBlue-1. The components are then individually assembled into expression vector pTrcHisB. CFP and YFP are mostly commonly used in the construction of FRET based sensors. During the course of this chapter different DNA polymerases are used in order to achieve optimum amplification. Once cloned into the vector the resulting recombinant clones are first analysed using an alkaline lysis procedure to verify the plasmid size before further analysis. The cloning strategy into pTrcHis B is represented below (Figure 3).

pTrcHis A,B,C
4.4 kb

Comments for pTrcHis B:
4404 nucleotides

Bgl II *Bam* HI



CFP

Eco RI *Hind III*

YFP

6xHis	CFP	TG2	YFP
-------	-----	-----	-----

ii) Multiple cloning site of pTrcHisB (invitrogen user manual, 2008)

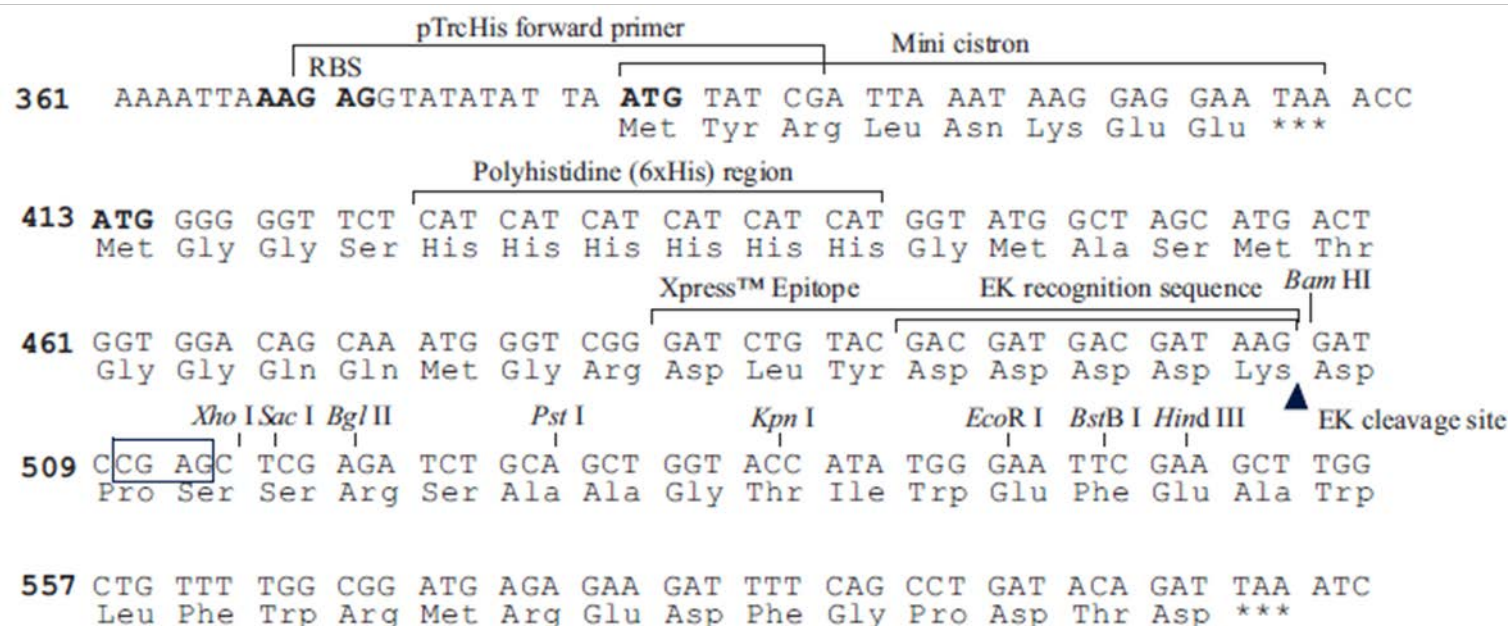


Figure 3 Overview of the cloning strategy showing the stepwise assembly of the TG2 FRET construct in expression vector pTrcHisB (vector map shown i). Step 1 showing the cloning of CFP into the *Bam*HI site of pTrcHisB present in the multiple cloning site (MCS shown in ii) as represented by the red arrow. Step 2 showing the cloning to TG2 into pTrcHisB-CFP. Step 3 showing the cloning of YFP into pTrcHis-CFP-TG2. The Vector map of pTrcHisB showing the HisTag and multiple cloning site highlighted in red circles. The restriction sites present on CFP, TG2, YFP used for cloning are indicated by blue arrows. Both Step 2 and Step 3 are directional cloning. The red box represents the final TG2 FRET construct in pTrcHisB with the His tag at the N terminal of the construct.

3.2 RESULTS

3.3 PCR amplification

Reactions were performed in triplicates in MWG Biotech Aviso Thermal cycler to avoid over-representation of polymerase-induced errors. Thermal cycling conditions were optimised for maximum amplification yield and specificity.

3.3.1 CFP amplification

Using primers CFP For3 and CFP Rev3, with the commercially available vector pAM cyan1-c1 as template, amplification was obtained as seen in Lanes 2, 3, 4 (Figure 3.1). Bands of correct size of about 0.7Kb were seen. Conditions for PCR were optimised to be initial denaturation at 98°C for 2 min, followed by 35 cycles of 98°C for 45 s, 65°C for 1 min, 72°C for 1 min, followed by a final extension step at 72°C for 10 min using Phusion Hot start polymerase.

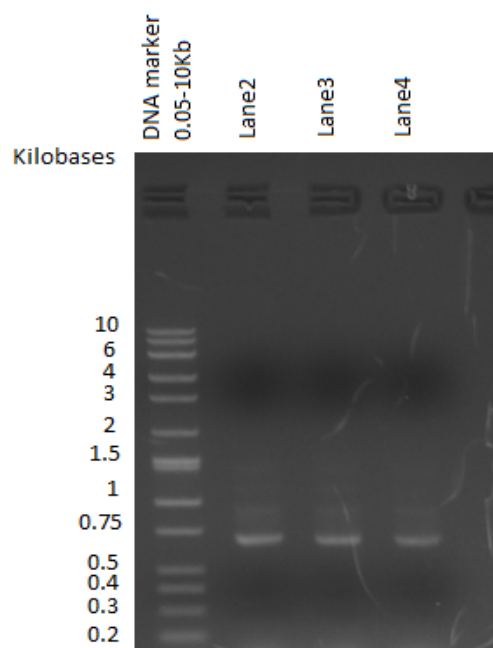


Figure 3.1 Agarose gel electrophoresis of amplified products using primers CFP For3/Rev3. Lane 1 represents the 2-log marker DNA. Lane 2, 3, 4 showing the amplified CFP which is 0.7 Kb in size.

3.3.4 YFP amplification

Using primers YFP For2 and YFP Rev2, with the commercially available vector pZs Yellow1- N1 as template, amplification was obtained as seen in Lanes 2, 3, 4 (Figure 3.2). Bands of correct size of about 0.7Kb were seen. Conditions for PCR were optimised to be initial denaturation at 98°C for 2 min, followed by 35 cycles of 98°C for 45 s, 65°C for 1 min, 72°C for 1.5 min, followed by a final extension step at 72°C for 10 min using Phusion Hot start polymerase.

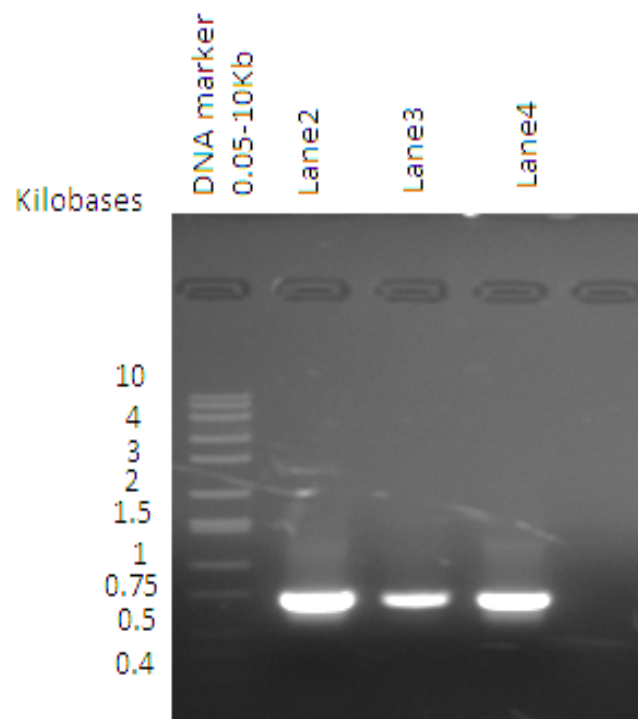


Figure 3.2 Agarose gel electrophoresis of amplified products using primers YFP For2/Rev2. Lane 1 represents the 2-log marker DNA. Lane 2, 3, 4 showing the amplified YFP which is 0.7 Kb in size.

3.3.4 TG2 amplification

Using primers TG2 For and TG2 Rev, with the vector pcDNA 3.1 CT GFP:hTG2 as template, amplification was obtained as seen in Lanes 2, 3, 4, 5, 6, 7 (Figure 3.3). Bands of correct size of about 2Kb were seen. Conditions for PCR were optimised to be initial denaturation at 98°C for 2 min, followed by 35 cycles of 98°C for 45 s, 65°C for 1 min, 72°C for 3 min, followed by a final extension step at 72°C for 10 min using Phusion Hot start polymerase.

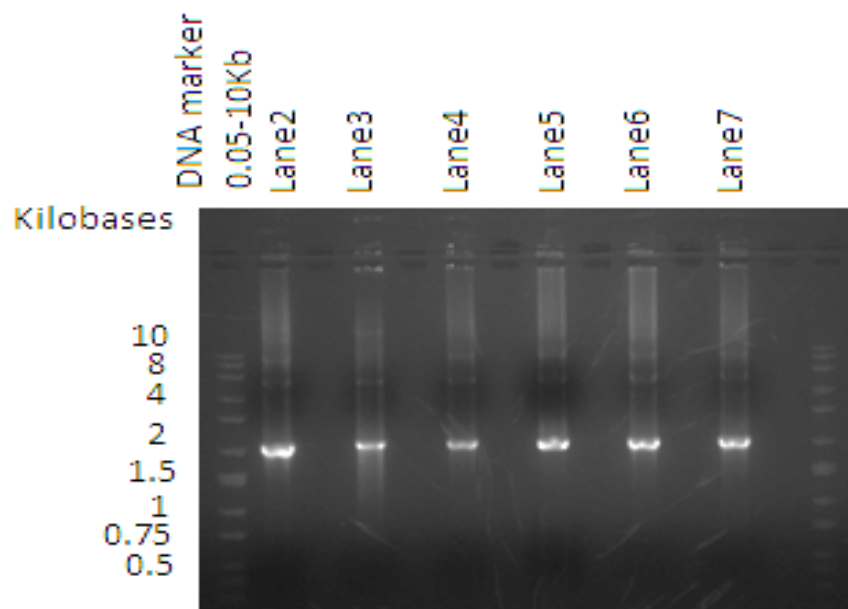


Figure 3.3 Agarose gel electrophoresis of amplified products using primers TG2 For/Rev. Lane 1 is the 2-log marker DNA. Lane 2, 3, 4, 5, 6, 7 showing the amplifiedTG2 which is 2 Kb in size.

3.4 Cloning amplified products into pSTBlue-1

3.4.1 Identification of recombinant pSTBlue-1 plasmids.

Using the pSTBlue-1 blunt cloning kit the amplified products of CFP, TG2 and YFP were ligated into pSTBlue-1 and transformed into NovaBlue competent cells. Blue/white screening was performed by spreading transformed cells onto plates containing 100µg/ml ampicillin, 100µM IPTG and 50µg/ml X-gal. White colonies, potentially containing inserted DNA, were screened for increased size compared to the empty vector pSTBlue-1 using a simple alkaline lysis procedure followed by agarose DNA electrophoresis (cracking).

3.4.2 CFP cracking

Following Blue/White screening, 14 white colonies were selected for the cracking procedure. A blue colony (parent pSTBlue-1) was also selected as a negative control for cracking. All samples were then run on an agarose gel for further analysis. All plasmids which were of a larger size than the parent pSTBlue-1 (blue colony) were selected for nucleotide sequencing. From Figure 3.4, clones CFP 4, CFP 6, CFP 7, CFP 11 and CFP 13 were larger than parent vector and were further analysed by sequencing.

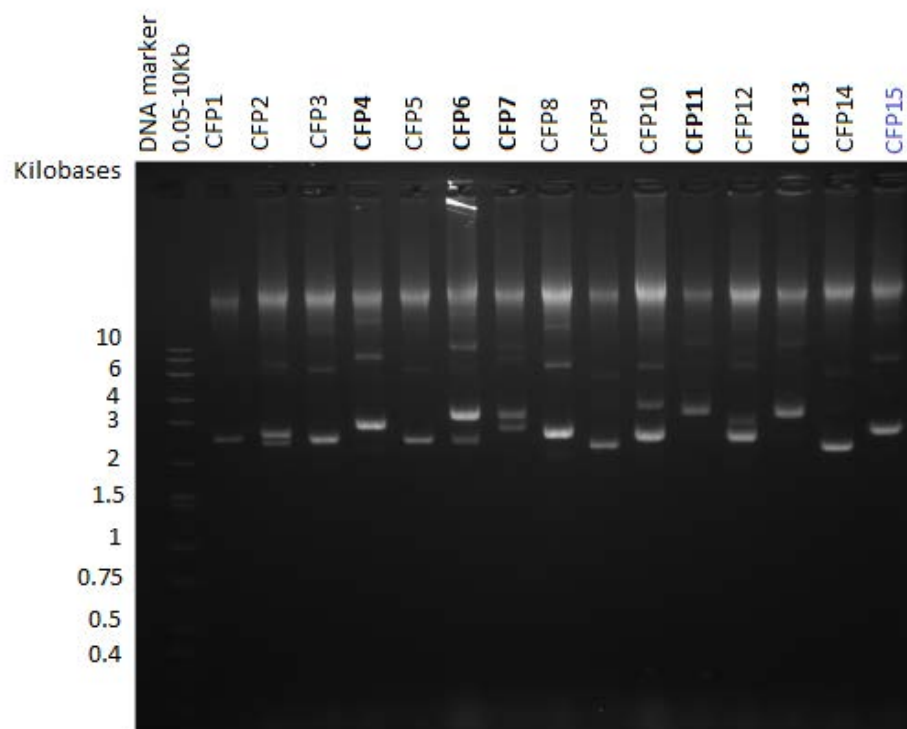


Figure 3.4 Agarose gel electrophoresis of the cracking procedure performed on the selected CFP colonies after Blue White screening. Lane 1 is the 2-log marker DNA. Lanes 2 to 15 showing CFP clones 1-14. Lane 16 showing the blue colony representing a negative control for selection. CFP 4, 6, 7, 11 and 13 were selected for sequencing.

3.4.3 YFP cracking

Similarly for YFP, 14 white colonies were selected for the cracking procedure. A blue colony was also selected as a negative control for cracking. All samples were then run on an agarose gel for further analysis. All plasmids which were bigger than parent vector (blue colony) were selected for nucleotide sequencing. From the gel Figure 3.5, clones YFP 3, YFP 7, YFP 8, YFP 9, YFP 10, YFP 11, YFP 12 and YFP 14 were larger than parent vector and were further analysed by sequencing.

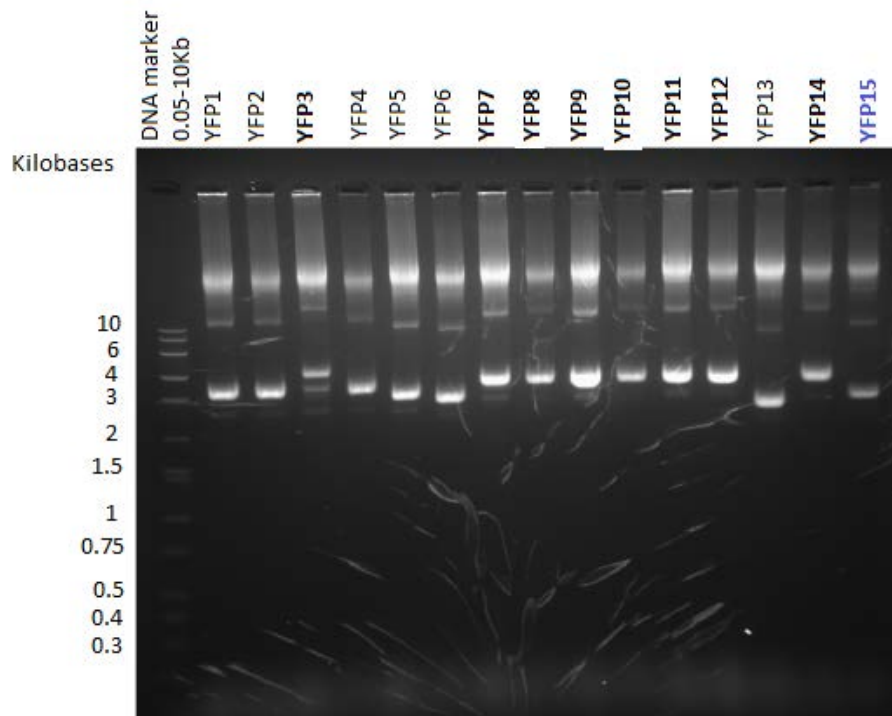


Figure 3.5 Agarose gel electrophoresis of the cracking procedure performed on the selected YFP colonies after Blue White screening. Lane 1 is the 2-log marker DNA. Lanes 2 to 15 showing YFP clones 1-14. Lane 16 showing the blue colony representing a negative control for selection. YFP 3, 7, 8, 9, 10, 11, 12, 14 were selected for sequencing.

3.4.5 TG2 cracking

For TG2, 7 white colonies were selected for the cracking procedure. A blue colony was also selected as a negative control for cracking. All samples were then run on an agarose gel for further analysis. All plasmids which were bigger than parent vector (blue colony) were selected for nucleotide sequencing. From the gel Figure 3.6, clones TG2 1, TG2 4, TG2 5 and TG2 7 were larger than parent vector and were further analysed by sequencing.

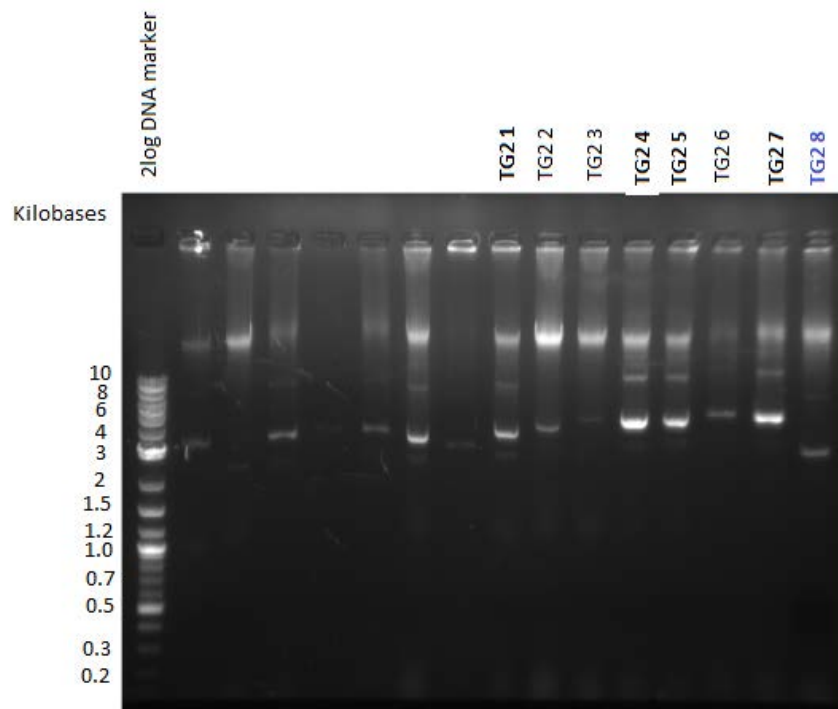


Figure 3.6 Agarose gel electrophoresis of the cracking procedure performed on the selected TG2 colonies after Blue White screening. Lane 1 is the 2-log marker DNA. Lanes 9 to 15 showing TG2 clones 1-7. Lane 16 showing the blue colony representing a negative control for selection. TG2 1, 4, 5, 7 were selected for sequencing.

On analysing the cracking agarose gel results, plasmids which were larger than the parent pSTBlue1 vector were selected for sequencing. Using the Promega Wizard Plus minipreps DNA purification Kit, plasmid purification was performed on the selected clones of CFP, YFP and TG2. These plasmids were then digested using *EcoRI* to test for inserts of the correct size (*EcoRI* digests close to each side of the cloning site in pSTBlue-1).

3.5 Cloning of CFP, YFP and TG2 into expression vector pTrcHisB

pTrcHis B vector was transformed into NovaBlue competent cells. Colonies were selected from the plate and then grown individually in 5ml LB broth containing ampicillin at 37°C in orbital shaking incubator overnight. Using the Promega Wizard Plus minipreps DNA purification Kit, plasmid purification was performed. The pTrcHis B purified plasmid was run on an agarose gel as showing Figure 3.7.

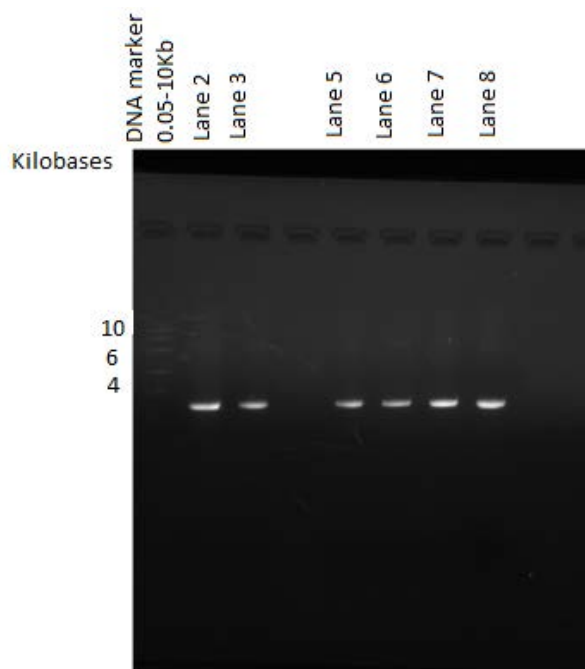


Figure 3.7 Agarose gel electrophoresis of the purified plasmid of pTrcHis B. Lane 1 is the 2-log marker DNA. Lanes 2, 3, 5, 6, 7, 8 showing pTrcHis B purified plasmid of about 4.4 Kb.

3.6 Cloning CFP into pTrcHis B

CFP was digested from the pSTBlue-1 plasmid using *Bam HI* and *Bgl II*. A double digestion was performed and the reaction was set up using buffer B (Promega). Gel electrophoresis (Figure 3.8) revealed the 0.7 Kb CFP insert released after digestion. pTrcHis B was digested using *Bam HI* only, with gel electrophoresis (Figure 3.9) showing undigested pTrcHis B and digested pTrcHis B (4.4 Kb). On digestion the purified undigested plasmid runs faster as it is super coiled but when digested a band about 4.4 Kb long was seen.

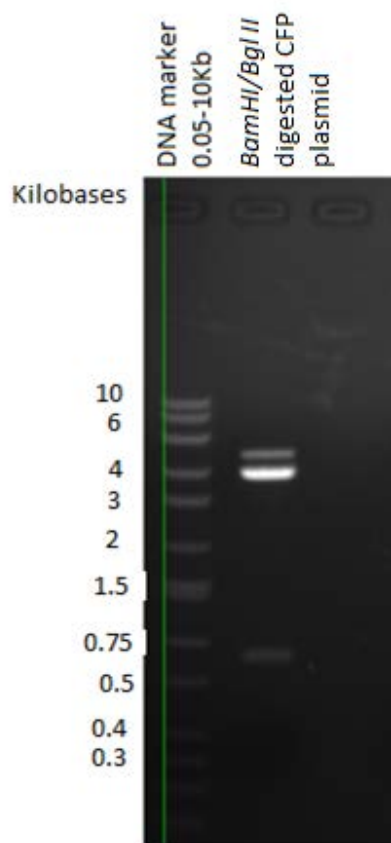


Figure 3.8 Agarose gel electrophoresis of the digestion of purified CFP using *Bam HI* and *Bgl II*. Lane 1 is the 2-log marker DNA. Lanes 2 shows the digested plasmid. A 0.7Kb long band is seen which represents the CFP insert.

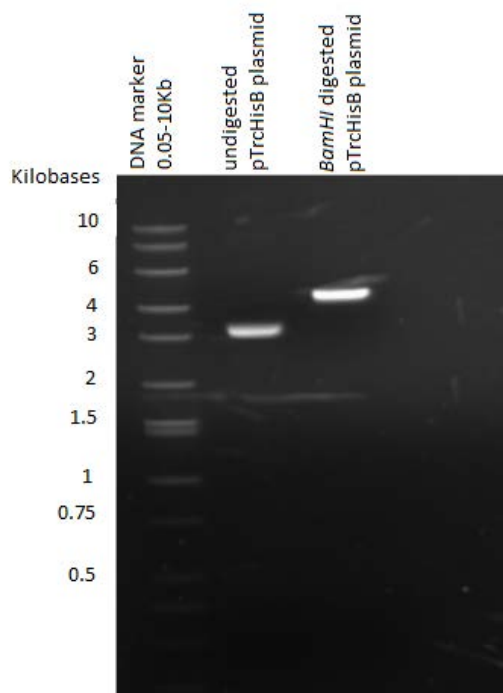


Figure 3.9 Agarose gel electrophoresis of the digestion of the purified pTrcHis B plasmid using *Bam HI*. Lane 1 is the 2-log marker DNA. Lanes 2 shows the undigested pTrcHis B plasmid and the digested plasmid of about 4.4 Kb in Lane 3.

The digested pTrcHis B and CFP were extracted and purified from a low melting point agarose gel. The purified pTrcHis B was further treated with Antarctic phosphatase to remove 5' phosphates and prevent religation. Further a ligation reaction was performed using Quick ligase to ligate pTrcHis B and CFP and was then transformed into Novablue competent cells.

Cracking procedure was repeated on the colonies grown. Clones showing plasmids of the right size were then selected for plasmid purification and then subjected to a restriction digest to determine orientation.

3.7 Screening of recombinant CFP-pTrcHisB plasmids

The screening of recombinant CFP-pTrcHis B plasmids were performed by analysing 20 transformed colonies via cracking procedure. Negative control used was

pTrcHisB colony. Plasmids which were larger than cloning vector pTrcHisB were selected as seen in Figure 3.10A and 3.10B. Based on size of the plasmid, three different colonies were expected. Firstly, plasmids similar to size of negative control representing pTrcHisB only. Second representing desired CFP insert into pTrcHisB and third representing concatemers (false positive) which represent multiple copies of the CFP insert sequence. Concatemers may be a result of DNA insert: plasmid ratio not being optimum. To differentiate and narrow down colony 3, 5, 6, 7, 8, 12 and 15 were grown for plasmid preparation and further restriction digestion.

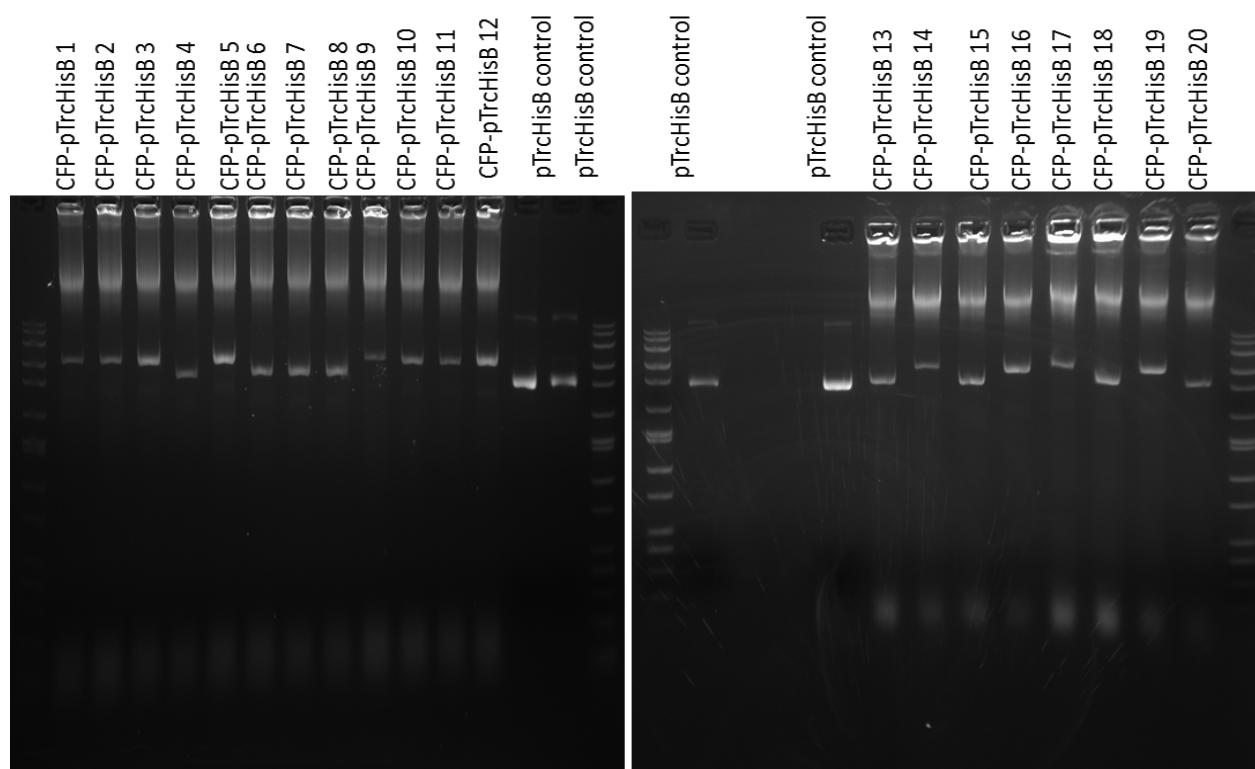


Figure 3.10A and 3.10B Agarose gel electrophoresis of the cracking procedure performed on the selected CFP-pTrcHisB clones. Figure A, Lane 1 and Lane15 are the 2-log marker DNA. Lanes 2 to 13 showing CFP-pTrcHisB clones 1-12. Lane 14 and Lane 15 represent the parent cloning vector pTrcHisB(negative control). Figure B, Lane 1 and 14 is the 2-log marker DNA. Lane 2 and Lane 5 represent the parent cloning vector pTrcHisB (negative control). Lanes 6 to 13 showing CFP-pTrcHisB clones 13-20. CFP-pTrcHisB 3, 5, 6, 7, 8, 12 and 15 were selected for further analysis.

3.8 Analysis of selected colonies of recombinant CFP-pTrcHis B clones.

CFP-pTrcHis B clones 3, 5, 6, 7, 8, 12 and 15 were selected from the agar plate and then grown individually in 5ml LB broth containing ampicillin at 37°C in orbital shaking incubator overnight. Using the Promega Wizard Plus minipreps DNA purification Kit, plasmid purification was performed. The pTrcHis B purified plasmid was run on a test agarose gel as shown below figure 3.11. Negative control of pTrcHis B was also simultaneously grown and a plasmid was purified and run on same gel. Negative control pTrcHis B plasmid was confirmed to be about 4.4Kb. Expected size of CFP-pTrcHis B clones should be about 5.1Kb and was observed in clones 3, 5, 12, 13 and 15. These plasmids were further analysed for the orientation of CFP into pTrcHis B.

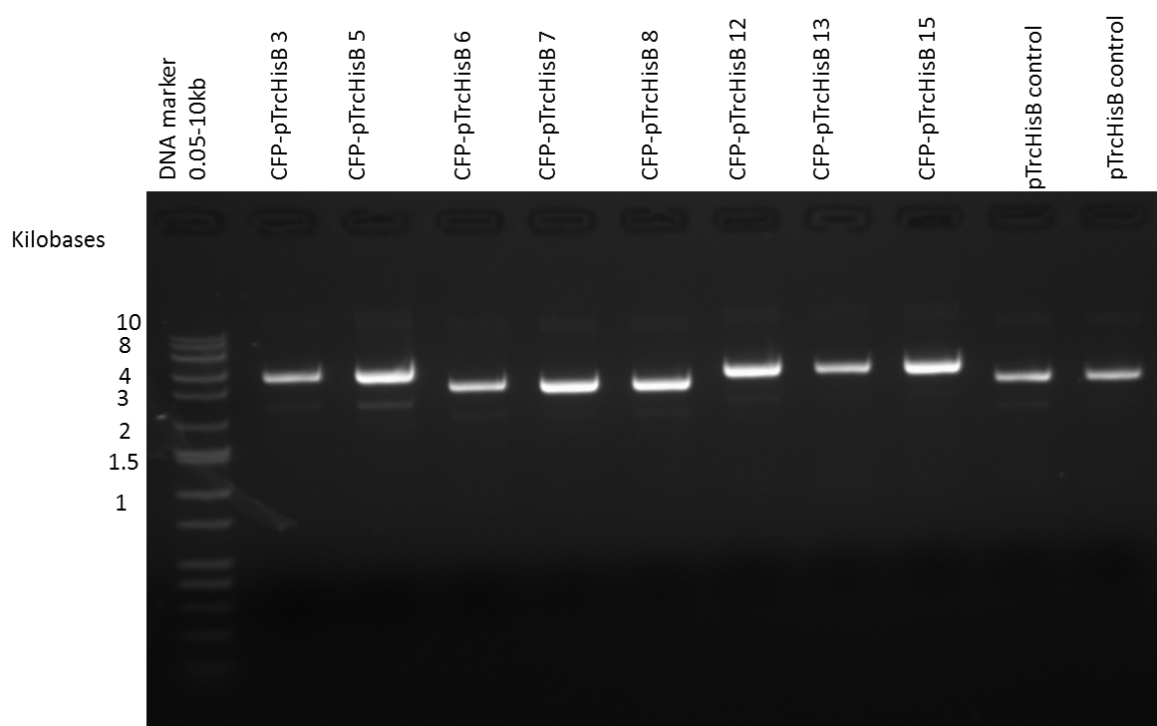
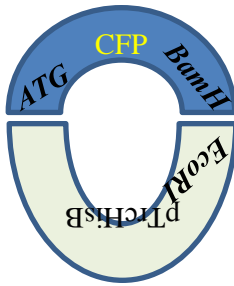


Figure 3.11 Agarose gel electrophoresis of the purified plasmid of CFP-pTrcHis B clones 3, 5, 6, 7, 8, 12, 13 and 15. Lane 1 is the 2-log marker DNA. Lanes 2 to 9 showing clones 3, 5, 6, 7, 8, 12, 13 and 15. Expected size of clones should be about 5.1Kb. Lane 10 and 11 showing pTrcHis B purified plasmid of about 4.4 Kb.

3.9 Orientation of CFP into pTrcHisB

Since the CFP fragment has *Bgl II*/*Bam HI* ends, the *Bam HI* site will be destroyed at the 5' end of the gene. Restriction digests of the CFP-pTrcHis B clones with *Bam HI* and any other enzyme 3' of the CFP in the pTrcHis B multiple cloning site (in this case *Eco RI*) would reveal its orientation. On digestion with *Bam HI* and *Eco RI* the plasmid was linearized indicating the correct orientation.



Correct orientation
 → *BamHI* destroyed at 5' end
 → *BamHI/EcoRI* digestion
 → plasmid linearizes



Wrong orientation
 → *BamHI/EcoRI* digestion
 → CFP cuts out

Plasmids of clones 3, 5, 6, 7, 8, 12 and 15 were digested with *BamHI* and *EcoRI* to reveal orientation of CFP into pTrcHisB (figure 3.12). Clones 3, 5, 12 and 15 were found to be of correct size as compared to negative control pTrcHisB vector. Out of these, clones 3, 5 and 12 were found to have correct orientation. Clone 15 digestion with *BamHI/EcoRI* reveals a smaller band of the size of CFP to cut out, indicating wrong orientation of CFP into pTrcHisB. Clone 3, 5 and 12 clones were further assessed for protein expression, colony PCR and sequence analysis.

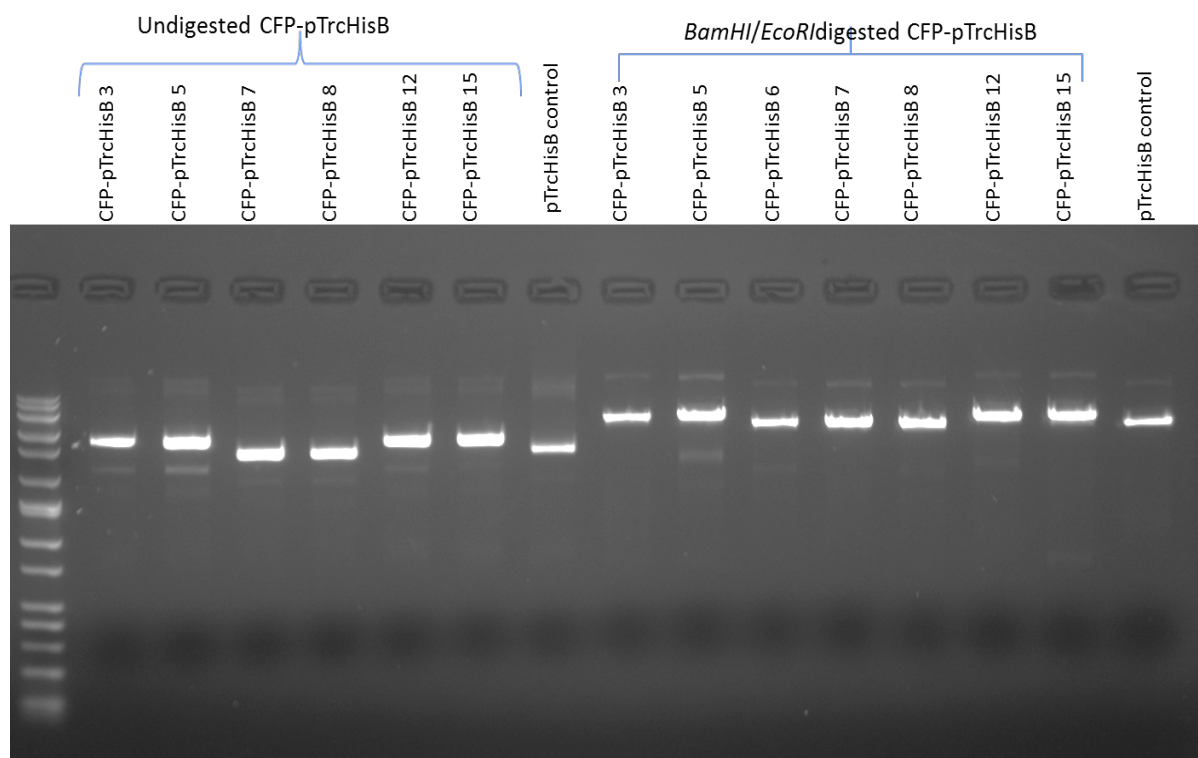


Figure 3.12 Agarose gel electrophoresis of the *Bam*HI/*Eco*RI digestion of the purified CFP-pTrcHisB clones. Lane 1 is the 2-log marker DNA. Lanes 2 to 8 represents undigested plasmid of clones 3, 5, 7, 8, 12, 15 and negative control pTrcHisB plasmid. Lanes 9 to 16 show the *Bam*HI/*Eco*RI double digested plasmids of clones 3, 5, 6, 7, 8, 12, 15 and control pTrcHisB vector.

3.10 Colony PCR

Colony PCR was set up using pTrcHisB forward primer (HispTrc) and CFP-pTrcHisB clones 3, 5 and 12 (Figure 3.13). If CFP was correctly orientated into pTrcHisB during cloning it was expected to result in successful amplification of CFP. Clone 3 and clone 5 did not show successful amplification of CFP whereas clone 12 subjected to colony PCR showed amplification of CFP. Agarose gel electrophoresis revealed a band of about 0.7Kb using clone 12 as a template for colony PCR.

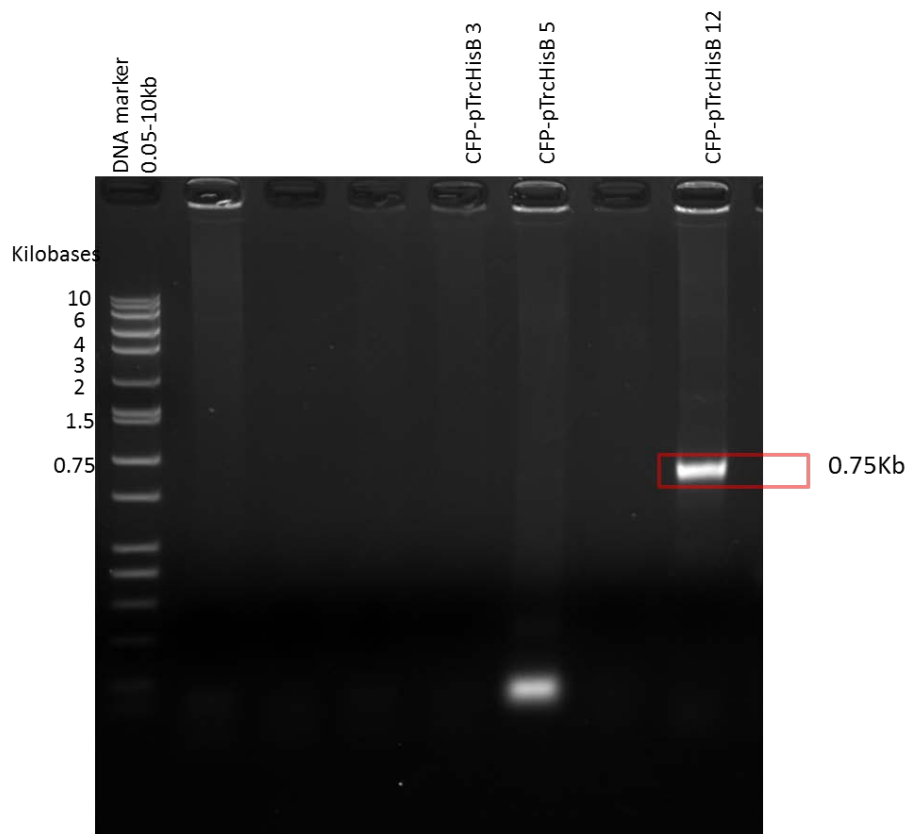


Figure 3.13 Agarose gel electrophoresis of the colony PCR performed using clones 3, 5 and 12 colonies as template DNA. Clone 12 showed amplification of CFP using pTrcHisB forward primer, indicating correct orientation.

3.11 Nucleotide sequencing

CFP-pTrcHisB clones 3, 5 and 12 was further analysed by nucleotide sequencing.

Clone 12 was confirmed to be of right sequence and orientation. CFP-pTrcHisB

clone 12 plasmid was stored at -80°C for further experiments. Glycerol stock

bacterial culture was stored -80°C.

3.12 Cloning of TG2 into CFP-pTrcHis B

CFP-pTrcHisB 12 clone was grown in 5ml LB broth containing ampicillin at 37°C in

orbital shaking incubator overnight. Using the Promega Wizard Plus minipreps DNA

purification Kit, plasmid purification was performed. TG2-pSTblue1 plasmid was also

grown for plasmid purification. Undigested plasmids CFP-pTrcHisB 12 and TG2-psTBlue1 were run on a 1% (w/v) agarose gel (figure 3.14). CFP-pTrcHisB purified plasmid above 5.1Kb but supercoiled plasmid runs faster.

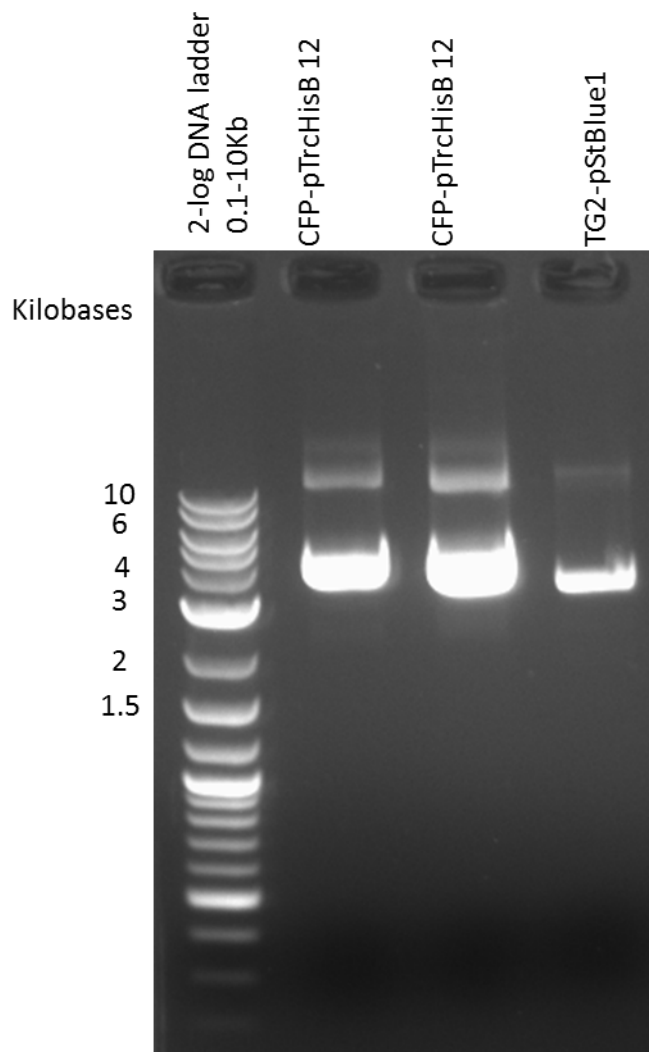


Figure 3.14 Agarose gel electrophoresis of the purified plasmid of CFP-pTrcHis B clones 12 and TG2-pSTblue 1 purified plasmid. Lane 1 is the 2-log marker DNA. Lanes 2 and 3 represents CFP-pTrcHisB 12 plasmid Expected size of clones should be about 5.1Kb. Lane 3 showing TG2-pSTblue-1 purified plasmid.

3.13 Restriction digestion of CFP-pTrcHisB 12 and TG2-pSTblue1 plasmid

CFP-pTrcHis B 12 purified plasmid and TG2-pSTblue 1 purified plasmid was digested with *EcoRI* and *BglII* digest in buffer D (Promega) for 4 hours at 37°C. The digested products were analysed on a test agarose gel (1%w/v) (figure 3.15). *EcoRI* digestion of CFP-pTrcHis B and TG2-psTBlue1 is seen in Lanes 4 and 5. *EcoRI* digestion of CFP-pTrcHis B 12 linearizes the plasmid. *EcoRI* digestion of TG2-pSTblue-1 was successful as a 2Kb lower band is observed representing TG2. The *EcoRI* digested plasmids were then digested with *BglII*. Lane 6 represents *BglII* digestion of *EcoRI* cut CFP-pTrcHisB 12 plasmid and Lane 7 represents the same for TG2-pSTblue1 plasmid. These digested plasmids were then purified on a low melting point agarose gel and a test 1% agarose gel was run to confirm purification (Figure 3.16). The gel purified plasmids were then ligated using T4 DNA ligase. A control ligation was setup using only purified CFP-pTrcHisB 12 plasmid (self-ligation).

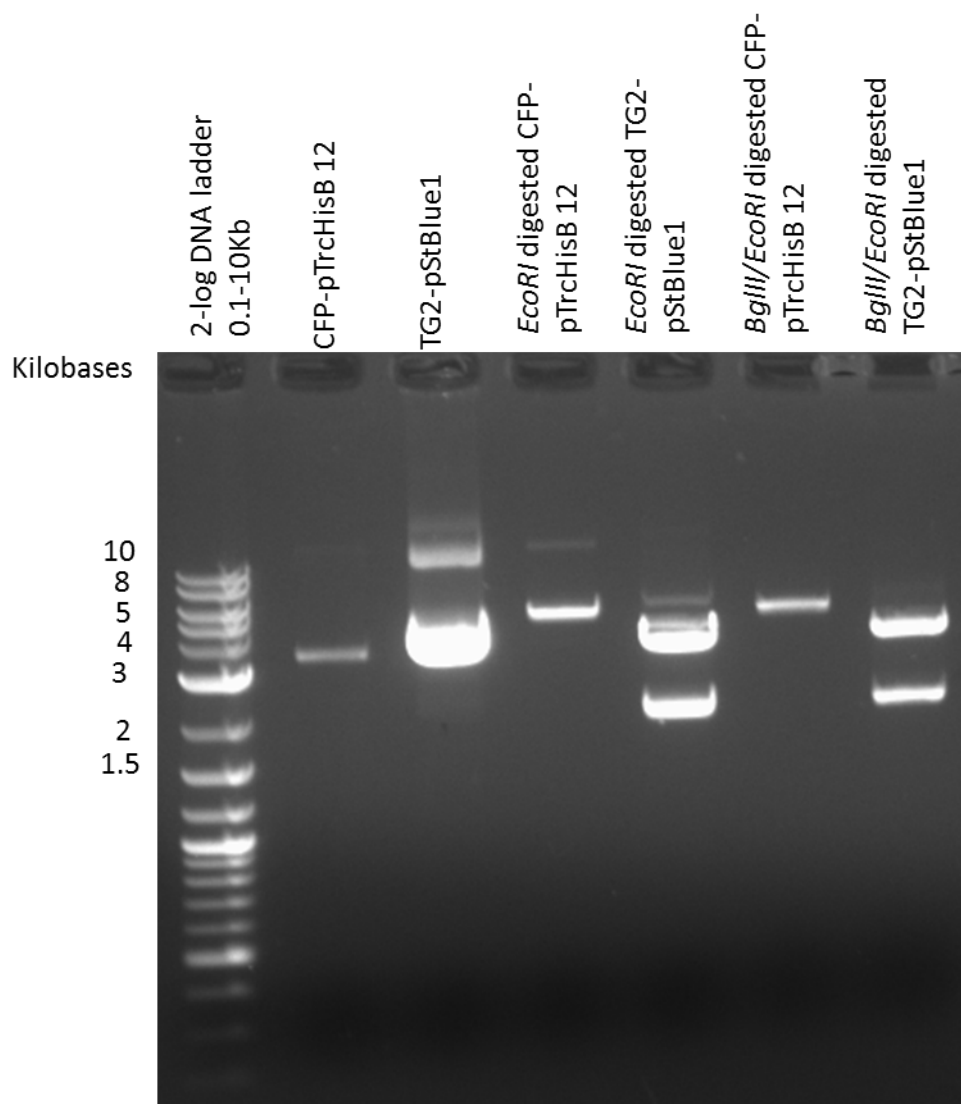


Figure 3.15 Agarose gel electrophoresis of *EcoRI*/*BglIII* digested CFP-pTrcHisB 12 and TG2-pSTBlue1 purified plasmid. Lane 1 is the 2-log marker DNA. Lanes 2 and 3 represents purified plasmids (undigested). Lane 4 showing *EcoRI* digestion of CFP-pTrcHisB 12 clone. Lane 5 representing *EcoRI* digestion of TG2-pSTblue-1 plasmid. Lane 6 and 7 indicate the *BglIII* digestion of previously digested (*EcoRI*) plasmids of CFP-pTrcHisB and TG2-psTblue1 plasmid respectively.

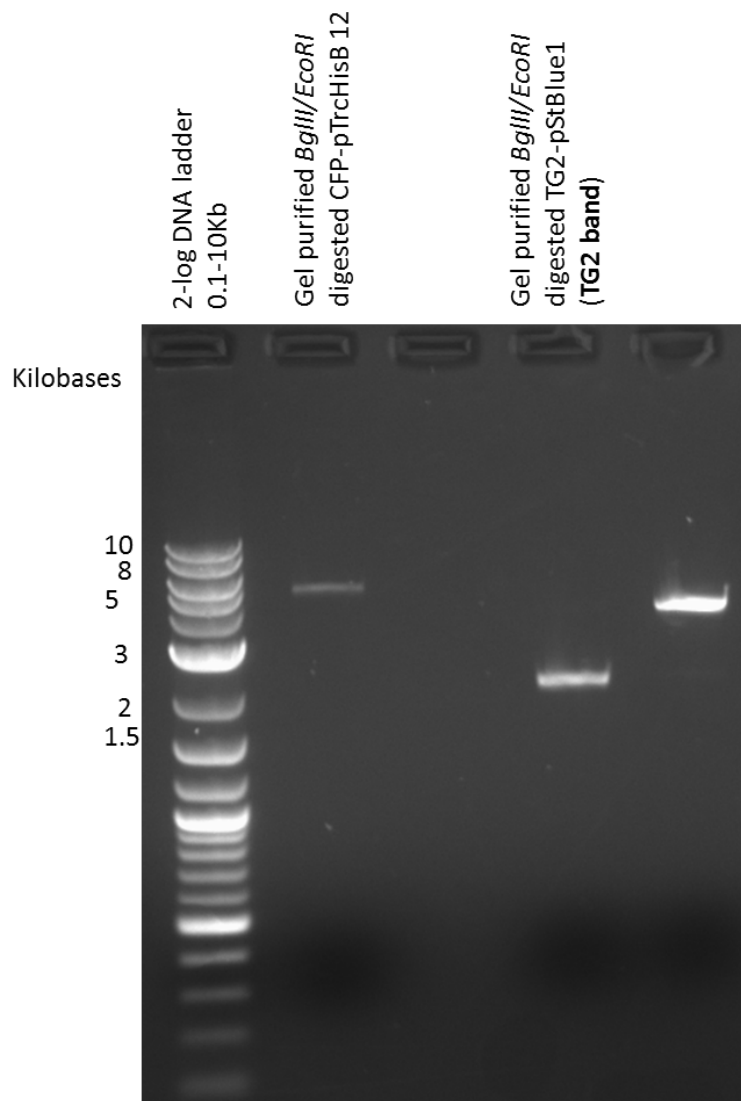


Figure 3.16 Agarose gel electrophoresis of gel purified plasmid of CFP-pTrcHis B clones 12 and TG2-pSTblue 1 purified plasmid. Lane 1 is the 2-log marker DNA. Lane 2 indicating gel purified *BglIII/EcoRI* digested CFP-pTrcHisB 12 plasmid. Lane 3 representing purified TG2 cut out after *BglIII/EcoRI* digestion of TG2-pSTblue1 plasmid.

3.14 Screening of CFP-TG2-pTrcHisB ligated colonies.

Ligation of purified CFP-pTrcHisB 12 vector and TG2 insert using T4 DNA ligase resulted in 15 colonies after transformation in Novablue competent cells. No colonies were seen in self ligated CFP-pTrcHisB12 vector as expected. These 15 colonies were then analysed using a cracking procedure and plasmids were run on an agarose gel (figure 3.17). Out of 15 transformed colonies CFP-TG2-pTrcHisB

clones 2, 3, 4, 11, 12, 14 and 15 were seen to be of the correct size. Other clones were of 2Kb size indicating insert only. A test *BglIII*/*EcoRI* digest was performed on these selected clones to make sure we can cut out TG2 again. Clone 12, 14, and 15 were then analysed by nucleotide sequencing.

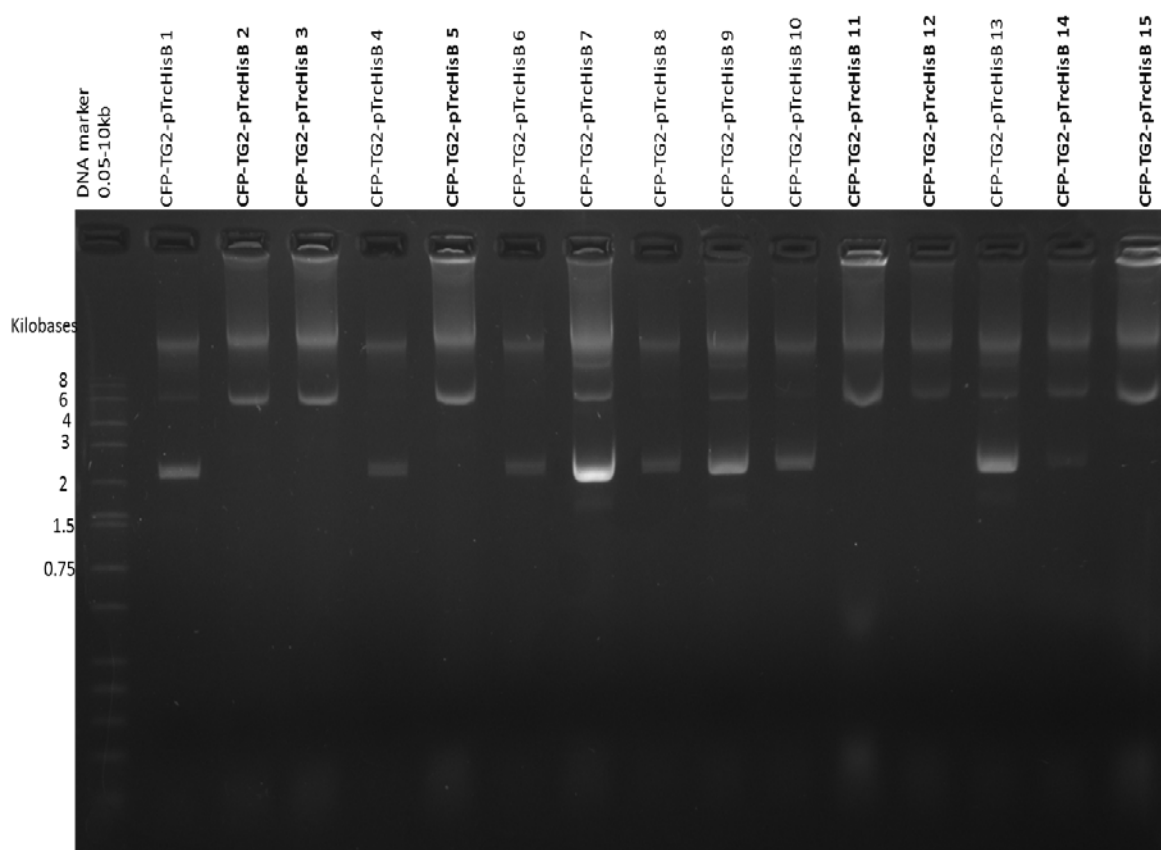


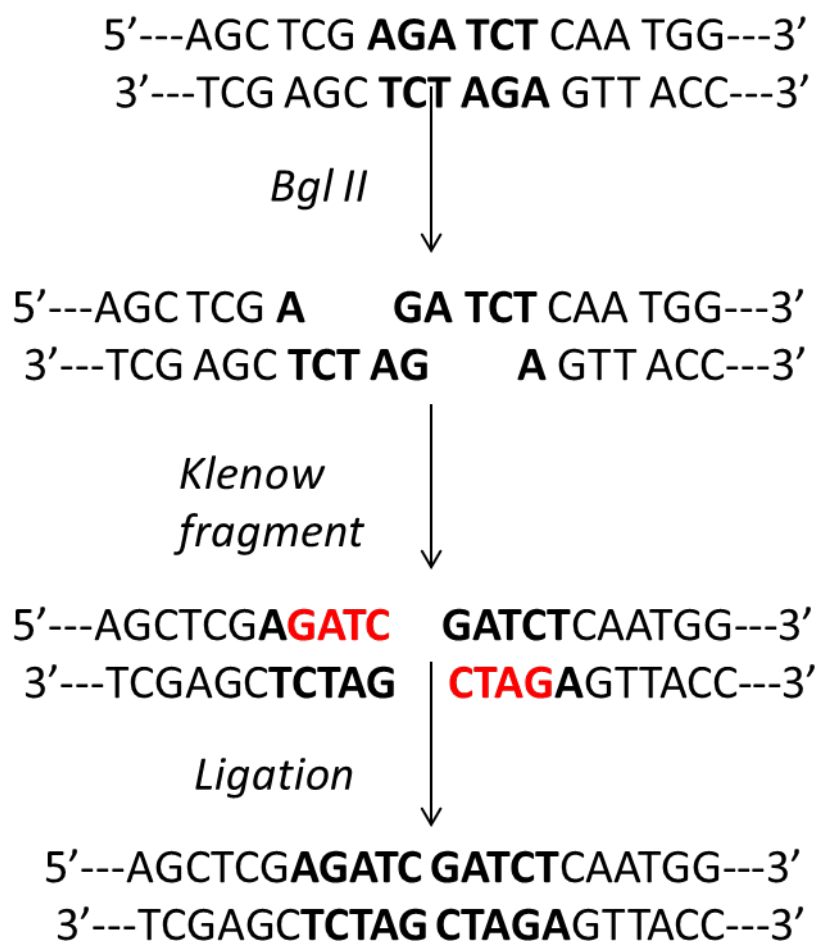
Figure 3.17 Agarose gel electrophoresis of the cracking procedure performed on the selected CFP-TG2-pTrcHisB clones. Lane 1 is the 2-log marker DNA. Lanes 2 to 16 showing CFP-pTrcHisB clones 1-15. Clones 2, 3, 5, 11, 12, 14 and 15 were found to be of correct size. After test digest of these clones with *BglIII*/*EcoRI* clones 12, 14 and 15 were selected for nucleotide sequencing.

3.15 Nucleotide sequencing of CFP-TG2-pTrcHisB clones

Nucleotide sequencing revealed an addition 'C' base pair in front of TG2 sequence. This disturbed the reading frame of CFP-TG2-pTrcHisB clones. The clones were then digested with *BglIII* and Klenow fragment infilling was performed. The clones were then re-ligated and transformed into Novablue competent cells (Figure 3.18).

As a result of this Klenow filling the *Bgl*III restriction site of TG2 was destroyed. A test gel was then performed with *Bgl*III to ensure that the plasmid does not get digested (figure 3.19). The resulting clones were then confirmed to have right sequence by nucleotide sequence analysis.

CFP-TG2 cloning into pTrcHisB infilled using Klenow fragment



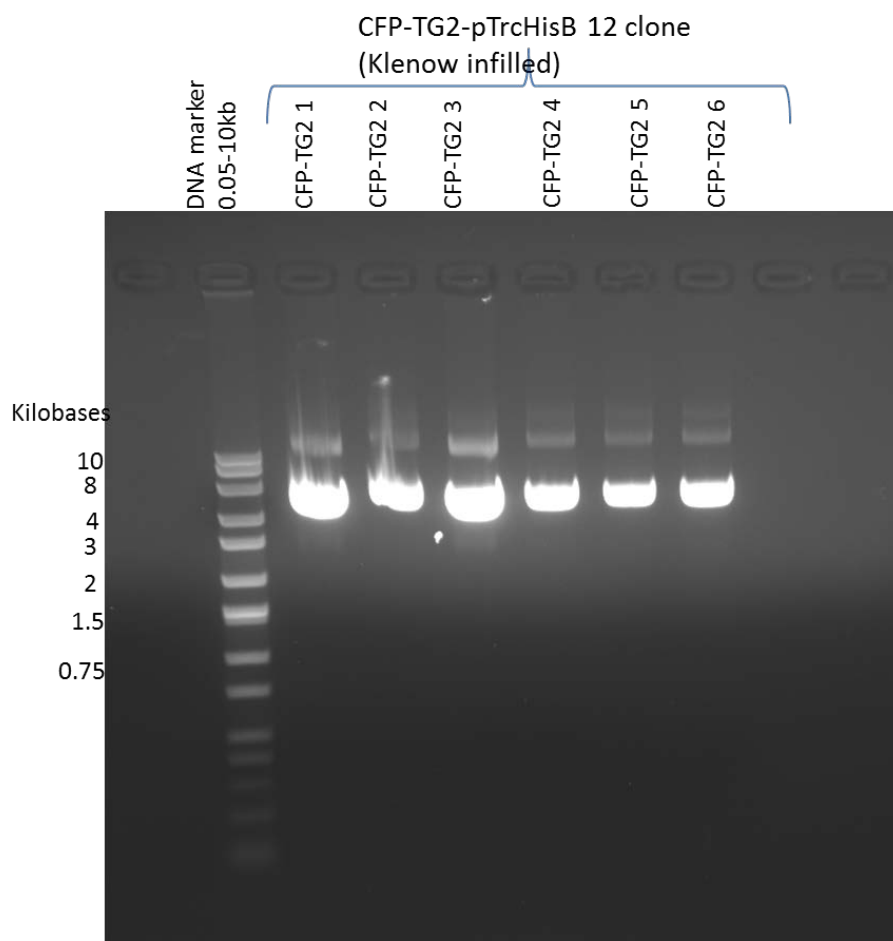


Figure 3.18 Agarose gel electrophoresis CFP-TG2-pTrcHisB clones which were treated with Klenow fragment and re-ligated. Lane 1 represents 2-log DNA marker. Lanes 2 to 7 represents clones 1 to 6 which is after treatment with Klenow and re-ligated.

3.16 Test *Bgl*III digest of CFP-TG2 clones

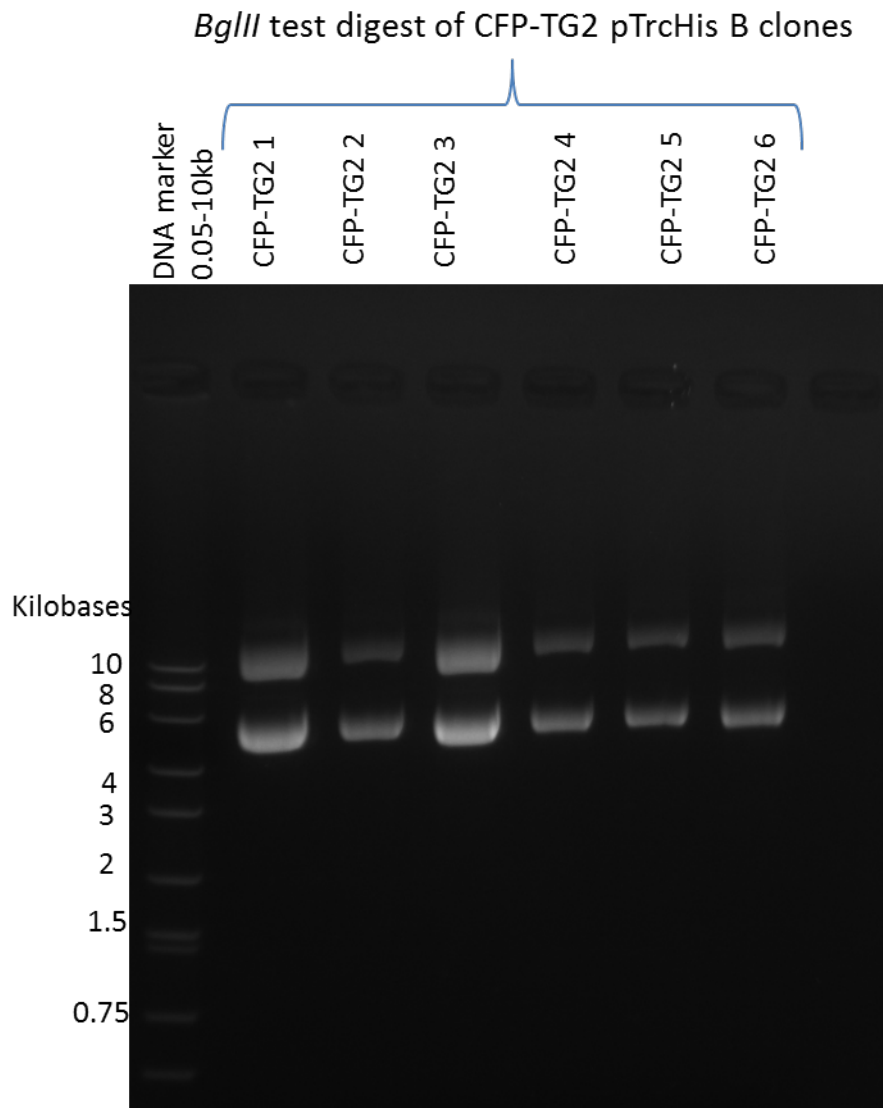


Figure 3.19 Agarose gel electrophoresis showing a test *Bgl*III digested of re-ligated clones indicated in Figure 3.18. Lane 1 indicates the 2-log DNA marker. Lane 2 to 7 represent the *Bgl*III digested clones 1 to 6. Clones 1 to 6 were not digested with *Bgl*III.

3.17 YFP cloning into CFP-TG2 pTrcHisB

YFP was digested from the pSTBlue-1 plasmid using *Hind*III and *Eco*RI. A sequential digestion was performed and the reaction was set up using buffer 2 (NEB). Gel electrophoresis (Figure 3.20 and Figure 3.21) revealed the 0.7 Kb YFP insert released after digestion. CFP-TG2-pTrcHisB was digested similarly with *Hind*III and

EcoRI, with gel electrophoresis (Figure 3.21 and 3.22) showing double digested CFP-TG2-pTrcHisB and a control *EcoRI* only digest.

3.18 *HindIII* digestion of YFP-psTBlue1 plasmid

YFP-pSTBlue-1 plasmids were purified and subjected to *HindIII* digestion using buffer 2(NEB) at 37°C for 4 hours. A test gel was run to analyse the digestion, which revealed successful digestion of plasmid resulting in YFP being cut out (0.7Kb) and upper band representing parent pSTblue1 vector (figure 3.20). The lower 0.7Kb band was then purified on a low melting point agarose gel (1.5%w/v) and purified using Promega SV gel and PCR Clean Up kit.

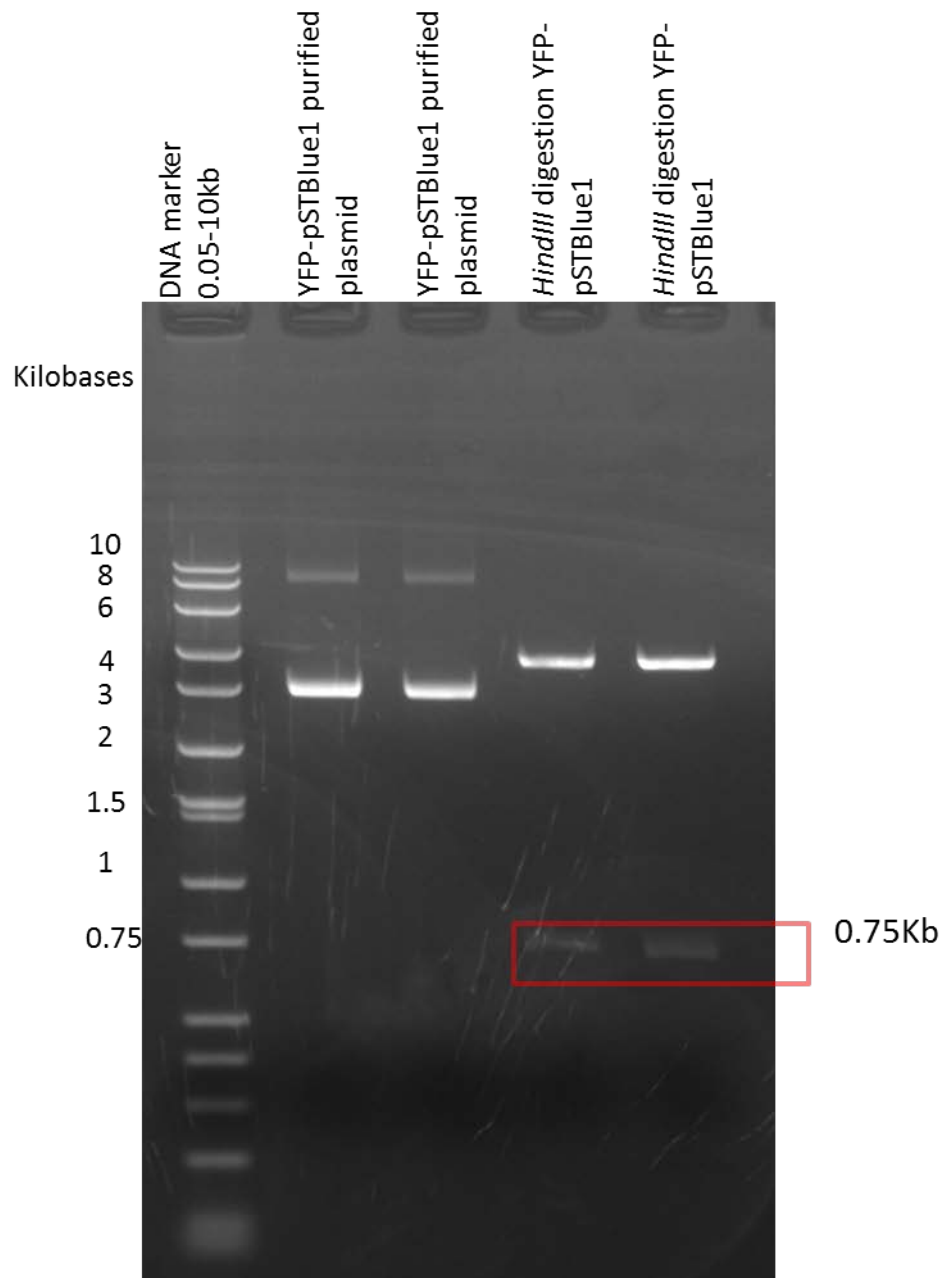


Figure 3.20 Agarose gel electrophoresis of the digestion of the purified YFP-pSTBlue1 plasmid using *HindIII*. Lane 1 is the 2-log marker DNA. Lanes 2 and 3 shows the purified undigested YFP-pSTBlue1 plasmids. Lane 4 and 5 show the *HINDIII* digested plasmid, 0.7Kb band of YFP cuts out and upper band represents cut pSTblue1 parent vector.

3.19 *EcoRI* digestion of YFP-psTBlue1 plasmid

The above (Figure 3.20) YFP 0.75 Kb insert DNA was then subjected to second digestion using *EcoRI* (NEB) in buffer 2 for 4 hours at 37°C. A control digestion of

YFP-pSTblue 1 plasmid using only *EcoRI* was set up to ensure the efficiency of the enzyme. Figure3.21 also represents digestion of CFP-TG2-pTrcHisB plasmid digestion using *HindIII*. It was observed that *EcoRI* digestion of YFP insert (*HindIII* digested) was successful as the control digestion cut out YFP insert (0.75Kb). CFP-TG2-pTrcHisB plasmid digestion with *HindIII* was confirmed (Figure3.22).

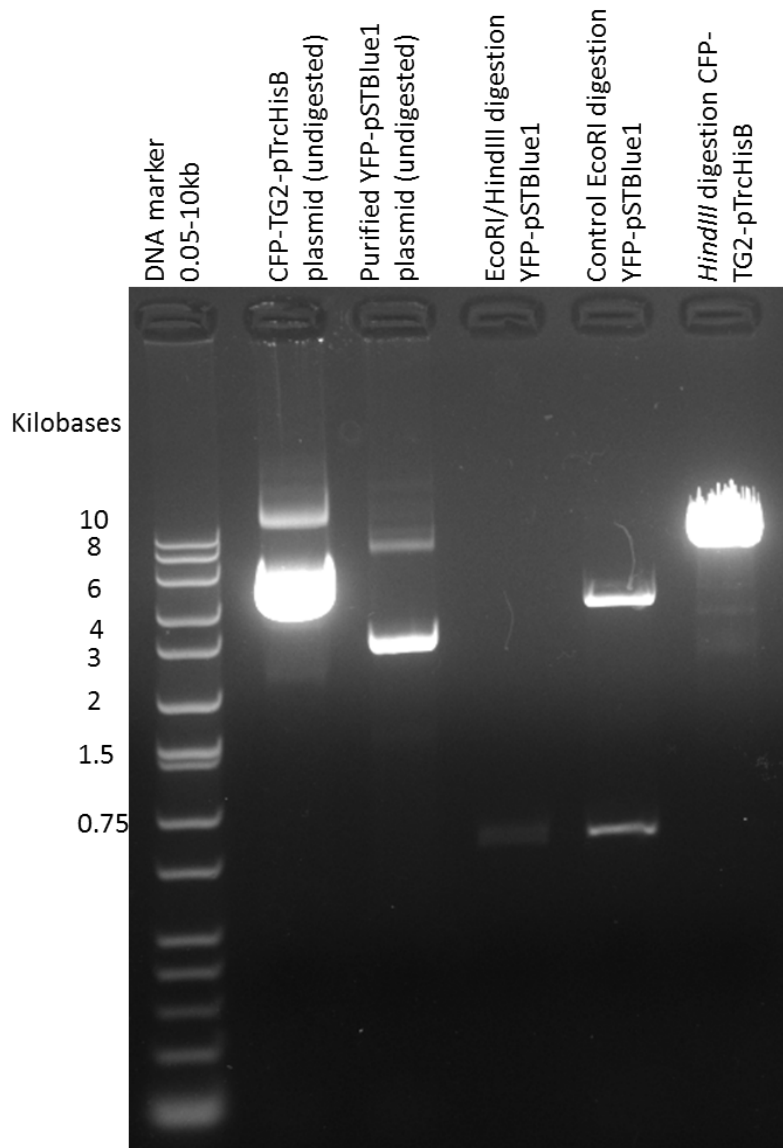


Figure 3.21 Agarose gel electrophoresis of the double digestion of the purified YFP-pSTBlue1 plasmid using *EcoRI/HindIII*. Lane 1 is the 2-log marker DNA. Lanes 2 shows purified CFP-TG2-pTrcHisB plasmid. Lane 3 shows the purified undigested YFP-pSTBlue1 plasmids. Lane 4 presents *EcoRI/HindIII* digestion of YFP-psTblue-1 with YFP band seen at 0.75Kb. Lane 5 show the control EcoRI digestion of YFP-psTblue1 plasmid, 0.75Kb band of YFP cuts out and upper band represents cut pSTblue1 parent vector. Lane 6 shows *HindIII* digestion of CFP-TG2-pTrcHisB plasmid.

3.20 *EcoRI* digestion of CFP-TG2-pTrcHisB plasmid

The CFP-TG2-pTrcHisB plasmid previously digested with *HindIII* was then digested with *EcoRI* (NEB) in buffer 2 for 4 hours at 37°C. A control CFP-TG2-pTrcHisB *EcoRI* only digest was simultaneously set up and resolved on a 1% (w/v) agarose gel (figure 3.22). It was observed that the control digestion showed some amount of uncut CFP-TG2-pTrcHisB plasmid (lower band).

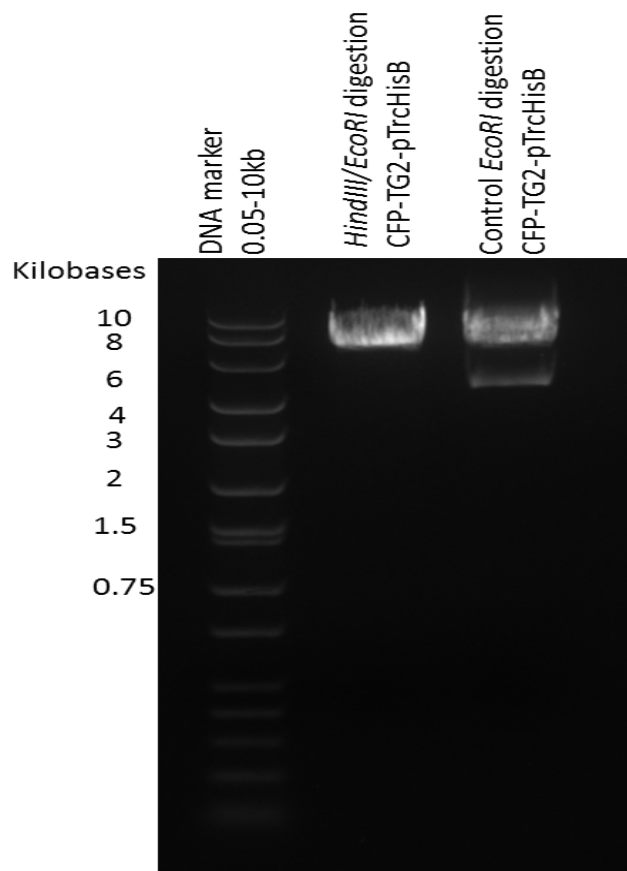


Figure 3.22 Agarose gel electrophoresis of the double digestion of CFP-TG2-pTrcHisB plasmid using *HindIII/EcoRI*. Lane 1 is the 2-log marker DNA. Lanes 2 shows double digested CFP-TG2-pTrcHisB plasmid of about 7.15Kb. Lane 3 shows the control *EcoRI* digestion of CFP-TG2-pTrcHisB plasmid.

3.21 Screening of recombinant CFP-TG2-YFP-pTrcHisB clones.

The double digested CFP-TG2-pTrcHis B plasmid and double digested YFP plasmid were extracted and purified from a low melting point agarose gel. Further a ligation reaction was performed using T4 DNA ligase and was then transformed into Novablue competent cells. A control self ligation (CFP-TG2 –pTrcHisB ligation) was also treated similarly. 21 transformed colonies were picked and further analysed by cracking procedure. Figure 3.23A and B reveals that all transformed colonies when run on test agarose gel show correct size of CFP-TG2-YFPpTrcHisB. The self ligated vector (CFP-TG2-pTrchisB) transformed colonies were analysed on the same gel (Figure 3. 23). An increase in size of plasmid (0.75Kb increase) was seen as compared to self ligated vector indicating the presence of YFP. Clones that indicated a larger plasmid size as compared to control were selected; clone 5, 6, 11, 12, 14, and 15. These were further grown and analysed.

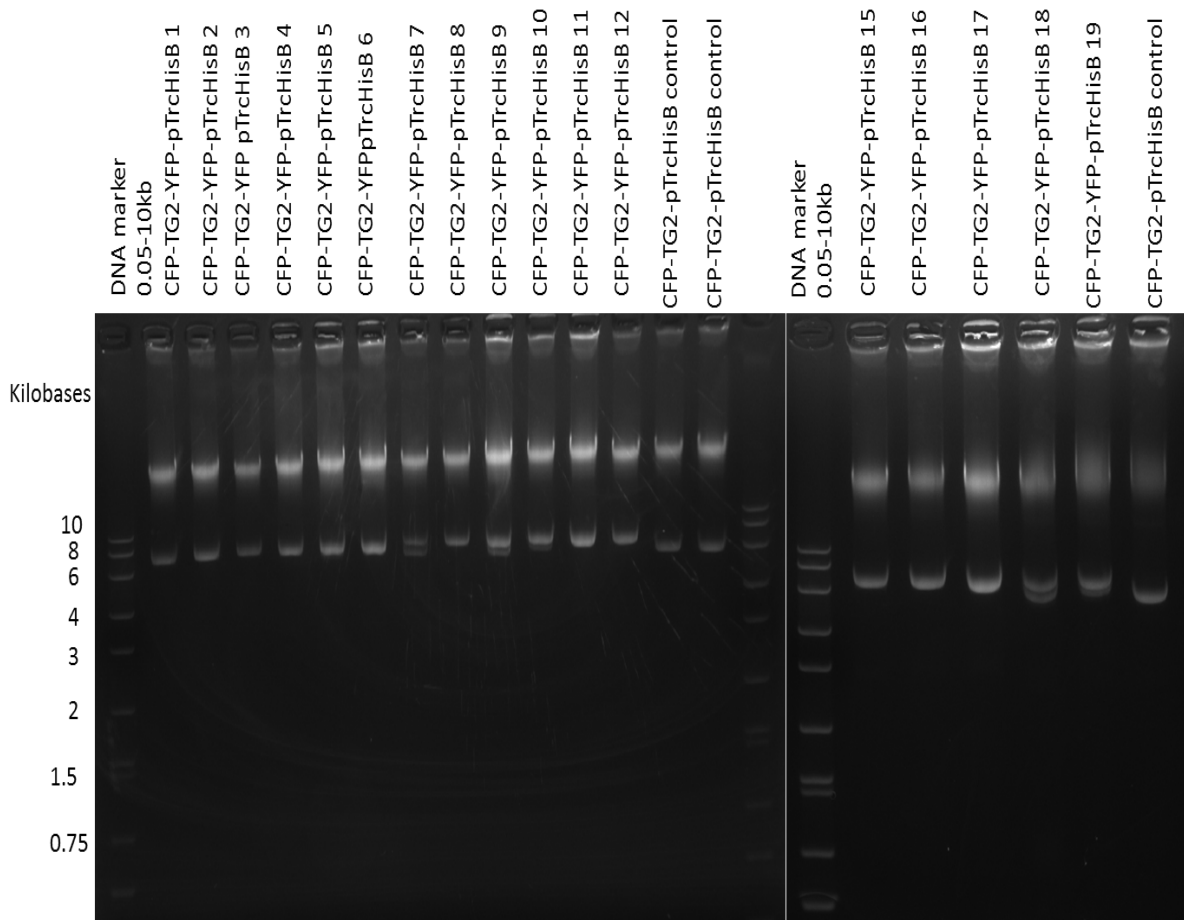


Figure 3.23A and 3.23B. Agarose gel electrophoresis of the cracking procedure performed on the selected CFP-TG2-YFP-pTrcHisB clones. Figure A, Lane 1 and Lane16 are the 2-log marker DNA. Lanes 2 to 13 showing CFP-TG2-YFP-pTrcHisB clones 1-12. Lane 14 and Lane 15 represent the cloning vector CFP-TG2-pTrcHisB (negative control). Figure B, Lane 1 is the 2-log marker DNA. Lane 7 represents the parent cloning vector pTrcHisB (negative control). Lanes 2 to 6 showing CFP-TG2-YFP-pTrcHisB clones 13-17. CFP-TG2-YFP-pTrcHisB clone 5, 6, 11, 12, 14 and 15 were selected for further analysis.

3.22 Restriction digestion test on selected CFP-TG2-YFP-pTrcHisB clones.

Clone 5, 6, 11, 12, 14, 15 (figure 3.23) were selected from the agar plate and then grown individually in 5ml LB broth containing ampicillin at 37°C in orbital shaking incubator overnight. Plasmids were isolated for further analysis. A test digest of these clones with *HindIII* and *EcoRI* should ideally result in YFP being cut out. With this in mind, clone5, 6, 11, 12, 14, 15 were digested with *HindIII*/*EcoRI* for 4 hours at 37°C. The digested products were run on a 1% (w/v) agarose gel and revealed

successful excision of YFP as seen by the 0.75Kb band (figure 3.24). The clones were further analysed by nucleotide sequencing. All clones were found to be of correct sequence.

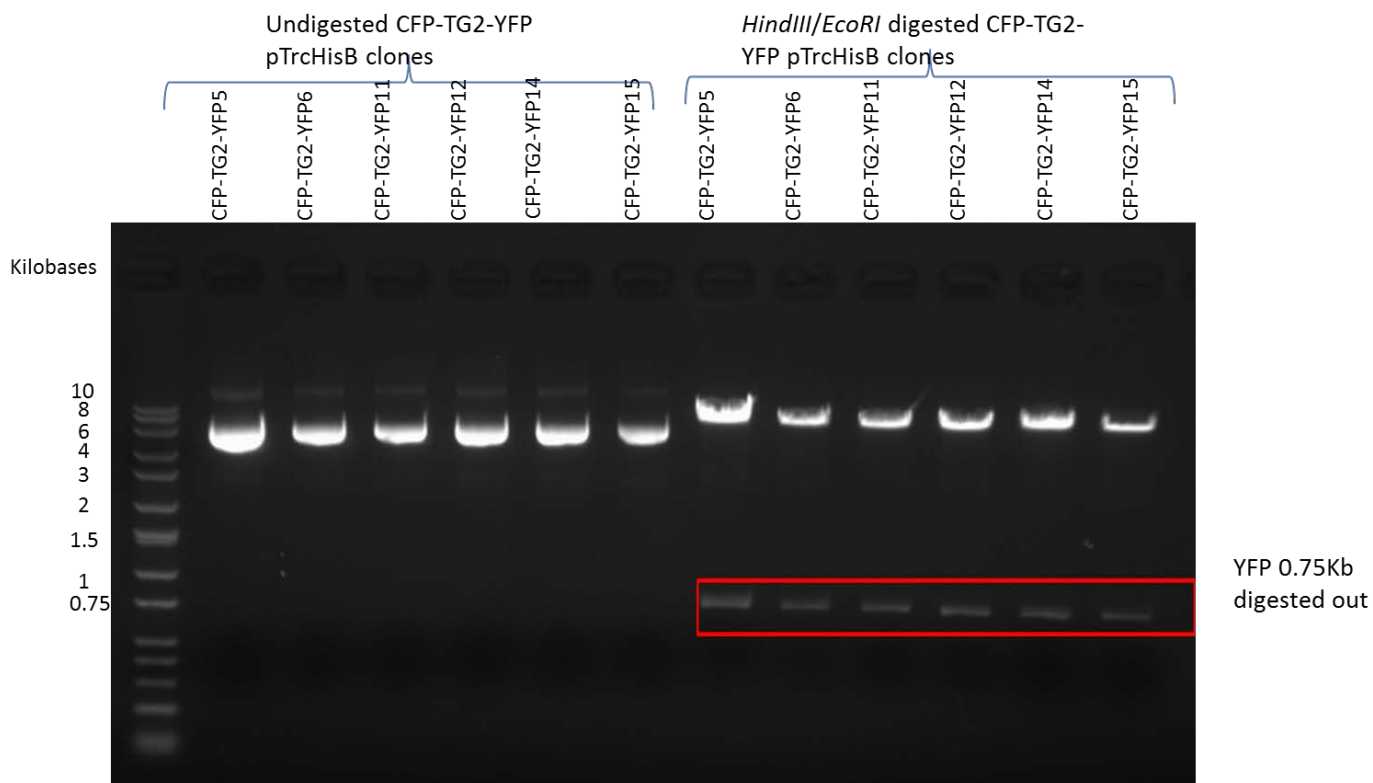


Figure 3.24 Agarose gel electrophoresis of the double digestion of the purified CFP-TG2-YFP-pTrcHisB clones. Lane 1 is the 2-log marker DNA. Lanes 2 to 7 shows purified CFP-TG2-pTrcHisB plasmids of clone 5, 6, 11, 12, 14 and 15. Lane 8 to 13 presents *HindIII* and *EcoRI* double digestion. The digestion resulted in excision of YFP as seen at 0.75Kb. These clones were further sent for nucleotide sequencing.

3.23 Discussion

The first part of the project was the construction of the TG2 FRET construct. In order to achieve this, the amplification of individual genes of CFP, YFP and TG2 was PCR amplified. One of the bottlenecks of this project was the PCR amplification of these fragments. In order to successfully amplify the CFP gene a variety of annealing temperatures were tried. In order to optimise the PCR amplification different reaction conditions were tested including the use of different polymerase, first including Pfu DNA polymerase. An attempt to alter the magnesium ion concentration to 1.5mM, 3.5mM and 6.5mM in its buffer to help stabilise the primer/template duplexes and reduce non-specific binding did not result in PCR amplification. By varying concentrations of DMSO from 1 to 10% didn't work and resulted in no amplification. The use of Taq polymerase with lower initial denaturation temperature also resulted in no amplification. It was then attempted to use a new vector for CFP, pAmcyan1-C1 and designed new primers accordingly. The PCR conditions for CFP were then optimised at initial denaturation at 98°C for 2 min, followed by 35 cycles of 98°C for 45 s, 65°C for 1 min, 72°C for 1 min, followed by a final extension step at 72°C for 10 min using Phusion Hot start polymerase. Similar PCR amplification was performed for TG2 and YFP. For TG2, conditions for PCR were optimised to be initial denaturation at 98°C for 2 min, followed by 35 cycles of 98°C for 45 s, 65°C for 1 min, 72°C for 3 min, followed by a final extension step at 72°C for 10 min using Phusion Hot start polymerase. For YFP, conditions for PCR were optimised to be initial denaturation at 98°C for 2 min, followed by 35 cycles of 98°C for 45 s, 65°C for 1 min, 72°C for 1.5 min, followed by a final extension step at 72°C for 10 min using Phusion Hot start polymerase.

The amplified PCR products were then sub-cloned into pSTblue-1, which is compatible with any DNA polymerase since the cloning kit contains a blunt ending step, and contains SP6/T7 promoters for in vitro transcription and sequencing. It also has dual EcoRI sites flanking the insert and also provides ampicillin selection. Utilising T4 DNA ligase, ligation reaction was set up effectively which favourably links sticky and blunt ends and also seals gaps in the phosphodiester backbone. This ligase is known to utilise ATP as the cofactor which is present in Quick buffer. The ligated reactions were transformed into E.coli Novablue competent cells. Cracking procedure was performed on selected white colonies and a blue colony used a negative control. Analysing the cracking results, all clones showing plasmids which were bigger than parent vector (blue colony) were sent for sequencing.

After the three components including CFP, TG2 and YFP were cloned and sequence confirmed in pSTblue-1, the assembly into pTrcHisB expression vector was performed. pTrcHis B expression vector was appropriately chosen for high levels of expression of recombinant protein using the *trc* promoter. The use of pTrcHisB expression vector also allowed the purification of recombinant proteins using immobilised metal affinity chromatography. CFP was inserted into the *Bam*HI site of pTrcHisB. Orientation of CFP cloning into pTrcHisB was important and clones of correct orientation were short-listed based on restriction digestion with *Bam*HI/*Bgl*II. The clones were further analysed on protein expression. No difference in protein expression was seen among the selected clones probably as CFP was optimised for mammalian expression. The cloning of TG2 and YFP into pTrcHisB was directional cloning. One of the problems faced during cloning of TG2 into pTrcHisB when the CFP-TG2-pTrcHisB clones were found to be of incorrect sequence due to the additional extra 'C' base pair in front of TG2 sequence. In order to save time, this

problem was solved using 3' end infilling. The sequence was then confirmed to have correct reading frame by nucleotide sequencing. The cloning of YFP was straightforward and the entire construct (CFP-TG2-YFP-pTrcHisB) was ready to be further analysed for expression.

Chapter 4

Expression and characterisation of construct

4.1 Introduction

After the cloning was completed, the construct was tested for its ability to retain properties of TG2. The recombinant protein was attempted to be expressed and purified over a nickel column. During the purification of recombinant CFP-TG2-YFP many conditions of elution were tried to find out the best optimum purification protocol. This construct was tested for its ability to be affected by the use of TG2 inhibitors. Since TG2 is known to bind to heparin sepharose, the constructed recombinant FRET sensor was also tested for its ability to bind to heparin sepharose. TG2 activity was assessed by incorporation of biotin cadaverin into fibronectin and N,N'dimethyl casein. Interestingly activity was TG2 was assessed with increasing concentration of calcium and GTP and then compared to RhTG2 and FRET control CFP-TG2.

4.2 Expression of CFP-pTrcHisB

A time course expression of CFP-pTrcHis B plasmid transformed into Novablue cells was set up. A single colony of Clone 3, 5 and 12 (figure 4.1) was inoculated in 2ml of LB broth containing ampicillin (50µg/ml) and grown overnight at 37°C in an orbital shaker. A 50ml culture was setup using this 1/10th volume of this overnight grown culture. Cells were grown at 37°C for 4 hours until mid-log phase and then induced with 1mM IPTG. 1ml sample were collected prior to IPTG induction as time zero sample. Samples were then collected after every one hour for and treated according to Invitrogen's Pilot expression protocol of pTrcHis recombinant protein. SDS page analysis of recombinant protein expression (CFP-pTrcHis B) showed expression of CFP at 30kDa but there was no difference seen in expression between clones 3, 5 and 12 as seen in figure 4.1.

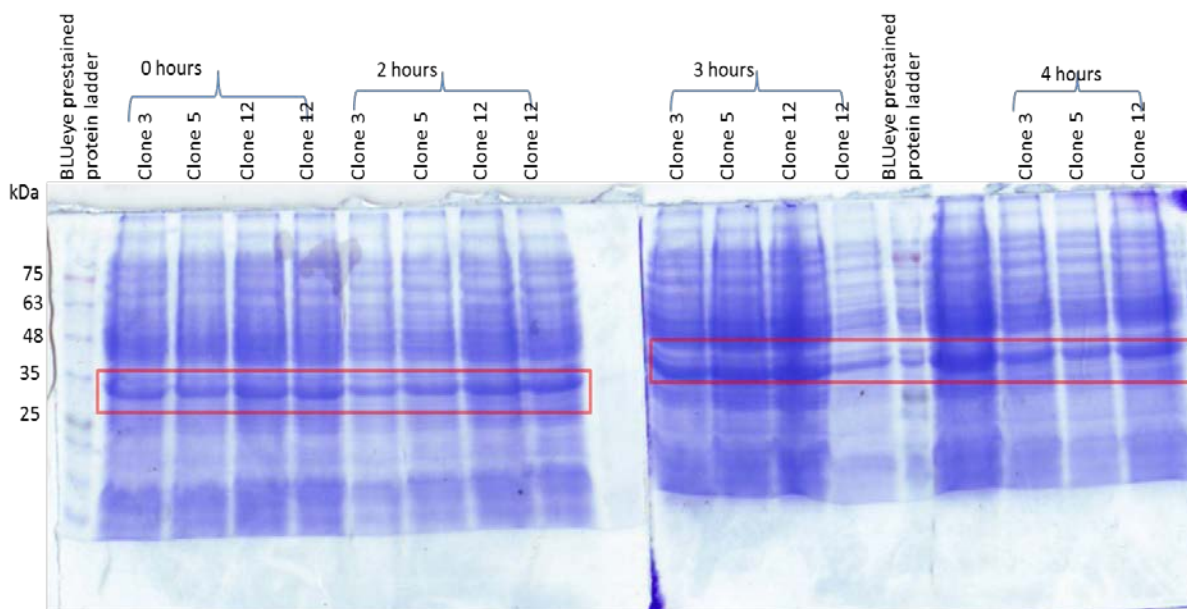


Figure 4.1 SDS PAGE analysis of expression of CFP by CFP-pTrcHisB clones. Lane 1 is the BLUeye prestained protein ladder. These clones were further sent for nucleotide sequencing. 30kDa protein is seen expressed in clones 3, 5 and 12. No significant difference was observed in expression between the clones. These clones were further analysed by nucleotide sequencing.

4.3 Expression and Purification of CFP-TG2-YFP recombinant protein

CFP-TG2-YFP clone 5 was randomly selected (all clones figure 4.1 were found to be of correct sequence), inoculated in 5 ml of LB with ampicillin (50µg/ml) and grown overnight at 37°C using an orbital shaker. This overnight grown culture was inoculated into 500ml of LB with ampicillin and grown for 4 hours until OD is about 1.0 at 600nm. The cells were then induced with 0.1mM IPTG and using the purification protocol cell lysate was applied to His GraviTrap column (GE Healthcare).

4.4 Chromatographic purification of His-tagged proteins using His GraviTrap column

CFP-TG2-YFP recombinant protein was expressed in Novablu cells and protein purification was performed using His GraviTrap columns. The recombinant protein was eluted using 10mls of elution buffer containing 200mM imidazole. The collected 1ml fractions were analysed using SDS-PAGE analysis (figure 4.2) to check expression and purification. It was observed that protein of correct size of about 135kDa was seen fractions 2 and 3 but the expression was weak. The load and flowthrough analysed on the SDS-PAGE also showed the presence of protein. Presence of protein in flow through indicated that all protein did not efficiently bind to the column. The CFP-TG2-YFP plasmid was then transformed into Rosetta 2 cells for efficient mammalian gene expression.

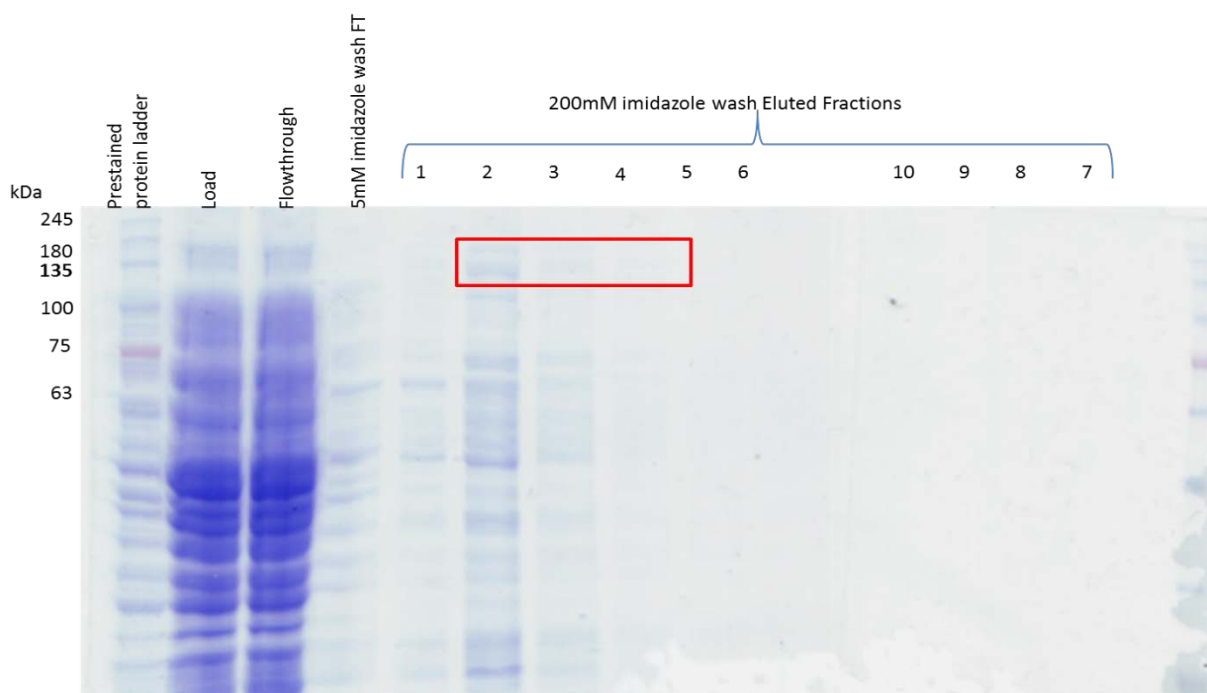


Figure 4.2 SDS PAGE analysis CFP-TG2-YFP recombinant protein expressed in Novablu cells and purified using His GraviTrap column (GE Healthcare). Prestained protein marker is seen in Lane 1. Lane 2 depicts the cell lysate applied to the column (load). The load flowthrough is collected and seen in Lane3. A 5mM imidazole wash was performed to get rid of unbound protein and is seen in Lane4. Protein elution was performed over 10ml using buffer containing 200mM imidazole. Protein of interest (135kDa, red box) was seen in fractions 2 and 3.

4.5 Fractions of protein purified on His GraviTrap column

Fractions that were eluted using 200mM wash of imidazole using His GraviTrap column were analysed by western blotting using Cub7402 (figure 4.3). CFP-TG2-YFP recombinant protein was seen present in the load, flowthrough, 5mM wash and eluted fractions using imidazole.

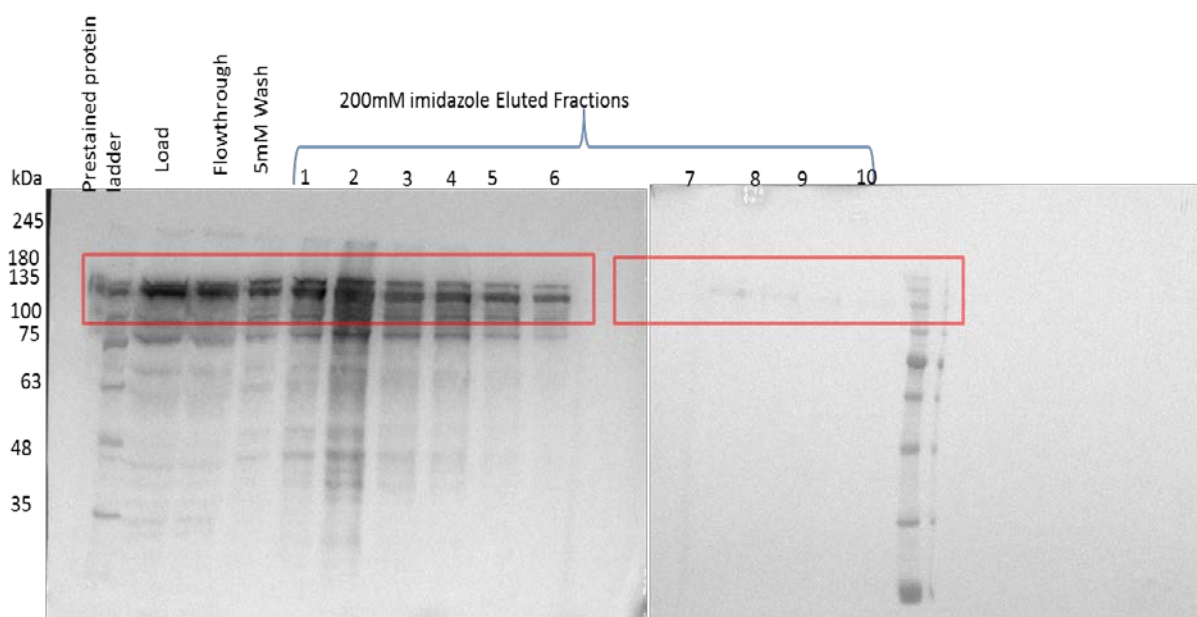


Figure 4.3 Western blot analysis of CFP-TG2-YFP recombinant protein purification using His GraviTrap column (GE Healthcare). Western blot analysis using anti-transglutaminase 2 antibody Cub7402 revealed presence of 135kDa recombinant protein.

4.6 Gradient purification using GE AKTA prime FPLC

To improve protein purification, CFP-TG2-YFP plasmid was transformed into Rosetta 2 cells. The cells were grown and induced using IPTG. Cells were further lysed and applied to Ni-NTA column. A 20mM imidazole wash was performed to elute unbound protein. The 20mM wash samples show non-specifically bound protein being eluted (contaminated protein). Gradient elution was performed from 20mM to 200mM imidazole. Protein of interest of about 135kDa was seen being eluted from 60mM to 110mM imidazole (figure 4.4). Specific activity of purified protein was found to be 4.5 OD490/min/mg.

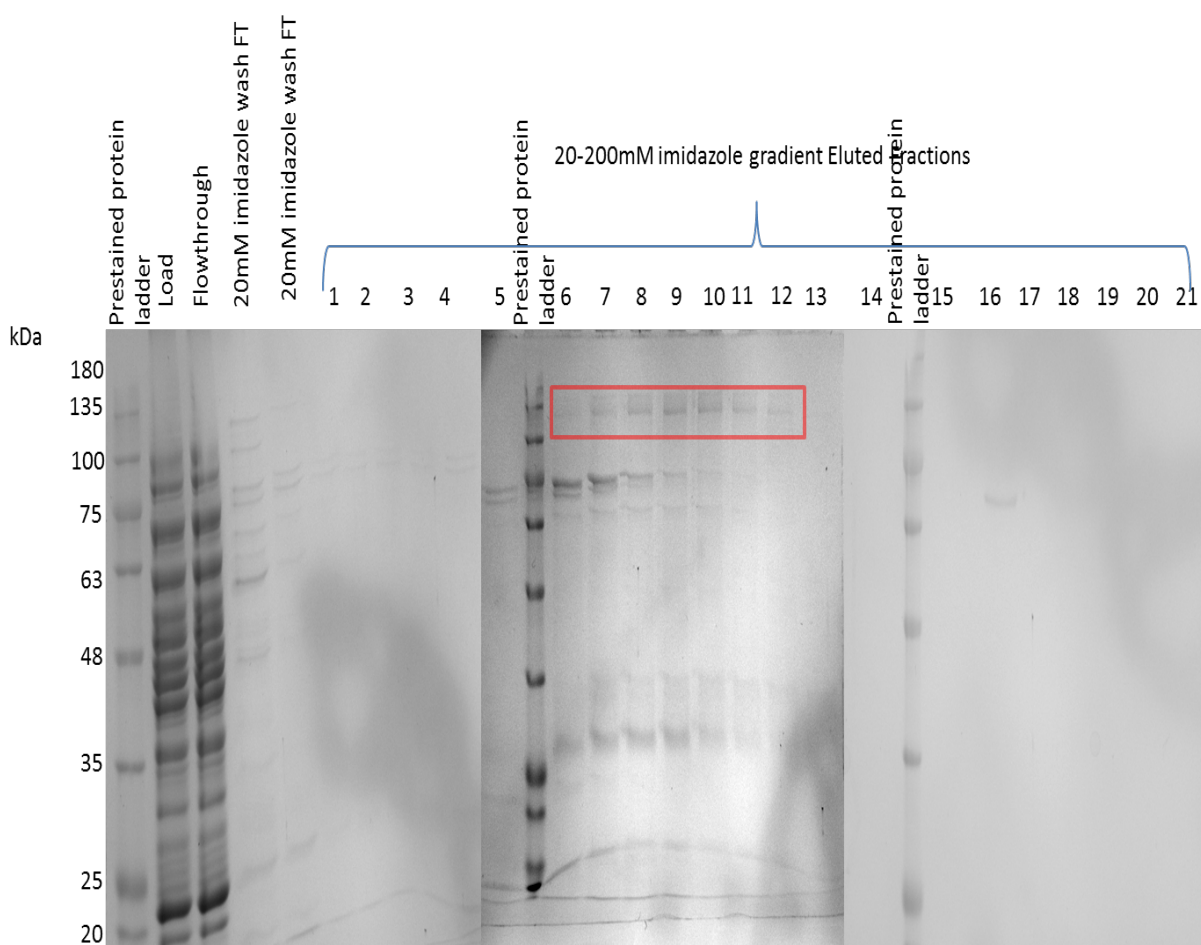


Figure 4.4 SDS PAGE analysis CFP-TG2-YFP recombinant protein expressed in Rosetta cells and purified using Ni-NTA column (GE AKTA prime FPLC). Prestained protein marker is seen in Lane 1. Lane 2 depicts the cell lysate applied to the column (load). The load flowthrough is collected and seen in Lane3. A 20mM imidazole wash was performed to get rid of unbound protein and is seen in Lane4 and Lane5. Protein elution was performed over 20ml using gradient elution from 20mM to 200mM imidazole. Protein of interest (135kDa, red box) was seen in fractions 7 and 11.

4.6.1 Western blot analysis of 20mM-200mM imidazole gradient eluted fractions

CFP-TG2-YFP recombinant protein was expressed in Rosetta 2 cells. The purification was performed using GE Ni-NTA column. The purification was performed using a 20mM imidazole wash, followed by a gradient elution from 20mM to 200mM (40ml/ 20 fractions) Western blotting was performed on peak fractions that were first

confirmed using SDS-PAGE stained using coomassie blue. The presence of TG2 antigen was analysed by western blotting using Cub7402. Protein of interest of about 135kDa was seen being eluted from 60mM to 110mM imidazole (figure 4.5).

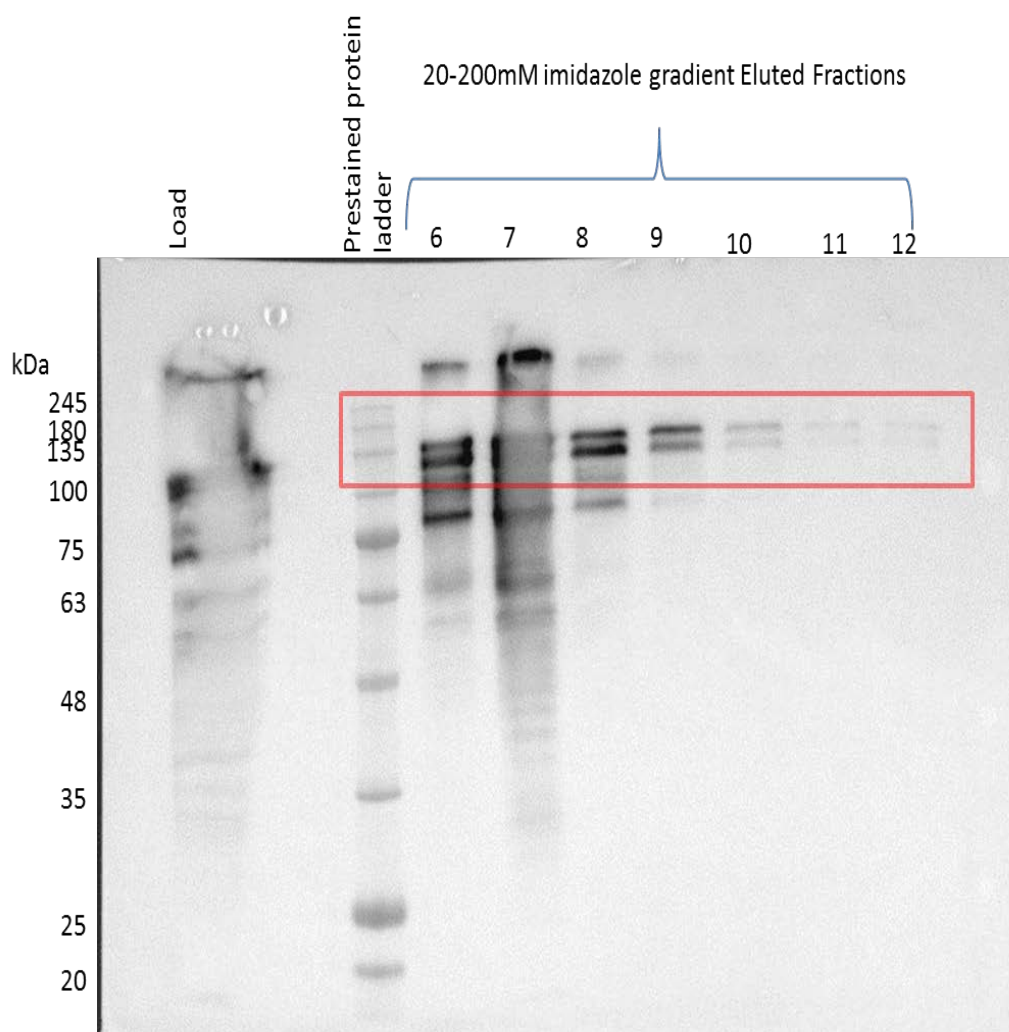


Figure 4.5 Western blot analysis of CFP-TG2-YFP recombinant protein purification using Ni-NTA column. Western blot analysis using anti-transglutaminase 2 antibody Cub7402 revealed presence of 135kDa recombinant protein.

Inspite of successful purification, the above purification showed non-specific interactions and unwanted protein was eluted with protein of interest. To get rid of the unwanted proteins (around 75kDa and below) an attempt was made to wash with higher concentration of imidazole. The figure 4.6 depicts CFP-TG2-YFP recombinant

protein purification. Prior to elution, a 25mM imidazole wash was performed to get rid of non-specific interactions. CFP-TG2-YFP recombinant protein was eluted in fractions 6 and 7. Specific activity was found to be 4.34 OD490/min/mg. Unwanted protein seen of size around 75kDa was still purified along with protein of interest.

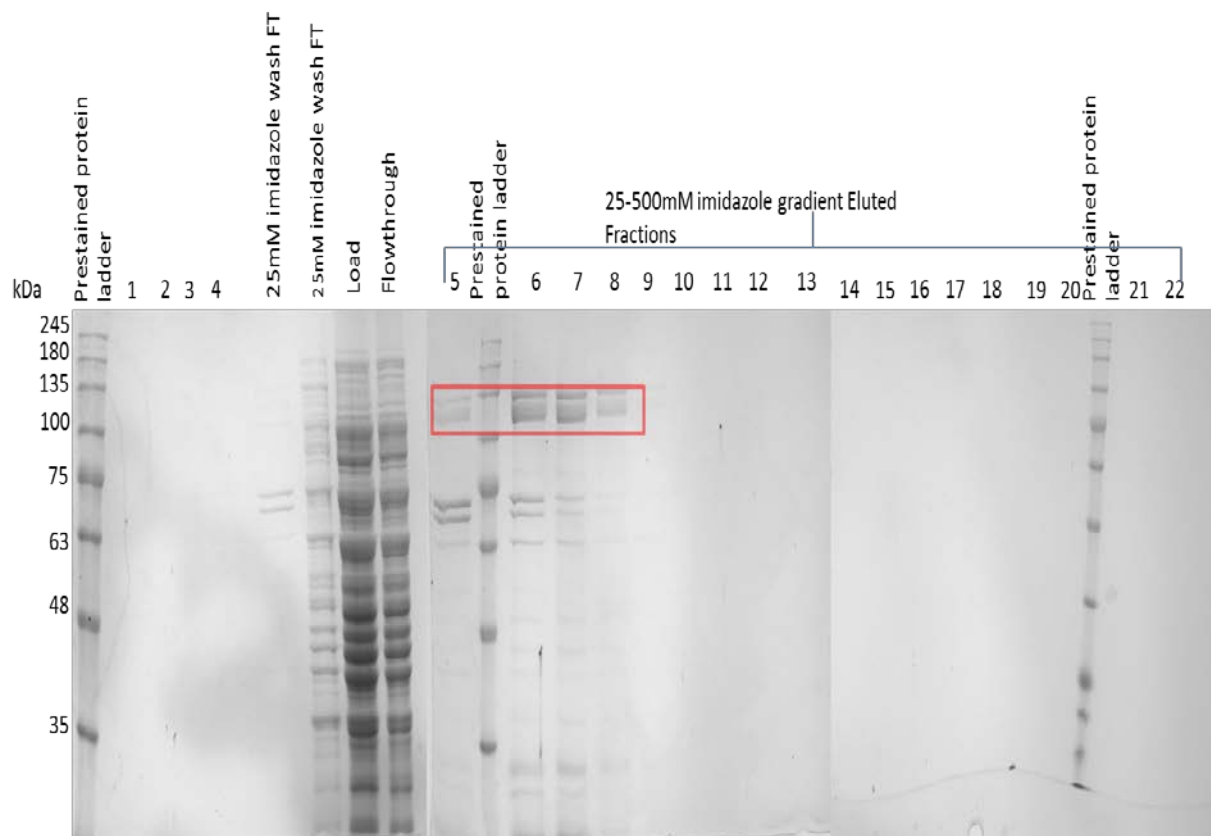


Figure 4.6 SDS PAGE analysis CFP-TG2-YFP recombinant protein expressed in Rosetta cells and purified using Ni-NTA column (GE AKTA prime FPLC). Prestained protein marker is seen in Lane 1. Lane 8 depicts the cell lysate applied to the column (load). The load flowthrough is collected and seen in Lane9. A 25mM imidazole wash was performed to get rid of unbound protein and is seen in Lane6and Lane7. Protein elution was performed over 20ml using gradient elution from 25mM to 500mM imidazole. Protein of interest (135kDa, red box) was seen in fractions 6 and 7. Fractions 21 and 25 represent elution at highest concentration (500mM) imidazole.

4.6.2 25mM-500mM imidazole gradient eluted fractions

The purification was performed using a 25mM imidazole wash, followed by a gradient elution from 25mM to 500mM (40ml/ 20 fractions) as seen in figure 4.7. Western blotting was performed on peak fractions that were first confirmed using SDS-PAGE stained using coomassie blue. The presence of TG2 antigen was analysed by western blotting using Cub7402.

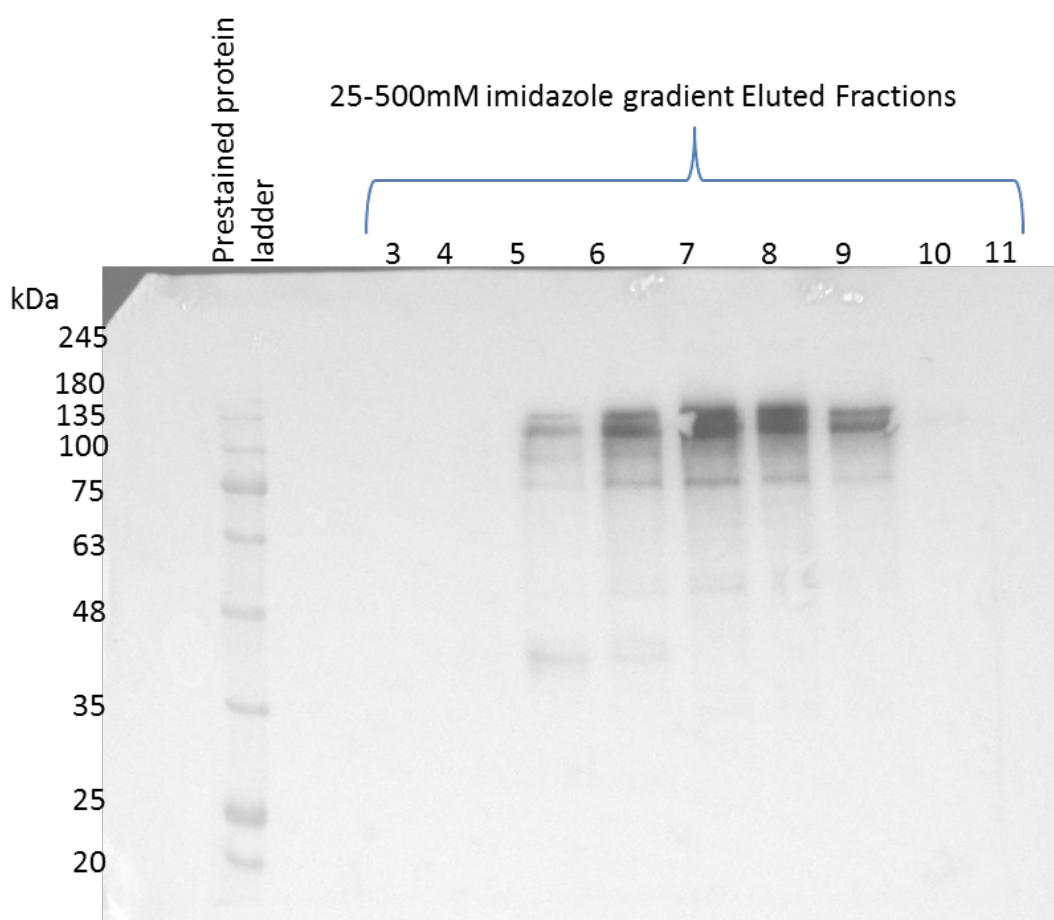


Figure 4.7 Western blot analysis of CFP-TG2-YFP recombinant protein purification using Ni-NTA column using 25-500mM imidazole gradient elution. Western blot analysis using anti-transglutaminase 2 antibody Cub7402 revealed presence of 135kDa recombinant protein.

Further purification was performed applying a 30mM imidazole wash followed by a gradient elution from 30mM to 500mM imidazole (figure 4.8). CFP-TG2-YFP recombinant protein was purified but the yield (specific activity 1.33 OD490/min/mg).

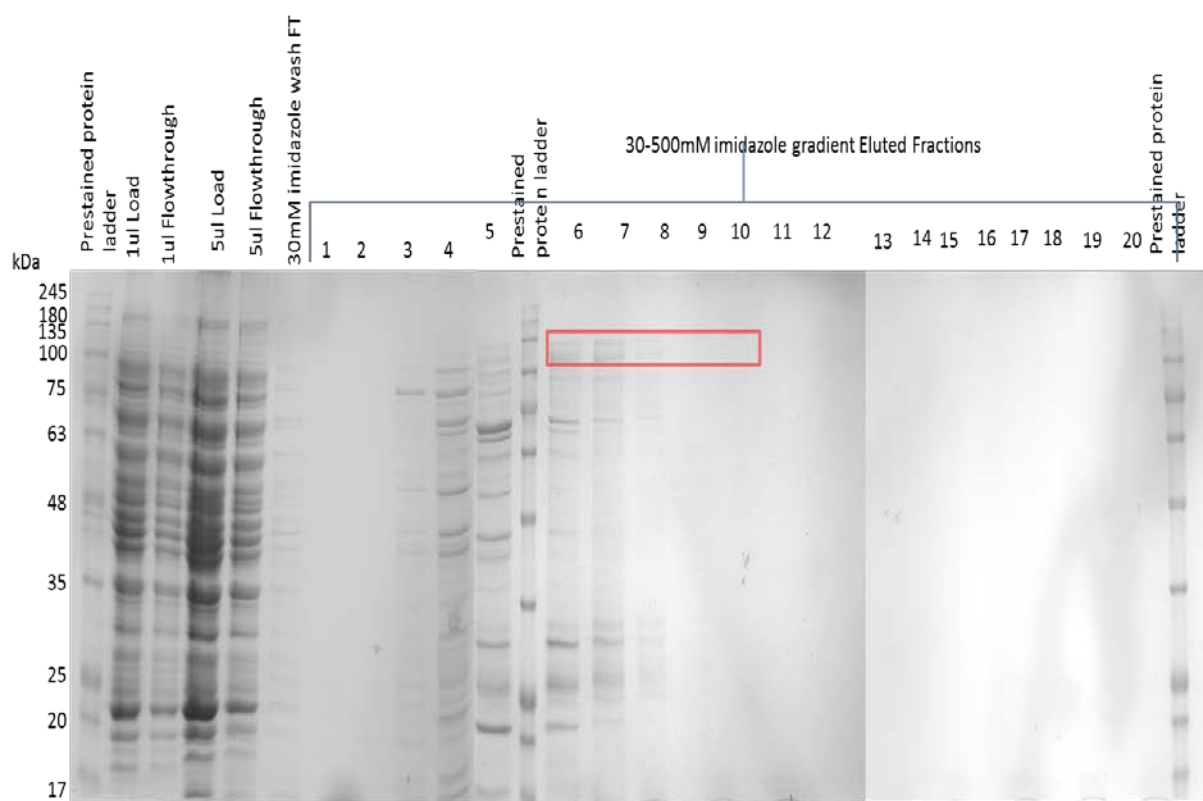


Figure 4.8 SDS PAGE analysis CFP-TG2-YFP recombinant protein expressed in Rosetta cells and purified using Ni-NTA column (GE AKTA prime FPLC). Prestained protein marker is seen in Lane 1. Lane 7 and 9 depicts the cell lysate applied to the column (load). The load flowthrough is collected and seen in Lane 6 and 8. A 30mM imidazole wash was performed to get rid of unbound protein and is seen in Lane 5. Protein elution was performed over 20ml using gradient elution from 30mM to 500mM imidazole. Protein of interest (135kDa, red box) was seen in fractions 7 and 8.

4.6.3 30mM-500mM imidazole gradient eluted fractions

The purification was performed using a 30mM imidazole wash, followed by a gradient elution from 30mM to 500mM (40ml/ 20 fractions) Western blotting was

performed on peak fractions that were first confirmed using SDS-PAGE stained using coomassie blue. The presence of TG2 antigen was analysed by western blotting using Cub7402. Protein of interest of about 135kDa was seen being eluted from 60mM to 110mM imidazole (figure 4.9).

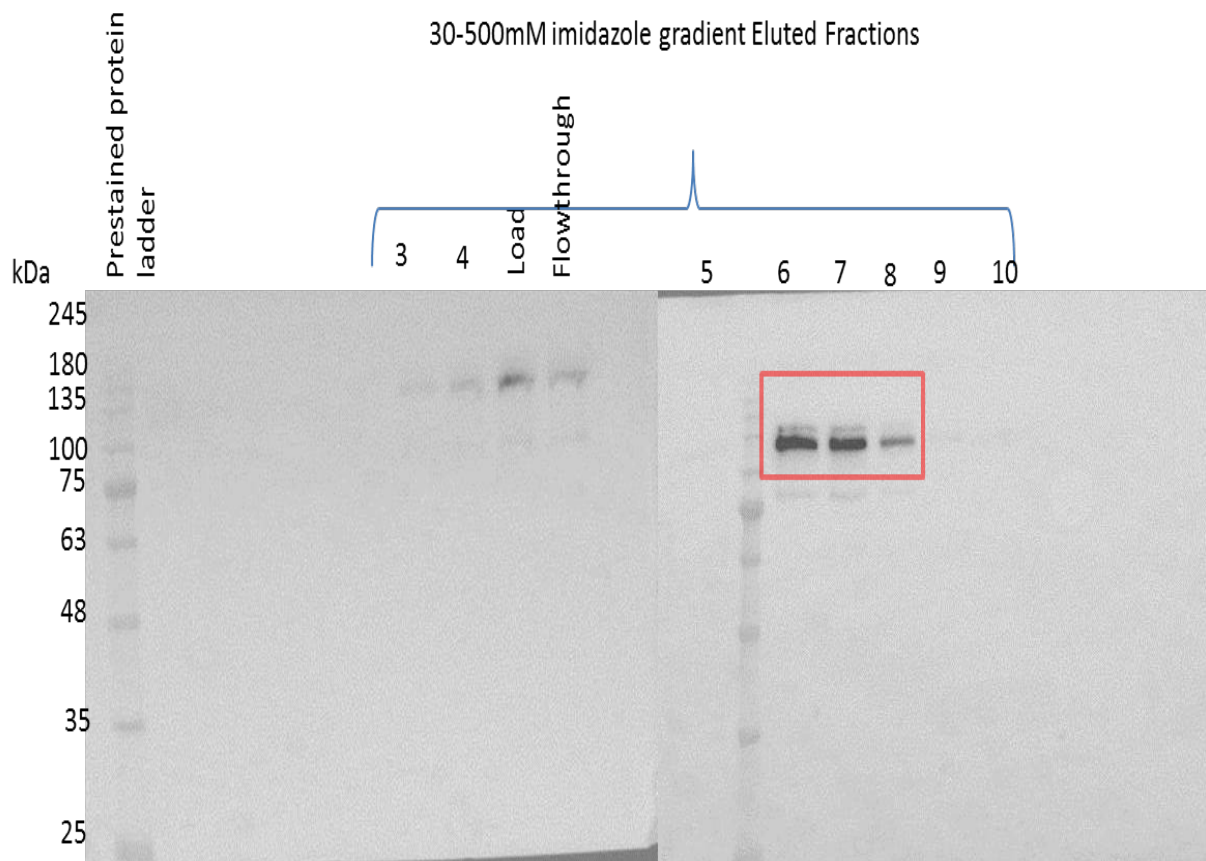


Figure 4.9 Western blot analysis of CFP-TG2-YFP recombinant protein purification using Ni-NTA column using 30-500mM imidazole gradient elution. Western blot analysis using anti-transglutaminase 2 antibody Cub7402 revealed presence of 135kDa recombinant protein.

Purification of CFP-TG2-YFP recombinant protein was repeated by gradient eluting protein over 20 ml (shallow gradient) figure 4.10. At the end of gradient elution, fractions were collected at 200mM imidazole. The purified fractions were then run and analysed using SDS-PAGE. Coomassie staining of SDS-PAGE did not show

presence of recombinant protein in eluted fractions. CFP-TG2-YFP recombinant protein (135kDa) was seen in load and flowthrough samples.

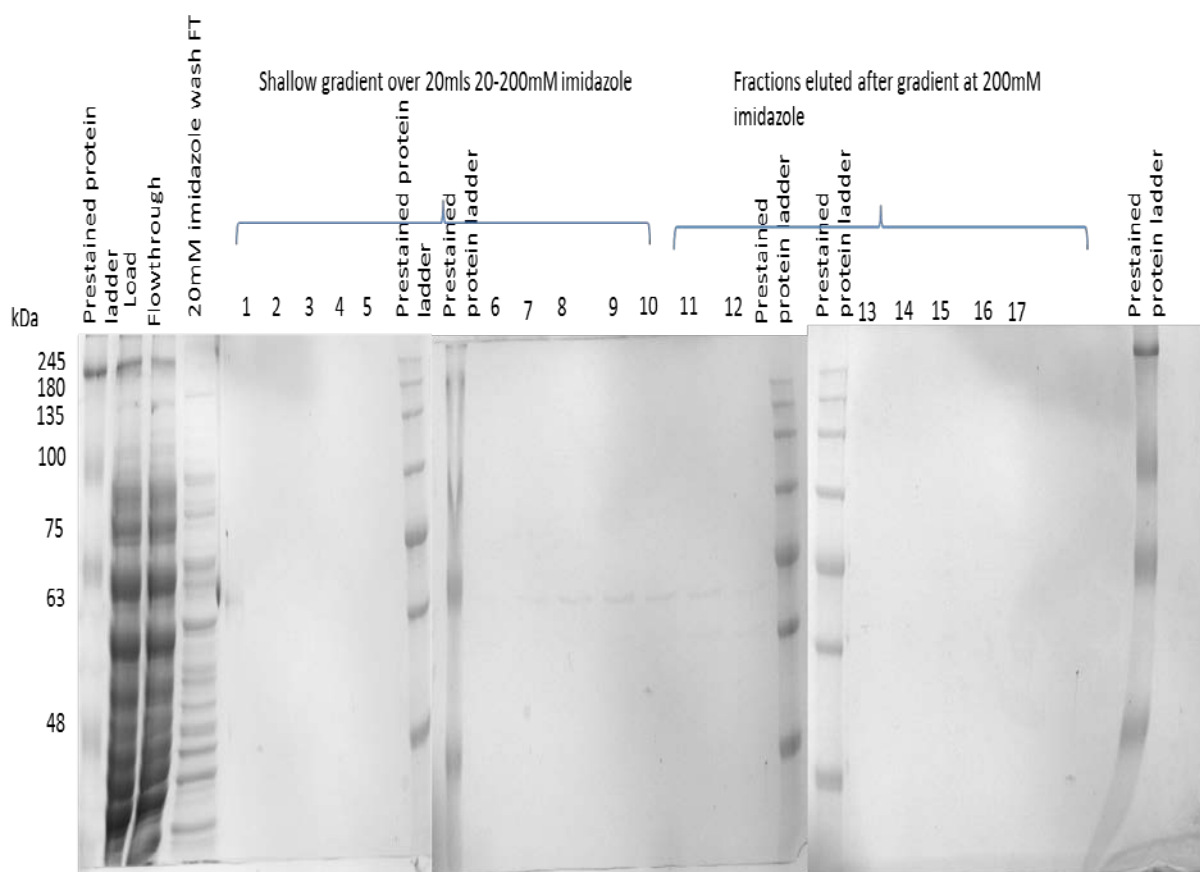


Figure 4.10 SDS PAGE analysis CFP-TG2-YFP recombinant protein using a shallow gradient of 20ml. Prestained protein marker is seen in Lane 1,10,11,20. Lane 2 depicts the cell lysate applied to the column (load). The load flowthrough is collected and seen in Lane 3. A 20mM imidazole wash was performed to get rid of unbound protein and is seen in Lane 4. Protein elution was performed over 20ml using gradient elution from 20mM to 200mM imidazole. Protein of interest 135kDa was not seen in purification.

Since the purification of CFP-TG2-YFP recombinant protein using shallow gradient (elution over 20mls) did not show presence of protein in eluted fractions , purification was repeated by gradient eluting protein over 40 ml (steep gradient).A wash was performed using 25mM imidazole wash. The purified fractions were then analysed

using SDS-PAGE revealed the presence of 135kDa in fractions 7, 8, 9, 10, 11 and 12 (figure 4.11). Specific activity was found to be 3.8 OD490/min/mg.

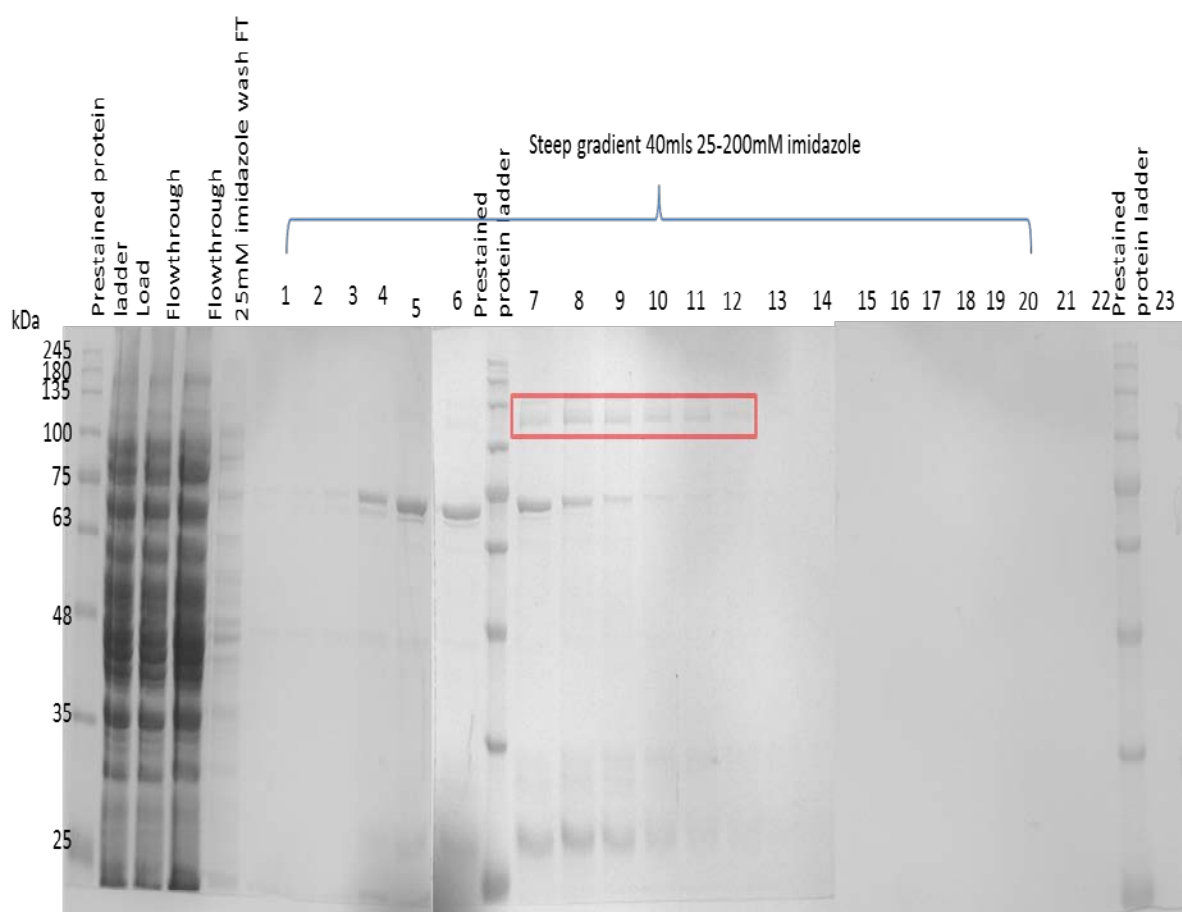


Figure 4.11 SDS PAGE analysis CFP-TG2-YFP recombinant protein expressed in Rosetta cells and purified using Ni-NTA column (GE AKTA prime FPLC). Prestained protein marker is seen in Lane 1. Lane 3 depicts the cell lysate applied to the column (load). The load flowthrough is collected and seen in Lane 4 and 5. A 25mM imidazole wash was performed to get rid of unbound protein and is seen in Lane 5. Protein elution was performed over 40ml using gradient elution from 25mM to 200mM imidazole. Protein of interest (135kDa, red box) was seen in fractions 7 to 12.

4.6.4 Steep 25mM-200mM imidazole gradient eluted fractions

The purification was performed using a 25mM imidazole wash, followed by a gradient elution from 25mM to 200mM (40ml/ 20 fractions) Western blotting was performed on peak fractions that were first confirmed using SDS-PAGE stained using coomassie blue. The presence of TG2 antigen was analysed by western blotting using Cub7402. Presence of protein of interest of about 135kDa was seen in fractions (figure 4.12).

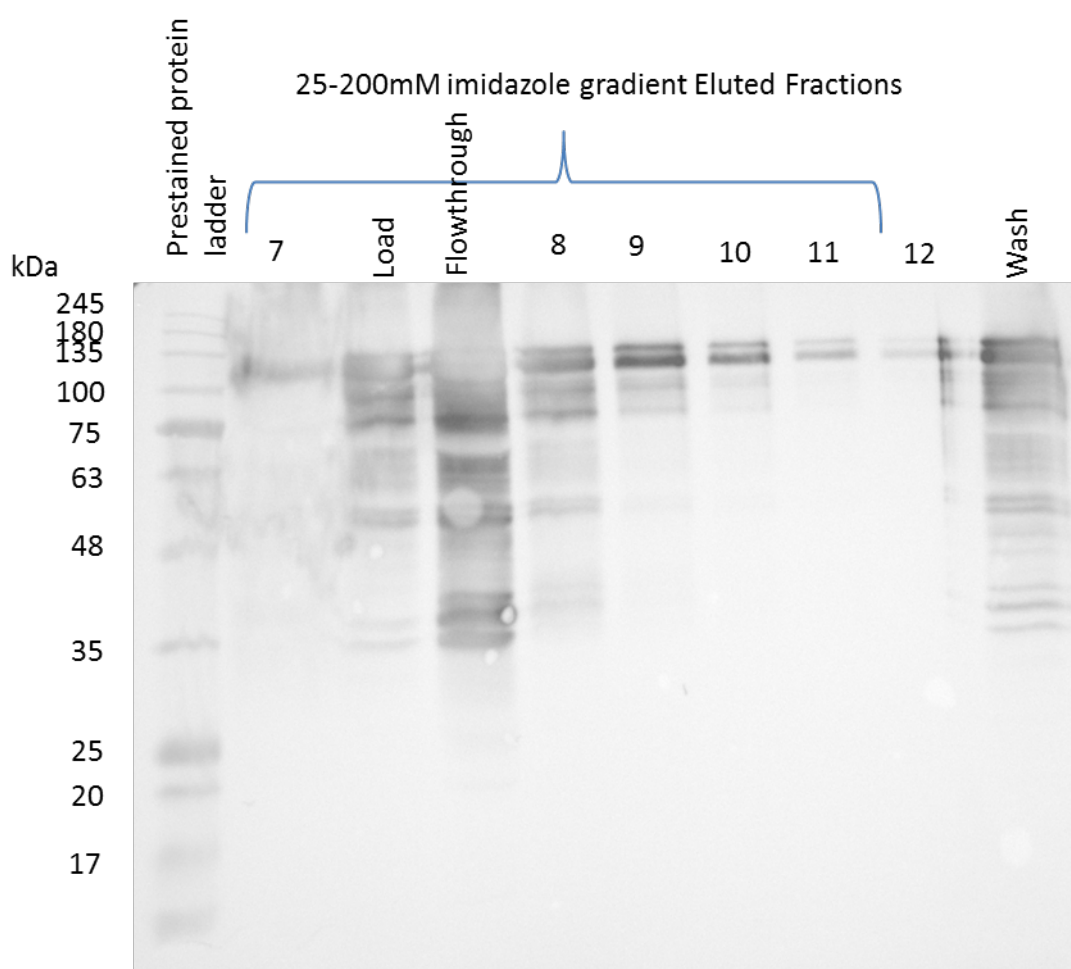


Figure 4.12 Western blot analysis of CFP-TG2-YFP recombinant protein purification using Ni-NTA column. Western blot analysis using anti-transglutaminase 2 antibody Cub7402 revealed presence of 135kDa recombinant protein.

4.7 Control CFP-TG2 recombinant protein purification

CFP-TG2 (control) recombinant protein was purified using same protocol as CFP-TG2-YFP recombinant protein purification using the Ni-NTA column. Protein was eluted using a 20-200mM imidazole gradient using 40ml volume. Out of the 20 fractions collected over the elution, fractions 5 to 20 and fraction 21, 22(200mM imidazole elution after gradient) fractions were run on a SDS-PAGE gel and analysed by coomassie staining. CFP-TG2 (100KDa) recombinant protein was seen (figure 4.13).

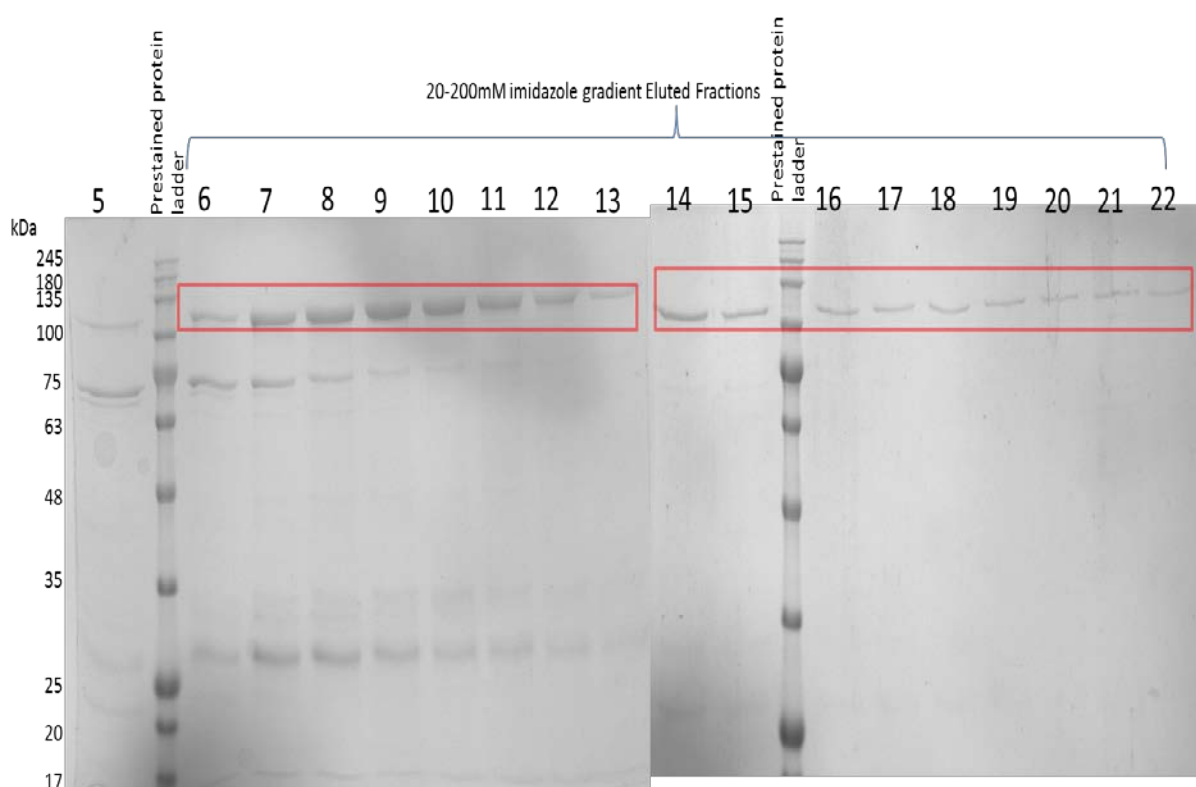


Figure 4.13 SDS PAGE analysis CFP-TG2 control recombinant protein expressed in Rosetta cells and purified using Ni-NTA column (GE AKTA prime FPLC). Prestained protein marker is seen in Lane 2. A 20mM imidazole wash was performed to get rid of unbound protein. Protein elution was performed over 40ml using gradient elution from 20mM to 200mM imidazole. Protein of interest (100kDa, red box) was seen in fractions elution fractions (7 to 12 peak fractions)

4.7.1 Western blot analysis of control CFP-TG2 purification eluted fractions

Western blotting was performed on peak fractions that were first confirmed using SDS-PAGE stained using coomassie blue. The presence of TG2 antigen was analysed by western blotting using Cub7402. Protein of interest of about 100Da was seen being eluted from 50mM to 110mM imidazole (peak fractions)

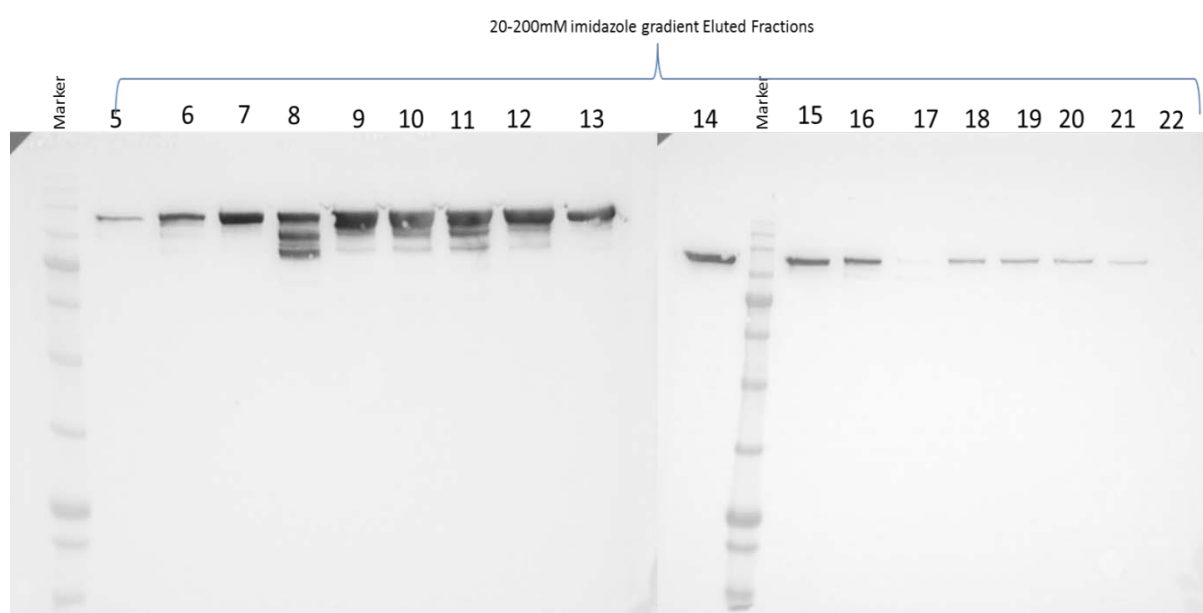


Figure 4.14 Western blot analysis of CFP-TG2 recombinant protein purification using Ni-NTA column over a 20-200mM imidazole gradient elution. Western blot analysis using anti-transglutaminase 2 antibody Cub7402 revealed presence of 100KDa recombinant protein.

4.8 Control wild type TG2-pET30ek/LIC purification (wild type TG2)

Wild type recombinant TG2 was purified using same protocol as CFP-TG2-YFP recombinant protein purification using the Ni-NTA column. Protein was eluted using a 20-200mM imidazole gradient using 40ml volume. All fractions of the purification

were analysed using SDS-PAGE analysis. Protein of correct size of about 80kDa was seen in fractions 5 to 13 (figure 4.15).

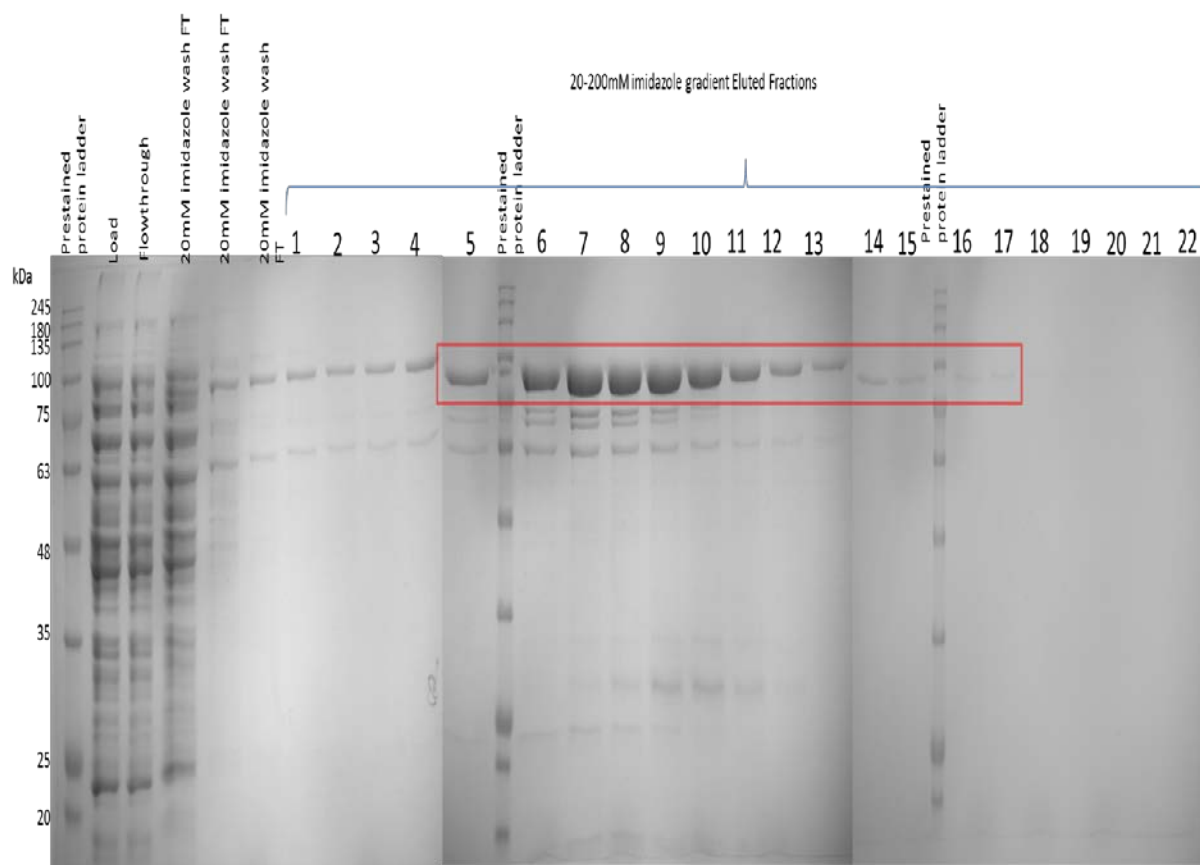


Figure 4.15 SDS PAGE analysis Control wild type TG2-pET30ek/LIC recombinant protein expressed in Rosetta cells and purified using Ni-NTA column (GE AKTA prime FPLC). Prestained protein marker is seen in Lane 1. Lane 2 depicts the cell lysate applied to the column (load). The load flowthrough is collected and seen in Lane 3. A 20mM imidazole wash was performed to get rid of unbound protein and is seen in Lane 4, 5 and 6. Protein elution was performed over 40ml using gradient elution from 20mM to 200mM imidazole. Protein of interest (80kDa, red box) was seen in fractions 5 to 13.

4.9 Binding of TG2 to Heparin-Sepharose

400ml of LB broth was inoculated with 20ml overnight culture of *E.coli* Rosetta2 CFPTG2YFP, cCFPTG2, pET30Ek/LIC TG2 and grown for 4 hours prior to induction with 1mM IPTG at 16°C overnight. Cells were centrifuged at 10000g for 15 min at 4°C. Cells were resuspended in bufferA (refer Material and methods) and thereafter

lysed. The cell lysate was centrifuged at 20000g for 30 min at 4°C. Heparin column was equilibrated using buffer A and the clarified lysate was loaded onto the column. Purification was performed using protocol by Wang *et al*, 2012. The column was washed with 25ml of buffer A and 1ml fractions were eluted with a linear gradient of increasing gradient of NaCl from 0 to 0.5M. Every alternate fraction of the gradient was run on a SDS page and analysed by western blotting.

4.9.1 Western blot analysis of CFPTG2YFP purification through heparin-Sepharose column

Western blot analysis revealed that recombinant CFP-TG2-YFP purified protein exhibited heparin binding capacity characteristic of tissue transglutaminase. The initial load and subsequent flow through were also collected and analysed on SDS-PAGE. After loading, wash fractions to get rid of unbound protein were also collected and analysed. Protein elution fractions (25 fractions of 1 ml each) were collected over a gradient of 0 to 0.5M NaCl. Every alternate fraction was analysed by running on SDS-PAGE and western blotting using Cub 7402 (figure 4.16).

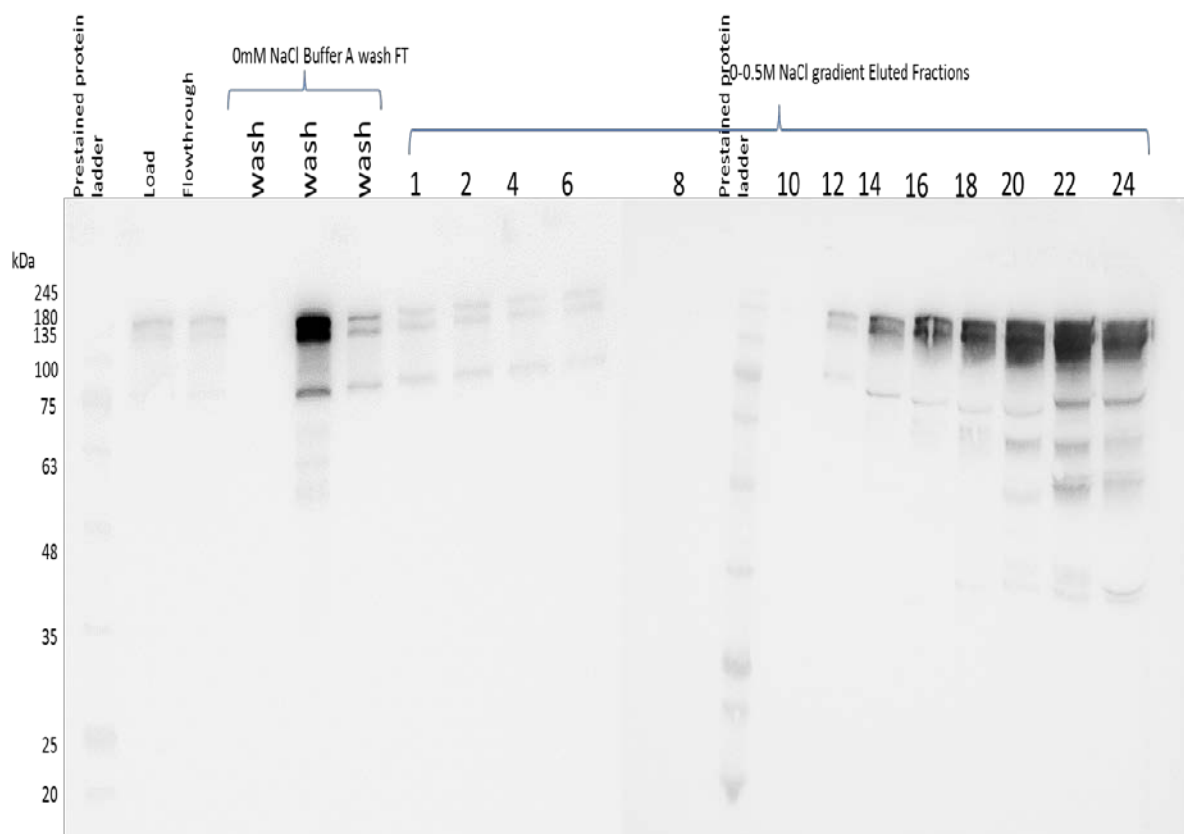


Figure 4.16 Western blot analysis of CFP-TG2-YFP recombinant protein purification over heparin sepharose column. Western blot analysis using Cub7402 revealed successfully purification of CFP-TG2-YFP recombinant protein as seen by band at about 135kDa. Load and flowthrough was seen in Lane 2 and 3 respectively. Subsequently loaded wash samples also showed presence protein of interest. CFP-TG2-YFP recombinant protein was seen being eluted from 12th fraction of gradient onwards (0.24M NaCl) upto 24th fraction (0.48M NaCl) with peak of elution seen at 22nd fraction (0.44M NaCl)

4.9.2 Western blot analysis of wild type TG2 purification eluted using heparin-Sepharose column

Similar to CFP-TG2-YFP recombinant protein purification, wild type TG2 (pET30Ek/LIC TG2) was also purified over the same heparin sepharose column. Load, flowthrough and subsequent wash samples were loaded and analysed (figure 4.17). Wild type TG2 showed affinity towards heparin sepharose column and purified protein fractions were eluted started from 0.28M NaCl upto 0.48M NaCl.

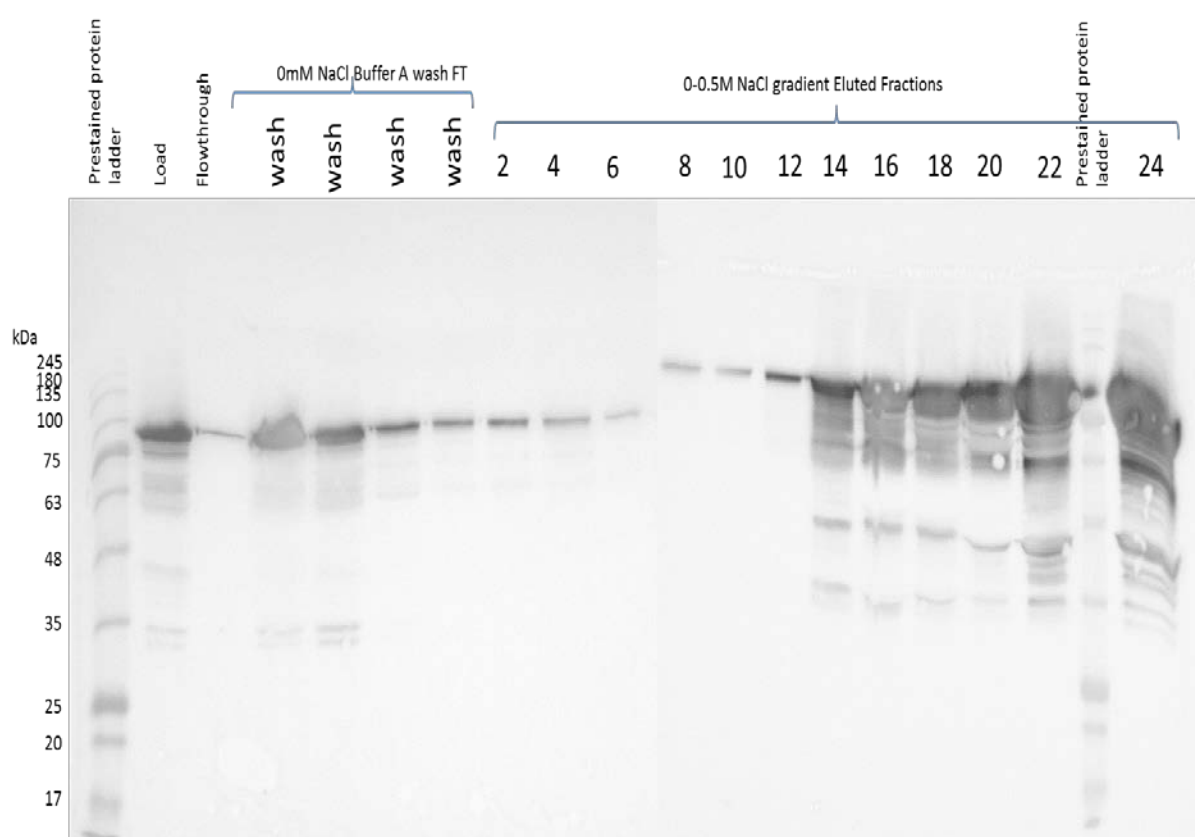


Figure 4.17 Western blot analysis of wild type recombinant protein purification over heparin sepharose column. Western blot analysis using Cubb7402 revealed successfully purification of TG2 recombinant protein as seen by band at about 78kDa. Load and flowthrough was seen in Lane 2 and 3 respectively. Subsequently loaded wash samples also showed presence protein of interest. Wild type TG2 recombinant protein was seen being eluted from 14th fraction of gradient onwards (0.28M NaCl) upto 24th fraction (0.48M NaCl) with peak of elution seen at 22nd fraction (0.44M NaCl)

4.9.3 Western blot analysis of CFPTG2 purification eluted fractions

As seen in figure 4.17, control CFP-TG2 recombinant protein was also purified using the heparin sepharose column. The eluted fractions were resolved using SDS-PAGE and analysed using western blot analysis. It was found that CFP-TG2 recombinant protein could also bind to heparin. The figure 4.18 represents load and flow through in lane 2 and 3 respectively. As compared to CFP-TG2-YFP recombinant protein purification seen above, CFP-TG2 exhibits enhanced binding to sepharose as less protein is seen in flowthrough sample. Wash fractions were collected and loaded in lane 4, 5 and 6. CFP-TG2 recombinant protein was eluted starting from 0.28M NaCl upto 0.48M NaCl of gradient.

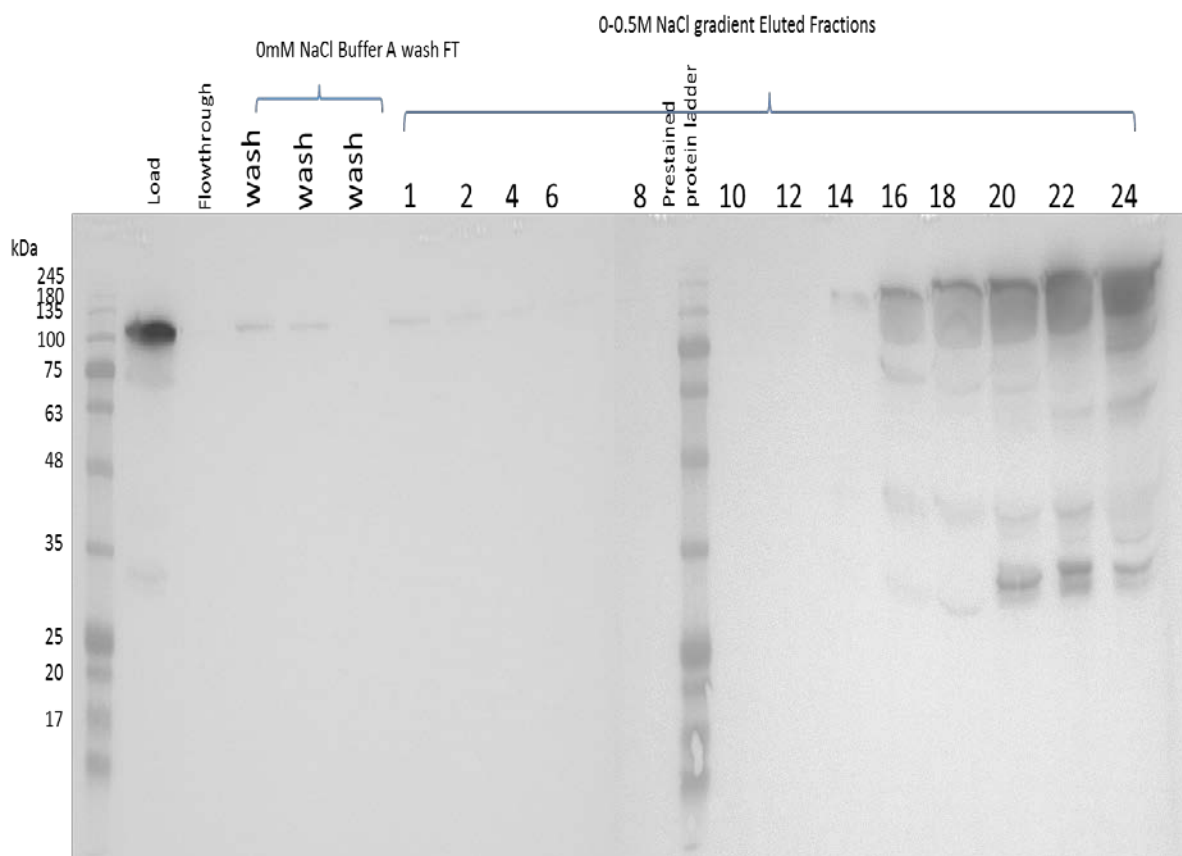


Figure 4.18 Western blot analysis of control CFP-TG2 recombinant protein purification over heparin sepharose column. Western blot analysis using Cubb7402 revealed successfully purification of TG2 recombinant protein as seen by band just over 100kDa. Load and flowthrough was seen in Lane 2 and 3 respectively. Subsequently loaded wash samples also showed presence protein of interest. Control CFP-TG2 recombinant protein was seen being eluted from 14th fraction of gradient onwards (0.28M NaCl) upto 24th fraction (0.48M NaCl) with peak of elution seen at 20nd fraction (0.4M NaCl)

4.9.4 Downstream cleaning of Ni-affinity purified protein using Heparin column

As both wildtype TG2 and CFP-TG2-YFP recombinant protein showed affinity toward heparin sepharose which is characteristic of tissue transglutaminase, an attempt was made to use this heparin column for downstream cleaning of protein that was purified using the Ni-column. The non-specific contaminated protein which was found in purification could possibly be eliminated and result in cleaner purified protein.

Control pET30Ek/LIC TG2 was affinity purified over Ni column (figure 4.19). Gradient eluted fractions were collected and desalted over PD10 column. Fractions 6 and 7 were pooled together desalted and applied to the Heparan column and elution was carried out at gradient between 0 to 0.5M NaCl. The fractions were then run on SDS gel and stained with coomassie.

4.10 Affinity purification of control pET30Ek/LIC TG2 using GE AKTA prime FPLC (Ni column purification)

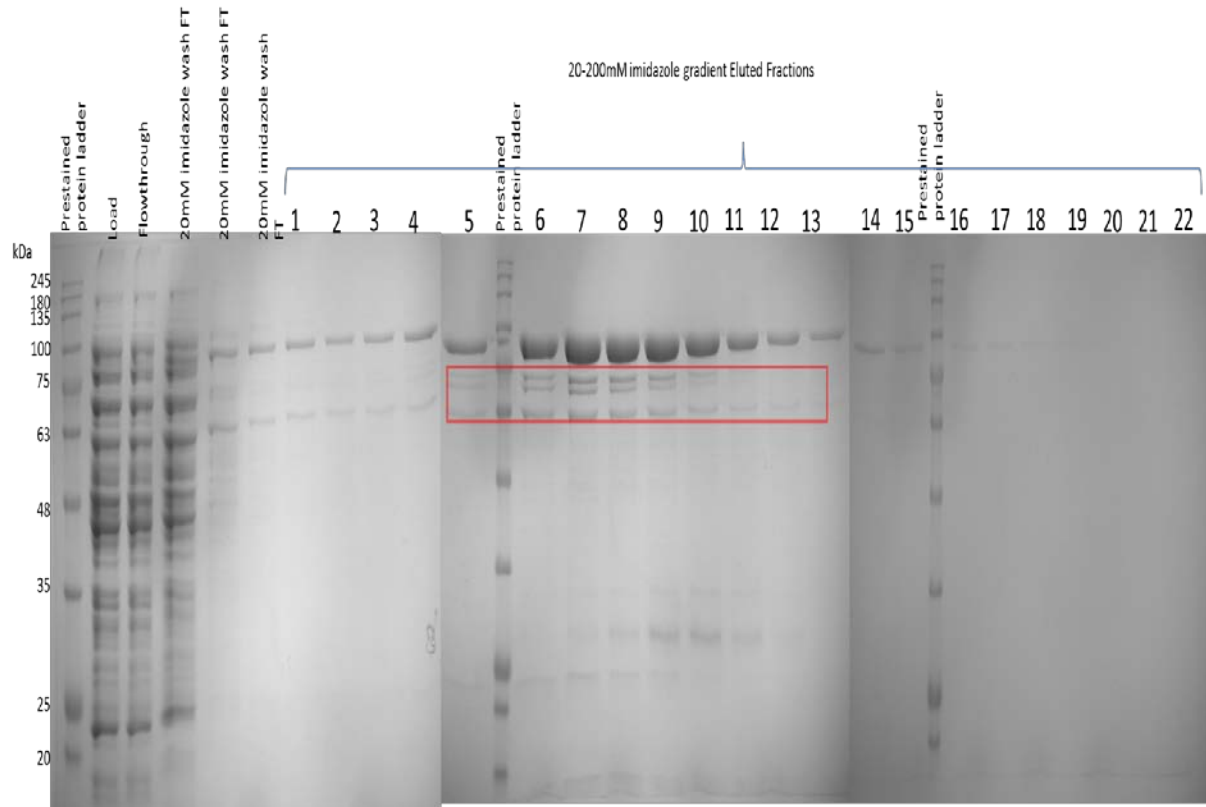


Figure 4.19 SDS PAGE analysis of wild type TG2 protein purification using Ni column. The non-specifically bound protein highlighted by the red box. Protein of interest was eluted as seen in fractions 5 to 12. Peak fraction 6 and 7 were further selected for downstream processing.

4.10.1 Purified wild type TG2 through heparin column

Wild type TG2 which was purified using the Ni column was then loaded onto the heparin sepharose column. In this case, fraction 6 and 7 were used as a load. Using the heparin sepharose protocol (refer material and methods) the purification was performed using a gradient from 0 to 0.5M NaCl over 12 mls. The wild type protein was eluted starting from 8th fraction (0.3M NaCl). This elution was similar to the previous wildtype purification performed using lysed cells as load (figure 4.20). The proteins were analysed using SDS-PAGE and revealed that the purification using heparin sepharose was cleaner and showed lesser non-specific bands. Hence the protein purified using Ni column was further processed using heparin sepharose column.

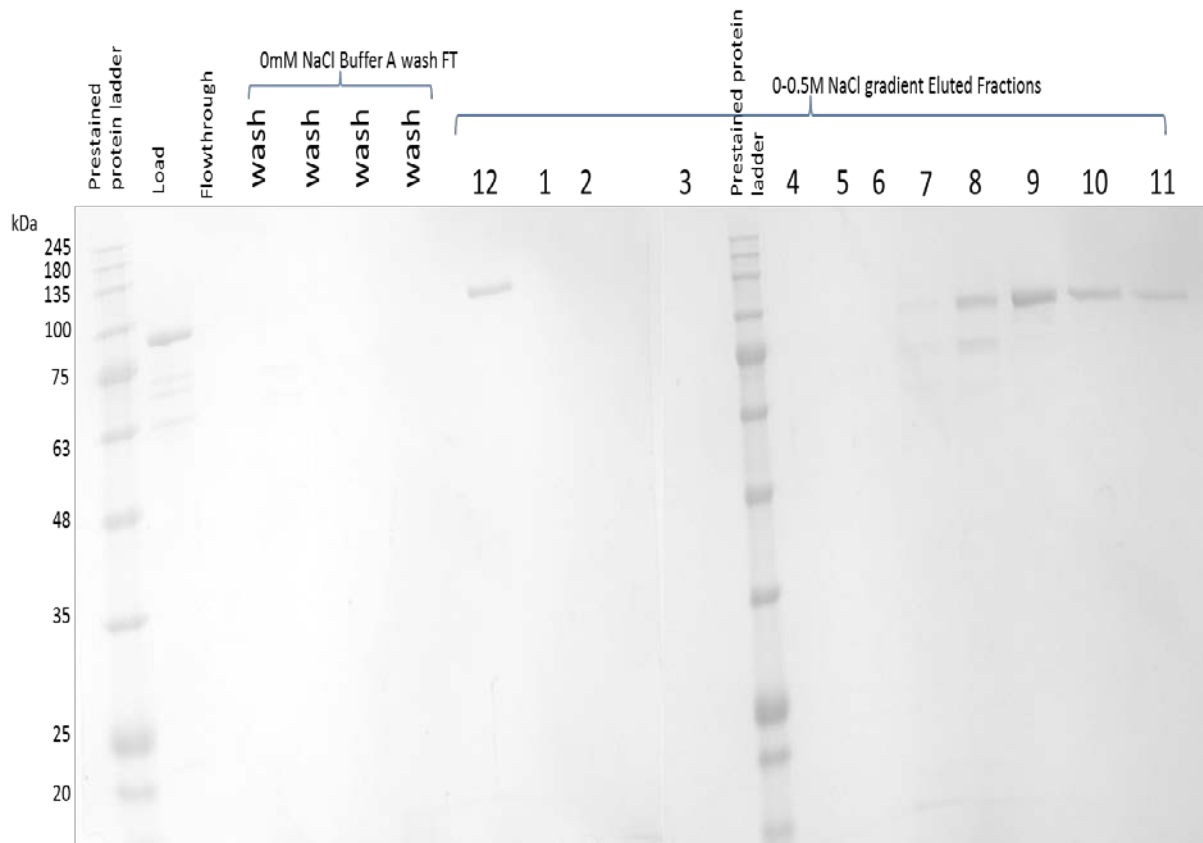


Figure 4.20 SDS PAGE analysis of purified fractions of wild type TG2 protein purification using heparin column. Fractions 6 and 7 of Ni column purification were loaded onto the heparin column. A gradient elution was performed from 0 to 0.5M NaCl. Protein was eluted as seen in fractions 8 to 12 and less non-specific binding observed as compared to Ni-column purification.

4.11 Affinity purification of CFP-TG2-YFP using GE AKTA prime FPLC

CFP-TG2-YFP was affinity purified over Ni column. Gradient eluted fractions were collected and desalted over PD10 column. Fractions 9 and 10 were desalted and applied to the Heparin column and elution was carried out at gradient between 0 to 0.5M NaCl over 12ml. The fractions were then run on SDS gel and stained with coomassie blue (figure 4.21).

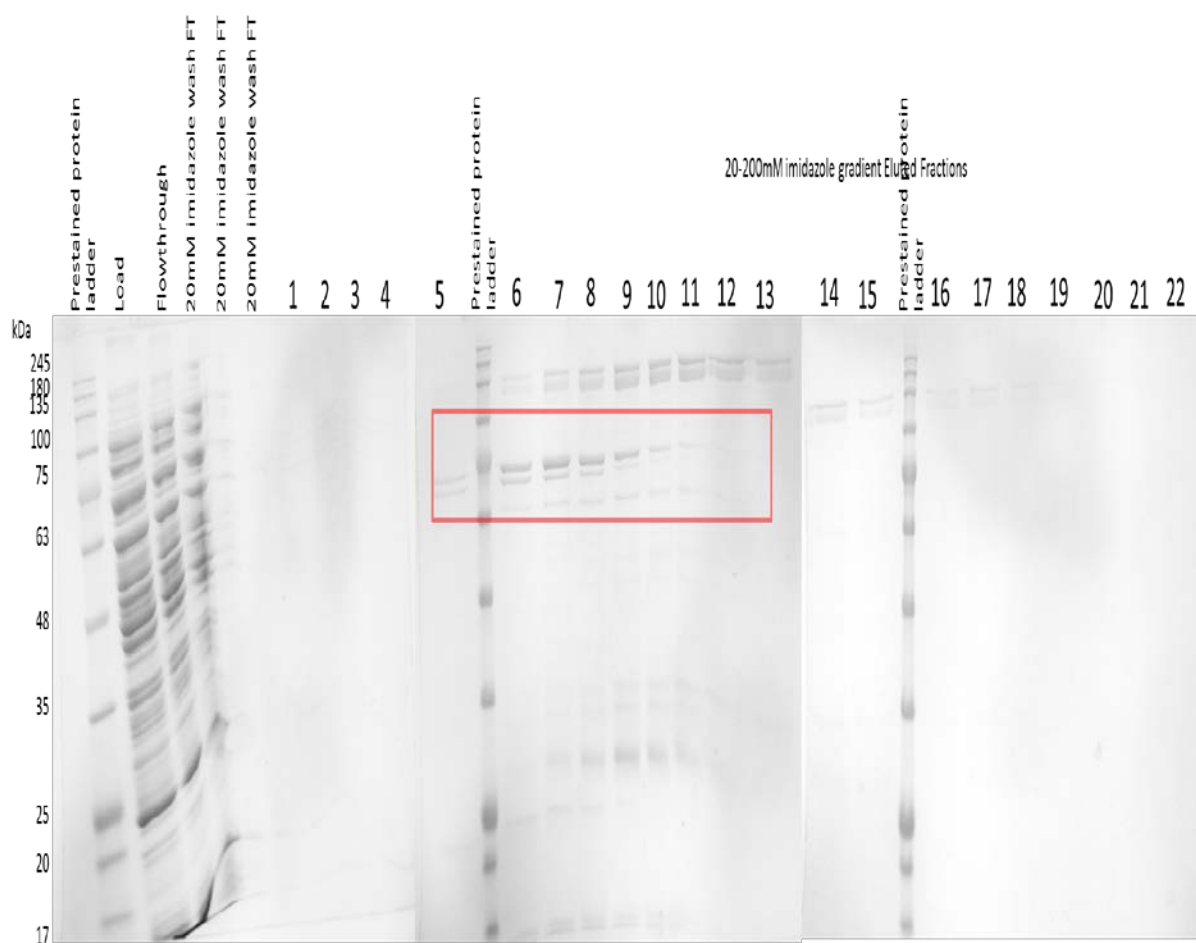


Figure 4.21 SDS PAGE analysis of CFP-TG2-YFP recombinant protein purification using Ni column. The non-specifically bound protein highlighted by the red box. Protein of interest was eluted as seen in fractions 7 to 13. Peak fraction 9 and 10 were further selected for downstream processing.

4.11.2 Purified CFP-TG2-YFP fractions through heparin column

Wild type TG2 which was purified using the Ni column was then loaded onto the heparin sepharose column. In this case, fraction 9 and 10 were used as a load. Using the heparin sepharose protocol (refer material and methods) the purification was performed using a gradient from 0 to 0.5M NaCl over 12 ml. The wild type protein elution from 8th fraction (0.3M NaCl). This elution was similar to the previous CFP-TG2-YFP recombinant purification performed using lysed cells as load. The proteins were analysed using SDS-PAGE (figure 4.22) and revealed that the purification using heparin sepharose was cleaner and showed lesser non-specific bands. Hence the protein purified using Ni column was further processed using heparin sepharose column.

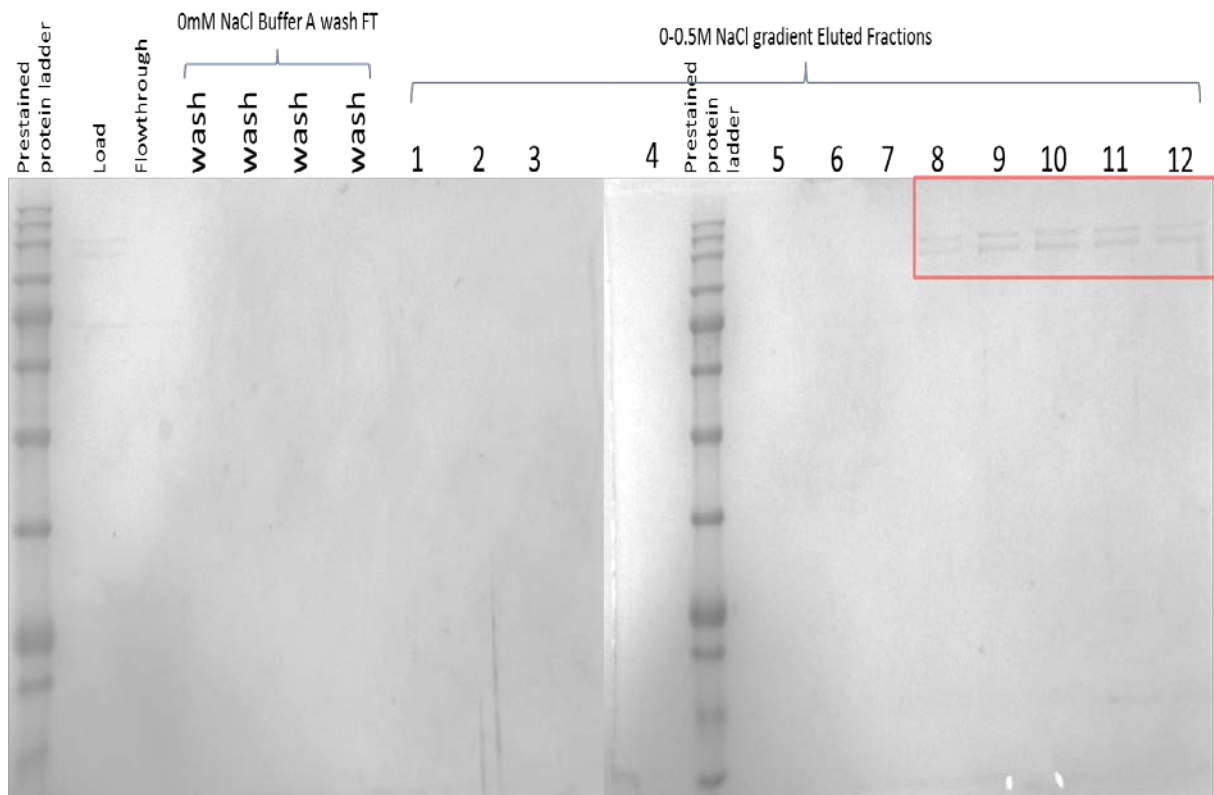


Figure 4.22 SDS PAGE analysis of purified fractions of CFP-TG2-YFP recombinant protein purification using heparin column. Fractions 9 and 10 of Ni column purification were loaded onto the heparin column. A gradient elution was performed from 0 to 0.5M NaCl. Protein was eluted as seen in fractions 8 to 12 and less non-specific binding observed as compared to Ni-column purification.

4.12 Conformational changes due to effect of monodansyl cadaverin, biotin cadaverin, inhibitors R281 / R283

The protease sensitivity of wild type TG2 (control pET30Ek/LIC TG2) and CFP-TG2-YFP recombinant protein was analysed. It has been suggested that when TG2 adapts a closed conformation it is less susceptible to protease digestion. When the structure opens, trypsin susceptibility increases resulting in digestion.

4.12.1 Effect of Biotin cadaverin (BTC)

Purified recombinant wild type TG2 (3 μ g) was treated with increasing concentrations of biotin cadaverin and then incubated with 80ng of trypsin on ice. After two hours of incubation the reaction was stopped by adding laemmli buffer and the results were analysed by resolving the protein using SDS PAGE (figure 4.23). The gels were then stained with coomassie blue and it was observed that with increasing concentration (0 to 1mM) of biotin cadaverin no difference in trypsin digestion was detected.

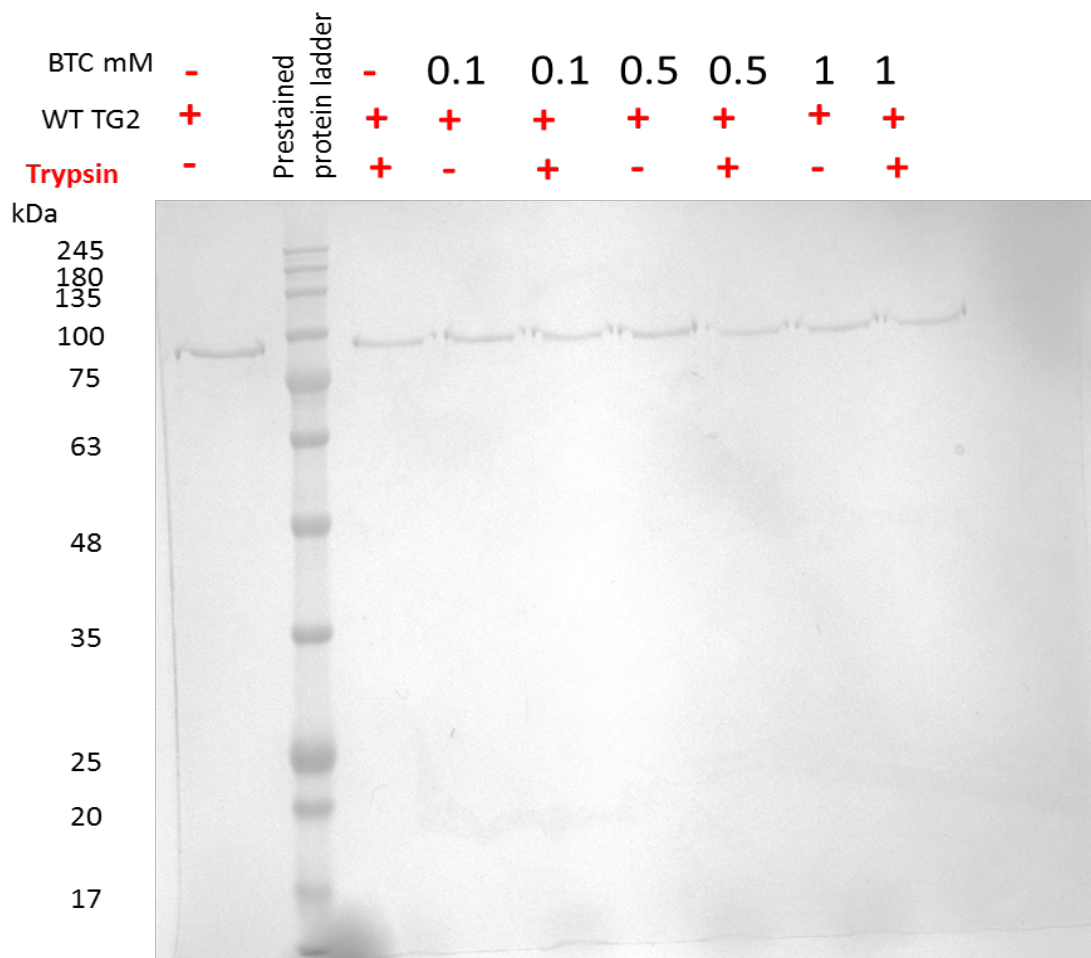


Figure 4.23 SDS PAGE analysis of BTC treated wild type TG2. 3 μ g of purified TG2 (recombinant wild type) was pre-treated with(+) or without (-) increasing concentrations of BTC;0mM, 0.1mM, 0.5mM and 1mM and subjected to trypsin digestion for 2 hours. The proteins were then resolved by SDS-PAGE and stained with coomassie blue. Lane 2 represents prestained protein ladder (245kDa). Lane 1 depicts purified recombinant TG2 (wildtype), Lanes 4, 6, 8 represent protein pre-treated with BTC without trypsin treatment (control).

Purified recombinant CFP-TG2-YFP protein was (3 μ g) was initially desalted in buffer containing 20mM Tris, 300mM NaCl and 10% glycerol and was similarly treated with increasing concentrations of biotin cadaverin for 1 hour at room temperature. It was then subjected to 80ng of trypsin on ice. After two hours of incubation the reaction was stopped by adding laemmili buffer and the results were analysed by resolving the protein using SDS PAGE. The gels were then stained with coomassie blue

(Figure 4.24) and it was observed that with increasing concentration (0 to 1mM) of biotin cadaverin no difference in trypsin digestion was detected. This result was similar to the effect observed on wild type TG2.

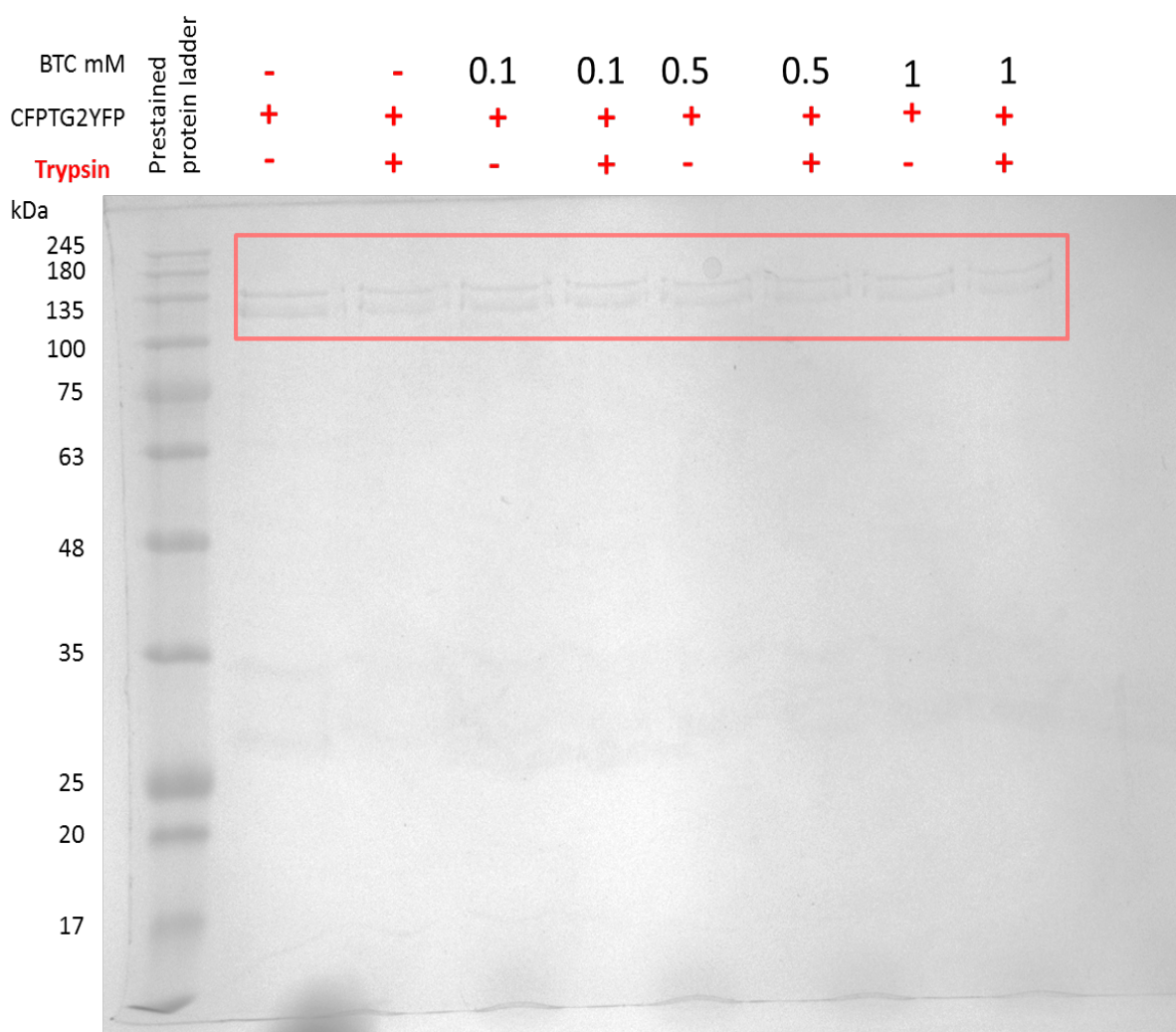


Figure 4.24 SDS PAGE analysis of BTC treated CFP-TG2-YFP recombinant protein. 3ug of purified recombinant CFP-TG2-YFP (construct protein) was pre-treated with(+) or without (-) increasing concentrations of BTC;0mM, 0.1mM, 0.5mM and 1mM and subjected to trypsin digestion for 2 hours. The proteins were then resolved by SDS-PAGE and stained with coomassie blue. Lane 1 represents prestained protein ladder (245kDa). Lane 2 depicts purified recombinant TG2 (wildtype), Lanes 4, 6, 8 represent protein pre-treated with BTC without trypsin treatment (control).

4.12.2 Effect of monodansyl cadaverin

Purified recombinant wild type TG2 (3 μ g) was treated with increasing concentrations of monodansyl cadaverin and then incubated with 80ng of trypsin on ice as previously reported by Zhang et al, 2013. (Zhang et al., 2013) After two hours of incubation the reaction was stopped by adding laemmili buffer and the results were analysed by resolving the protein using SDS PAGE. The gels were then stained with coomassie blue (figure 4.25) and it was observed that with increasing concentration (0 to 1mM) of monodansyl cadaverin, no difference in trypsin digestion was detected similar to biotin cadaverin treatment. With the increasing concentration of monodansyl cadaverin there was no increase in trypsin susceptibility as a result of conformational change as indicated by Zhang et al (2013).

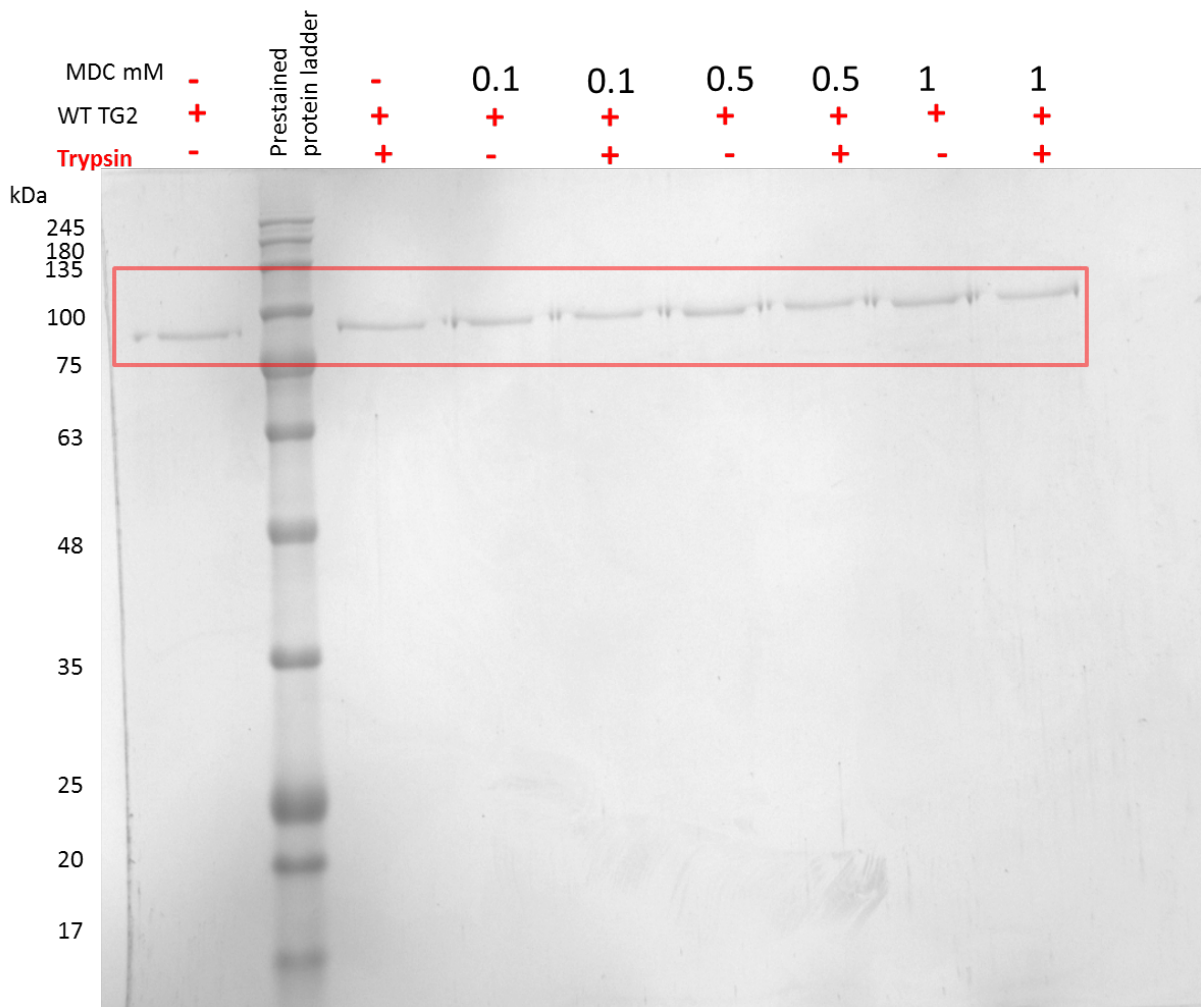


Figure 4.25 SDS PAGE analysis of MDC treated wild type TG2. 3 μ g of purified TG2 (recombinant wild type) was pre-treated with(+) or without (-) increasing concentrations of MDC; 0mM, 0.1mM, 0.5mM and 1mM and subjected to trypsin digestion for 2 hours. The proteins were then resolved by SDS-PAGE and stained with coomassie blue. Lane 2 represents prestained protein ladder (245kDa). Lane 1 depicts purified recombinant TG2 (wildtype), Lanes 4, 6, 8 represent protein pre-treated with BTC without trypsin treatment (control).

Purified recombinant CFP-TG2-YFP protein was (3 μ g) was initially desalted in buffer containing 20mM Tris, 300mM NaCl and 10% glycerol and was similarly treated with increasing concentrations of monodansyl cadaverin (MDC) for 1 hour at room temperature. It was then subjected to 80ng of trypsin on ice. After two hours of incubation the reaction was stopped by adding laemmli buffer and the results were

analysed by resolving the protein using SDS PAGE. The gels were then stained with coomassie blue (figure 4.26) and it was observed that with increasing concentration (0 to 1mM) of monodansyl cadaverin no difference in trypsin digestion was detected. This result was similar to the effect observed on control wild type TG2.

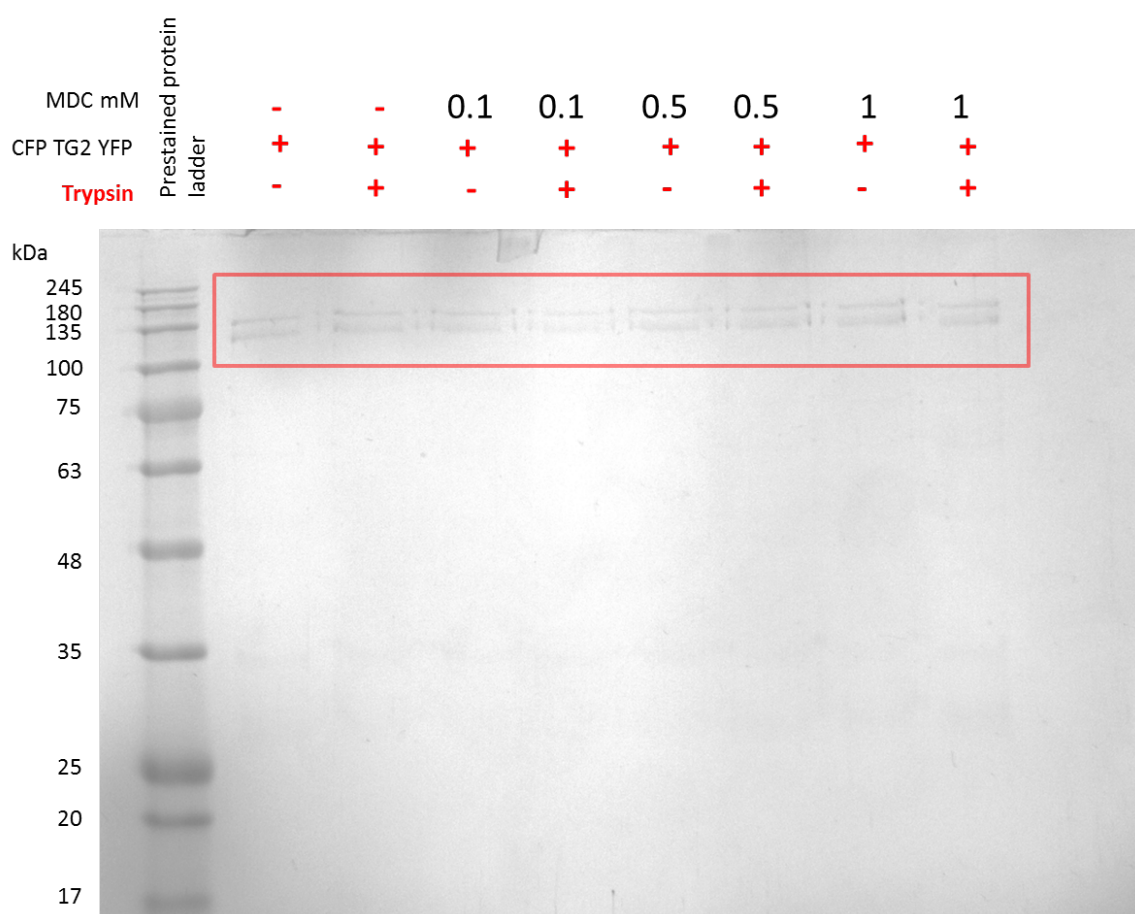


Figure 4.26 SDS PAGE analysis of BTC treated CFP-TG2-YFP recombinant protein. 3ug of purified recombinant CFP-TG2-YFP (construct protein) was pre-treated with(+) or without (-) increasing concentrations of MDC;0mM, 0.1mM, 0.5mM and 1mM and subjected to trypsin digestion for 2 hours. The proteins were then resolved by SDS-PAGE and stained with coomassie blue. Lane 1 represents prestained protein ladder (245kDa). Lane 2 depicts purified recombinant TG2 (wildtype), Lanes 4, 6, 8 represent protein pre-treated with MDC without trypsin treatment (control).

4.12.3 Effect of Inhibitors R281 and R283

TG2 cell permeable inhibitor R283 and cell impermeable TG2 inhibitor R281 are known to interfere with transamidating activity of TG2 by targeting the active cysteine. Inhibitor bound TG2 adapts an open conformation. (Griffin et al., 2008) R281 and R283 were used to assess the effect of trypsin on both wild type TG2 and CFP-TG2-YFP recombinant protein.

4.12.4 R281 and wild type

3ug of recombinant protein was pre-treated with 20mM calcium chloride, 1mM DTT and 500μM R281 for 1 hour on ice. The inhibitor treated protein was then mixed with increasing concentrations of trypsin. Two controls were used, one without addition of inhibitor and trypsin (purified protein) and second control without pre-treatment with inhibitor (only trypsin digested protein). It was observed that wild type TG2 treated with R281 was completely digested with lowest concentration of 80ngs of trypsin. Control sample with no R281 treatment and only addition of trypsin showed no digestion suggesting that TG2 could be in closed conformation, not susceptible to protease digestion (figure 4.27). Once treated with inhibitor TG2 (open conformation), trypsin was seen to completely digest protein.

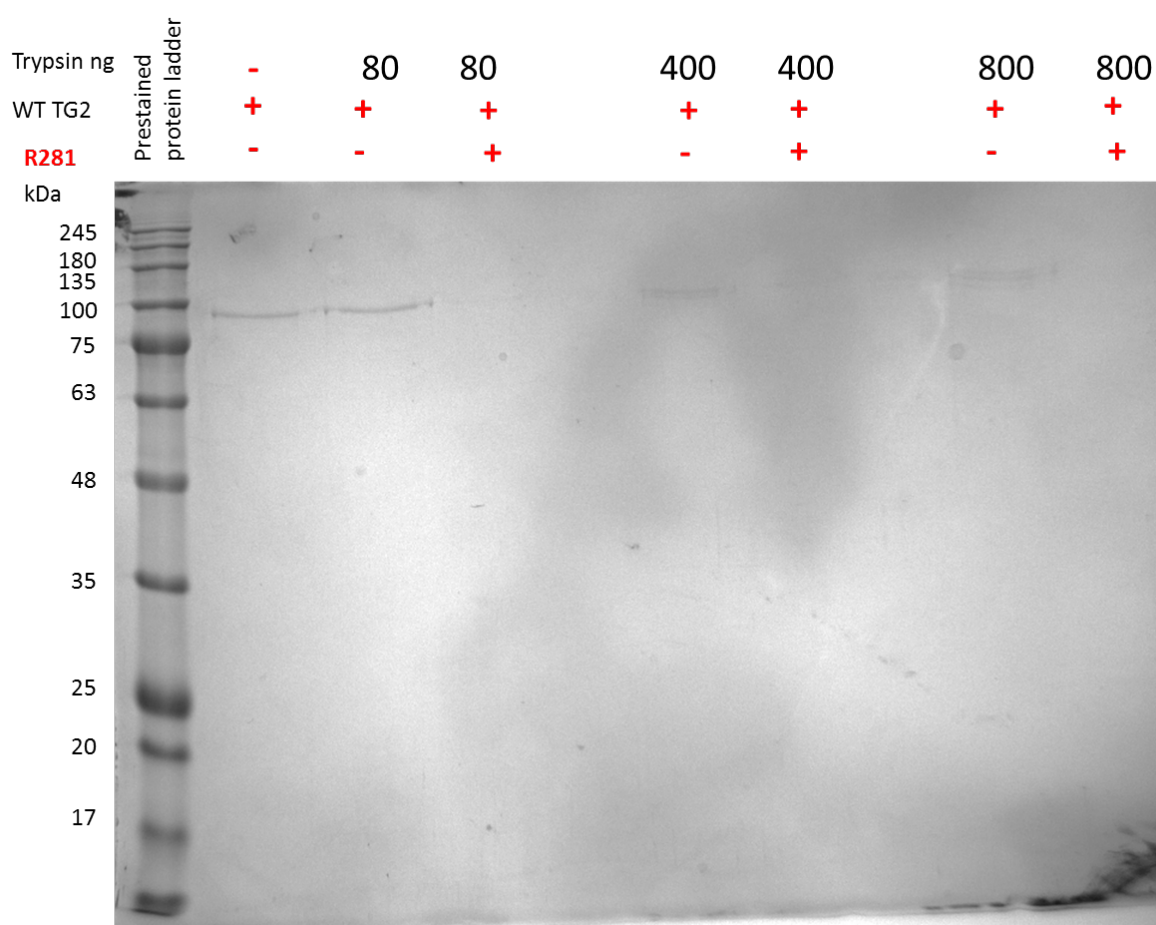


Figure 4.27 SDS PAGE analysis of R281 treated wild type recombinant TG2 protein. 3 μ g of purified recombinant wild type TG2 was pre-treated with (+) or without (-) 500 μ M R281 and subjected to trypsin digestion for 2 hours. The proteins were then resolved by SDS-PAGE and stained with coomassie blue. Lane 1 represents prestained protein ladder (245kDa). Lane 2 depicts purified recombinant TG2 (wildtype), Lanes 3 and 4 shows protein digested with 80ngs of trypsin. Lane 5 and 7 shows control without pre-treatment with inhibitor and digested with trypsin.

4.12.5 R283 and wild type

Similar to R281 treatment 3 μ g of wild type TG2 was treated with R283, followed by digestion with increasing concentrations of trypsin. Two controls were used, one without addition of inhibitor and trypsin (purified protein) and second control without pre-treatment with inhibitor (only trypsin digested protein). It was observed that wild

type TG2 treated with R281 was completely digested with lowest concentration of 80ngs of trypsin. Control sample with no R283 treatment and only addition of trypsin showed no digestion suggesting that TG2 could be in closed conformation, not susceptible to protease digestion. Once treated with inhibitor TG2 (open conformation), trypsin was seen to digest protein but at higher concentrations as compared to R281 treatment as seen above. At low concentrations of 80ngs to 0.8µg no digestion of R283 treated protein was observed (figure 4.28). Digestion of R283 treated protein was observed at 3.2µg of trypsin and higher suggesting a probable slight difference in conformation and protease digestion.

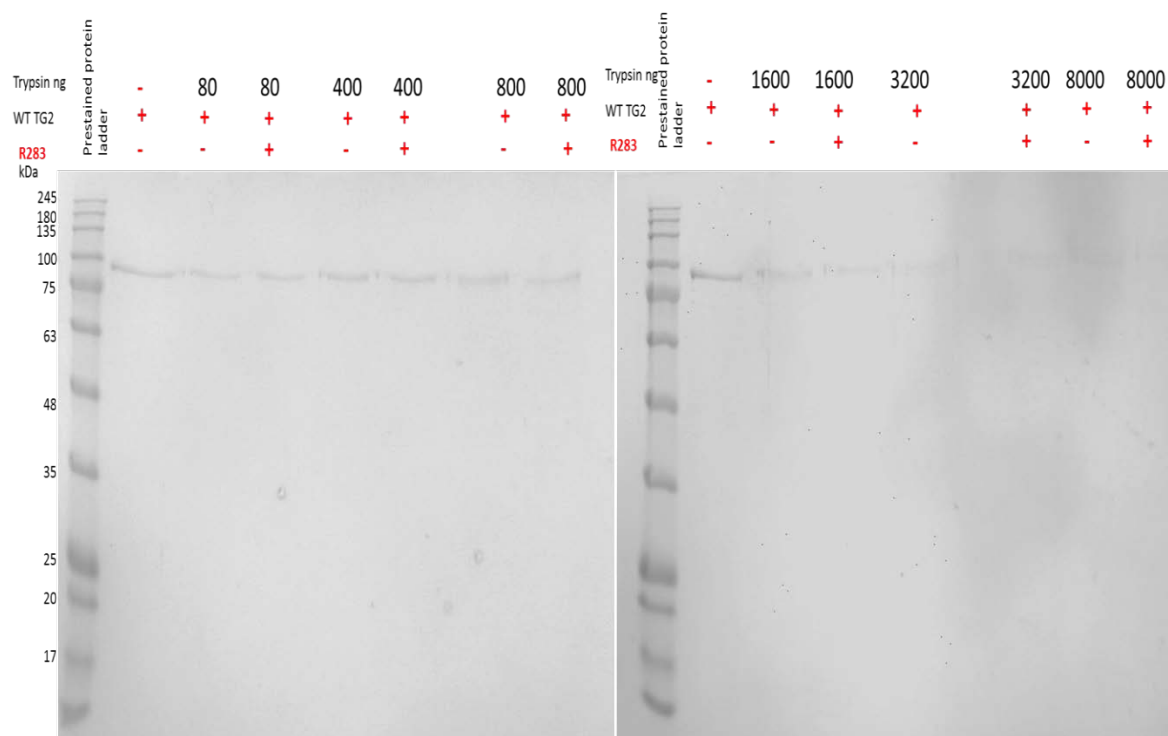


Figure 4.28 A and B SDS PAGE analysis of R283 treated wild type recombinant TG2 protein. 3ug of purified recombinant wild type TG2 was pre-treated with (+) or without (-) 500 μ M R283 and subjected to trypsin digestion for 2 hours. The proteins were then resolved by SDS-PAGE and stained with coomassie blue. Lane 1 represents prestained protein ladder (245kDa) figure A and B. Lane 2 depicts purified recombinant TG2 (wildtype), Lanes 3 and 4 shows protein digested with 80ngs of trypsin in figure A. Lane 5 and 7 shows control without pre-treatment with inhibitor and digested with trypsin in figure A. Figure B depicts higher concentrations of trypsin digestion from 1.6 μ g to 8 μ g. Digestion of R283 treated wild type protein was observed at higher concentration than R281 as seen in figure B.

4.12.6 R281 and CFP-TG2-YFP recombinant protein

3ug of recombinant protein was pre-treated with 20mM calcium chloride, 1mM DTT and 500 μ M R281 for 1 hour on ice. The inhibitor treated protein was then mixed with increasing concentrations of trypsin. Two controls were used, one without addition of inhibitor and trypsin (purified protein) and second control without pre-treatment with

inhibitor (only trypsin digested protein). It was observed that wild type TG2 treated with R281 was partially digested with lowest concentration of 80ngs of trypsin and complete digestion was seen with R281 pre-treated protein using 0.8µg of trypsin. Control sample with no R281 treatment and only addition of trypsin showed no digestion suggesting that TG2 could be in closed conformation, not susceptible to protease digestion (figure 4.29). Once treated with inhibitor TG2 (open conformation), trypsin was seen to completely digest protein. It is observed that R281 treated wild type TG2 and CFP-TG2-YFP recombinant protein show difference in concentration of trypsin required for complete digestion possibly due the difference in size.

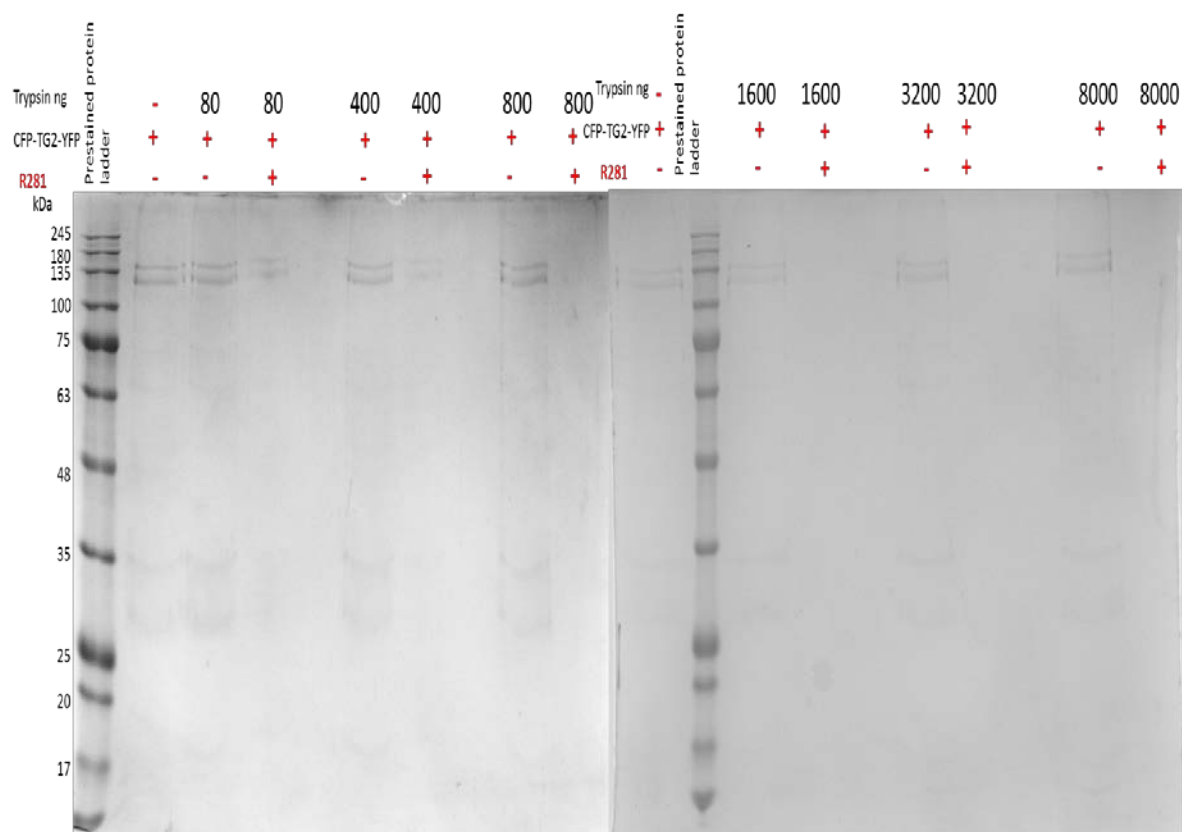


Figure 4.29 A and B SDS PAGE analysis of R281 treated wild type recombinant TG2 protein. 3ug of purified recombinant CFP-TG2-YFP recombinant protein was pre-treated with (+) or without (-) 500μM R281 and subjected to trypsin digestion for 2 hours. The proteins were then resolved by SDS-PAGE and stained with coomassie blue. Lane 1 represents prestained protein ladder (245kDa). Lane 2 depicts purified recombinant CFP-TG2-YFP, Lanes 4 shows protein partially digested with 80ngs of trypsin in figure A. Lane 5 and 7 shows control without pre-treatment with inhibitor and digested with trypsin in figure A. Complete digestion of protein was observed at 0.8μg trypsin as seen in Lane 8 of figure A. Figure B depicts higher concentrations of trypsin digestion from 1.6μg to 8μg.

4.13 Presence of TG2 antigen by ELISA

CFP-TG2-YFP recombinant protein and CFP-TG2 recombinant protein were purified and presence of TG2 antigen was detected using enzyme linked immunosorbent assay. Cub 7402 anti-TG2 monoclonal antibody was used (refer material and methods for protocol) CFP-TG2-YFP recombinant protein exhibits similar incorporation of fibronectin as compared to recombinant TG2 (RhTG2). The assay was repeated using anti-TG2 1D10 monoclonal antibody. The results were compared between Cub7402 and 1D10 and it was found that Cub 7402 has higher affinity to TG2 as compared to 1D10.

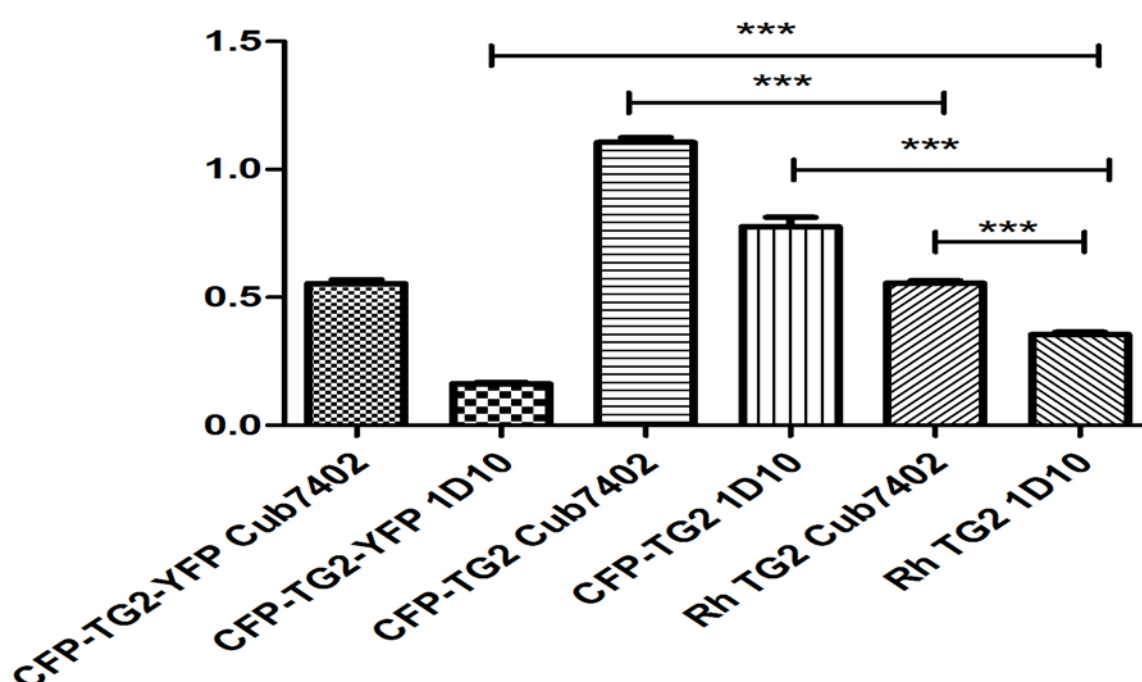


Figure 4.30 Detection of TG2 antigen using ELISA. The results represent TG2 activity comparison of RhTG2, purified CFP-TG2-YFP recombinant protein and CFP-TG2 recombinant protein. The experiment was performed using Cub7402 and 1D10 monoclonal TG2 antibody. Results show mean \pm S.E.M of three independent experiments done performed in triplicates. Statistical analysis was done using ANOVA applying Bonferroni post-test (***) $P<0.001$

4.14 Biotin-cadaverine incorporation into N,N'-dimethylcasein

Purified CFP-TG2-YFP recombinant protein was tested and compared to RhTG2 for its ability to incorporate biotin-cadaverin into N, N-dimethylcasein. The reaction was performed at three concentration of calcium. The specific activity was seen to be less than half of RhTG2 when using casein.

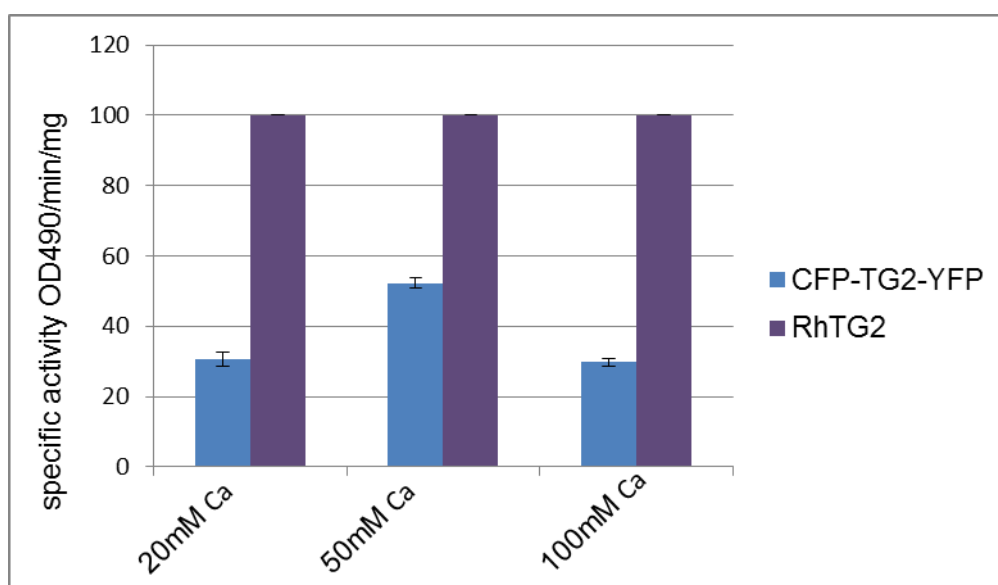


Figure 4.31 Comparison of specific activity of RhTG2 and purified CFP-TG2-YFP recombinant with respect to biotin cadaverin incorporation into N, N'-dimethylcasein. The experiment was performed at three different concentration of calcium. Results show mean \pm S.D of three independent experiments done performed

4.15 Biotin-cadaverine incorporation into Fibronectin

Purified CFP-TG2-YFP recombinant protein was tested and compared to RhTG2 for its ability to incorporate biotin-cadaverin into fibronectin. The reaction was performed at three concentration of calcium. The specific activity was seen to be more than half of RhTG2 when using fibronectin.

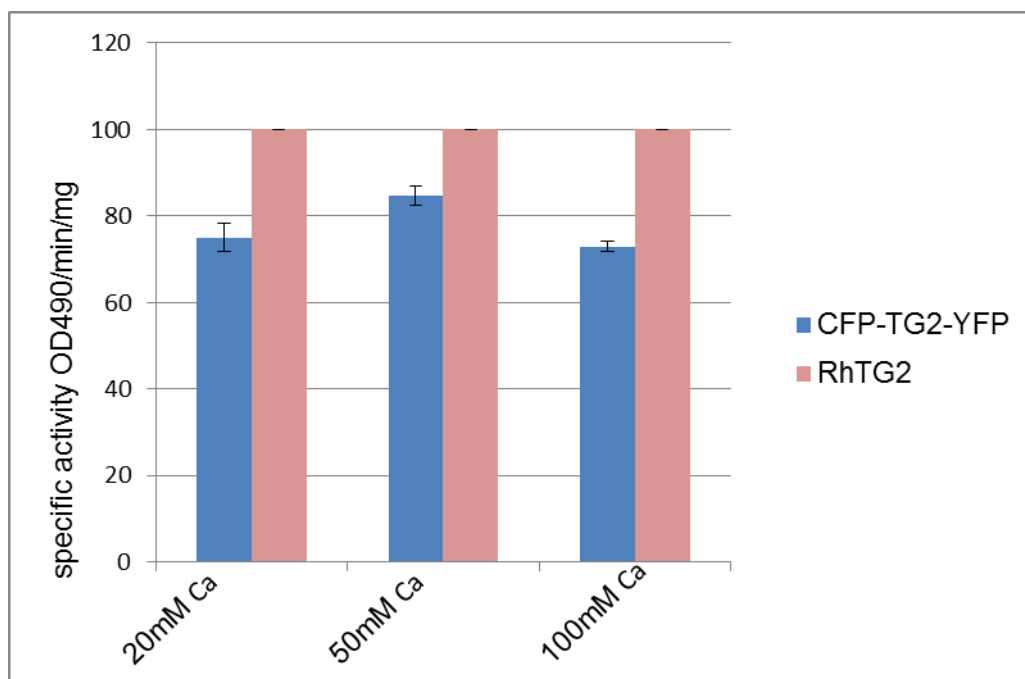


Figure 4.32 Comparison of specific activity of RhTG2 and purified CFP-TG2-YFP recombinant with respect to biotin cadaverin incorporation into fibronectin. The experiment was performed at three different concentration of calcium. Results show mean \pm S.D of three independent experiments done performed

4.16 Calcium activation assay

To compare calcium sensitivity biotin-X-cadaverin activity assay was performed based on incorporation into immobilised fibronectin (refer material and methods). Transglutaminase activity was measured over a range of varying calcium concentrations using 5 μ M, 10 μ M, 50 μ M, 0.1mM, 0.25mM, 0.5mM, 0.75mM, 1mM, 5mM, 10mM of calcium chloride with 1 μ g TG2 (using RhTG2, CFP-TG2-YFP recombinant protein and CFP-TG2 recombinant protein) CFP-TG2-YFP recombinant protein and CFP-TG2 recombinant protein was purified using Ni-NTA column and desalted using PD-10 column in the presence of 1mM EGTA. Addition calcium was added to compensate for EGTA chelation. TG2 activity was measured and analysed

using Michelis-Menten equation. The curve was plotted in Graphpad prism and the K_m value was calculated for RhTG2 $K_m=59.49\mu\text{M} \pm 0.03$, CFP-TG2-YFP recombinant protein $K_m=98.19\mu\text{M} \pm 0.03$ and CFP-TG2 recombinant protein $K_m=87.54\mu\text{M} \pm 0.03$. The results indicate a difference in calcium sensitivity between RhTG2 and fluorescent protein tagged TG2.

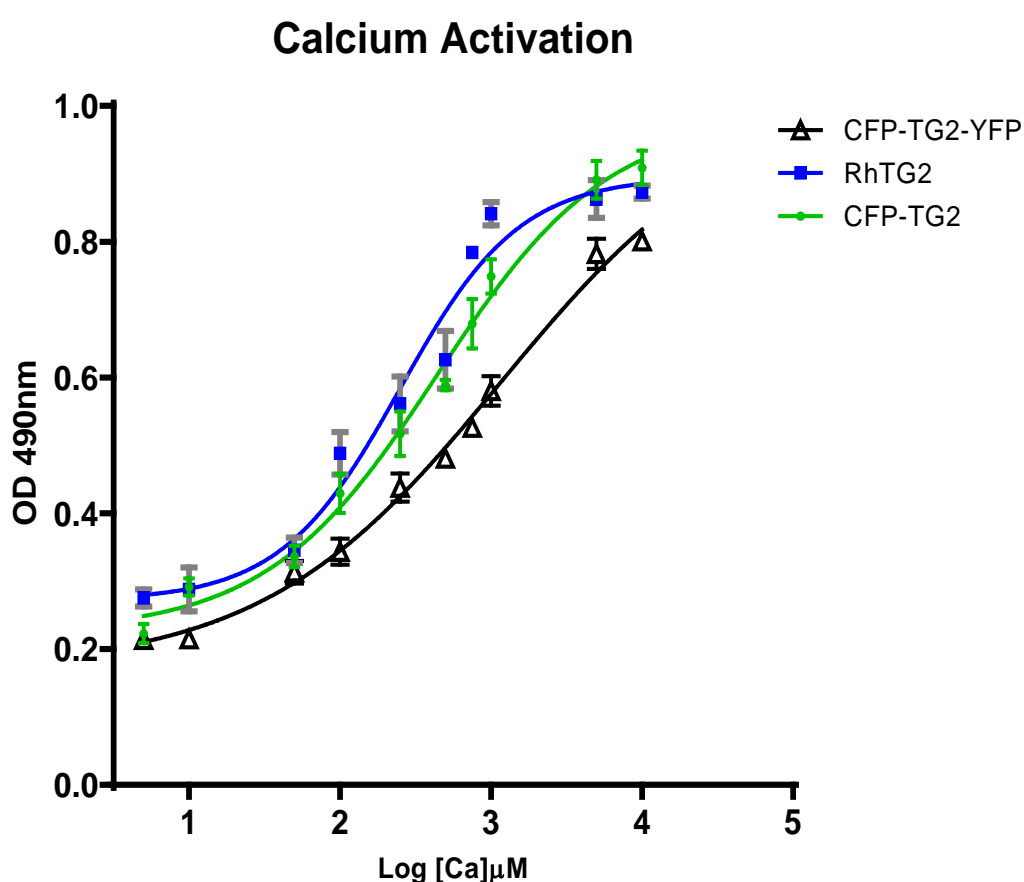
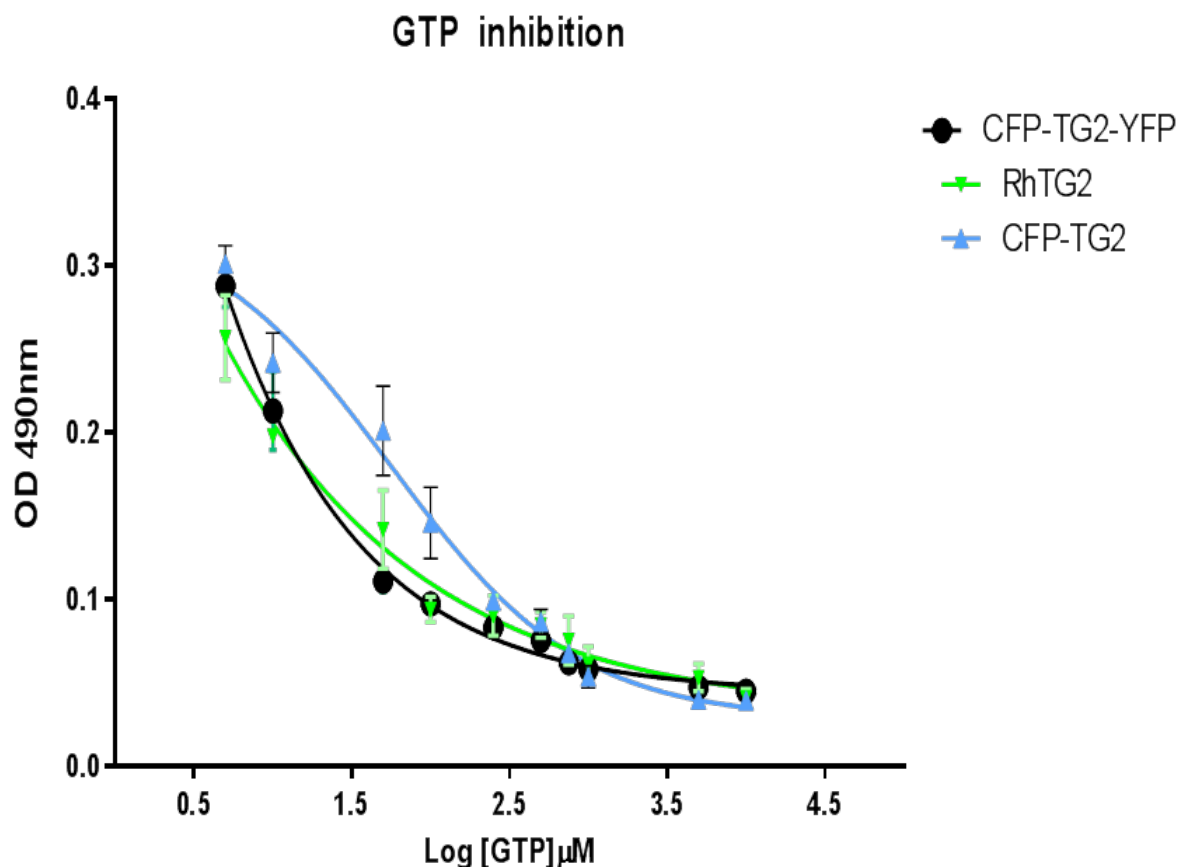


Figure 4.33 Dose-response curve of transglutaminase activity for calcium with values plotted on a logarithmic scale. Transglutaminase activity with calcium concentration ranging from $5\mu\text{M}$ to 10mM was compared for RhTG2, purified CFP-TG2-YFP recombinant protein and purified CFP-TG2 recombinant protein. Rh TG2 $K_m= 59.49 \mu\text{M}$ and CFP-TG2-YFP recombinant protein $K_m=98.19\mu\text{M}$. CFP-TG2 recombinant protein $K_m=87.54\mu\text{M}$. The results represent mean \pm S.E.M of three independent experiments done performed in triplicates.

4.17 GTP inhibition curve

GTP is known to negatively regulated activity of tissue transglutaminase. To compare GTP inhibition, biotin-X- cadaverin activity assay was performed based on incorporation into immobilised fibronectin (refer material and methods). Transglutaminase activity was measure over a range of varying GTP concentrations using 5 μ M, 10 μ M, 50 μ M, 0.1mM, 0.25mM, 0.5mM, 0.75mM, 1mM, 5mM, 10mM of GTP and 250 μ M calcium chloride with 1 μ g TG2 (using RhTG2, CFP-TG2-YFP recombinant protein and CFP-TG2 recombinant protein) CFP-TG2-YFP recombinant protein and CFP-TG2 recombinant protein was purified using Ni-NTA column and desalted using PD-10. TG2 activity was measured and plotted using Morrison Ki equation. The curve was plotted in Graphpad prism and the KI value was calculated for RhTG2 $K_m=1.14\mu\text{M} \pm 0.02$, CFP-TG2-YFP recombinant protein $K_m=4.56\mu\text{M} \pm 0.02$ and CFP-TG2 recombinant protein $K_m=11.73\mu\text{M} \pm 0.02$. The result show RhTG2, recombinant CFP-TG2-YFP protein and CFP-TG2 recombinant protein show a decrease in transamidating activity with increase in GTP concentration.



4.34 Figure Dose-response curve of transglutaminase activity for GTP with values plotted on a logarithmic scale. Transglutaminase activity with GTP concentration ranging from $5\mu\text{M}$ to 10mM was compared for RhTG2, purified CFP-TG2-YFP recombinant protein and purified CFP-TG2 recombinant protein. Rh TG2 $K_i = 1.146\ \mu\text{M}$ and CFP-TG2-YFP recombinant protein $K_i = 4.562\ \mu\text{M}$. CFP-TG2 recombinant protein $K_m = 11.73\ \mu\text{M}$. The results represent mean \pm S.E.M of three independent experiments done performed in triplicates.

4.18 Discussion

The second part of the project was the characterisation of the TG2 FRET construct. In order to achieve this, the expression of the construct was first tested. The expression of CFP-pTrcHisB clones revealed a 35kDa protein but no difference was observed in the expression based on the time course. Changing the time course could be another option to assess the expression over time. For example a shorter time course where samples are collected every 30mins or less within the first hour of expression. Nevertheless the presence of protein of correct size seen via SDS page analysis could mean that CFP was expressed. The western blot analysis using anti-CFP antibody could be another option to be sure the 35kDa protein seen is CFP. For the analysis of CFT-TG2-YFP expression the use of alternate antibodies specific to CFP or YFP could also be useful. For expression of this construct the possibility of expression in yeast could also be another interesting area of investigation. Yeast cells are known to support the expression of protein with the advantages like faster growth, low cost and easy genetic manipulations. It would also be interesting to investigate the truncated products seen in the expression. The use of alternate antibodies specific to CFP or YFP rather than TG2 could indicate what sort of truncated proteins are seen in the western blots during protein expression. Also the use of silver staining for SDS gels could prove to be more sensitive than coomassie blue staining. The use of other size exclusion chromatography would also provide a cleaner purification and get rid of smaller products that are seen in the SDS gels stained with coomassie and western blot analysis using Cub7402. Another future prospective could be introducing point mutations within the construct and check how it affects the expression of TG2. The use of Gly spacers between the fluorescent proteins and TG2 and if it affects expression and activity of the construct could also

broaden the existing research. The conformational changes due to monodansyl cadaverin, biotin cadaverin and inhibitors could also be assessed using a different protease other than trypsin to check digestion. The difference seen by ELISA comparing Cub7402 and 1D10 could also indicate a difference in epitope. The epitope of Cub7402 is known but epitope of our laboratory produced ID10 still needs investigation. A difference in antibody reactivity is observed. An interesting difference in affinities of TG2 binding fibronectin and casein is observed via biotin cadaverin incorporation using a saturating calcium concentration. This could be due to steric hindrance to substrate accessibility using a solid phase assay.

Chapter 5

FRET analysis

5.1 Introduction

FRET is the non-radiative transfer of energy from the donor to the acceptor. This chapter focuses on analysis the fluorescence changes that occur as a result of TG2 structure opening and closing. TG2 opening structure is assessed by increasing concentration of calcium and closed form of TG2 is assessed by binding of GTP. This chapter also encompasses the use of FRET controls including the fluorescence changes occurring in CFP-TG2 construct only, as a result of calcium and GTP. The raw fluorescence reading was then processed for FRET efficiency. The activity curve seen previously was compared to the FRET efficiency to determine whether or not this system is valid.

5.2 FRET data analysis

5.2.1 Effect of GTP on conformation using FRET analysis

When GTP binds to TG2, structure adapts a closed conformation and not allowing access to its active site. Here we investigate the effect of GTP on the conformation of TG2 using FRET. An increasing concentration of GTP ranging from 5 μ M, 10 μ M, 50 μ M, 0.1mM, 0.25mM, 0.5mM, 0.75mM, 1mM, 5mM, 10mM. 250 μ M of calcium was added to the reaction. CFP-TG2-YFP recombinant protein was purified using Ni-NTA column and desalted in 50mM Tris buffer, 1mM DTT, 1mM EGTA. 1 μ g of protein was used in each reaction. The figure 5.1 represents the normalised fluorescence measure when CFP is excited at 436nm and emission was measured at 476nm (cut off selected 455nm). As the GTP concentration increases there is a decrease in CFP emission as the TG2 structure closes. A significant difference was observed between mean fluorescence at 5 μ M (lowest GTP concentration) and 10mM (highest concentration) of GTP.

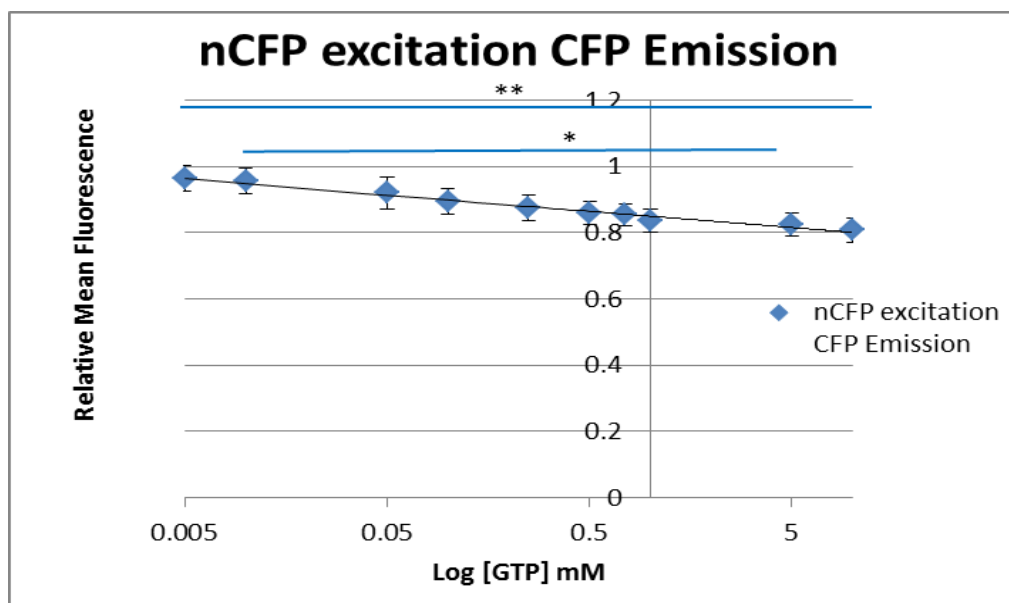


Figure 5.1 Effect of increasing concentration of GTP on CFP emission analysing CFP-TG2-YFP recombinant protein. The graph was plotted using log of GTP concentration from 5 μ M to 10mM. The decrease in fluorescence is represented as normalised mean fluorescence. The results represent mean \pm S.D of three independent experiments done performed in triplicates. Statistical analysis was done using ANOVA applying Bonferroni post-test ($P < 0.001$)**

The figure 5.2 represents the normalised fluorescence measure when YFP is excited at 516nm and emission was measured at 538nm (cut off selected 530nm). As the GTP concentration increases the YFP emission increases. YFP emission indicated in figure below is an indication of the amount of protein. Although there is an increase with increase in GTP concentration observed in YFP emission, this increase was corrected for during FRET efficiency calculation.

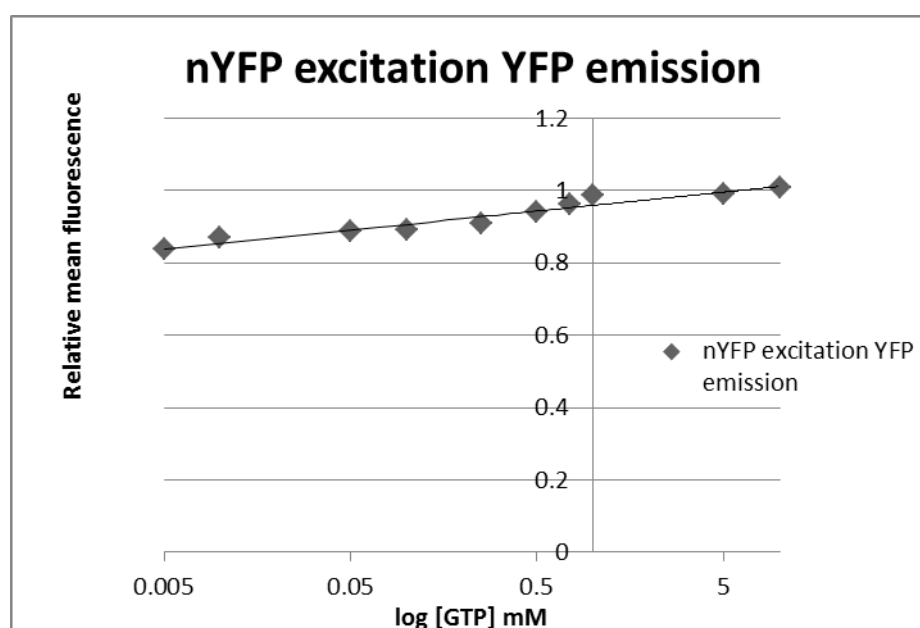


Figure 5.2 Effect of increasing concentration of GTP on YFP emission analysing CFP-TG2-YFP recombinant protein. The graph was plotted using log of GTP concentration from 5 μ M to 10mM. The fluorescence is represented as normalised mean fluorescence represented on the Y axis. The results represent mean \pm S.D of three independent experiments done performed in triplicates.

The figure 5.3 represents the normalised fluorescence measure when CFP is excited at 436nm and emission was measured at 538nm (cut off selected 530nm). As the GTP concentration increases there is a significant increase in YFP emission as the TG2 structure closes. A significant difference was observed between mean fluorescence at 5 μ M (lowest calcium concentration) and 10mM (highest concentration) of GTP. This increase in FRET indicates the structure of recombinant CFP-TG2-YFP closes as the GTP concentration increases. As the structure closes more energy is transferred from the donor to acceptor and hence an increase in FRET is observed.

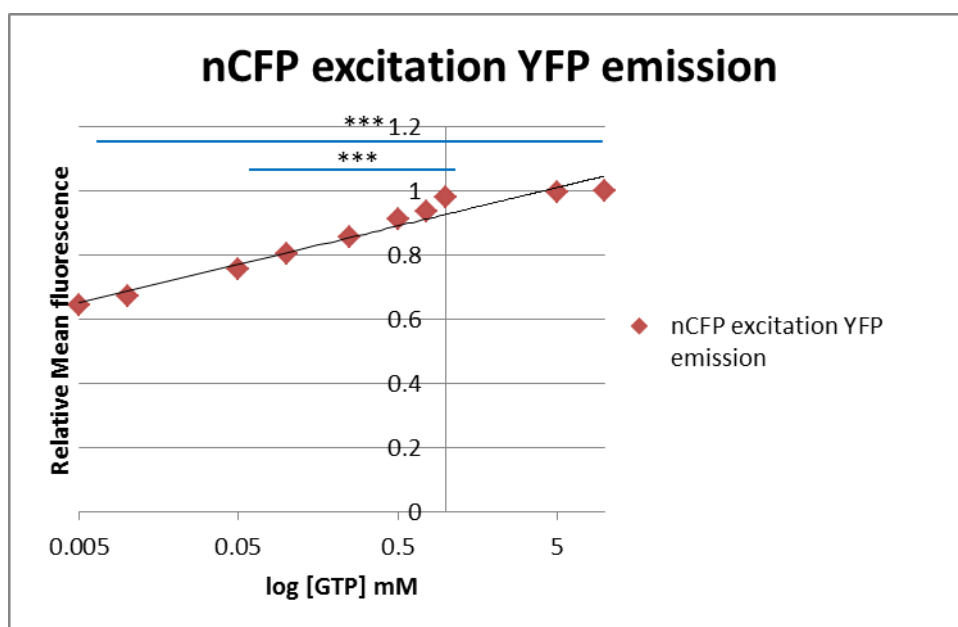


Figure 5.3 Effect of increasing concentration of GTP on CFP excitation YFP emission analysing CFP-TG2-YFP recombinant protein. The graph was plotted using log of calcium concentration from 5 μ M to 10mM. The increase in fluorescence is represented as normalised mean fluorescence. The results represent mean \pm S.D of three independent experiments done performed in triplicates. Statistical analysis was done using ANOVA applying Bonferroni post-test ($P < 0.001$)**

5.3 Control CFP-TG2 recombinant protein FRET analysis

The figure 5.4 represents the normalised fluorescence measured for CFP-TG2 recombinant protein when CFP is excited at 436nm and emission was measured at 476nm (cut off selected 455nm). As the GTP concentration increases no significant difference was observed in CFP emission.

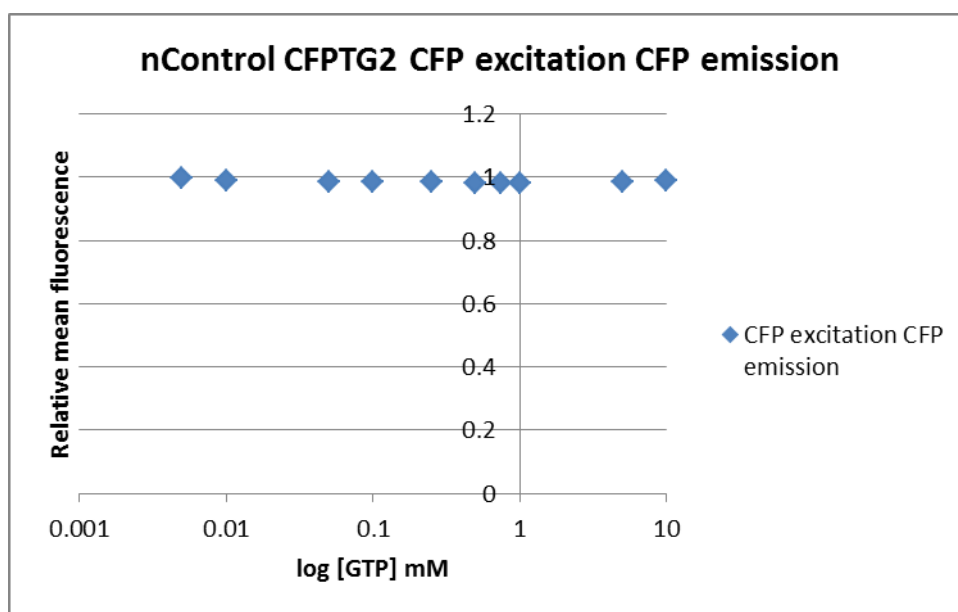


Figure 5.4 Effect of increasing concentration of GTP on CFP emission analysing control CFP-TG2 recombinant protein. The graph was plotted using log of calcium concentration from 5 μ M to 10mM. The fluorescence is represented as normalised mean fluorescence on Y axis. The results represent mean \pm S.D of three independent experiments done performed in triplicates.

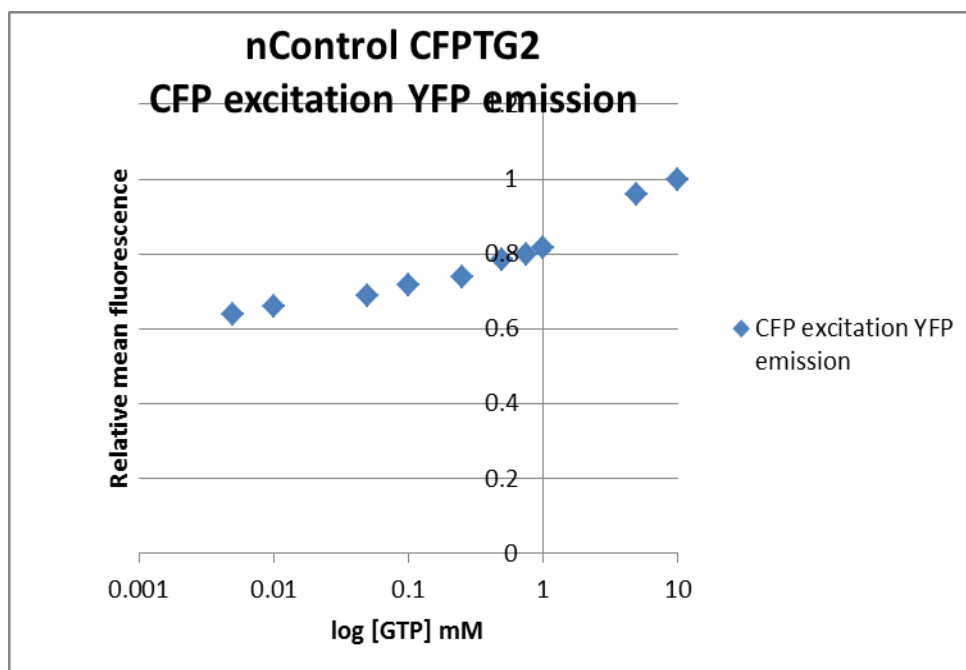


Figure 5.5 Effect of increasing concentration of GTP on CFP excitation YFP emission analysing control CFP-TG2 recombinant protein. The graph was plotted using log of calcium concentration from 5 μ M to 10mM. The increase in fluorescence is represented as normalised mean fluorescence. The results represent mean \pm S.D of three independent experiments done performed in triplicates.

Calculated FRET

A part of above represented YFP emission seen as CFP excitation YFP emission of CFP-TG2-YFP recombinant protein also includes bleedthrough. To correct for bleedthrough, we first calculated bleedthrough by

$$\text{Bleedthrough} = \frac{(\text{CFP}_{\text{ex}} \text{ YFP}_{\text{em}})_{\text{control CFP-TG2}}}{(\text{CFP}_{\text{ex}} \text{ CFP}_{\text{em}})_{\text{control CFP-TG2}}} \times (\text{CFP}_{\text{ex}} \text{ CFP}_{\text{em}})_{\text{CFP-TG2-YFP}}$$

$$\begin{array}{l} \text{YFP emission} \\ \text{corrected for} \\ \text{Bleedthrough} \end{array} = (\text{CFP}_{\text{ex}} \text{ YFP}_{\text{em}})_{\text{CFP-TG2-YFP}} - \text{Bleedthrough}$$

where “ex” is excitation and “em” represents emission

$$\begin{array}{l} \text{Sensitised YFP} \\ \text{emission corrected} \\ \text{for YFP} \end{array} = \begin{array}{l} \text{Sensitised YFP} \\ \text{emission corrected} \\ \text{for Bleedthrough} \end{array} - \text{Correction factor of YFP}$$

The calculated YFP emission corrected for bleedthrough is represented in the figure 5.6. With increase in GTP concentration there is an increase in FRET indicating the closing of the structure.

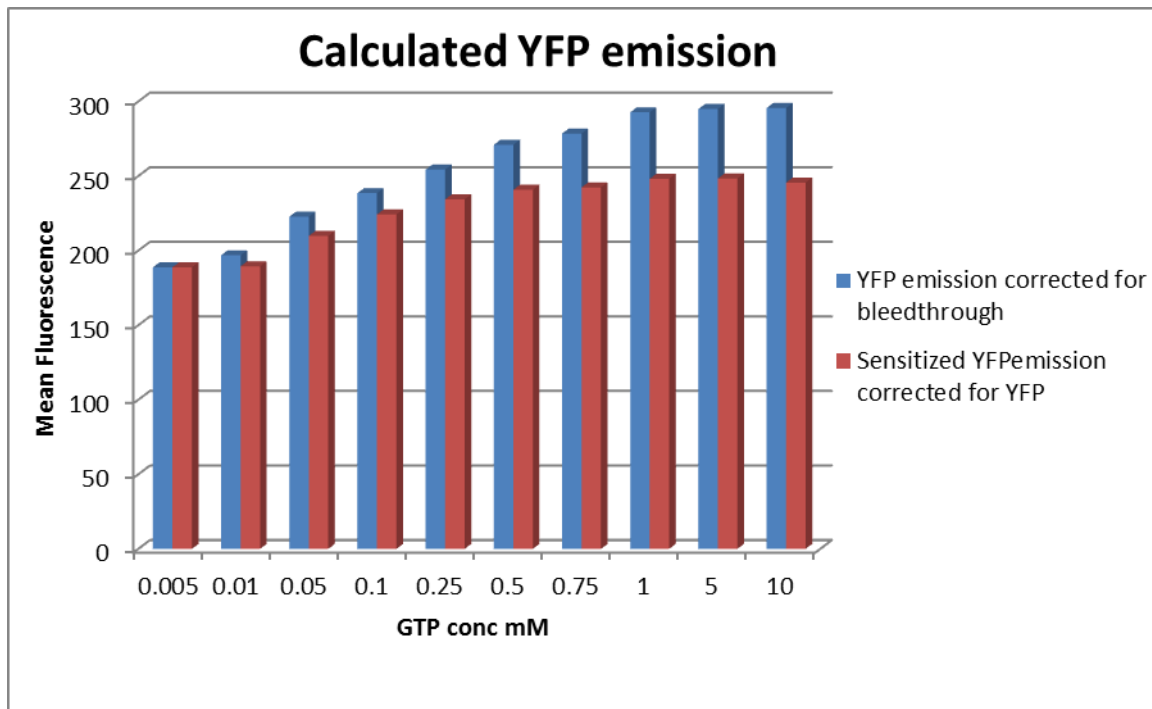


Figure 5.6 Effect of increasing concentration of GTP on FRET. The graph was plotted using log of GTP concentration from 5 μ M to 10mM. The figure shows the increase in YFP emission corrected for bleedthrough as represented in blue. As represented in red is the fluorescence corrected for the increase in YFP emission.

For calculating FRET efficiency,

$$\text{FRET efficiency} = \frac{\text{corrected(CFPex YFPem)A} - \text{corrected(CFPex YFPem)B}}{\text{corrected(CFPex YFPem)A}}$$

where A and B represent concentrations of GTP

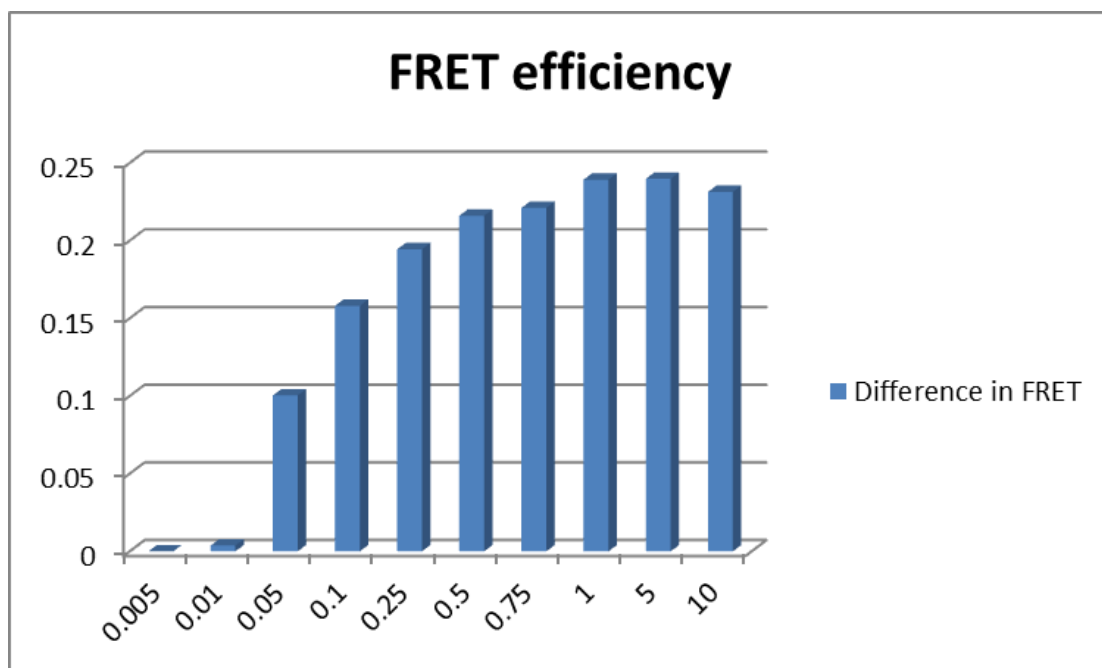


Figure 5.7 Effect of increasing concentration of GTP on FRET efficiency. The graph was plotted using log of GTP concentration from 5 μ M to 10mM.

5.4 Effect of Calcium on conformation using FRET analysis

TG2 activity is dependent of calcium binding. It is known that when calcium binds TG2 structure opens up to adapt an extended conformation allowing access to its active site. Here we investigate the calcium induced change in conformation of TG2 using FRET. An increasing concentration of calcium ranging from 5 μ M, 10 μ M, 50 μ M, 0.1mM, 0.25mM, 0.5mM, 0.75mM, 1mM, 5mM, 10mM. Additional calcium was added to compensate for EGTA chelation. CFP-TG2-YFP recombinant protein was purified using Ni-NTA column and desalted in 50mM Tris buffer, 1mMDTT, 1mM EGTA. 1 μ g of protein was used in each reaction. The figure 5.8 represents the normalised fluorescence measure when CFP is excited at 436nm and emission was measured at 476nm (cut off selected 455nm). As the calcium concentration increases there is an increase in CFP emission as the TG2 structure opens. A significant difference was observed between mean fluorescence at 5 μ M (lowest calcium concentration) and 10mM (highest concentration) of calcium. No significant difference was observed between 5mM and 10mM of calcium.

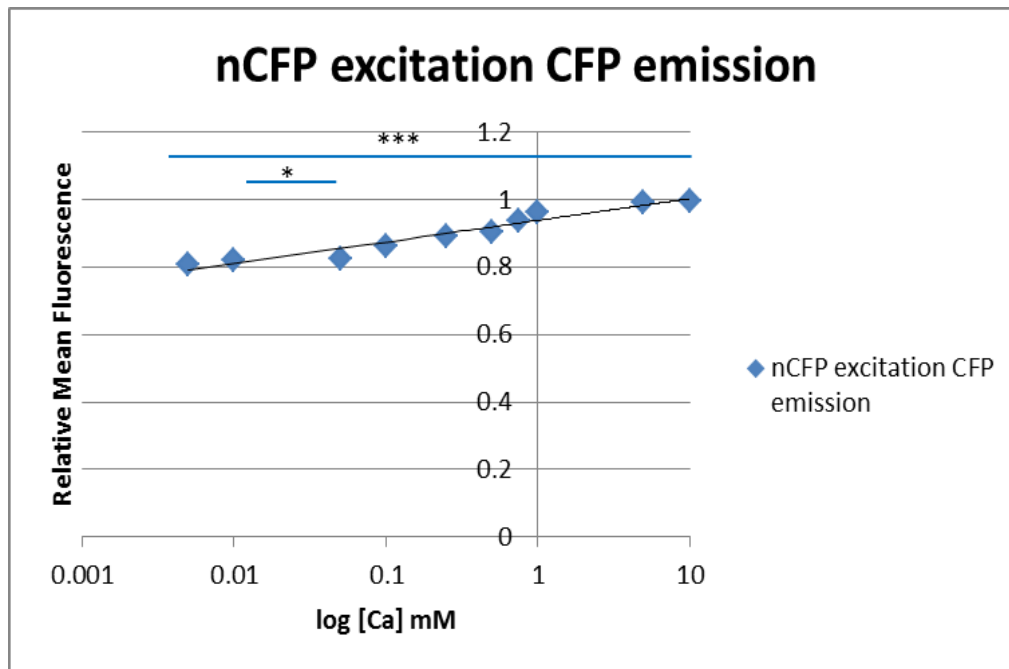


Figure 5.8 Effect of increasing concentration of calcium on CFP emission analysing CFP-TG2-YFP recombinant protein. The graph was plotted using log of calcium concentration from 5 μ M to 10mM. The increase in fluorescence is represented as normalised mean fluorescence. The results represent mean \pm S.D of three independent experiments done performed in triplicates. Statistical analysis was done using ANOVA applying Bonferroni post-test (*) $P < 0.001$)**

The figure 5.9 represents the normalised fluorescence measure when YFP is excited at 516nm and emission was measured at 538nm (cut off selected 530nm). As the calcium concentration increases the YFP emission does not show much difference in mean fluorescence. YFP emission indicated in figure below is a good indication of the amount of protein. Although there is a slight decrease with increase in calcium concentration observed in YFP emission, this decrease was corrected for during FRET efficiency calculation.

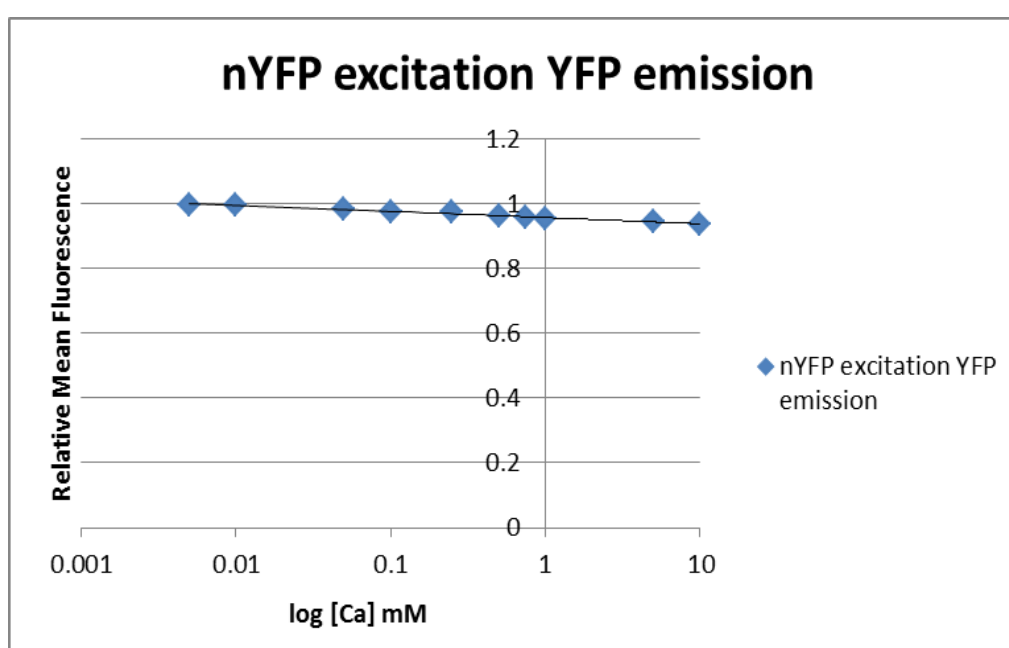


Figure 5.9 Effect of increasing concentration of calcium on YFP emission analysing CFP-TG2-YFP recombinant protein. The graph was plotted using log of calcium concentration from 5 μ M to 10mM. The fluorescence is represented as normalised mean fluorescence represented on the Y axis. The results represent mean \pm S.D of three independent experiments done performed in triplicates.

The figure 5.10 represents the normalised fluorescence measure when CFP is excited at 436nm and emission was measured at 538nm (cut off selected 530nm). As the calcium concentration increases there is a significant decrease in YFP emission as the TG2 structure opens. A significant difference was observed between mean fluorescence at 5 μ M (lowest calcium concentration) and 10mM (highest concentration) of calcium. This decrease in FRET indicates the structure of recombinant CFP-TG2-YFP opens as the calcium concentration increases. As the structure opens less energy is transferred from the donor to acceptor and hence a decrease in FRET is observed.

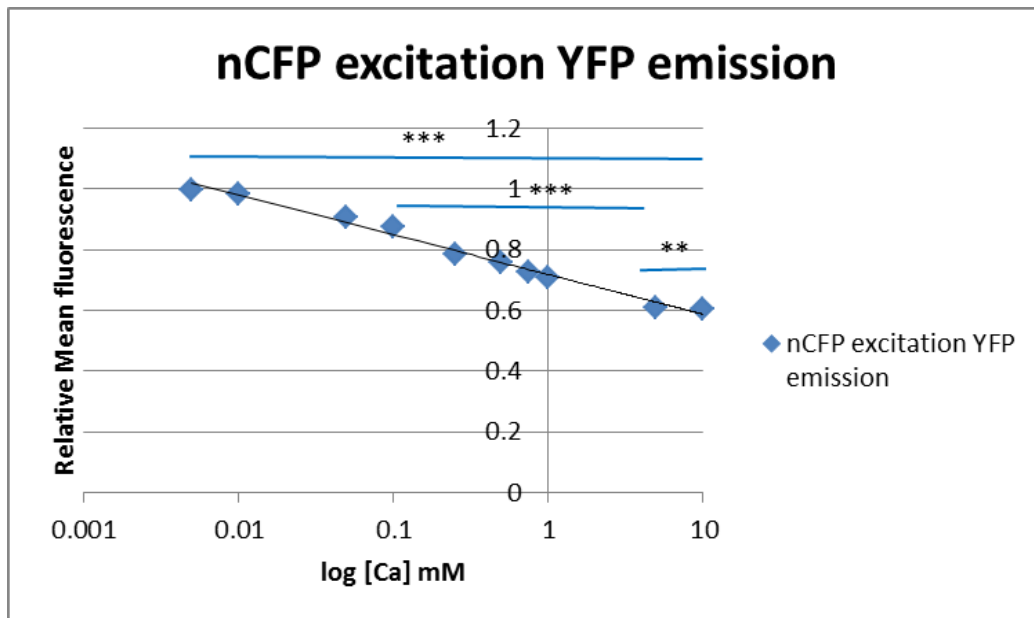


Figure 5.10 Effect of increasing concentration of calcium on CFP excitation YFP emission analysing CFP-TG2-YFP recombinant protein. The graph was plotted using log of calcium concentration from 5 μ M to 10mM. The decrease in fluorescence is represented as normalised mean fluorescence. The results represent mean \pm S.D of three independent experiments done performed in triplicates. Statistical analysis was done using ANOVA applying Bonferroni post-test (*) $P < 0.001$)**

5.5 Control CFP-TG2 recombinant protein FRET analysis

The figure 5.11 represents the normalised fluorescence measured for CFP-TG2 recombinant protein when CFP is excited at 436nm and emission was measured at 476nm (cut off selected 455nm). As the calcium concentration increases no significant difference was observed in CFP emission.

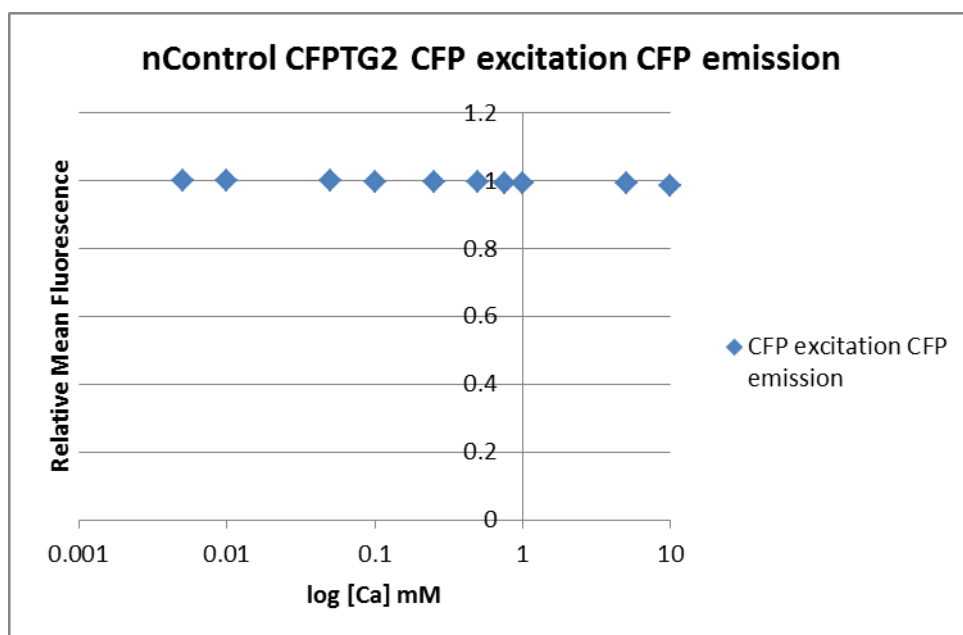


Figure 5.11 Effect of increasing concentration of calcium on CFP emission analysing control CFP-TG2 recombinant protein. The graph was plotted using log of calcium concentration from 5 μ M to 10mM. The fluorescence is represented as normalised mean fluorescence on Y axis. The results represent mean \pm S.D of three independent experiments done performed in triplicates.

The figure 5.12 represents the normalised fluorescence measure for CFP-TG2 recombinant protein when CFP is excited at 436nm and emission was measured at 538nm (cut off selected 530nm). As the calcium concentration increases there is a significant decrease in YFP emission as the TG2 structure opens. This control CFP-TG2 recombinant protein is important for the calculation of bleedthrough and FRET efficiency.

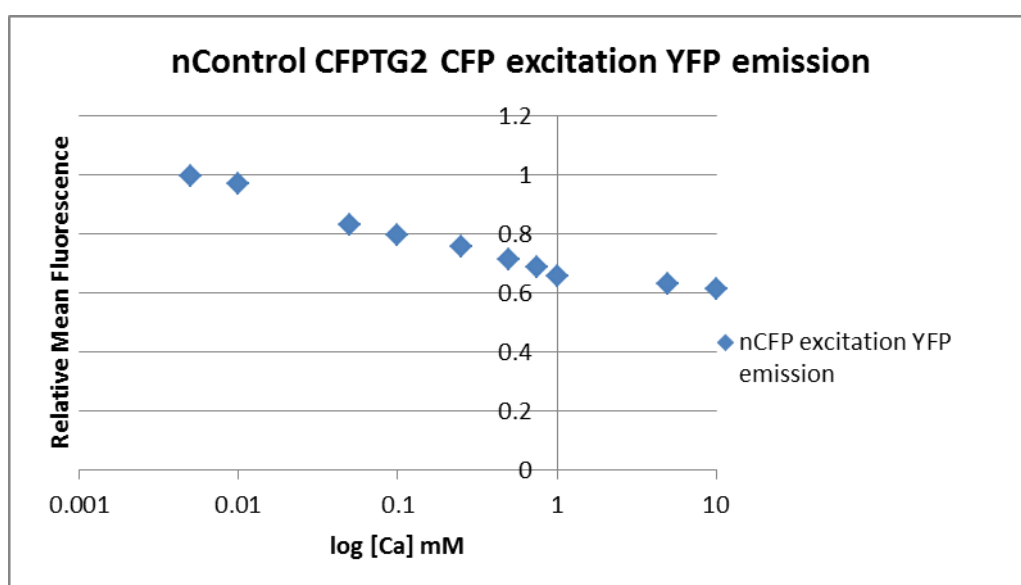


Figure 5.12 Effect of increasing concentration of calcium on CFP excitation YFP emission analysing CFP-TG2 recombinant protein. The graph was plotted using log of calcium concentration from 5 μ M to 10mM. The decrease in fluorescence is represented as normalised mean fluorescence. The results represent mean \pm S.D of three independent experiments done performed in triplicates.

Calculated FRET

A part of above represented YFP emission seen as CFP excitation YFP emission of CFP-TG2-YFP recombinant protein also includes bleedthrough. To correct for bleedthrough, we first calculated bleedthrough by

$$\text{Bleedthrough} = \frac{(\text{CFPex YFPem})_{\text{control CFP-TG2}}}{(\text{CFPex CFPem})_{\text{control CFP-TG2}}} \times (\text{CFPex CFPem})_{\text{CFP-TG2-YFP}}$$

$$\begin{array}{l} \text{YFP emission} \\ \text{corrected for} \\ \text{Bleedthrough} \end{array} = (\text{CFPex YFPem})_{\text{CFP-TG2-YFP}} - \text{Bleedthrough}$$

where “ex” is excitation and “em” represents emission

$$\begin{array}{l} \text{Sensitised YFP} \\ \text{emission corrected} \\ \text{for YFP} \end{array} = \begin{array}{l} \text{Sensitised YFP} \\ \text{emission corrected} \\ \text{for Bleedthrough} \end{array} - \text{Correction factor of YFP}$$

The calculated YFP emission corrected for bleedthrough is represented in the figure 5.13. With increase in calcium concentration there is a decrease in FRET indicating the opening of the structure.

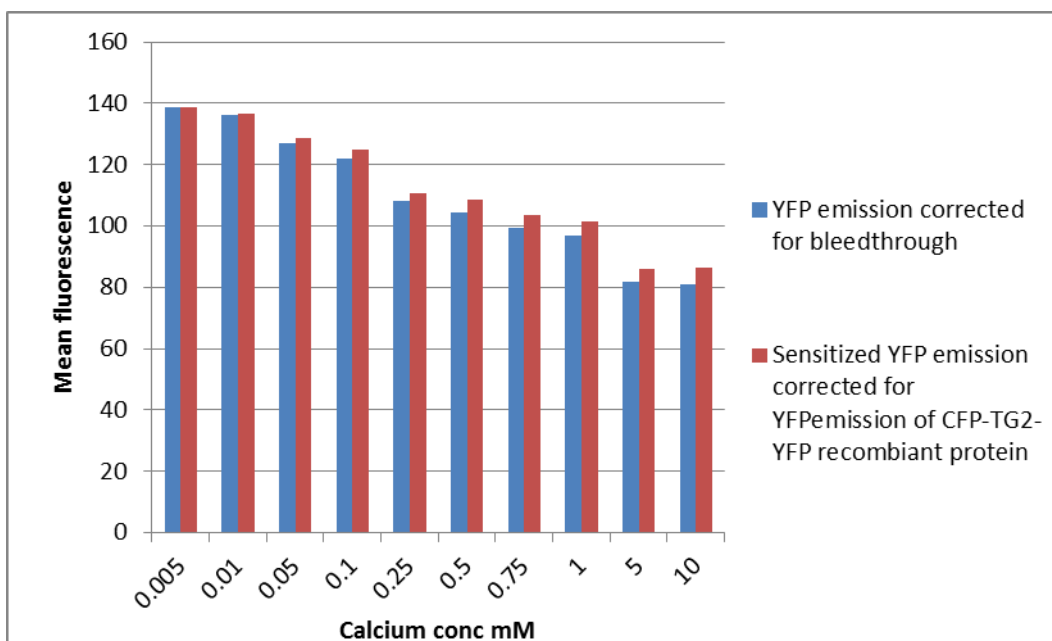


Figure 5.13 Effect of increasing concentration of calcium on FRET. The graph was plotted using calcium concentration from 5 μ M to 10mM against mean fluorescence. The figure shows the decrease in YFP emission corrected for bleedthrough as represented in blue. As represented in red is the fluorescence corrected for the increase in YFP emission.

For calculating FRET efficiency,

$$\text{FRET efficiency} = \frac{\text{corrected(CFPex YFPem)A} - \text{corrected(CFPex YFPem)B}}{\text{corrected(CFPex YFPem)A}}$$

where A and B represent concentrations of calcium

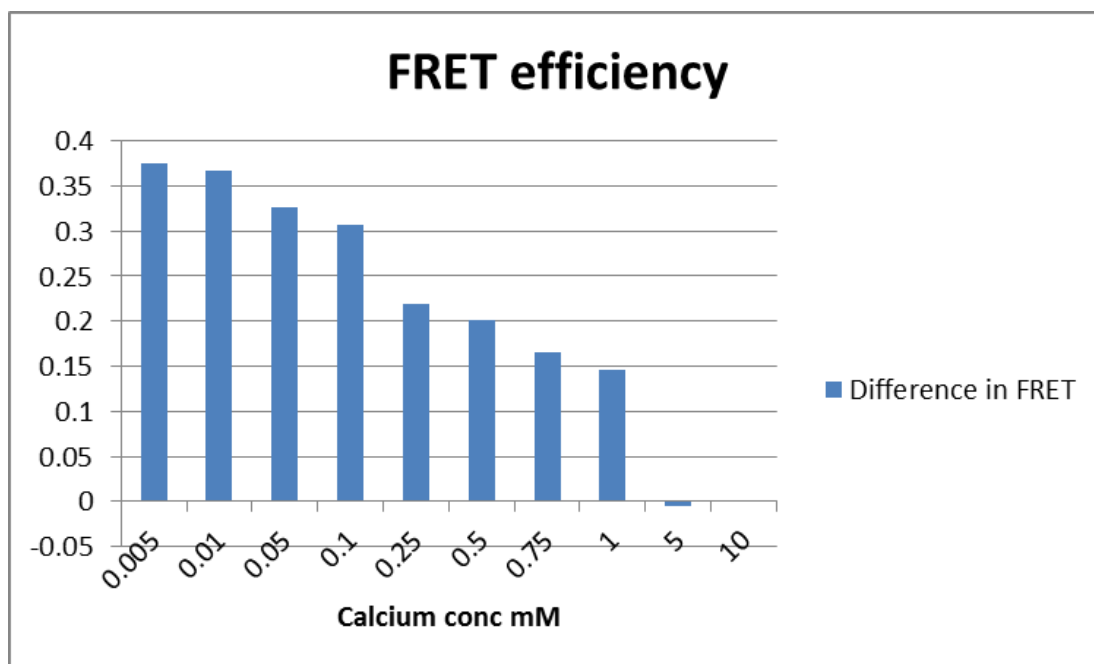


Figure 5.14 Effect of increasing concentration of calcium on FRET efficiency. The graph was plotted using log of calcium concentration from 5 μ M to 10mM.

5.6 Comparison of Calcium activity curve and FRET efficiency

The calcium activity curve was plotted on the same graph as the calculated FRET efficiency (negative FRET efficiency values) to compare the curve. Both curves follow the same trend indicating that we could correlate the effect of calcium on TG2 activity with the calculated FRET (figure 5.15).

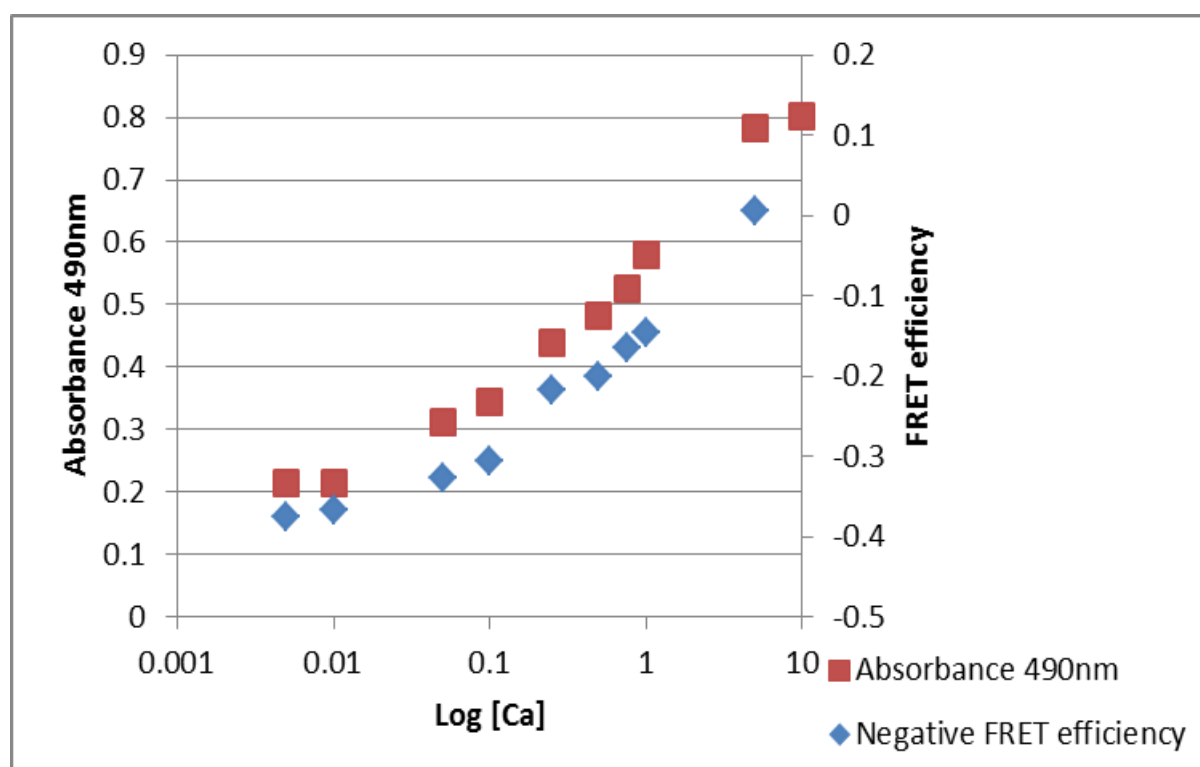


Figure 5.15 Comparison of calcium activity and FRET efficiency. The X axis represents the log of calcium concentration plotted against one Y axis represents increase in TG2 activity and second Y axis depicts the negative value of FRET efficiency.

5.7 Discussion

The TG2 FRET construct CFP-TG2-YFP was characterised to have properties similar to that of TG2. Although the construct and CFP-TG2 control was successfully constructed, the only YFP control TG2-YFP needs further investigation. This control would be helpful in FRET efficiency calculations. For the TG2-YFP construction a PCR cycle could be set up using TG2 forward primer and YFP reverse primer. This TG2-YFP construct would be subjected to nucleotide sequencing, expression and characterisation similar to that of CFP-TG2-YFP and CFP-TG2 construct. The only CFP-TG2 construct could also be applied to further studies investigating inter-molecular FRET with TG2 binding partners. The FRET data showed that with increasing concentration of GTP the TG2 structure adapts a closed conformation as accounted by the increase in the fluorescence. It could also be interesting to check the conformation when TG2 interacts with other molecules like integrin, heparin and syndecan. With increasing concentration of calcium the FRET data suggests the opening of the molecule as indicated by the decrease in fluorescence. The validation of the FRET construct is also seen by comparing the activity curve of TG2 and FRET efficiency.

Chapter 6

Construction of CFP-TG2-YFP recombinant protein in mammalian system

6.1 Introduction

Since the characterisation of the TG2 sensor was investigated, this FRET sensor was attempted to be cloned into mammalian expression vector. In this chapter it was attempted to describe the cloning strategy for mammalian expression vector. This chapter also focuses on some commonly faced problems with cloning. The CFP-TG2-YFP recombinant protein was attempted to be cloned into mammalian expression vector pcDNA3.1-. The use of new primer to amplify the construct were designed such that two proteins can be produced with or without the His tag.

6.2 PCR amplification

For expression of CFP-TG2-YFP recombinant protein in mammalian system, CFP-TG2-YFP in pTrcHisB construct (refer chapter 3) was attempted to be cloned into pcDNA3.1- (Invitrogen).

6.3 CFP-TG2-YFP amplification

Using primers NotICFP(for NotICFP-TG2-YFP construct) and HispTrc (for His-tag CFP-TG2-YFP construct) as forward primers and YFP reverse primer(YFP Rev2) was using to amplify the entire CFP-TG2-YFP construct using CFP-YFP-TG2 plasmid (chapter 3) Reactions were performed in triplicates in MWG Biotech Aviso Thermal cycler to avoid over-representation of polymerase-induced errors. Thermal cycling conditions were optimised for maximum amplification yield and specificity. Amplification of His-CFP-TG2-YFP was obtained as seen in Lanes 2, 3, 4 in figure 6.1. Amplification of NotICFP-TG2-YFP was obtained as seen in Lanes 5, 6, 7 in figure 6.1. Bands of correct size of about 3.5Kb were seen. Conditions for PCR were optimised to be initial denaturation at 95°C for 2 min, followed by 35 cycles of 95°C for 45 s, 70°C for 1 min, 72°C for 1 min, followed by a final extension step at 72°C for 10 min using KOD Hot start polymerase using 10X KOD hot start buffer and 1mM MgSO₄.

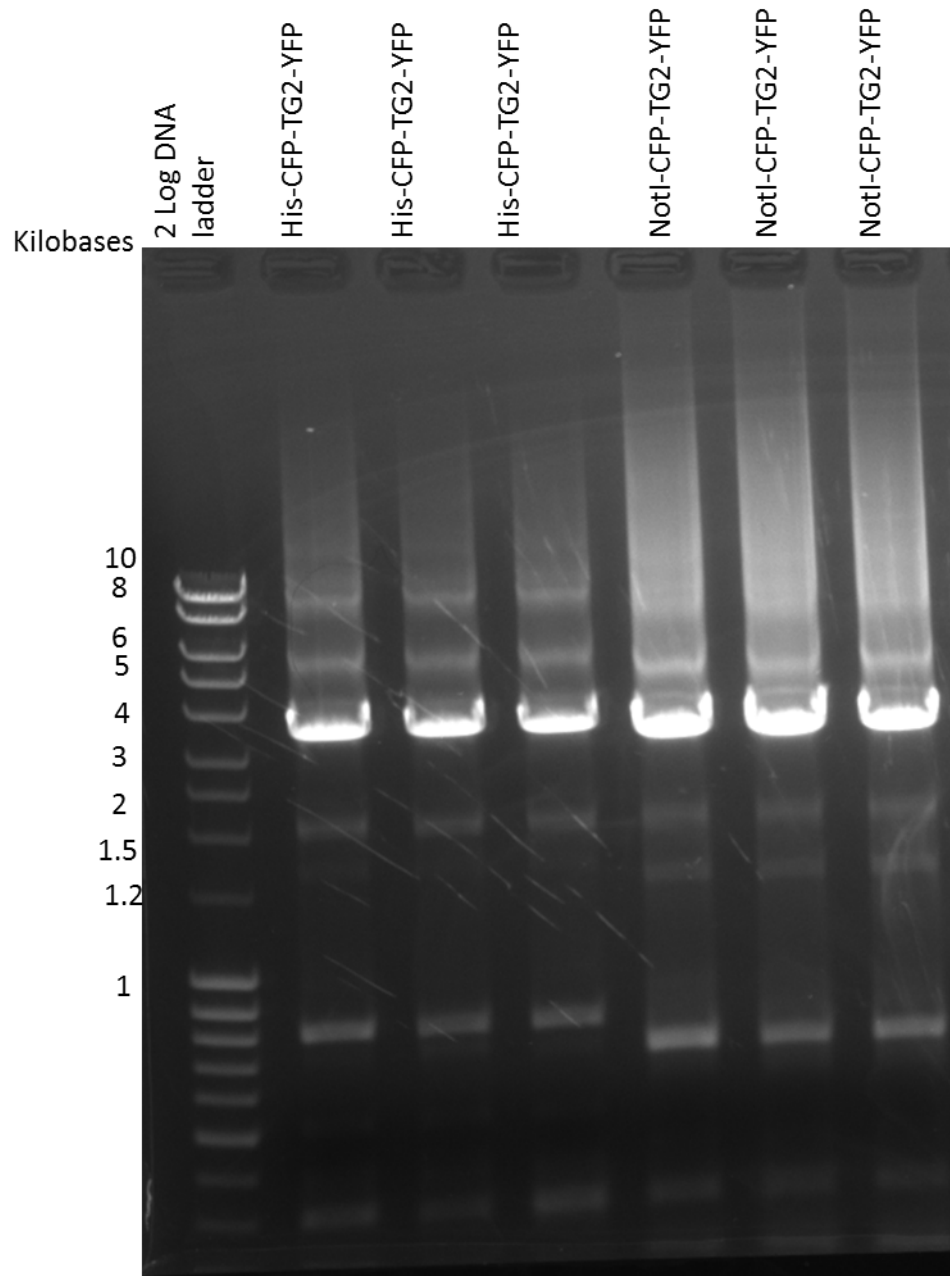


Figure 6.1 Agarose gel electrophoresis of amplified CFP-TG2-YFP plasmid using forward primers NotICFP and HispTrc and YFP Rev2 primer. Lane 1 is the 2-log marker DNA. Lane 2, 3, 4 showing amplified His-CFP-TG2-YFP plasmid and Lane 5, 6, 7 showing the amplified NotICFP-TG2-YFP which is 3.5 Kb in size.

6.4 Cloning amplified products into pSTBlue-1

Identification of recombinant pSTBlue-1 plasmids.

Using the pSTBlue-1 blunt cloning kit the amplified products His-CFP-TG2-YFP and NotICFP-TG2-YFP were ligated into pSTBlue-1 and transformed into NovaBlue competent cells. Blue/white screening was performed by spreading transformed cells onto plates containing 100µg/ml ampicillin, 100µM IPTG and 50µg/ml X-gal. White colonies, potentially containing inserted DNA, were screened for increased size compared to the empty vector pSTBlue-1 using a simple alkaline lysis procedure followed by agarose DNA electrophoresis (cracking).

6.5 His-CFP-TG2-YFP cracking

Following Blue/White screening, 13 white colonies were selected for the cracking procedure. A blue colony (parent pSTBlue-1) was also selected as a negative control for cracking. All samples were then run on an agarose gel for further analysis. All plasmids which were of a larger size than the parent pSTBlue-1 (blue colony) were selected for further analysis. From the figure 6.2, clones His-CFP-TG2-YFP 5, 6, 8, 9, 10, 11, 14 were found to be larger than parent vector.

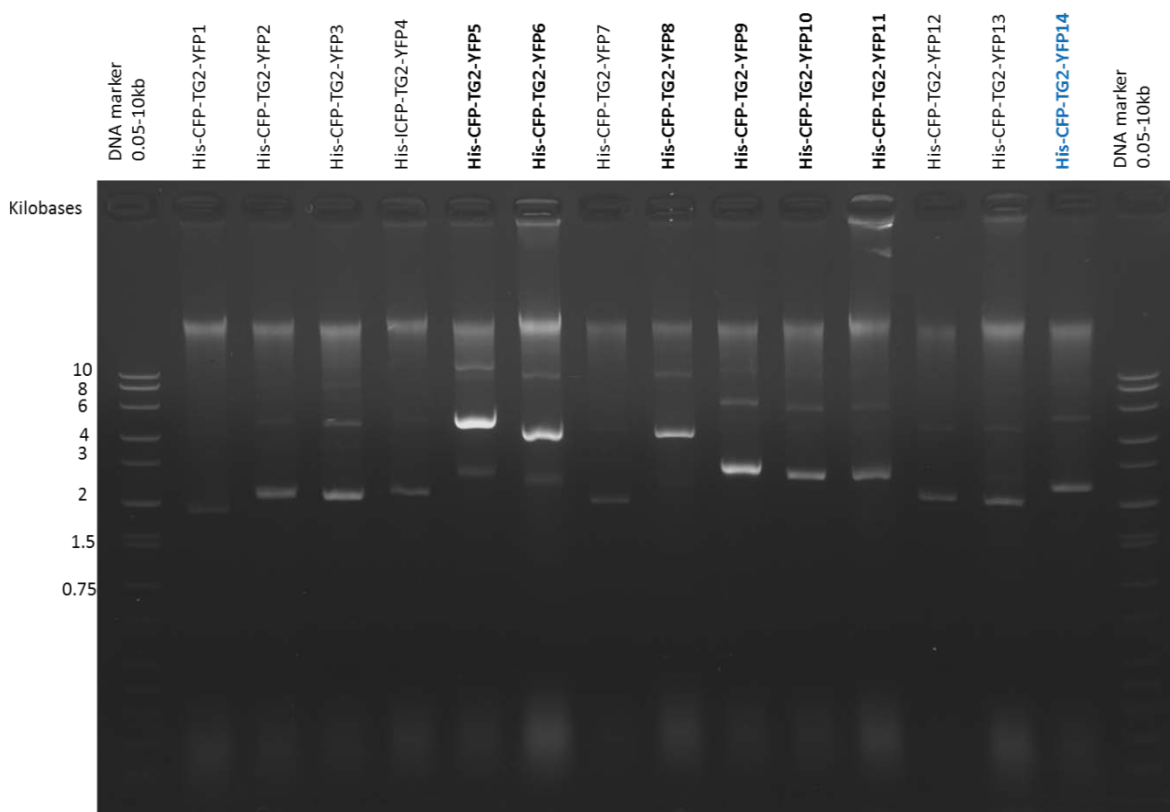


Figure 6.2 Agarose gel electrophoresis of the cracking procedure performed on the selected His CFP-TG2-YFP colonies after Blue White screening. Lane 1 is the 2-log marker DNA. Lanes 2 to 14 showing His-CFP-TG2-YFP clones 1-13. Lane 15 showing the blue colony representing a negative control for selection. CFP 5, 6, 8, 9, 10, 11 and 14 were found to be of correct size.

6.6 NotICFP-TG2-YFP cracking

Following Blue/White screening, 14 white colonies were selected for the cracking procedure. A blue colony (parent pSTBlue-1) was also selected as a negative control for cracking. All samples were then run on an agarose gel for further analysis. All plasmids which were of a larger size than the parent pSTBlue-1 (blue colony) were selected for further analysis. From the figure 6.3, clones NotICFP-TG2-YFP 4, 5, 8, 10, 12, 13 were found to be larger than parent vector.

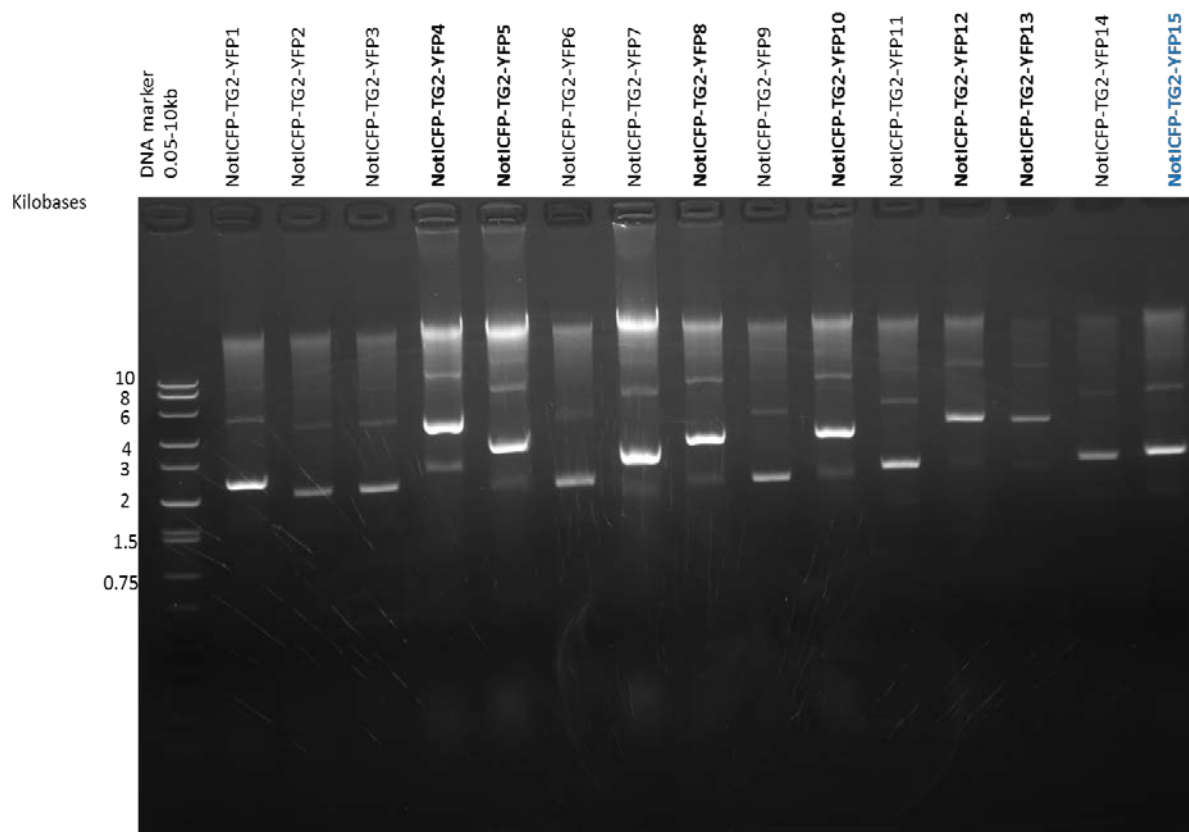


Figure 6.3 Agarose gel electrophoresis of the cracking procedure performed on the selected NotI CFP-TG2-YFP colonies after Blue White screening. Lane 1 is the 2-log marker DNA. Lanes 2 to 15 showing His-CFP-TG2-YFP clones 1-15. Lane 16 showing the blue colony representing a negative control for selection. CFP 4, 5, 8, 10, 12 and 13 were found to be of correct size.

On analysing the cracking agarose gel results, plasmids which were larger than the parent pSTBlue1 vector were selected. Using the Promega Wizard Plus minipreps DNA purification Kit, plasmid purification was performed on the selected clones of His-CFP-TG2-YFP and NotCFP-TG2-YFP. These plasmids were then digested using *EcoRI* to test for inserts of the correct size (*EcoRI* digestion cuts out YFP (0.75Kb insert), around 2.75Kb insert of CFP-TG2 insert and 3.8Kb insert of pSTBlue1).

6.7 Cloning of CFP-TG2-YFP construct into expression vector pcDNA3.1-

pcDNA3.1- vector was transformed into NovaBlue competent cells. Colonies were selected from the plate and then grown individually in 5ml LB broth containing ampicillin at 37°C in orbital shaking incubator overnight. Using the Promega Wizard Plus minipreps DNA purification Kit, plasmid purification was performed. The pcDNA3.1- purified plasmid was run on an agarose gel as shown in figure 6.4.

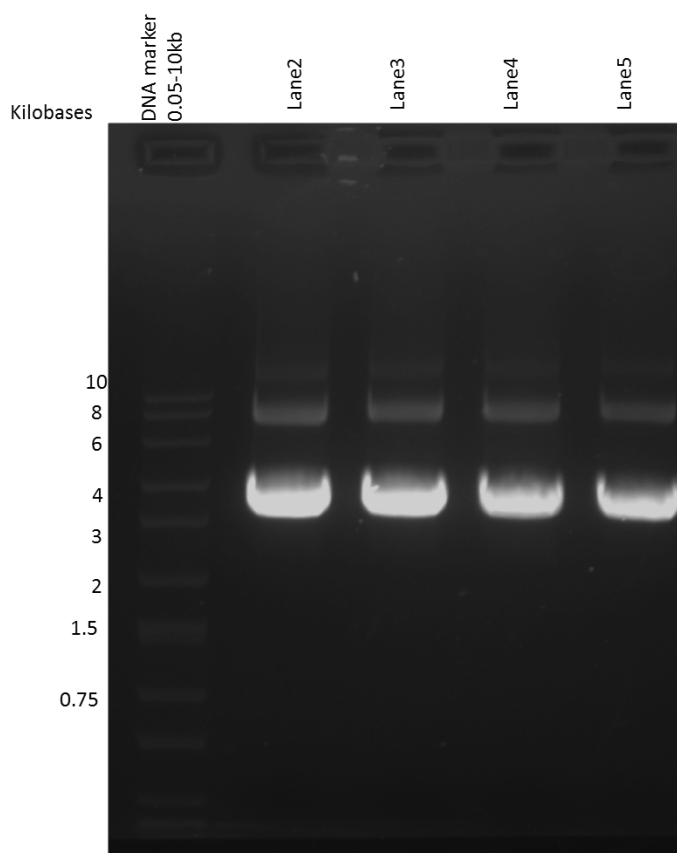


Figure 6.4 Agarose gel electrophoresis of the purified plasmid of pcDNA3.1-. Lane 1 is the 2-log marker DNA. Lanes 2, 3, 5 showing pcDNA3.1- purified plasmid of about 5.5 Kb.

6.8 Cloning NotCFP-TG2-YFP and HisCFP-TG2-YFP into pcDNA3.1-

His-CFP-TG2-YFP/NotCFP-TG2-YFP plasmid was digested from the pSTBlue-1 plasmid using *HindIII* and *NotI*. The *HindIII* digestion was performed and the reaction was set up using buffer 2 (NEB) followed by *NotI*/*PvuI* double digestion in buffer 3. *PvuI* was used to cut the 3.8Kb pSTblue1 parent vector into smaller fragments to facilitate easy agarose gel purification of His-CFP-TG2-YFP insert of 3.5Kb (figure 6.5). Similar digestion was performed on NotCFP-TG2-YFP plasmid. pcDNA3.1- was digested using *NotI* and *HindIII*, with gel electrophoresis (Figure 6.6) showing double digested pcDNA3.1- (5.4 Kb). On digestion the purified undigested plasmid runs faster as it is super coiled but when digested a band about 5.5 Kb was seen.

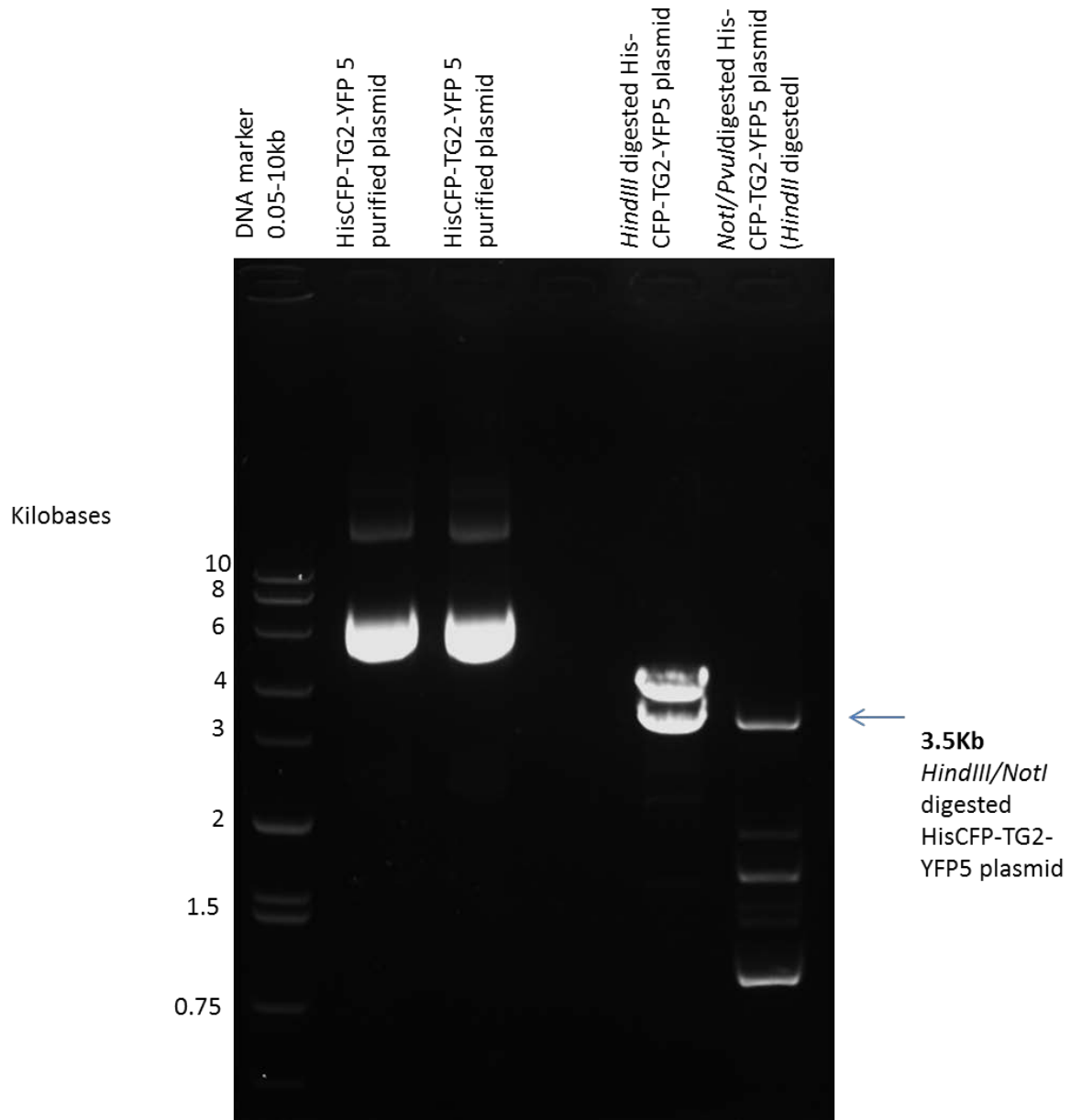


Figure 6.5 Agarose gel electrophoresis of the digestion of the His-CFP-TG2-YFP5 plasmid using *NotI* and *HindIII*. Lane 1 is the 2-log marker DNA. Lane 2 and 3 shows purified plasmid of His-CFP-TG2-YFP5. Lanes 4 shows *HindIII* digestion showing 3.8Kb band of pSTblue1 and 3.5Kb band of His-CFP-TG2-YFP insert. Lane5 shows *NotI/PvuI* digestion revealing 3.5Kb band of insert and lower bands indicated pSTblue1 vector digested into smaller fragments.

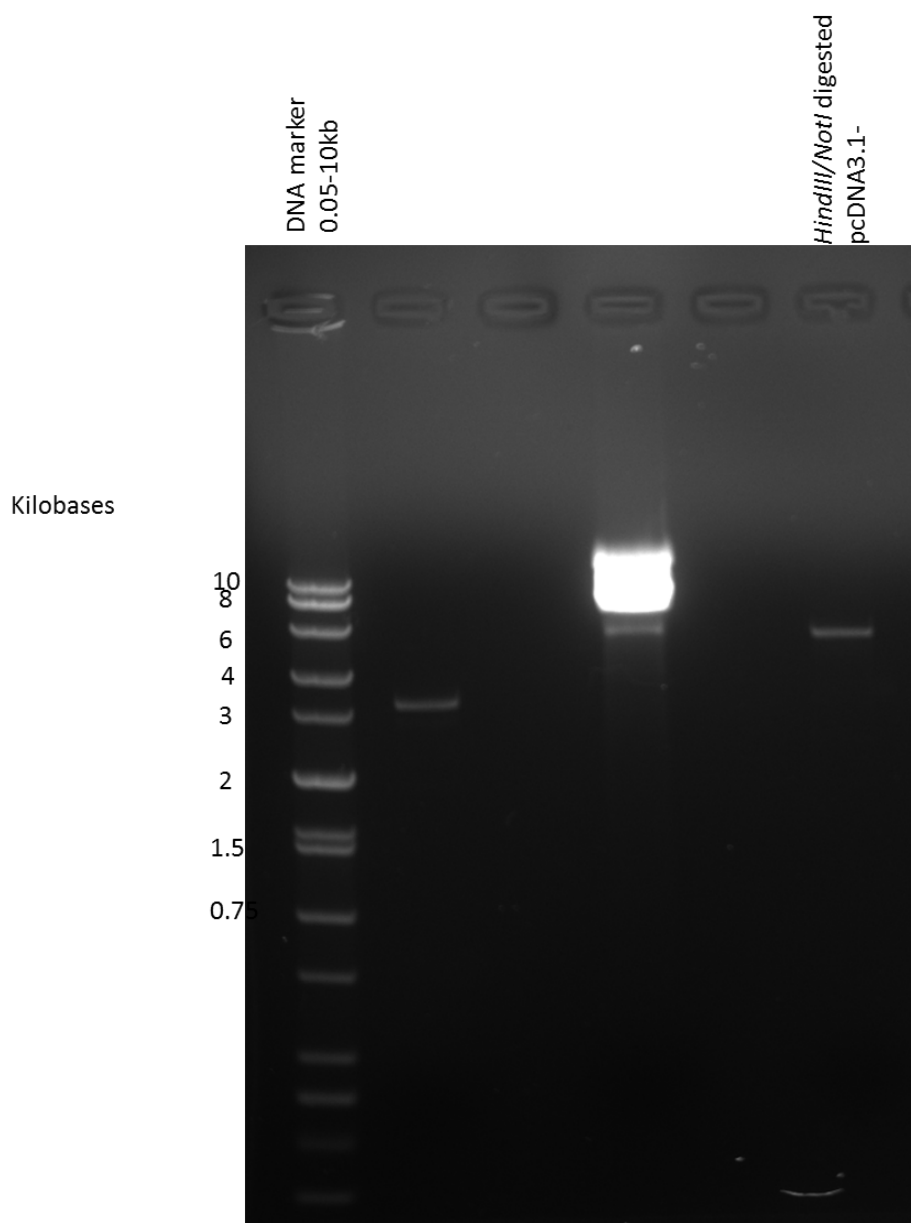


Figure 6.6 Agarose gel electrophoresis of the digestion of the purified pcDNA3.1- plasmid using *NotI* and *HindIII*. Lane 1 is the 2-log marker DNA. Lanes 4 shows double digested plasmid of about 5.5 Kb.

The digested pcDNA 3.1-, His-CFP-TG2-YFP plasmid, Not-CFP-TG2-YFP plasmids were extracted and purified from a low melting point agarose gel. The purified pcDNA3.1- was further treated with Antarctic phosphatase to remove 5' phosphates and prevent religation. Further a ligation reaction was performed using Quick ligase

to ligate pTrcHis B and CFP and was then transformed into Novablue competent cells. Cracking procedure was repeated on the colonies grown.

6.9 Screening of recombinant CFP-TG2-YFP-pcDNA3.1- plasmids

The screening of recombinant plasmids were performed by analysing transformed colonies via cracking procedure. Negative control used was pcDNA3.1- self ligated control. Cracking procedure did not reveal colonies of correct size. Analysed colonies seen in the figure 6.7, 6.8, 6.9 showed plasmid of size similar to that of negative control indicating unsuccessful cloning of insert into pcDNA3.1- vector.

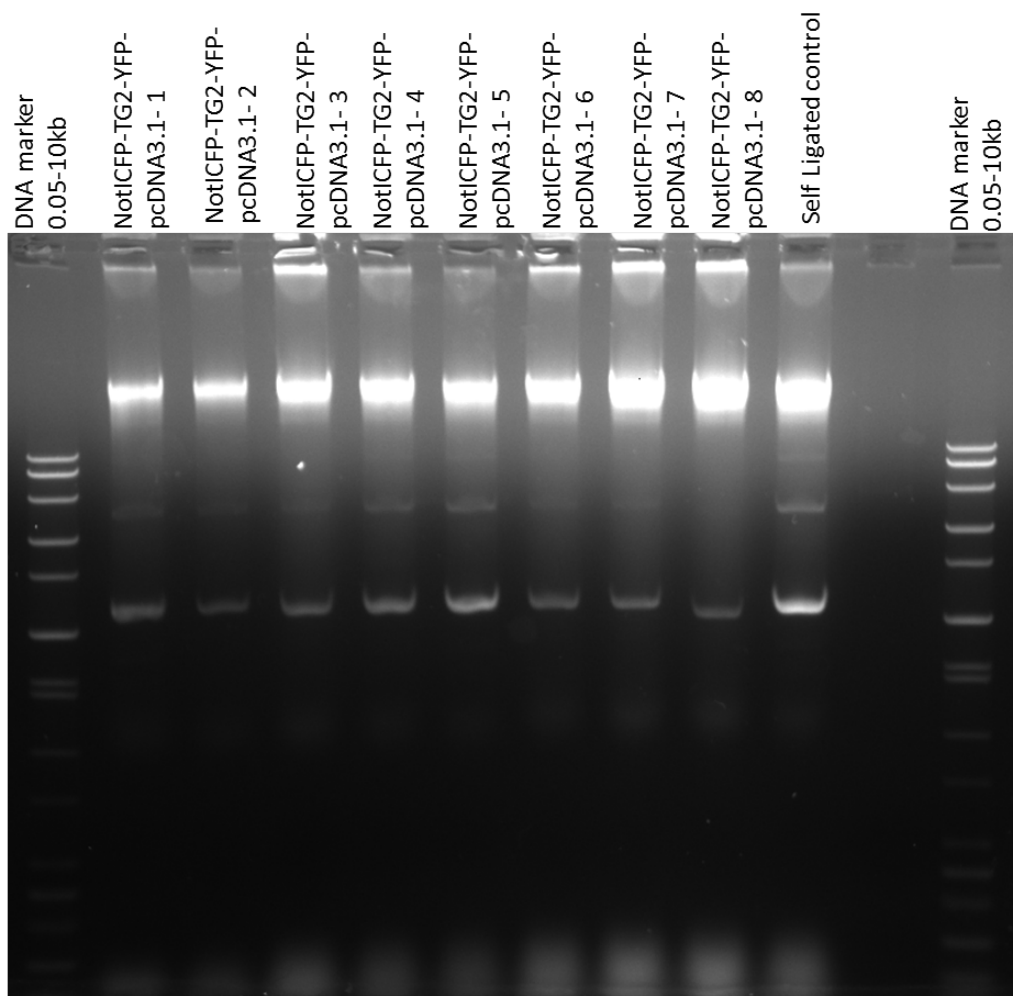


Figure 6.7 Agarose gel electrophoresis of the cracking procedure performed on the selected NotICFP-TG2-YFP-pcDNA3.1- colonies after transformation. Lane 1 and 11 is the 2-log marker DNA. Lanes 2 to 9 showing NotICFP-TG2-YFP-pcDNA3.1- clones 1-8. Lane 10 representing a negative control (self ligated vector) for selection.

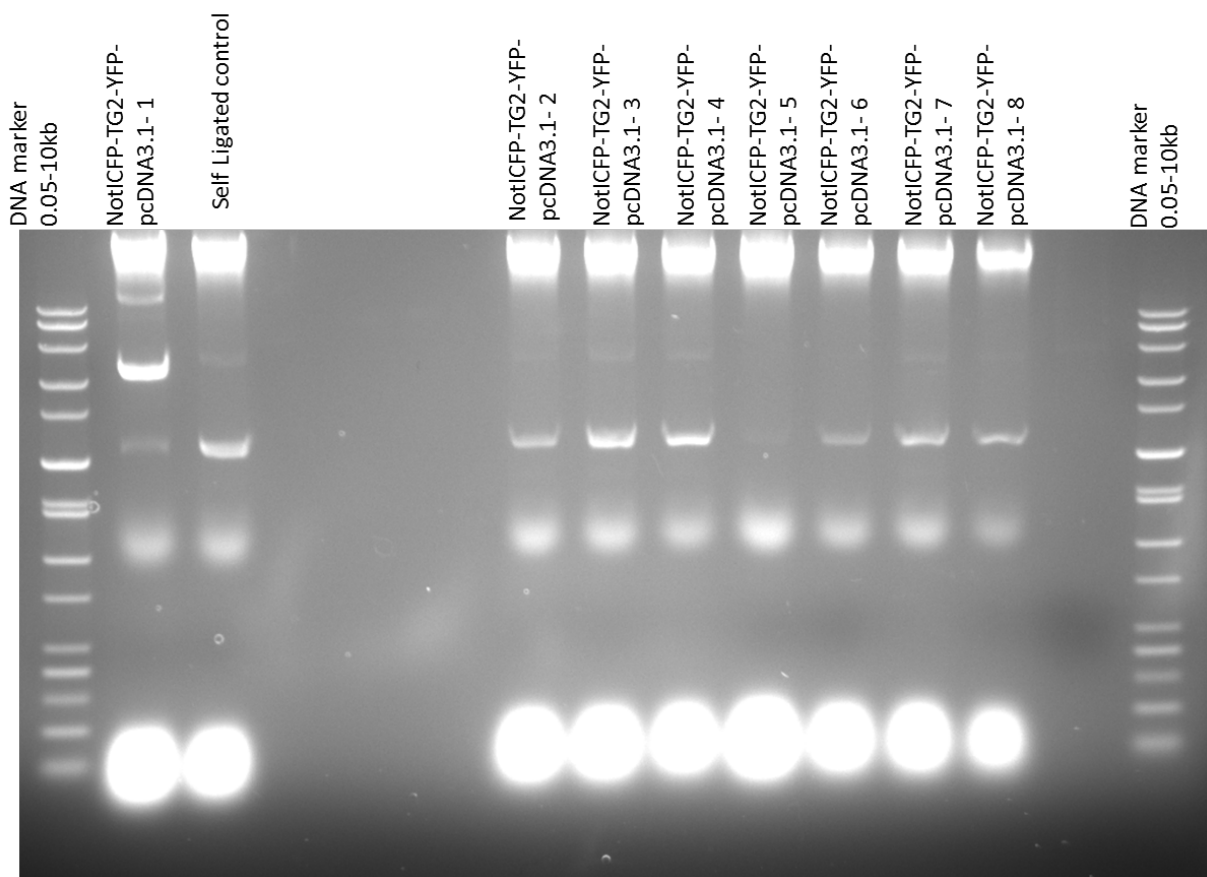


Figure 6.8 NotICFP-TG2-YFP-pcDNA3.1- colonies after transformation. Lane 1 and 11 is the 2-log marker DNA. Lanes 2, 4 to 10 showing NotICFP-TG2-YFP-pcDNA3.1- clones 1-8. Lane 3 representing a negative control (self ligated vector) for selection.

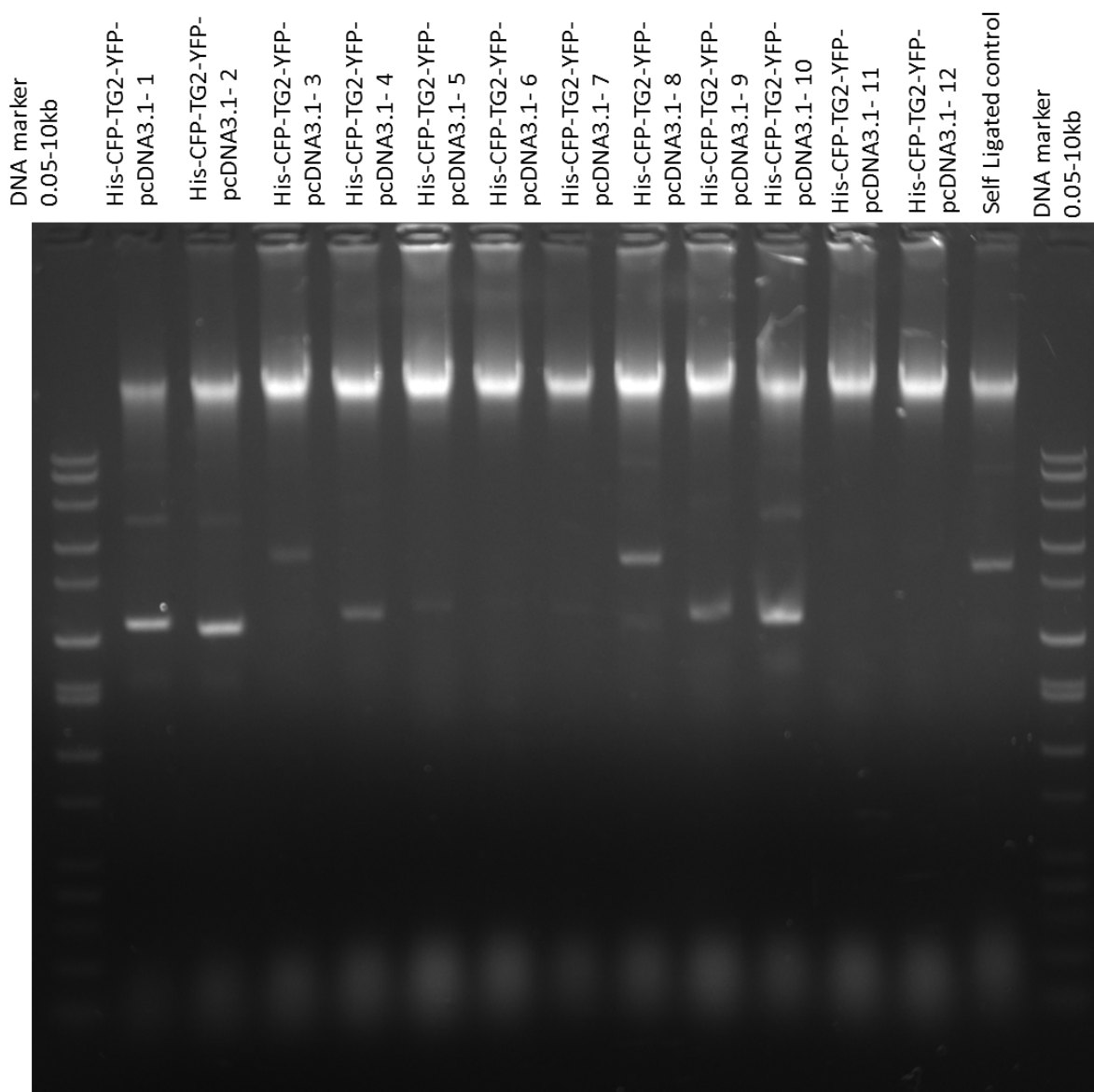


Figure 6.9 Agarose gel electrophoresis of the cracking procedure performed on the selected His-CFP-TG2-YFP-pcDNA3.1- colonies after transformation. Lane 1 and 15 is the 2-log marker DNA. Lanes 2 to 13 showing His-CFP-TG2-YFP-pcDNA3.1- clones 1-12. Lane 14 representing a negative control (self-ligated vector) for selection.

6.10 Discussion

The cloning of the construct into mammalian expression vector still needs further investigation. The use of pcDNA3.1- was the choice of expression vector. The use of alternate expression vector like LIC vector could be a better option. These vectors are better designed to accommodate larger fragments of DNA for mammalian expression. The other option is to clone CFP-TG2-YFP into pcDNA3.1+ but changing the restriction sites and cloning strategy. Also it could be worth sequencing the pcDNA3.1- expression vector to ensure no mutations have occurred and the restriction sites are intact for successful cloning. Such point mutations could have been introduced during the freezing-thawing of plasmids. The same nucleotide sequencing could be done to ensure NotCFP-TG2-YFP and HisCFP-TG2-YFP plasmid to ensure no mutations have been introducing during PCR amplification.

Chapter 7

Discussion

Transglutaminase is a commercially important enzyme that catalyses the posttranslational modifications of proteins, converting the primary amide group of the peptidyl-glutamine substrate into a secondary amide by formation of an isopeptide bond. The final products undergo polyamidation or are cross-linked aggregated proteins.(Bergamini et al., 2011) Tissue transglutaminase is a calcium dependent enzyme and its transamidating activity is regulated by the binding of calcium ions and exposure of the active site for interaction with glutamine substrate. GTP acts as an inhibitor of this reaction by binding to the protein and bringing the core domain and β - barrel 1 together adapting a compact form. This conformational change thereby also affects the binding of other molecules like fibronectin, heparan sulphate and integrins. To have a better understanding of conformation of TG2, that is brought about by the binding of calcium and GTP this study incorporated the construction of a novel TG2 FRET biosensor. The construction of this FRET sensor involved a pair of fluorescent proteins fused on the N and C termini of TG2. For this construct CFP and YFP were recruited as the choice of fluorescent proteins. CFP-YFP is the most commonly used FRET pair due to their small size. This pair was preferred such that the use of small fluorescent protein would not interfere with the conformational change that TG2 undergoes.(Pinkas et al., 2007) The use of other FRET pair like mcerulean C1 and eYFP for TG2 has also been reported. (Caron et al., 2012) For the assembly of this TG2 FRET sensor the cloning strategy was to clone the CFP first with TG2 and check expression in the expression vector pTrcHisB. This would not only serve as a FRET control CFP-TG2 construct but also assess the effect of tagging one fluorescent protein onto TG2. The stepwise cloning strategy would also ensure the correct sequence of the construct and if it behaves similar to protein without the fluorescent tag. The other alternative to step wise cloning would be the

PCR amplification of the entire construct. This would require a massive screening of recombinant TG2. Also the chances of entire sequence to be correct without point mutations would be critical. This alternate strategy of constructing the FRET sensor could definitely be quicker provided the screening of recombinant clones is performed systematically. This method could also be disadvantageous for orientation of fluorescent tags and the screening of constructs with correct orientation could be time consuming. The step wise cloning also has the advantage of checking whether the expression of TG2 is affected because of fluorescent tags attached. PCR amplification of the entire construct has the risk that once constructed the expression may not be ideal or construct may not function properly. To avoid this risk the step wise cloning and checking of construct after attachment of each tag would reduce the risk of the entire construct not working altogether. This method would also require another protocol to be established for the generated of FRET controls including CFP-TG2 and TG2-YFP constructs. This cloning strategy would also determine if there is a difference between single tagged CFP-TG2 and double tagged CFP-TG2-YFP recombinant protein. Having only one fluorescent protein attached to TG2 either CFP-TG2 or TG2-YFP could be applied to study intermolecular FRET by binding the other fluorescent protein on to TG2 binding partners like integrin, syndecan or heparin and investigate ECM interactions. The use of other expression vectors including pTrcHisA or pTrcHisC would also be another possibility but dependent on the restriction sites for cloning. It could also be further investigated whether how the expression is increased or decreased using another expression vector. This construct was then characterised on the basis of its expression and purification in bacterial system. The synthesised CFP-TG2-YFP recombinant protein was also tested for its ability to bind to heparin sepharose. The

CFP-TG2-YFP recombinant protein was further examined for its protease sensitivity after reacting with monodansyl cadaverin, biotin cadaverin and R281/R283 (TG2 inhibitors). An increasing concentration of calcium and GTP was applied to analyse the activity curve of CFP-TG2-YFP recombinant protein. Its ability to bind to fibronectin was also examined using an enzyme linked immunosorbent assay. Using this FRET-based TG2 biosensor the changes in fluorescence are measured with respect to the conformational changes of TG2.

For the cloning part of this project, Novablue competent cells were used as they are highly efficient for transformation and support blue-white screening. Expression of CFP-TG2-YFP recombinant protein was tested in Novablue cells first. The construct was then transferred into Rosetta 2 cells as they are designed to express mammalian genes as the cells have tRNAs necessary for protein expression. The use of Rosetta 2 for expression definitely showed enhanced protein expression as compared to Novablue cells. Initial expression and purification was performed using GE Healthcare His-GraviTrap column. Although CFP-TG2-YFP was successfully purified using the pre-packed column, it was limiting with respect to optimisation of the gradient. The purification performed using His-GraviTrap column was performed using gravity protocol according to manufacturer's instruction which often was time consuming. The use of GE AKTA prime FPLC was better for purification of the recombinant CFP-TG2-YFP protein as a higher volume of initial load could be loaded onto the column with less difficulty, a better control over protein elution with respect to gradient elution and higher yield of purification was seen. The gradient elution for purification of recombinant CFP-TG2-YFP was optimised by altering the elution step with respect to volume of the elution step. The initial wash step preceding the elution

was altered to reduce non-specifically bound proteins. Different concentrations of imidazole were tried to optimise the purification of desired protein. The most optimum purification of CFP-TG2-YFP recombinant protein was seen when applying a 20mM imidazole wash followed by a 20-200mM imidazole gradient elution where the specific activity was found to be 4.5 OD490/min/mg. Using this purification protocol it is observed that apart from desired protein seen at 135kDa, a simultaneous band of around 75kDa is observed in the SDS-PAGE analysis of the purified protein. This band is also seen the western blot plot analysis of purified protein using Cub7402 mouse monoclonal antibody. This band could possibly be due to presence of start codon in the sequence of the construct or due to proteolytic cleavage during purification. Subsequent purifications were performed incorporating 1mM phenylmethylsulfonyl fluoride (PMSF) just before lysing the bacterial cells via sonication. But no change in purity of protein was observed, the 75KDa band was still eluted simultaneously with CFP-TG2-YFP recombinant protein. The purification of control CFP-TG2-pTrcHisB was performed similarly. SDS PAGE analysis stained with coomassie blue staining and western blot analysis both confirmed the successful purification of the control CFP-TG2 recombinant protein required as a FRET control.

To characterise the CFP-TG2-YFP construct further, the heparin binding ability of the newly synthesised recombinant CFP-TG2-YFP recombinant protein was verified. As a control to test the heparin sepharose column, purification of pET30Ek/LIC TG2 (wild type TG2) using Ni-NTA column was performed. The eluted protein was then loaded onto the heparin sepharose column and it was observed that wild type TG2 successfully binds to the heparin column and its presence in eluted fractions was confirmed by western blot analysis. The heparin binding ability of CFP-TG2-YFP and

CFP-TG2 recombinant protein was tested using the same heparin sepharose column. The results revealed that both CFP-TG2-YFP recombinant protein and CFP-TG2 recombinant protein successfully bind to heparin sepharose column. CFP-TG2-YFP recombinant protein was purified over Ni-NTA column was processed further using heparin sepharose column to get a cleaner purification. A reduction in non-specifically bound protein was observed after down streaming processing of CFP-TG2-YFP purified recombinant protein.

Analysis of protease sensitivity of biotin cadaverin (BTC) treated wild type TG2 revealed that no digestion of protein was observed with increasing concentrations of BTC. The same was observed with purified CFP-TG2-YFP recombinant protein. The use of monodansyl cadaverin (MDC) to pre-treat wild type TG2 and recombinant CFP-TG2-YFP protein revealed no digestion of protein on treatment with trypsin. This probably suggests that TG2 adapts a closed conformation which is less susceptible to trypsin digestion. As a positive control we treated wild-type TG2 with R281 inhibitors that locks TG2 into its open conformation. R281 treated wild type TG2 was then subjected to trypsin digestion and complete digestion of protein was observed with 80ngs of trypsin. This could indicate that the open conformation of TG2 is susceptible to trypsin digestion. It was further attempted to test the effect of R283 inhibitor on the conformation of TG2. Wild type TG2 was treated with R283 and subjected to trypsin digestion. The results revealed that when wild-type TG2 was treated with R283 no digestion was observed until 3.2 μ g of trypsin. This indicating altered conformation as compared to R281 inhibitor. R281 inhibitor treated CFP-TG2-YFP recombinant protein shows a partial digestion of protein using trypsin treatment. Altered trypsin susceptibility of CFP-TG2-YFP recombinant protein could be due to attachment of two fluorescent proteins to TG2. Due to the difference in

molecular size of wild-type TG2 and CFP-TG2-YFP recombinant protein probably a higher concentration of trypsin is required for complete digestion of CFP-TG2-YFP recombinant protein.

Comparison between fibronectin incorporation using a modified ELISA revealed CFP-TG2-YFP and RhTG2 show similar fibronectin binding while using Cub7402. Control CFP-TG2 recombinant protein showed higher fibronectin incorporation as compared to CFP-TG2-YFP recombinant protein and RhTG2 using both Cub7402 and 1D10. While comparing Cub7402 and 1D10 a difference was observed in fibronectin incorporation between CFP-TG2-YFP recombinant protein and RhTG2. This could possibly be due to steric hindrance by attaching two fluorescent protein and thereby differential binding to 1D10 to TG2.

Biotin cadaverin incorporation into N, N' dimethyl casein and fibronectin showed that higher specific activity was observed while using fibronectin. It was observed that with casein the specific activity was less than half. Using fibronectin the showed an increase in specific activity of recombinant CFP-TG2-YFP.

Further analysis of activity of TG2 with increasing concentrations of calcium showed that with the increase in calcium TG2 activity is also upregulated. Comparing RhTG2, CFP-TG2-YFP recombinant protein and CFP-TG2 protein followed the same curve. It was observed that the K_m value for recombinant CFP-TG2-YFP protein was higher as compared to RhTG2. A similar curve was plotted using increasing concentration of GTP. It was seen that all three proteins followed the same curve. RhTG2 and CFP-TG2-YFP recombinant protein has all most overlapping curve. With the increasing concentration of GTP TG2 activity is inhibited. This is also true for CFP-TG2-YFP recombinant protein and CFP-TG2.

It was observed that CFP-TG2-YFP FRET sensor constructed showed similar characteristic properties to TG2. To analyse the FRET changes in-vitro, CFP-TG2-YFP recombinant protein was purified using the Ni-NTA column. Appropriate FRET controls include CFP-TG2 and TG2-YFP only constructs. Since *Bgl*III the restriction site at the start of TG2 was destroyed during infilling the 3'ends, restriction digestion of TG2-YFP construct was not possible. CFP-TG2 construct was similarly expressed and purified in bacterial cells for FRET analysis. In order to measure the changes in fluorescence using an increasing concentration of calcium and GTP were incorporated with CFP-TG2-YFP and CFP-TG2 recombinant proteins. Analysing the effect of GTP on fluorescence we excited CFP at 436nm and YFP emission was measured at 538nm. It was observed that with increasing concentration of GTP, as the structure closes more energy is transferred from CFP to YFP and hence an increase in YFP emission was observed. An opposing effect was seen in fluorescence while measuring CFP emission by exciting CFP. This again is in accordance with the closing of TG2 with GTP. Since more energy is transferred to YFP, CFP fluorescence is bound to decrease as observed. Exciting YFP and emitting YFP should ideally remain constant if the same amount of protein is excited. A slight increase in YFP emission that is observed should be accounted for when calculating FRET efficiency. All calculations were performed on raw data and was observed that with the increase in GTP concentration, the YFP emission and FRET efficiency also increases. This suggests with increasing concentration of GTP the structure of TG2 closes, bringing the fluorophores together and increasing the fluorescence. The opposite effect was observed when increasing calcium concentration in solution. As calcium concentration increases a decrease in YFP emission was seen when exciting CFP. This suggests that as TG2 structure opens,

less energy is transferred from CFP to YFP which explains the decrease seen. While measuring fluorescence by exciting CFP, emission of CFP fluorescence was observed to increase correctly. The efficiency of FRET with increasing concentration of calcium was noted to decrease. This implies that as the structure of TG2 opens up with increasing concentration of calcium the fluorophores move apart from each other and hence less energy is transferred. A graphical representation of TG2 activity curve and negative value of FRET efficiency shows that both activity and FRET follow the same curve and thereby validating the constructed FRET sensor. This sensor can be suggested to work efficiently even in mammalian cells.

For the expression of this FRET sensor in mammalian cells, it must be subcloned into pcDNA3.1-. New primers were designed to express the entire CFP-TG2-YFP construct and another construct was aimed to have a polyhistidine tag CFP-TG2-YFP for purification purposes. PCR amplification using NotICFP and HispTrc forwards primers with YFP reverse primers showed successful amplification of 3.5Kb construct. For optimisation of PCR various concentrations of magnesium sulphate were tried. Concentration of DMSO was varied with different dilutions of template DNA. Condition of PCR were optimised as initial denaturation at 95°C for 2 min, followed by 35 cycles of 95°C for 45 s, 70°C for 1 min, 72°C for 1 min, followed by a final extension step at 72°C for 10 min using KOD Hot start polymerase using 10X KOD hot start buffer and 1mM MgSO₄. Non-specific bands were still observed on agarose gel electrophoresis of PCR products. NotICFP-TG2-YFP and His-CFP-TG2-YFP were ligated into pSTlue1 and the colonies were screened for plasmid larger than parent vector were selected for test digestion with *EcoRI*. For cloning into mammalian expression vector pcDNA3.1-, *NotI* and *HindIII* digestion was successfully performed. In order to help easy gel purification of HisCFP-TG2-YFP

insert from pSTlue1 cloning vector another restriction enzyme *PvuI* was employed. Ligation was performed to insert HisCFP-TG2-YFP and NotICFP-TG2-YFP into pcDNA3.1-. All resulting colonies were screened but showed self ligated plasmid only. This could be due to incomplete digestion of insert or due to improper vector: insert ratio. Another problem could be the large size of the insert which needs further optimisation for successful cloning into pcDNA3.1-.

Future work

Now that the basis of constructing FRET sensors has been laid, it would certainly be interesting to monitor the real-time changes *in-vivo* in mammalian cells. Once the cloning of this construct into pcDNA3.1- is successful, it can be transfected into H293T/17 cells. The construct can be assessed on its expression, activity, stability like performed in the bacterial system. It could also be interesting to analyse the difference of TG2 behaviour *in vitro* and *in vivo*. TG2 conformation in HEK293T/17 cells could be assessed using FRET, its response to calcium and GTP influx. The real-time monitoring of TG2 could be interesting and take this project further. Also the introduction of mutations into this FRET construct could open a new area of investigation. The validating of existing mutations using this FRET construct would also be possible. The use of inter-molecular FRET could also provide newer insights into TG2 interactions. The use of CFP-TG2 only construct could be applied for such inter-molecular FRET based studies. It would also be an interesting study to specifically direct this construct using signal peptides into different compartments like the nucleus, extracellular matrix to check its response and interactions specific to that environment. The effect of calcimycin or other ionophores could also be assessed using this sensor. The use of other TG2 inhibitors and determine the effect of such inhibitors could not only contribute to TG2 investigation but also may provide

a quicker method for testing inhibitors. The same FRET construct could also be applied to study TG2 in plant cells. The use of other FRET pairs like that of turbo sapphire and ds Red could also open up new possibilities of exploring and comparing the effect of different FRET pairs.

References

References

- ACHYUTHAN, K. E. & CHARLES, G. S. 1987. Identification of a guanosine triphosphate-binding site on guinea pig liver transglutaminase. *The Journal of Biological Chemistry*, 262, 1901-1906.
- ADAMS, S. R., ALEC, H. T., JI, B. Y., SUSAN, T. S. & ROGER, T. Y. 1991. Fluorescence ration imaging of cyclic AMP in single cells. *Nature*, 349, 694-697.
- AHVAZI, B., KAREN, B. M., WILLIAM, I., ULRICH, B. & PETER, S. M. 2003. Role of calcium ions in the activation and activity of transglutaminase 3 enzyme. *The Journal of Biological Chemistry*, 278, 23834-23841.
- AKIMOV, S. S., DMITRY, K., LAURIE, F. F. & ALEXEY, B. M. 2000. Tissue Transglutaminase is an integrin binding adhesion coreceptor for fibronectin. *Journal of Cell Biology*, 147, 825-838.
- ANDRINGA, G., LAM, K. Y., CHEGARY, M., WANG, X., CHASE, T. N. & BENNETT, M. C. 2004. Tissue transglutaminase catalyses the formation of alpha-synuclein crosslinks in Parkinson's disease. *The FASEB Journal*, 18, 932-4.
- ARENTZ-HANSEN, H., KORNER, R., MOLBERG, O., QUARSTEN, H., VADER, W., KOOY, Y., LUNDIN, K. E. A., KONING, F., ROESTRORFF, P., SOLLID, L. M. & MCADAM, S. N. 2000. The intestinal T cell response to α -Gliadin in adult celiac disease is focused on a single deamidated glutamine targeted by tissue transglutaminase. *The journal of Experimental Medicine*, 191, 603-612.
- AZIM, A. C., SHIRIN, M. M., CATHERINE, K., ELIZABETH, D., COHEN, C. M. & CHISHTI, A. H. 1996. Human erythrocyte dematin and protein 4.2 (pallidin) are ATP binding proteins. *Biochemistry*, 35, 3001-3006.
- BAILEY, C. D. C. & JOHNSON, G. V. W. 2004. Developmental regulation of tissue transglutaminase in the mouse forebrain. *Journal of Neurochemistry*, 91, 1396-1379.
- BEGG, G. E., LYLE, C., STOKES, P. H., JACQUELINE, N. M., MERRIDEE, W. A., AHSAN, H., LASZLO, L., SIIRI, I. & ROBERT, G. M. 2006. Mechanism of allosteric regulation of transglutaminase 2 by GTP. *PNAS*, 103, 19683-19688.
- BELKIN, A. M. 2011. Extracellular TG2: emerging functions and regulation. *FEBS Journal*, 278, 4704-4716.
- BELKIN, A. M., AKIMOV, S. S., ZARITSKAYA, L. S., RATNIKOV, B. I., DERYUGINA, E. I. & STRONGIN, A. Y. 2001. Matrix-dependent proteolysis of surface transglutaminase by membrane-type metalloproteinase regulates cancer cell adhesion and locomotion. *J Biol Chem*, 276, 18415-22.
- BERGAMINI, C. M., COLLIGHAN, R. J., WANG, Z. & GRIFFIN, M. 2011. Structure and Regulation of Type 2 Transglutaminase in Relation to its Physiological Functions and Pathological Roles. *Advances in Enzymology*. John Wiley & Sons, Inc.

- BOWDEN, P. E. 2011. Peeling skin syndrome: genetic defects in late terminal differentiation of the epidermis. *Journal of Investigative dermatology*, 131, 561-564.
- BREJC, K., TITIA, S. K., PAUL, K. A., STEVEN, K. R., ROGER, T. Y., MATS, O. & JAMES, R. S. 1997. Structural basis for dual excitation and photoisomerization of the *Aequorea victoria* green fluorescent protein. *Proc. Natl. Acad. Sci, USA*, 94, 2306-2311.
- BROECKELMANN, T. J., LIMPER, A. H., COLBY, T. V. & MCDONALD, J. A. 1991. Transforming growth factor beta 1 is present at sites of extracellular matrix gene expression in human pulmonary fibrosis. *Proc Natl Acad Sci U S A*, 88, 6642-6.
- CANDI, E., SERGIO, O., ALESSANDRO, T., ANDREA, P., MARCO, R., ALESSANDRO, F.-A. & GERRY, M. 2001. Transglutaminase 5 cross-links loricrin, involucrin, and small proline-rich proteins in vitro. *The Journal of Biological Chemistry*, 276, 35014-23.
- CANDI, E., SERGIO, O., ANDREA, P., ALESSANDRO, T., MARCO, R., PATRIZIA, T., GENNARO, C., SILVIA, S., PIETRO, P. & GERRY, M. 2002. Expression of transglutaminase 5 in normal and pathologic human epidermis. *Journal of Investigative Dermatology*, 119, 670-677.
- CAO, Z., YANG, W., ZHI-YONG, L., ZHEN-SHENG, Z., SHAN-CHENG, R., YONG-WEI, Y., MENG, Q., BEI-BEI, Z. & YING-HAO, S. 2013. Overexpression of transglutaminase 4 and prostate cancer progression : a potential predictor of less favourable outcomes. *Asian Journal of Andriology*, 15, 742-746.
- CARON, N. S., MUNSIE, L. N., KEILLOR, J. W. & TRUANT, R. 2012. Using FLIM-FRET to measure conformational changes of transglutaminase type 2 in live cells. *PLoS One*, 7, e44159.
- CASCELLA, N. G., DEBBY, S., PATRICIA, G., KELLY, D. L., ALESSIO, F. & EATON, W. W. 2013. Increased prevalence of transglutaminase 6 antibodies in sera from schizophrenia patients. *Schizophrenia Bulletin*, 39, 867-871.
- CASE, A. & STEIN, R. L. 2007. Kinetic analysis of the interaction of tissue transglutaminase with a nonpeptidic slow-binding inhibitor. *Biochemistry*, 46, 1106-15.
- CASSIDY, A. J., STEENSEL, M. A. M. V., STEIJLEN, P. M., MICHEL, V. G., VELDEN, J. V. D., MORLEY, S. M., TERRINONI, A., MELINO, G., CANDI, E. & MCLEAN, I. W. H. 2005. A homozygous missense mutation in TGM5 abolishes epidermal transglutaminase 5 activity and causes acral peeling skin syndrome. *American journal of human genetics*, 77, 909-917.
- CHALFIE, M., YUAN, T., GHIA, E., WARD, W. W. & PRASHER, D. C. 1994. Green Fluorescent protein as a marker for gene expression. *Science*, 263, 802-805.

- CHUDAKOV, D. M., MATZ, M. V., SERGEY, L. & LUKYANOV, K. A. 2010. Fluorescent proteins and their applications in imaging living cells and tissue. *Physiological Reviews*, 90, 1103-1163.
- CITRON, B. A., ZHIMING, S., KAREN, S., DAVIES, P. J. A., FRANK, Q. & FESTOFF, B. W. 2002. Protein crosslinking, tissue transglutaminase, alternative splicing and neurodegeneration. *Neurochemistry International*, 40, 69-78.
- COLLIGHAN, R. J. & GRIFFIN, M. 2009. Transglutaminase 2 cross-linking of matrix proteins: biological significance and medical applications. *Amino Acids*, 36, 659-670.
- DAY, R. N. & DAVIDSON, M. 2012. Fluorescent proteins for FRET microscopy: monitoring protein interactions in living cells. *Bioessays*, 34, 341-350.
- DEL DUCA, S., BENINATI, S. & SERAFINI-FRACASSINI, D. 1995. Polyamines in chloroplasts: identification of their glutamyl and acetyl derivatives. *Biochemical Journal*, 305, 233-237.
- DUBBINK, H. J., VERKAIK, S. N., FABER, P. W., TRAPMAN, J., SCHRODER, F. H. & ROMIJN, J. C. 1996. Tissue specific and androgen regulated expression of human prostate-specific transglutaminase. *Biochem. J*, 315, 901-908.
- DUDEK, S. M. & JOHNSON, G. V. W. 1994. Transglutaminase facilitates the formation of polymers of the β -amyloid peptide. *Brain Research*, 651, 129-133.
- DUVAL, E., CASE, A., STEIN, R. L. & CUNY, G. D. 2005. Structure-activity relationship study of novel tissue transglutaminase inhibitors. *Bioorg Med Chem Lett*, 15, 1885-9.
- FENG, J.-F., MELISSA, R., YADAV, S. P. & IM, M.-J. 1999. Calreticulin down regulates both GTP binding and transglutaminase activities of transglutaminase II. *Biochemistry*, 38, 10743-10749.
- FOX, B. A., YEE, V. C., PEDERSEN, L. C., TRONG, I. L., BISHOP, P. D., STENKAMP, R. E. & TELLER, D. C. 1999. Identification of the calcium binding site and novel Ytterbium site in blood coagulation factor XIII by X-ray crystallography. *The Journal of Biological Chemistry*, 274, 4917-4923.
- GRECARD, P., BRESSON-HADNI, S., EL ALAOUI, S. D., CHEVALLIER, M., VUITTON, D. A. & RICARD-BLUM, S. 2001a. Transglutaminase-mediated cross-linking is involved in the stabilization of extracellular matrix in human liver fibrosis. *Journal of Hepatology*, 35, 367-375.
- GRECARD, P., KAY, B. M. & DANIEL, A. 2001b. Evolution of transglutaminase gene: identification of transglutaminase gene cluster on human chromosome 15q15: structure of the gene encoding transglutaminase x and a novel gene family member, Transglutaminase Z. *The Journal of Biological Chemistry*, 276, 33066-33078.

- GRIFFIN, M., CASADIO, R. & BERGAMINI, C. M. 2002. Transglutaminases: nature's biological glues. *Biochem J*, 368, 377-96.
- GRIFFIN, M., MONGEOT, A., COLLIGHAN, R., SAINT, R. E., JONES, R. A., COUTTS, I. G. & RATHBONE, D. L. 2008. Synthesis of potent water-soluble tissue transglutaminase inhibitors. *Bioorg Med Chem Lett*, 18, 5559-62.
- GUNDEMIR, S., GOZDE, C., JANUSZ, T. & V.W, J. G. 2012. Transglutaminase 2: A molecular swiss army knife. *Biochim Biophys Acta*, 1823, 409-419.
- GUNDEMIR, S. & JOHNSON, G. V. W. 2009. Intracellular localisation and conformational state of transglutaminase 2: implication for cell death. *Plos One*, 4, 1-13.
- GUSELLA, J. F., MACDONALD, M. E., AMBROSE, M. C. & DUYAO, M. P. 1993. Molecular genetics of huntington's disease. *Archives of Neurology*, 50, 1157-63.
- HADJIVASSILIOU, M., PASCALE, A., SANDERS, D. S., NICOLA, W. & DANIEL, A. 2008. Autoantibodies in gluten ataxia recognize a novel neuronal transglutaminase. *Annals of Neurology*, 64, 332-343.
- HAN, B.-G., CHO, J.-W., CHO, Y. D., JEONG, K.-C., KIM, S.-Y. & LEE, B. L. 2010. Crystal structure of human transglutaminase 2 in complex with adenosine triphosphate. *International journal of biological macromolecules*, 47, 190-195.
- HANG, J., ZEMSKOV, E. A., LASZLO, L. & BELKIN, A. M. 2005. Identification of a novel recognition sequence for fibronectin within NH₂- terminal B-sandwich domain of tissue transglutaminase. *The Journal of Biological Chemistry*, 280, 23675-23683.
- HASEGAWA, G., SUWA, M., ICHIKAWA, Y., OHTSUKA, T., KUMAGAI, S., KIKUCHI, M., SATO, Y. & SAITO, Y. 2003. A novel function of tissue-type transglutaminase: protein disulphide isomerase. *Biochem J.*, 373, 793-803.
- HEIM, R. & TSEIN, Y. R. 1996. Engineering green flurescent protein for improved brightness, longer wavelengths and flurorescence resonance energy transfer. *Current Biology*, 6, 178-182.
- HIIRAGI, T., HIROYUKI, S., AKIRA, N., HISATAKA, S., SHEN, S. C., MASATO, M., KIYOFUMI, Y. & SHOICHIRO, T. 1999. Transglutaminase Type 1 and its cross linking activity are concentrated at adherens junctions in simple epithelial cells. *The Journal of Biological Chemistry*, 274, 34148-34154.
- IISMAA, S. E., MEARNES, B. M., LASZLO, L. & GRAHAM, R. M. 2009. Transglutaminases and disease: lessons from genetically engineered mouse models and inherited disorders. *Physiological Reviews*, 89, 991-1023.
- IISMAA, S. E., MING-JIE, W., NISHA, N., CHURCH, B. W. & GRAHAM, R. M. 2000. GTP binding and Signaling by G_H/transglutaminase II involves distinct residues in a unique GTP-binding pocket. *The Journal of Biological Chemistry*, 275, 18259-18265.

- JABRI, B. & SOLLID, L. M. 2009. Tissue mediated control of immunopathology in coeliac disease. *Nature Reviews Immunology*, 9, 858-870.
- JANG, T.-H., DONG-SUP, L., KIHANG, C., MAN, J. E., IN-GYU, K., WHAN, K. Y., NYEO, C. J., JU-HONG, J. & HYUN, P. H. 2014. Crystal Structure of Transglutaminase 2 with GTP complex and amino acid sequence evidence of evolution of GTP binding site. *Plos One*, 9, 1-8.
- JIANG, W. & ALBIN, R. J. 2011. Prostate transglutaminase: a unique transglutaminase and its role in prostate cancer. *Biomark Med*, 5, 285-291.
- JOHNSON, G. V. W., COX, T. M., LOCKHART, J. P., ZINNERMAN, M. D., MILLER, M. L. & POWERS, R. E. 1997a. Transglutaminase activity is increased in Alzheimer's disease brain. *Brain Research*, 751, 323-329.
- JOHNSON, T. S., MARTIN, G., GRAHAM, T. L., JAMES, S., ANN, C., BIN, Y., BEN, N., J., B. P., CHIWONESO, M.-K. & NAHAS A, M. E. 1997b. The role of transglutaminase in the rat subtotal nephrectomy model of renal fibrosis. *The journal of clinical investigation*, 99, 2950-2960.
- KANAJI, T., HIROSHI, O., TOSHIFUMI, T., HIDEO, K., MASAO, M. & YASUTSUGU, S. 1993. Primary structure of microbiaql transglutaminase from *Streptovortillum* sp. Strain S-8112. *The Journal of Biological Chemistry*, 268, 11565-11572.
- KEVIN, T. & MITSUHIKO, I. 2001. The use of FRET imaging microscopy to detect protein-protein interactions and protein conformational changes in vivo. *Current opinion in structural biology*, 11, 573-578.
- KIM, H. C., LEWIS, M. S., GORMAN, J. J., PARK, S. C., GIRAND, J. E., FOLK, J. E. & CHUNG, S. I. 1990. Protransglutaminase E from guinea pig skin. Isolation and partial characterisation. *The Journal of Biological Chemistry*, 265, 21971-8.
- KIM, S.-Y., CHUNG, S.-I. & STEINERT, P. M. 1995. Highly active soluble processed forms of the transglutaminase 1 enzyme in epidermal keratinocytes. *The Journal of Biological Chemistry*, 270, 18026-35.
- KIRALY, R., EVA, C., TIBOR, K., SANDOR, A., KRISZTIAN, S., ZSOFIA, S.-V., IIMA, K.-S., ZSOLT, K. & LASZLO, F. 2009. Functional significance of five noncanonical Ca^{2+} binding sites of human transglutaminase 2 characterised by site directed mutagenesis. *FEBS*, 276, 7083-7096.
- KOTSAKIS, P. & GRIFFIN, M. 2007. Tissue transglutaminase in tumour progression: friend or foe? *Amino Acids*, 33, 373-384.
- KULASAKARAN, P., SCAVONE, C. A., ROGERS, D. S., ARENBERG, D. A., THANNICKAL, V. J. & HOROWITZ, J. C. 2009. Endothelin-1 and Transforming Growth Factor- β 1 Independently Induce Fibroblast Resistance to Apoptosis via AKT Activation. *American Journal of Respiratory cell and molecular biology*, 41, 484-493.

- LAI, T.-S., BIELAWSKA, A., PEOPLES, K. A., HANNUN, Y. A. & GREENBERG, C. S. 1997. Sphingosylphosphocholine reduces the calcium ion requirement for activating tissue transglutaminase. *The Journal of Biological Chemistry*, 272, 16295-16300.
- LAI, T. S., HAUSLADEN, A., SLAUGHTER, T. F., EU, J. P., STAMLER, J. S. & GREENBERG, C. S. 2001. Calcium regulates S-nitrosylation, denitrosylation, and activity of tissue transglutaminase. *Biochemistry*, 40, 4904-10.
- LAI, T. S., SLAUGHTER, T. F., PEOPLES, K. A., HETTASCH, J. M. & GREENBERG, C. S. 1998. Regulation of human tissue transglutaminase function by magnesium-nucleotide complexes. Identification of distinct binding sites for Mg-GTP and Mg-ATP. *J Biol Chem*, 273, 1776-81.
- LEHTHINEN, M. J., SEPPO, M. & SAKARI, J. T. 2004. Interdomain contact regions and angles between adjacent short consensus repeat domains. *Journal of Molecular Biology*, 344, 1385-1396.
- LESORT, M., KALAYA, A., JIANWEN, Z. & JOHNSON, G. V. W. 1998. Distinct nuclear localisation and activity of tissue transglutaminase. *The Journal of Biological Chemistry*, 273, 11991-11994.
- LI, I. T., ELIZABETH, P. & KEVIN, T. 2006. Protein biosensors based on the principle of fluorescence resonance energy transfer for monitoring cellular dynamics. *Biotechnol Lett*, 28, 1971-1982.
- LIECA, M. 2007. FRET acceptor photobleaching. *Resolution Confocal application letter*, Dec 2007.
- LIU, S., CERIONE, R. A. & CLARDY, J. 2002. Structural basis for the guanine nucleotide-binding activity of tissue transglutaminase and its regulation of transamidation activity. *Proc. Natl. Acad. Sci, USA*, 99, 2743-2747.
- MANN, A. P., VERMA, A., SETHI, G., MANAVATHI, B., WANG, H., FOK, J. Y., KUNNUMAKKARA, A. B., KUMAR, R., AGGARWAL, B. B. & MEHTA, K. 2006. Overexpression of tissue transglutaminase leads to constitutive activation of nuclear factor-kappaB in cancer cells: delineation of a novel pathway. *Cancer Res*, 66, 8788-95.
- MEHTA, K., KUMAR, A. & KIM, H. I. 2010. Transglutaminase 2: A multi-tasking protein in the complex circuitry of inflammation and cancer. *Biochemical Pharmacology*, 80, 1921-1929.
- MIAN, S., ALAOUI, S. E., J., L., GENTILE, V., DAVIES, P. J. A. & MARTIN, G. 1995. The importance of the GTP-binding protein tissue transglutaminase in the regulation of cell cycle progression. *FEBS*, 370.
- MICHALIK, A. & VAN BROECKHOVEN, C. 2003. Pathogenesis of polyglutamine disorders: aggregation revisited. *Hum Mol Genet*, 12 Spec No 2, R173-86.
- MISHRA, S. & MURPHY, L. J. 2004. Tissue transglutaminase has intrinsic kinase activity. *The Journal of Biological Chemistry*, 279, 23863-23868.

- MIYAWAKI, A. & TSEIN, Y. R. 2000. Monitoring protein conformations and interactions by fluorescence resonance energy transfer between mutants of green fluorescent protein. *Methods in enzymology*, 327, 472-500.
- MONSONEGO, A., Yael, S., IGOR, F., YOAV, P., ORYL, E. & MACHAL, S. 1997. Expression of GTP dependent and GTP independent tissue type transglutaminase in cytokine treated rat brain astrocytes. *The Journal of Biological Chemistry*, 272, 3724-3732.
- MUKHERJEE, D. C., AGARWAL, A. K., MANJUNATH, R. & MUKHERJEE, A. B. 1983. Suppression of epididymal sperm antigenicity in the rabbit by uteroglobin and transglutaminase in vitro. *Science*, 219, 989-91.
- MURTHY, S. N. P., LOMASNEY, J. W., MAK, E. C. & LASZLO, L. 1999. Interactions of Ghyltransglutaminase with phospholipase C δ 1 and with GTP. *PNAS*, 96, 11815-11819.
- MURTHY, S. N. P., SIIRI, I., BEGG, G. E., FREYMAN, D. M., GRAHAM, R. M. & LASZLO, L. 2002. Conserved tryptophan in the core domain of transglutaminase is essential for catalytic activity. *Proc. Natl. Acad. Sci, USA*, 99, 2738-2742.
- MYRSKY, E., KAUKINEN, K., SYRJANEN, M., KORPONAY-SZABO, I., MAKI, M. & LINDFORS, K. 2008. Coeliac disease-specific autoantibodies targeted against transglutaminase 2 disturbs angiogenesis. *Clinical and Experimental Immunology*, 152, 111-119.
- NAKAOKA, H., PEREZ, D., KJ, B., T, D., A, H., K, M., IM, M. & GRAHAM, R. 1994. Gh: a GTP-binding protein with transglutaminase activity and receptor signaling function. *Science*, 264, 1593-6.
- OLSEN, K. C., SAPINORO, R. E., KOTTMANN, R. M., KULKARNI, A. A., IISMAA, S. E., JOHNSON, G. V., THATCHER, T. H., PHIPPS, R. P. & SIME, P. J. 2011. Transglutaminase 2 and its role in pulmonary fibrosis. *Am J Respir Crit Care Med*, 184, 699-707.
- PALOTAS, A., BOTOND, P., LAJOS, K., ZOLTAN, J. & JANOS, K. 2004. A chapter in the unity of variety-calcium is the sole author? *Brain Research*, 1000, 57-59.
- PARK, D., SHIM, C. S. & KNON-SOO, H. 2010. Transglutaminase 2 :a multifunctional protein in multiple subcellular compartments. *Amino Acids*, 39, 619-631.
- PENG, X., YONHUI, Z., HAIFAN, Z., SCOTT, G., WILLIAMS, J. F., LEVITT, M. L. & ANNA, L. 1999. Interaction of tissue transglutaminase with nuclear transport protein α 3. *FEBS*, 446, 35-39.
- PINKAS, D. M., PAVEL, S., ALEX, B. T. & CHAITAN, K. 2007. Transglutaminase 2 undergoes a large conformational change upon activation. *Plos Biology*, 5, e327.

- PISTON, D. W. & KREMERS, G.-J. 2007. Fluorescent protein FRET: the good, the bad and the ugly. *TRENDS in Biochemical Sciences*, 32, 407-414.
- PUSZKIN, E. G. & RAGHURAMAN, V. 1985. Catalytic properties of a calmodulin-regulated transglutaminase from human platelet and chicken gizzard. *J Biol Chem*, 260, 16012-20.
- RASCOL, O., PIERRE, P., FABIENNE, O., J., F. J., CHRISTINE, B.-C. & JEAN-LOUIS, M. 2003. Limitations of current Parkinson's disease therapy. *Annals of Neurology*, 53, S3-S15.
- RITCHIE, H., LAWRIE, L. C., CROMBIE, P. W., MOSESSON, M. W. & BOOTH, N. A. 2000. Cross-linking of Plasminogen Activator Inhibitor 2 and α 2-Antiplasmin to Fibrin(ogen). *Journal of Biological Chemistry*, 275, 24915-24920.
- ROSE, C., PAUL, A. F., JANA, R., BERND-WOLFGANG, I., DETLEF, Z. & IAKOV, S. 2009. Autoantibodies against epidermal transglutaminase are a sensitive diagnostic marker in patients with dermatitis herpetiformis on a normal or gluten-free diet. *Journal of the American Academy of Dermatology*, 61, 39-43.
- RUAN, Q. & JONHSON, G. V. W. 2007. Transglutaminase 2 in neurodegenerative disorders. *Frontiers in Biosciences*, 12, 891-904.
- SAITO, M., ASAKURA, H., YOSHIDA, T., ITO, K., OKAFUJI, K., YOSHIDA, T. & MATSUDA, T. 1990. A familial factor XIII subunit B deficiency. *British Journal of haematology*, 74, 290-4.
- SHANER, N. C., PATTERSON, G. H. & DAVIDSON, M. W. 2007. Advances in fluorescent protein technology. *Journal of Cell Science*, 120, 4247-4260.
- SHANER, N. C., STEINBACH, A. P. & TSEIN, Y. R. 2005. A guide to choosing fluorescent proteins. *Nature methods*, 2, 905-909.
- SHIMOMURA, O., FRANK, J. H. & YO, S. 1962. Extraction, purification and properties of a bioluminescent protein from the luminescent hydromedusa, *Aequorea*. *Journal of Cellular and Comparative Physiology*, 59, 223-239.
- SIEGEL, M. & KHOSLA, C. 2007. Transglutaminase 2 inhibitors and their therapeutic role in disease states. *Pharmacol Ther*, 115, 232-45.
- SIEGEL, M., PAVEL, S., EDWARD, W. R., KIHANG, C., BANA, J., BISHR, O. M. & CHAITAN, K. 2008. Extracellular Transglutaminase 2 is catalytically inactive but is transiently activated upon tissue injury. *Plos One*, 3, 1-11.
- SINGH, R. N. & MEHTA, K. 1994. Purification and characterisation of a novel transglutaminase from filarial nematode *Brugia malayi*. *European Journal of Biochemistry*, 225, 625-634.
- SMETHURST, P. A. & GRIFFIN, M. 1996. Measurement of tissue transglutaminase activity in a permeabilised cell system: its regulation by Ca^{2+} and nucleotides. *Biochem J.*, 313, 803-808.

- SPINA, A. M., ESPOSITO, C., PAGANO, M., CHIOSI, E., MARINIELLO, L., COZZOLINO, A., PORTA, R. & ILLIANO, G. 1999 GTPase and transglutaminase are associated in the secretion of the rat anterior prostate. *Biochemical and Biophysical Research Communications*, 260, 351-356.
- STACEY, S. N., SULEM, P., GUDBJARTSSON, D. F., JONASDOTTIR, A., GUDMAR THORLEIFSSON, GUDJONSSON, S. A., MASSON, G., GUDMUNDSSON, J., SIGURGEIRSSON, B., BENEDIKTSDOTTIR, K. R., THORISDOTTIR, K., RAGNARSSON, R., FUENTELES, V., CORREDERA, C., GRASA, M., PLANELLES, D., SANMARTIN, O., RUDNAI, P., GURZAU, E., KOPPOVA, K., HEMMINKI, K., NEXØ, B. A., TJØNNELAND, A., OVERVAD, K., JOHANNSDOTTIR, H., HELGADOTTIR, H. T., THORSTEINSDOTTIR, U., KONG, A., VOGEL, U., KUMAR, R., NAGORE, E., MAYORDOMO, J. I., RAFNAR, T., OLAFSSON, J. H. & STEFANSSON, K. 2014. Germline sequence variants in TGM3 and RGS22 confer risk of basal cell carcinoma. *Human Molecular Genetics*, 23, 3045-3053.
- STAMNAES, J., M., P. D., BURKHARD, F., CHAITAN, K. & M., S. L. 2009. Redox regulation of transglutaminase 2 activity. *The Journal of Biological Chemistry*, 285, 25402-25409.
- STURNIOLO, M. T., CHANRARATNA, R. A. & ECKERT, R. L. 2005. A novel transglutaminase activator forms a complex with type 1 transglutaminase. *Oncogene*, 24, 2963-2972.
- TAKANISHI, C. L., EKATERINA, A. B., WEI, C. & JIE, Z. 2006. GFP-based FRET analysis in live cells. *Brain Research*, 1091, 132-139.
- TARCSA, E., MAREKOV, L. N., ANDEROLI, J., IDLER, W., CANDI, E., CHUNG, S. I. & STEINERT, P. M. 1997. The fate of trichohyalin. Sequential post-translational modifications by peptidyl-arginine deiminase and transglutaminases. *The Journal of Biological Chemistry*, 272, 27893-278901.
- TELICI, D., COLLIGHAN, R. J., HUVEYDA, B. & MARTIN, G. 2009. Increases TG2 expression can result in induction of transforming growth factor β -1, causing increases synthesis and deposition of matrix proteins, which can be regulated by nitric oxide. *The Journal of Biological Chemistry*, 284, 29547-29558.
- TELICI, D., WANG, Z., LI, X., VERDERIO, E., MARTIN, H. J., MANUELA, B., HUVEYDA, B. & GRIFFIN, M. 2008. Fibronectin-Tissue transglutaminase matrix rescues RGD-impaired cell adhesion through syndecan-4 and β_1 integrin co-signaling. *The Journal of Biological Chemistry*, 283, 20937-20947.
- THIEBACH, L., JOHN, S., PAULSSON, M. & SMYTH, N. 2007. The role of TG3 and TG6 in hair morphogenesis and in establishment of the skin barrier *In*: LINKING, T. I. C. O. T. A. P. C. (ed.). Morocco.
- THOMAS, H., KONRAD, B., MAGDALENA, A., PASCALE, A., MARTIN, L., C., O. R., LARS, T., MARTIN, H. & DANIEL, A. 2013. Transglutaminase 6 a protein associated with central nervous system development and motor function. *Amino Acids*, 44, 161-177.

- TRUONG, K. & IKURA, M. 2001. The use of FRET imaging microscopy to detect protein-protein interactions and protein conformational changes in vivo. *Current Opinion in Structural Biology*, 11, 573-587.
- TSAI, Y.-H., LAI, W.-F. T., CHEN, S.-H. & JOHNSON, L. R. 1998. A Novel Calcium-Independent Enzyme Capable of Incorporating Putrescine into Proteins. *Biochemical and Biophysical Research Communications*, 244, 161-166.
- TSEIN, R. Y. 1998. The green fluorescent protein. *Annu. Rev, Biochem*, 67, 509-544.
- VERDERIO, E. A., TIMOTHY, J. & MARTIN, G. 2004. Tissue transglutaminase in normal and abnormal wound healing: review article. *Amino Acids*, 26, 387-404.
- VERDERIO, E. A. M., JOHNSON, T. S. & GRIFFIN, M. 2005. Transglutaminases in wound healing and inflammation. *Progress in experimental tumor research*, 38, 89-114.
- WAL, Y. V. D., YVONNE, K., PETER, V. V., SALVADOR, P., LUISA, M., GEORGE, P. & FRITS, K. 1998. Cutting Edge: selective deamination by tissue transglutaminase strongly enhances gliadin specific T cell reactivity. *The Journal of Immunology*, 161, 1585-1588.
- WANG, Y. & WANG, N. 2009. FRET and mechanobiology. *Integr Biol (Camb)*, 1, 565-573.
- WANG, Z., COLLIGHAN, R. J., GROSS, S. R., DANEN, E. H., OREND, G., TELCI, D. & GRIFFIN, M. 2010. RGD-independent cell adhesion via a tissue transglutaminase-fibronectin matrix promotes fibronectin fibril deposition and requires syndecan-4/2 and $\alpha_5\beta_1$ integrin co-signaling. *J Biol Chem*, 285, 40212-40229.
- WANG, Z., COLLIGHAN, R. J., KAMILA, P., RATHBONE, D. L., XIAOLING, L. & MARTIN, G. 2012. Characterisation of Heparin-binding site of tissue transglutaminase. *The Journal of Biological Chemistry*, 287, 13063-83.
- WARD, W. W. & BOKMAN, S. H. 1982. Reversible denaturation of Aequorea green-fluorescent protein: physical separation and characterization of the renatured protein. *Biochemistry*, 21, 4535-4540.
- YASUEDA, H., KUMAZAWA, Y. & MOTOKI, M. 1994. Purification and characterization of a tissue-type transglutaminase from red sea bream (*Pagrus major*). *Biosci Biotechnol Biochem*, 58, 2041-5.
- ZEMSKOV, E. A., MIKHAILENKO, I., HSIA, R.-C., ZARITSKAYA, L. & BELKIN, A. M. 2011. Unconventional secretion of tissue transglutaminase involves phospholipid-dependent delivery into recycling endosomes. *PLoS ONE*, 6, e19414.

- ZHANG, J., ANTONYAK, M. A., SINGH, G. & CERIONE, R. A. 2013. A mechanism for the upregulation of EGF receptor levels in glioblastomas. *Cell Reports*, 3, 2008-2020.
- ZHANG, J. & MASUI, Y. 1997. Role of amphibian egg transglutaminase in the development of secondary cytotstatic factor in vitro. *Mol Reprod Dev*, 47, 302-11.
- ZHU, L., B., K. S. & LONG-SHENG, C. 1998. Developmental expression of mouse erythrocyte protein 4.2 mRNA: evidence for specific expression in erythroid cells. *Blood*, 91, 695-705.